Characterization of Novel Regulators of FoxO Transcription Factors

by

Kathleen Johanna Dumas

A dissertation submitted in partial fulfillment
of the requirements for the degree of
Doctor of Philosophy
(Cellular and Molecular Biology)
in the University of Michigan
2013

Doctoral Committee:

Assistant Professor Patrick J. Hu, Chair
Associate Professor Scott E. Barolo
Assistant Professor Diane C. Fingar
Professor Gary D. Hammer
Assistant Professor John Kim

Dedication

To my parents, for their constant love, support, and encouragement.

Acknowledgements

My graduate experience has been shaped most significantly by the guidance and support of my mentor, Dr. Patrick Hu. Patrick's enthusiasm, intellect, passion, and scientific vision have been integral to my development as a scientist. I am honored to have worked with Patrick and owe him a great debt of gratitude for the time and energy he has invested in my training and development.

I would like to thank my thesis committee members, Dr. John Kim, Dr. Scott Barolo, Dr. Diane Fingar, and Dr. Gary Hammer. My committee has been an excellent sounding board for my scientific questions and has helped to guide the development of my dissertation projects. Moreover, they have continually been my champions and there support has opened many doors for my future career. Most of all, I would like to thank John, Scott, Diane, and Gary for the mentoring and advice they have shared with me through many conversation outside of my formal committee meetings. I know that what I have learned from these individuals will continue to help shape my science and my career well beyond graduate school, and for that I am truly grateful.

The members of the Hu lab, both past and present, have provided invaluable help with my projects and have made the lab an enjoyable place to be. Travis Williams, Chunfang Guo, and I entered the field of worm biology together as complete novices and we learned the ropes with each other's support; I thank them for their enthusiasm, dedication, and friendship throughout our time as colleagues. I thank Titan Shih, Albert Chen, Andy Polzin, and Ian Waters for their help and contributions to my projects, and for being my sounding board for new ideas.

I had the good fortune to work with excellent colleagues and collaborators whose effort and support were integral to successful completion of my dissertation. I thank all of my co-authors for their efforts on the studies described herein. My sincere thanks go out to Stephane Flibotte and Don Moerman (University of British Columbia) for their advice and expertise with the bioinformatic analysis of genome sequencing data collected for the *seak* gene projects. I thank Attila Stetak and Alex Hajnal (University of Zurich) for

reagents pertinent to the GAP-3 project, and I thank Gyorgyi Csankovszki (University of Michigan) for introducing us to the field of dosage compensation and providing invaluable expertise and reagents. I would also like to thank Frank Schroeder and members of the Schroeder lab for their efforts to help us understand the role of HSD-1 in the synthesis of dafachronic acids and for their generosity with reagents and technical advice.

I sincerely thank the members of the Kim lab, our neighbors at the Life Sciences Institute, for their technical advice, generosity with their time, equipment and reagents, and most of all, for their friendship: Ting Han, Vishal Khivansara, Arun Prasad Manoharan, Allison Billi, Amanda Day, Ameila Alessi, Mallory Freeberg, Danny Yang and Natasha Weiser.

Lastly, I thank my family and friends for their unwavering support encouragement, through this endeavor and all of my life. I could not have completed this without you.

Preface

FoxO transcription factors: Master regulators of the biology of aging

Aging is the leading risk factor for cancer and heart disease, as well as the majority of adult diseases. By improving our understanding of the biology of aging, we hope to uncover strategies to interfere with the underlying aging process, and as a result prevent or mitigate the effects of age-associated diseases.

FoxO transcription factors play important roles in the biology of aging; understanding the regulation of these factors promises to shed light on the aging process and illuminate new therapeutic targets for the treatment of age-associated diseases. FoxO transcription factors were first implicated as regulators of longevity in the round worm *C. elegans.* Reducing insulin/insulin-like growth factor signaling (ILS) or ablating the germline extends *C. elegans* lifespan in a manner dependent on the FoxO transcription factor DAF-16. The reduction of ILS is also known to enhance mammalian longevity, suggesting potential conservation of the lifespan-promoting role of FoxO transcription factors. Recent evidence supports this hypothesis, as studies in multiple independent human cohorts have found that specific FoxO polymorphisms are associated with extreme longevity. Additionally, evidence supports roles for FoxO in modulating age-associated diseases in humans, including cancer, Type 2 diabetes, and osteoporosis. Increasing FoxO activity protects against tumor development and osteoporosis, but is also sufficient to induce metabolic dysregulation. The ability to modulate FoxO activity is therefore desirable as a potential therapeutic strategy to combat the progression of cancer, Type 2 diabetes, and potentially other age-associated diseases. Moreover, understanding the regulatory mechanisms controlling FoxO activity will likely contribute to our broader understanding of the biology of aging.

The current paradigm for the regulation of the FoxO family of transcription factors is that activity is dependent on subcellular localization of the factor; when FoxO is in the cytoplasm, its function as a transcription factor is inhibited. When it is in the nucleus, FoxO is active and can initiate transcriptional programs controlling cell cycle

progression, stress resistance and apoptosis. In *C. elegans* and in mammals, insulin activation of the phosphatidylinositol 3-kinase (PI3K)/Akt signaling pathway causes phosphorylation of FoxO by Akt, resulting in cytoplasmic sequestration and consequent inhibition of the transcription factor. In worms, ILS reduction or germline removal causes DAF-16/FoxO to translocate to the nucleus, increasing its activity. Nuclear DAF-16/FoxO induces transcriptional programs that promote longevity.

Nuclear localization is necessary for DAF-16/FoxO activity, however, evidence indicates that it is not sufficient for full activation of the transcription factor, suggesting the existence of a second pathway controlling DAF-16/FoxO. Our lab has recently discovered the EAK pathway, a conserved pathway which inhibits the *C. elegans* DAF-16/FoxO by a novel mechanism.

The EAK pathway was identified in a genetic screen for enhancers of an *akt-1* mutant phenotype. In animals deficient in AKT-1, DAF-16/FoxO accumulates in the nucleus but is not fully active. The *akt-1* mutation therefore provides a sensitized background to identify molecules that, when mutated, further activate DAF-16/FoxO. Genes identified by the *eak* screen encode molecules that normally function in parallel to AKT-1 to inhibit DAF-16/FoxO. Twenty-one independent alleles defining seven *eak* genes were isolated by the screen. My thesis involves characterizing the EAK pathway and elucidating the mechanism by which it controls DAF-16/FoxO. I describe my thesis in the following three parts.

Part I: Characterization of EAK-2/HSD-1, a conserved FoxO regulator

The first aim of my thesis, corresponding to Chapter 2, was to characterize one of two conserved *eak* genes, *eak-2/hsd-1*. The human ortholog of *eak-2/hsd-1,* SDR42E1, is highly expressed in the liver but its function is unknown. It is a member of the 3-beta hydroxysteroid dehydrogenase family of enzymes, which are involved in steroid hormone and bile acid synthesis. In *C. elegans,* EAK-2/HSD-1 is predicted to play a role in the biosynthesis of steroid hormones known as dafachronic acids (DAs). DAs have a structure similar to that of bile acids, and act as ligands for an important nuclear hormone

receptor in the worm, DAF-12. DAF-12 is orthologous to human Liver X Receptor, which is a key regulator of lipid homeostasis. In the worm, DAF-12 regulates the transition into a developmental state known as dauer diapause. Importantly, DAF-16 is also required for this transition.

I determined that EAK-2/HSD-1 acts with the other *eaks* in parallel to PI3K/Akt to inhibit DAF-16/FoxO activity, independent of controlling its subcellular localization. Loss of EAK-2/HSD-1 activity increases DAF-16/FoxO activation during larval development. Interestingly, deletion of *eak-2/hsd-1* reduces longevity that is induced by ILS abrogation, suggesting *eak-2/hsd-1* mutation has the opposite impact on DAF-16/FoxO in the context of aging. It is noteworthy that all *eak* genes characterized to date act in one genetic pathway. Moreover, *eak-2/hsd-1* and all but one of the other characterized *eak* genes are expressed only in two endocrine cells in the worm. Importantly, DAF-16 is not expressed in these cells, suggesting the *eaks* exert their function on DAF-16 non-autonomously, possibly through steroid hormone/DAF-12 signaling.

Part II: Characterization of convergence of steroid hormone signaling and insulin signaling in the control of DAF-16-dependent longevity

Given its ability to both potentiate and antagonize the activity of DAF-16/FoxO, I sought to further understand the mechanistic underpinnings of DAF-16/FoxO control by *eak-2/hsd-1* and steroid hormone/DAF-12 signaling. DAF-12 and DAs we previously known to impinge on DAF-16/FoxO in longevity control, however the nature of the interaction was unclear. My second aim, corresponding to Chapter 3, was to unravel the intersection of these two signaling axes in longevity control. Using animals with mutations in key DA synthetic enzymes, I tested the role of DAs and DAF-12 in regulating longevity *via* DAF-16/FoxO. I found that in animals with reduced ILS, mutations that reduce DA biosynthesis or abrogate DAF-12 activity shorten life span, suggesting that liganded DAF-12 promotes longevity. In animals with weakly reduced ILS, unliganded DAF-12 also promotes longevity. However, with a greater reduction in ILS, as conferred by insulin/IGF-1 receptor mutation, and in germline-ablated animals, unliganded DAF-12

shortens life span. Thus, multiple DAF-12 activities influence life span in a context-dependent manner. These findings highlight the complexity of interactions among DA biosynthetic pathways, DAF-12, and DAF-16/FoxO in aging.

Part III: Genetic screen to identify DAF-16/FoxO activators

My work in parts I and II helped to reveal that all characterized *eak* genes act in one genetic pathway to control the nuclear pool of DAF-16/FoxO. The pathway is endocrine; all EAKs but one, *eak-7* (the other conserved *eak*), act in cells distant from those which express DAF-16/FoxO and are the important sites for influencing development and aging. EAK-7, which is active in the same cells as DAF-16/FoxO and DAF-12, is anchored to the plasma membrane while it acts on the nuclear pool of DAF-16/FoxO. Given its expression pattern, EAK-7 is likely the most downstream EAK, yet how it transduces signals to DAF-16/FoxO is not known.

My final aim was to illuminate the mechanism underlying EAK pathway inhibition of DAF-16/FoxO activity. To accomplish this, I designed an approach to identify molecules which may relay EAK pathway signals to DAF-16/FoxO. I reasoned that by using *akt-1* mutant animals, we could move DAF-16 into the nucleus, and *via* the addition of an *eak-7* mutation, we could induce activation of nuclear DAF-16/FoxO. In this sensitized background, we could then ask for components which, when mutated, suppress the activation of DAF-16/FoxO. As such, I sought to identify suppressors of an *eak-7;akt-1* mutant phenotype (*seak* mutants). We hypothesize that *seak* genes will encode molecules that activate DAF-16/FoxO by acting in the PI3K/Akt or EAK pathways, or that exert their function in parallel to both pathways.

We took two approaches to identifying *seak* mutants. The first approach, described in Chapter 4, was to take advantage of the fact that we isolated a strain of *eak-7;akt*-1 mutant animals that spontaneously lost its dauer arrest phenotype. Dauer arrest delays the onset of the reproductive period in *C. elegans*. Because of this delay in reaching sexual maturity, there is selection pressure on the population that favors the accumulation of spontaneous mutations which promote bypass of the dauer stage. Thus, isolation of a

strain that lost its arrest phenotype suggested to us that the strain acquired a *de novo* mutation that suppressed dauer, potentially in a gene whose activity was normally required to activate DAF-16/FoxO. We therefore pursued identification of the spontaneous *seak* mutations in the strain via whole-genome DNA sequencing. This analysis revealed a point mutation in the gene *gap-3*, a conserved Ras GTPase activating protein (RasGAP) orthologous to human RASA1, which is associated with the *seak* phenotype.

My studies of GAP-3 revealed that reducing its function suppresses phenotypes associated with DAF-16 activity, including dauer arrest and longevity. Interestingly, this trait is specific to *gap-3*, as mutation of neither *gap-1* nor *gap-2* (the other *C. elegans* RasGAPs) suppresses dauer or longevity. Moreover, *gap-3* loss-of-function is not phenocopied by a *let-60*/Ras gain-of-function mutation, which renders Ras insensitive to inactivation by GAP. Together, this suggests GAP-3 regulates DAF-16 independently of LET-60/Ras, potentially through a distinct small GTPase.

Our second approach to identifying novel DAF-16/FoxO activators (*seak* genes) was a forward genetic screen, described in Chapter 5. Based on the utility of our first approach which implicated *gap-3* as a *seak* gene, I pursued a pilot mutagenesis screen to uncover more *seak* genes. I screened approximately 1,200 haploid genomes and isolated sixteen independent *seak* mutants. Using whole-genome DNA sequencing, we identified all lesions in each mutant strain, and I used SNP mapping to rapidly locate the causative *seak* mutation in each. To date, I have characterized one *seak* mutant from the genetic screen, *dpy-21*, which encodes a conserved component of the *C. elegans* dosage compensation machinery.

Like *gap-3, dpy-21* is a *bona fide seak* gene as its mutation suppresses dauer arrest of *eak-7;akt-1* mutants. DPY-21 is a component of the dosage compensation complex (DCC) which functions to equate sex chromosome gene dosage between the sexes. Via RNAi-mediated knockdown of individual DCC components in hermaphrodite and male animals, I demonstrated that the dauer suppression phenotype of *dpy-21* mutants is due to

a defect in dosage compensation *per se*. Expression of several X-linked dauer regulatory genes that promote dauer bypass is elevated in *dpy-21* null animals, including four genes encoding components of the ILS pathway that antagonize DAF-16/FoxO activity. Accordingly, *dpy-21* mutation reduced the expression of DAF-16/FoxO target genes. This work establishes a post-embryonic function for dosage compensation and demonstrates that chromosome-wide regulation of gene expression can influence the developmental response of an organism to environmental cues.

The causative mutation remains to be identified in thirteen of the seak mutant strains; we believe *seak* gene identity and characterization will illuminate regulatory mechanisms controlling FoxO transcription factors that might be implicated in the pathogenesis of aging and age-associated disease.

Summary

In summary, little is known about the regulation of FoxO factors by components outside of the PI3kinase/Akt pathway. My thesis research provides important insights into alternative regulatory paradigms of FoxO control with the characterization of the *eak* genes and discovery of novel *seak* genes. These new paradigms may represent avenues amenable to pharmacologic intervention, providing potential therapeutic benefit for aging and age-associated disease.

Table of Contents

Dedication ii

Acknowledgements iii

Preface v

List of Figures xiv

List of Tables xvi

List of Supplemental Figures xvii

List of Supplemental Tables xviii

Chapter 1: Introduction 1

FoxO transcription factors 1

Regulation of FoxO by insulin/insulin-like signaling 2

Discovery of FoxO as a longevity promoting factor 3

FoxO in the control of mammalian aging 4

FoxO controls mammalian age-associated disease 4

Caenorhabditis elegans as a model to study FoxO 5

A genetic screen for molecules that regulate nuclear DAF-16/FoxO activity 11

Outstanding questions 14

References 15

Chapter 2: Functional divergence of dafachronic acid pathways in the control of *Caenorhabditis elegans* development and life span 21

Abstract 21

Introduction 22

Materials and Methods 25

Results 27

Discussion 37

Supplemental Material 41

References 47

Chapter 3: The influence of steroid hormone signaling on life span control by *Caenorhabditis elegans* insulin-like signaling 51

Abstract 51

Introduction 52

Materials and Methods 56

Results 58

Discussion 69

Supplemental Information 73

References 81

Chapter 4: The p120RasGAP family member GAP-3 is a novel regulator of dauer arrest and longevity in *Caenorhabditis elegans* 85

Abstract 85

Introduction 86

Materials and Methods 87

Results 89

Discussion 99

Supplemental Information 102

References 103

Chapter 5: Post-embryonic control of *Caenorhabditis elegans* DAF-2 insulin-like signaling by the conserved dosage compensation protein DPY-21 106

Abstract 106

Introduction 107

Materials and Methods 108

Results 113

Discussion 127

Supplemental Information 131

References 140

Chapter 6: Conclusions 146

HSD-1 and dafachronic acids 146

seak gene identification 149

SEAK screen methodology and findings 151

References 153

List of Figures

Figure 1.1: Lifecycle of *C. elegans*..... 7

Figure 1.2: Signaling pathways controlling dauer arrest. 8

Figure 2.1. Hypothetical model of dafachronic acid (DA) biosynthetic pathways. 23

Figure 2.2: HSD-1 regulation of dauer arrest. 30

Figure 2.3. HSD-1 regulation of DAF-16/FoxO target gene expression. 32

Figure 2.4 HSD-1 inhibits nuclear DAF-16/FoxO activity without promoting its translocation from the nucleus to the cytoplasm..... 34

Figure 2.5. Impact of *hsd-1* mutation on life span and gonadal migration. 36

Figure 2.6. Hypothetical models of insulin-like and DA pathways in the control of diapause, longevity, and gonadal migration. 39

Figure 3.1: Models of dafachronic acid (DA) biosynthetic pathways and DAF-12 complexes in the control of dauer arrest and life span..... 53

Figure 3.2: Modulation of life span by *daf-12(null)* mutation in animals with reduced DAF-2/InsR activity..... 61

Figure 3.3: Mutations that reduce DA biosynthesis promote dauer arrest and shorten life span in animals with reduced DAF-2/InsR signaling. 64

Figure 3.4: Unliganded DAF-12 influences life span in a context-dependent manner. ... 68

Figure 3.5: New functions of DAF-12 complexes in life span control. 72

Figure 4.1: *gap-3* is a *seak* gene..... 91

Figure 4.2: Genetic structure of *gap-1*, *gap-2*, and *gap-3*, the three putative RasGAPs encoded in the *C. elegans* genome. 91

Figure 4.3: *seak* activity is specific to *gap-3*. 94

Figure 4.4: *gap-3* inactivation partially suppresses life span extension of *eak-7;akt-1* mutant animals. 95

Figure 4.5*: gap-3(ga139)* mutation suppresses dauer arrest of *eak-7* single mutants but not of *akt-1(null)* nor TGFβ-like pathway mutants, *daf-8* and *daf-14*. 96

Figure 4.6: GAP-3 inactivation does not change DAF-16::GFP nuclear localization..... 97

Figure 4.7: An activating mutation in *let-60/Ras* that renders Ras insensitive to inactivation by GAP activity does not recapitulate *gap-3* loss-of-function mutations..... 98

Figure 5.1: *dpy-21* inactivation suppresses the dauer phenotype of *eak-7;akt-1* mutants. 115

Figure 5.2: DPY-21 is a general regulator of dauer arrest. 118

Figure 5.3: Dosage compensation influences dauer arrest..... 121

Figure 5.4: DPY-21 activates DAF-16/FoxO. 126

Figure 5.5: Model of DAF-2/IGFR pathway regulation by DPY-21..... 128

Figure 6.1: Revised model of dafachronic acid biosynthesis. 147

Figure 6.2: Hypothetical role of SEAK protein, suppressors of *eak-7;akt-1*..... 149

List of Tables

Table 1.1: Seven EAK proteins were identified from the *eak* screen. 12

Table 3.1: Summary of effects of *daf-12* and *daf-36* null mutations on life span in three contexts of DAF-16 activation. 69

Table 4.1: Candidate *seak* mutations. 90

List of Supplemental Figures

Supplemental Figure 2.1: Phylogenetic relationship among *C. elegans* and human 3βHSD family members. 42

Supplemental Figure 2.2: *hsd-1* cDNA structures. 42

Supplemental Figure 2.3: The *hsd-1* promoter drives expression specifically in the XXX cells. 44

Supplemental Figure 2.4: Dafachronic acid precursors rescue the dauer arrest phenotype of *hsd-1;akt-1* double mutants. 45

Supplemental Figure 2.5: Subcellular DAF-16::GFP localization. 45

Supplemental Figure 2.6: *hsd-1* mutants do not exhibit the gonadal migration (Mig) phenotype characteristic of other DA biosynthetic mutants. 46

Supplemental Figure 3.1: *daf-12* gene structure, transcripts, and relevant mutations. 73

Supplemental Figure 3.2: Larval arrest phenotypes of *daf-2;daf-12(null)* mutants. 73

Supplemental Figure 3.3: *daf-12(null)* does not cause an RNAi-defective phenotype. ... 74

Supplemental Figure 3.4: Enhancement of the dauer-constitutive phenotype *daf-2(e1368)* by mutations in genes encoding DA biosynthetic pathway components. 75

Supplemental Figure 4.1: *gap-3* RNAi does not suppress *eak-7;akt-1* dauer arrest. 102

Supplemental Figure 5.1: DPY-21 regulates dauer arrest. 131

Supplemental Figure 5.2: Representative images of animals exhibiting cytoplasmic and nuclear DAF-16A::GFP localization. 132

Supplemental Figure 5.3: X-linked and autosomal gene expression replicate data. 133

Supplemental Figure 5.4: DAF-16/FoxO target gene expression replicate data. 134

List of Supplemental Tables

Supplemental Table 3.1: Mutant alleles used in this study. 75

Supplemental Table 3.2: Life span and dauer statistics. 76

Supplemental Table 5.1: Raw data and statistics for dauer assays. 135

Supplemental Table 5.2: Primers used for real-time quantitative PCR. 138

Supplemental Table 5.3: Dosage compensation of X-linked dauer regulatory genes. ... 139

Chapter 1: Introduction

FoxO transcription factors

FoxO transcription factors translate environmental stimuli into gene expression programs that result in control of stress resistance, metabolism, and cell growth and proliferation. Thus, they play a key role in enabling the appropriate physiological response of an organism to its environment.

FoxO transcription factors belong to the conserved forkhead transcription superfamily; all members of this family are characterized by their forkhead box DNA binding domain (Kaestner et al., 2000). Forkhead transcription factors are conserved across animal phylogeny and are also present in fungi and yeast, but they are absent in plants (Mazet et al., 2003). In mammals, the FoxO subgroup of forkhead transcription factors has four members, FOXO1, FOXO3, FOXO4, and FOX6. *Caenorhabditis elegans* has only one FoxO ortholog, DAF-16. Likewise, *Drosophila* also has a single FoxO ortholog, dFOXO.

FoxO factors typically act as transcriptional activators but they can also repress transcription. FoxOs interact with DNA via their winged-helix DNA binding domain in the forkhead box of the protein. Specificity and targeting of FoxO factors to target genes occurs via presence of the core recognition motif, TTGTTTAC (Furuyama et al., 2000; Greer and Brunet, 2008). By controlling expression of many target genes, FoxO transcription factors promote a range of cellular responses including apoptosis, differentiation, cell cycle arrest, and resistance to oxidative stress. At an organismal level, the integration of FoxO-dependent cellular responses results in promotion of development, metabolism, tumor suppression, and longevity.

Regulation of FoxO by insulin/insulin-like signaling

Mammalian FoxO transcription factors are negatively regulated by insulin and insulin-like growth factor signaling (ILS), via signaling through the phosphoinositide 3-kinase (PI3kinase)/protein kinase B (Akt) pathway. Insulin and insulin-like growth factor exert their effects by binding to their respective receptor tyrosine kinase, the insulin receptor or the insulin-like growth factor receptor (Ullrich et al., 1985, 1986). In response to engagement of receptor by ligand, the intrinsic tyrosine kinase activity of the receptor is activated, triggering a phosphorylation cascade. The active receptor phosphorylates its substrate proteins, which include insulin receptor substrate (IRS) proteins and subsequently PI3kinase. Activated PI3kinase phosphorylates phosphatidylinositol (4,5)-bisphosphate (PIP_2) in the plasma membrane, converting it to phosphatidylinositol (3,4,5)-trisphosphate (PIP_3) (Vanhaesebroeck and Alessi, 2000). PIP_3 serves as a recruitment signal for other downstream kinases. The pleckstrin homology domains of phosphoinositide-dependent kinase (PDK) and Akt cause their recruitment to PIP_3 in the plasma membrane. Once co-located at the plasma membrane, PDK phosphorylates Akt on threonine 308 which resides within the activation loop. Subsequently other kinases phosphorylate Akt on a second site, serine 473 in the C-terminal hydrophobic motif of the protein. Phosphorylation of Akt on both residues results in maximal activation of the kinase. Activated Akt translocates through the cytosol to the nucleus, allowing it to phosphorylate its substrate proteins in both compartments (Andjelković et al., 1997). Akt has numerous substrate proteins whose activities collectively allow Akt to promote cell survival, proliferation, and growth; FoxO transcription factors are substrates of Akt.

Active Akt promotes the phosphorylation of FoxO on three consensus phosphorylation sites that are conserved from nematodes to mammals (Greer and Brunet, 2009). Akt directly phosphorylates FoxO on a gatekeeper phosphorylation site, thereby promoting phosphorylation of the other two sites. This phosphorylation results in recognition of FoxO by 14-3-3 chaperone proteins, which then bind to FoxO. 14-3-3 binding to FoxO both exposes a nuclear export sequence (Brunet et al., 2002) and obscures a nuclear localization sequence on FoxO (Obsilova et al., 2005). As a result, phosphorylated FoxO and associated 14-3-3 are exported from the nucleus and FoxO is sequestered in the

cytoplasm. Moreover, ubiquitin-mediated proteasomal degradation of FoxO protein is triggered by Akt phosphorylation (Huang et al., 2005; Calnan and Brunet, 2008), reinforcing the inhibition of FoxO by ILS. Signaling through InsR/PI3kinase/Akt is inhibited by the activity of phosphatase and tensin homolog (PTEN) (Stambolic et al., 1998). PTEN converts PIP_3 back to PIP_2, thereby reversing the effect of PI3kinase. In this way, PTEN activity promotes the activation of FoxO.

In summary, activation of ILS results in phosphorylation of FoxO and subsequent redistribution of the transcription factor to the cytoplasm. Once sequestered in the cytosol, FoxOs are unable to carry out transactivation of gene expression and the cytoplasmic pool of the protein is degraded. Thus, signaling through PI3kinase and Akt inhibits FoxO activity principally through its nuclear exclusion, but also by promoting degradation of FoxO protein.

Discovery of FoxO as a longevity promoting factor

Work in *C. elegans* first revealed that FoxO is a critical longevity factor. Investigation of a panel of mutants that constitutively entered an alternative, long-lived larval stage known as dauer arrest facilitated the discovery that mutations in the gene *daf-2* increase adult life span two-fold. Moreover, this *daf-2* mutant longevity completely required the activity of a second gene, *daf-16* (Kenyon et al., 1993). It was subsequently discovered that *daf-2* encodes the *C. elegans* ortholog of the insulin and insulin-like growth factor receptor (InsR) (Kimura et al., 1997), and *daf-16* encodes the *C. elegans* FoxO ortholog (Lin et al., 1997; Ogg et al., 1997). Ensuing studies illustrated that over-expression of wild-type FoxO can extend life span in both worms and flies (Henderson and Johnson, 2001; Giannakou et al., 2004; Hwangbo et al., 2004). Collectively, this work demonstrated that a mutation in a single gene, the insulin/insulin-like growth factor receptor, was capable of extending organismal life span. Moreover, it revealed that FoxO is a key regulator of the transcriptional outputs of ILS. These discoveries suggested for the first time that the insulin signaling axis, through its interaction with FoxO transcription factors, might play a role in regulating the aging process in higher organisms.

FoxO in the control of mammalian aging

It remains an open question as to whether FoxO transcription factors regulate life span in humans. As in model organisms, the reduction of ILS also promotes longevity in mammals (Blüher et al., 2003; Holzenberger et al., 2003; Taguchi et al., 2007), but it is not yet known whether this life span extension requires FoxO transcription factors. Interestingly, recent studies have identified specific FoxO polymorphisms that are associated with extreme longevity in multiple cohorts of humans (Lunetta, 2007; Willcox et al., 2008; Anselmi, 2009; Flachsbart et al., 2009; Li, 2009; Pawlikowska, 2009). Together, this evidence is suggestive of the possibility that FoxO transcription factors might in fact play a role in longevity control in humans, as is the case in worms and flies.

FoxO controls mammalian age-associated disease

While a direct connection between mammalian FoxO transcription factors and life span control has not been established experimentally, recent work in conditional knockout mice supports a role for FoxO in modulating phenotypes that are reminiscent of aging-associated diseases in humans, including cancer, osteoporosis, and diabetes. Studies in mice illustrate that mammalian FoxOs function as tumor suppressors with the finding that loss of FoxO1, FoxO3, and FoxO4 in adults results in a cancer-prone phenotype characterized by thymic lymphomas and hemangiomas (Paik et al., 2007). Furthermore, deletion of FoxO factors in mouse osteoblasts results in reduced bone mass secondary to increased osteoblast apoptosis (Ambrogini et al., 2010; Rached et al., 2010), suggesting that FoxO transcription factors are protective against osteoporosis. In contrast to these apparent beneficial effects of FoxO, FoxO1 can contribute to metabolic dysregulation similar to that observed in Type 2 diabetes; FoxO1 haploinsufficiency protects mice against insulin resistance induced by a high-fat diet (Nakae et al., 2003), and both liver-specific and osteoblast-specific FoxO1 deletion ameliorate glucose intolerance in mouse models of insulin resistance (Matsumoto et al., 2007; Dong et al., 2008; Rached et al., 2010). Thus, in mammals, FoxO transcription factors have context-dependent effects on the development of phenotypes associated with age-related disease. Elucidating the regulatory mechanisms that maintain the balance of FoxO transcription factor activity

may prove to be crucial for understanding and combating the progression of age-related disease.

Caenorhabditis elegans as a model to study FoxO

Caenorhabditis elegans is an excellent model system for revealing and dissecting the signaling networks that control the activity of FoxO transcription factors. In addition to being the system in which the life span promoting function of FoxO was first discovered, there are several advantages to using *C. elegans* as a model system. First, the key molecules and pathways implicated in mammalian FoxO regulation have orthologs in *C. elegans* (Taniguchi et al., 2006). Secondly, the *C. elegans* system is simplified in that there is only one FoxO transcription factor, DAF-16, compared to four FoxO factors in mammals, as well as one InsR, in contrast to multiple mammalian insulin and insulin-like receptors. Importantly, in contrast to early embryonic lethality of total FoxO deletion in mice (Greer and Brunet, 2008), the *C. elegans daf-16 null* mutant is viable, facilitating genetic analysis. Moreover, in addition to regulating longevity, the *C. elegans* ILS pathway and DAF-16/FoxO control a well characterized, easily observable developmental phenotype known as dauer arrest. These facts, combined with the experimental manipulability and relatively short, approximately two-week life span of the organism, make *C. elegans* a well suited tool for the rapid identification and characterization of novel regulators of FoxO transcription factors.

Dauer arrest

In favorable environments, *C. elegans* larvae develop through four larval stages, becoming reproductively competent adults in approximately two days. When faced with adverse environmental conditions such as high population density, elevated temperatures or food scarcity, larvae undergo an alternative developmental pathway and enter a persistent larval stage known as dauer arrest (Figure 1.1). Dauer larvae are morphologically distinct from their non-arrested L3 counterparts and have undergone a series of physiologic changes that make them extremely stress resistant and long lived. Animals can remain in the dauer stage for several months. When dauer larvae encounter a

favorable environment, they rapidly exit the dauer stage and resume reproductive development at the L4 stage.

Dissection of the genetics of the dauer formation phenotype led to the identification of many genes responsible for regulating dauer formation, known as *daf* genes (abnormal DAuer Formation). Characterization of *daf* genes revealed four conserved signaling pathways which control dauer formation (Figure 1.2); a guanylyl cyclase/cGMP sensing pathway defined by dauer-constitutive (daf-c) mutants *daf-11* and *daf-21* (Figure 1.2A); a TGFβ-like pathway defined by daf-c mutants *daf-1, daf-4, daf-7, daf-8,* and *daf-14* (Figure 1.2B); the ILS pathway defined by daf-c mutant, InsR ortholog *daf-2,* and dauer-defective (daf-d) mutants PTEN ortholog *daf-18* and *daf-16/*FoxO (Figure 1.2C); and a hormonal signaling pathway defined by daf-c mutants *daf-36* and *daf-9,* each encoding enzymes involved in biosynthesis of steroid hormones known as dafachronic acids (DAs), and daf-d mutant *daf-12*, which encodes a nuclear hormone receptor that is the target of the DAs (Figure 1.2D) (Riddle et al., 1981; Vowels and Thomas, 1992; Gottlieb and Ruvkun, 1994; Gerisch et al., 2001; Jia et al., 2002; Motola et al., 2006). Genetic analysis of the dauer pathways indicate that DAF-16 acts downstream of the ILS pathway, and this pathway functions in parallel to the guanylyl cyclase/TGFβ pathways (Thomas et al., 1993; Gottlieb and Ruvkun, 1994). The hormonal DA/DAF-12 pathway functions downstream of all other dauer pathways; however there is some evidence to suggest that DAF-12 may also function in parallel to the ILS pathway and DAF-16/FoxO (Vowels and Thomas, 1992; Larsen et al., 1995; Dumas et al., 2010). Together, the dauer signaling pathways integrate environmental stimuli and coordinate an appropriate organism-wide physiologic response, promoting reproductive development when conditions are replete and triggering arrest when conditions are adverse.

The elucidation of *daf* genes led to the first identification of the ILS pathway in *C. elegans* and facilitated the discovery of DAF-2/InsR and DAF-16/FoxO as longevity regulators. Because of the enhanced longevity of dauer animals, the *daf* genes were used for the initial life span extension screens, resulting in the previously mentioned discovery that *daf-2* mutation extends life span. Investigation of dauer arrest in *C. elegans* therefore

directly facilitated the discovery DAF-16/FoxO as a key longevity promoting factor. Building on this initial work, dauer arrest remains a convenient phenotype for dissection of DAF-16/FoxO regulation. Loss-of-function mutation of *daf-16* renders animals dauer-defective, indicating DAF-16/FoxO activity is required for arrest. Because of this, dauer arrest can be used as a surrogate phenotype for DAF-16/FoxO activation, providing an experimental avenue for identification of novel FoxO regulators. It is noteworthy that each of the signaling pathways controlling dauer also impinges on adult longevity regulation in *C. elegans*, suggesting that novel DAF-16/FoxO regulators uncovered in the context of dauer arrest are likely to also be regulators of life span.

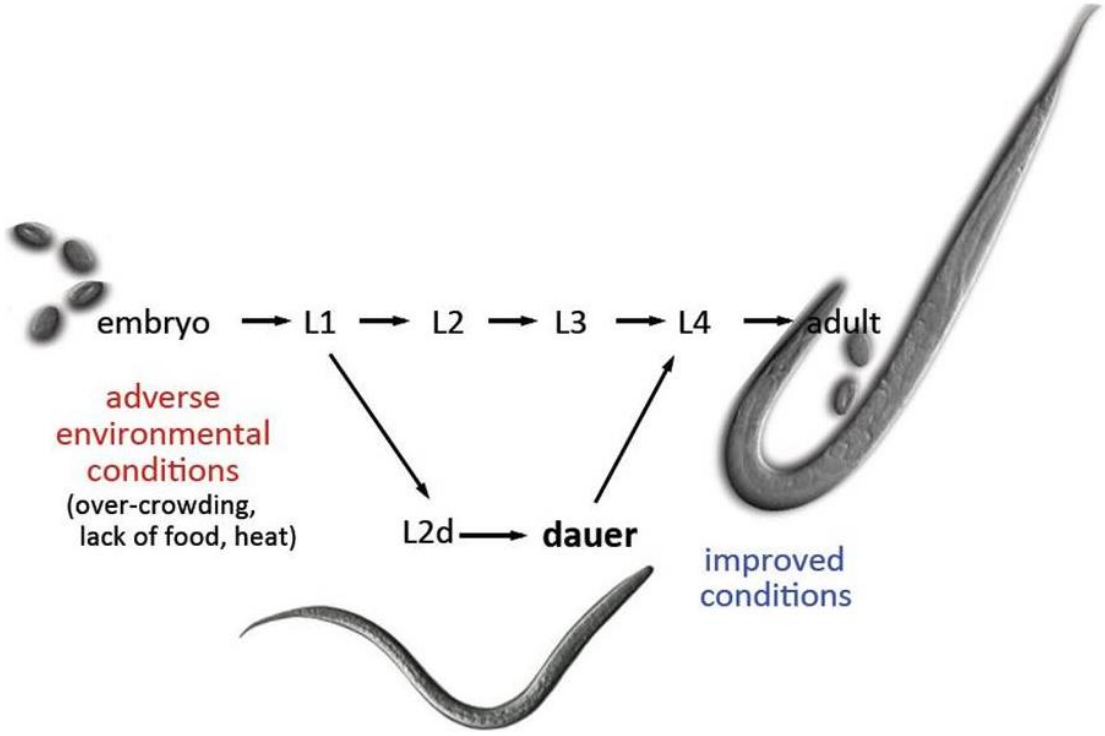

Figure 1.1: Lifecycle of *C. elegans*.

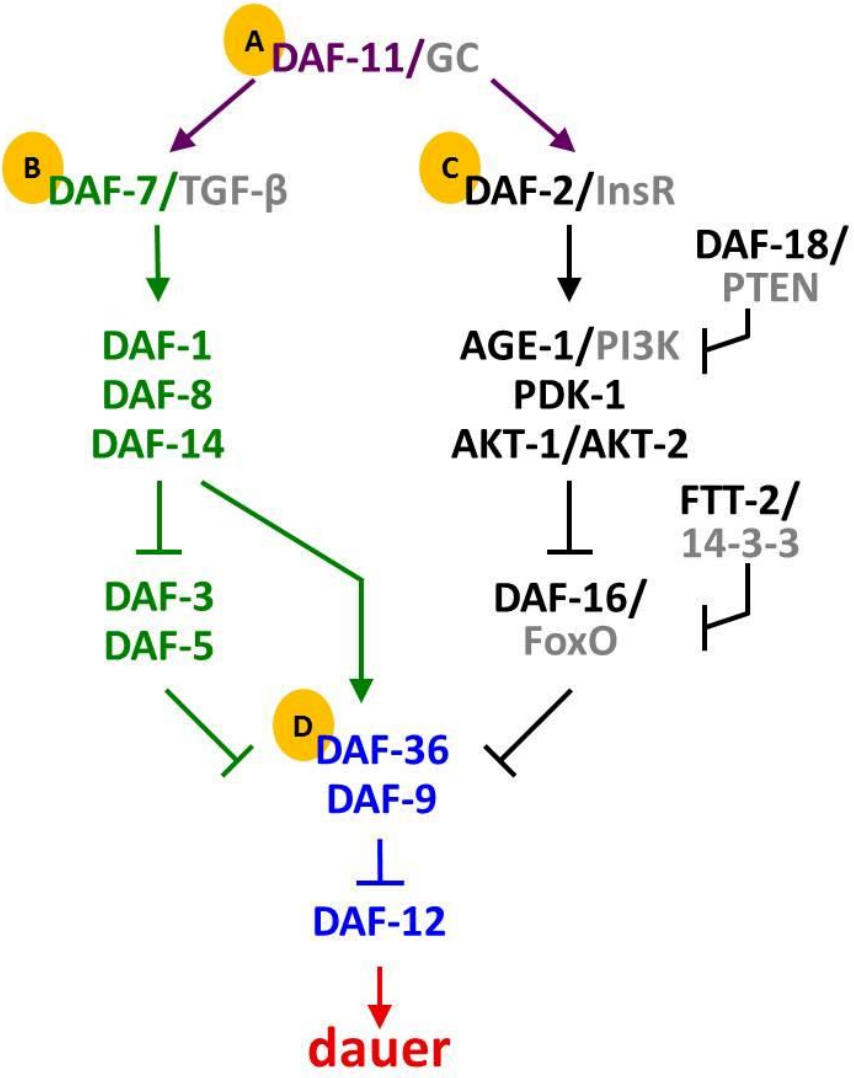

Figure 1.2: Signaling pathways controlling dauer arrest.
(A.) A guanylyl cyclase pathway, (B.) TGFβ-like pathway, (C.) Insulin/insulin-like signaling pathway, and (D.) a steroid hormone pathway regulate dauer arrest.

Known inputs to *C. elegans* DAF-16/FoxO regulation

Since its initial discovery as a critical longevity promoting factor, much work has focused on identifying and characterizing the regulatory inputs controlling the activity of DAF-16/FoxO, resulting in the elucidation of a network of factors involved in controlling activity of the transcription factor. In *C. elegans*, as in mammals, DAF-16/FoxO is regulated canonically by the insulin/insulin-like signaling pathway. Activation of DAF-

2/InsR triggers a PI3kinase/PDK/Akt signaling cascade resulting in the phosphorylation of DAF-16/FoxO (Lee et al., 2001; Lin et al., 2001), which causes the cytoplasmic sequestration of DAF-16/FoxO through its direct association with the 14-3-3 protein, FTT-2 (Berdichevsky et al., 2006; Li et al., 2007). PI3kinase is encoded by *C. elegans age-1*, the catalytic subunit, and *aap-1*, which encodes the adaptor subunit. Two Akt orthologs are responsible for inhibitory phosphorylation of DAF-16/FoxO, AKT-1 and AKT-2. Both AKT-1 and AKT-2 are widely expressed in *C. elegans* and they are activated by phosphorylation on sites corresponding to threonine 308 and serine 473 in mammalian Akt (Paradis and Ruvkun, 1998). AKT-2 appears to play a lesser role in DAF-16/FoxO regulation than AKT-1, as phenotypes associated with *akt-2* loss-of-function mutation are weaker than those associated with *akt-1* loss-of-function mutation (Paradis and Ruvkun, 1998; Hertweck et al., 2004; Quevedo et al., 2007). Additionally, ablation of *akt*-1 is sufficient to drive GFP tagged DAF-16 into the nucleus; however AKT-2 does not significantly influence DAF-16 localization (Hertweck et al., 2004).

In addition to the ILS pathway, a second pathway in *C. elegans* governs longevity via regulation of DAF-16 nuclear localization. Building on the finding that DAF-2/InsR mutation significantly extends *C. elegans* life span, subsequent work showed that removing the germline also results in life span extension in a DAF-16/FoxO dependent manner (Hsin and Kenyon, 1999). When the germline is ablated, DAF-16/FoxO translocates to the nucleus of intestinal cells (Lin et al., 2001), suggesting the germline normally produces an endocrine signal that promotes the cytoplasmic sequestration of intestinal DAF-16/FoxO. Interestingly, the somatic gonad is required for germline removal to extend life span, as animals lacking both the somatic gonad and the germline are not long lived (Hsin and Kenyon, 1999). This suggests that in addition to the FoxO-inhibitory signal from the germline, there is also a life span-promoting signal emanating from the somatic gonad. The nature of the endocrine signals deriving from the germline and the somatic gonad is not well understood; however, dafachronic acids (DAs), sterol ligands for the nuclear hormone receptor DAF-12, are likely involved (Yamawaki et al., 2010).

The mechanisms by which the ILS pathway and the germline control DAF-16/FoxO subcellular localization are distinct. The germline signal likely acts in parallel to ILS pathway activity, as germline removal further extends life span of animals with reduced ILS (Hsin and Kenyon, 1999). However, the consequence of germline removal in the context of *daf-2/InsR null* mutation is unknown; *daf-2 null* mutants arrest non-conditionally and do not reach adulthood, precluding the assessment of adult life span in the total absence of DAF-2/InsR. In contrast to ILS, DAF-16/FoxO nuclear localization as a result of germline removal requires activity of the nuclear hormone receptor DAF-12 and the presence of its ligands, DAs (Berman and Kenyon, 2006; Motola et al., 2006; Yamawaki et al., 2010). DAF-16/FoxO nuclear localization in the absence of the germline also requires the conserved protein KRI-1; however KRI-1 is dispensable for DAF-16/FoxO nuclear accumulation in the absence of ILS (Berman and Kenyon, 2006).

Together, this evidence supports the paradigm of endocrine regulation of DAF-16/FoxO by controlling its subcellular localization. Nuclear exclusion inhibits the activity of the transcription factor whereas, in the absence of an inhibitory signal (either ILS or signals from the germline), DAF-16/FoxO translocates to the nucleus where it can activate its transcriptional programs.

Paradigm shift: What controls nuclear DAF-16/FoxO?

Although nuclear localization of DAF-16/FoxO is clearly necessary for DAF-16/FoxO-dependent life span extension, multiple lines of evidence indicate that it is not sufficient for full DAF-16/FoxO activation. For example, reducing the activity of the 14-3-3 protein FTT-2 by RNAi mediated knock-down results in nuclear accumulation of DAF-16/FoxO but does not cause dauer arrest in wild-type animals (Li et al., 2007; Alam et al., 2010). Moreover, mutation of the consensus AKT phosphorylation sites on DAF-16/FoxO results in protein that is constitutively nuclear, but is not fully active (Lin et al., 2001).

In addition to nuclear localization being insufficient for full activation of DAF-16/FoxO, at least two findings support the existence of DAF-16/FoxO regulatory components

distinct from PI3kinase/Akt. First, partial loss-of-function mutation in *daf-18*/PTEN suppresses dauer arrest of *age-1*/PI3kinase mutants but does not suppress arrest of *daf-2*/InsR loss-of-function mutants (Gil et al., 1999). Second, *pdk-1* and *akt-1* activating mutations suppress *age-1*/PI3kinase mutant dauer arrest to a greater extent than they suppress *daf-2*/InsR mutant dauer arrest (Paradis and Ruvkun, 1998; Paradis et al., 1999).

Together, this evidence suggests that there is likely a signal that controls DAF-16/FoxO activity independently of PI3kinase, perhaps acting on the nuclear pool of the protein. The biologic importance of FoxO, together with the dearth of knowledge regarding what might control its activity once in the nucleus, prompted an attempt to uncover components of this parallel regulatory pathway.

A genetic screen for molecules that regulate nuclear DAF-16/FoxO activity

To identify components of the regulatory pathway acting on the nuclear pool of DAF-16/FoxO, a genetic screen was undertaken that exploited the fact that DAF-16/FoxO activity promotes dauer arrest. The screen was designed to uncover mutants that enhance the weak dauer-constitutive phenotype of an *akt-1* null mutant (*eak* screen, enhancer of *akt-1*). As mentioned previously, *akt-1* null mutation promotes nuclear localization of DAF-16/FoxO, potentiating its activation. However, *akt-1* null mutant animals develop reproductively at the elevated temperature of 25°C and do not arrest as dauer larvae, indicating DAF-16/FoxO is not fully active in the context of AKT-1 absence. *akt-1* null animals were subjected to mutagenesis and animals that subsequently arrested as a dauer larvae at 25°C in a *daf-16*-dependent manner were selected as harboring an *eak* mutation, as they likely acquired a mutation that causes the activation of DAF-16/FoxO. *eak* genes therefore encode molecules that normally function to inhibit the activity of nuclear DAF-16/FoxO.

Characterization of the EAK pathway

The *eak* screen identified twenty-one independent mutants that define seven *eak* genes, five of which have been cloned prior to this work (see Table 1.1) (Hu et al., 2006; Zhang

et al., 2008; Alam et al., 2010). The phenotypic similarity of all *eak* single mutants and the observation that no *eak;eak* double mutant combination tested to date exhibits phenotypic enhancement compared to *eak* single mutants indicate that the EAK proteins are components of a single pathway. EAK proteins and AKT-1 both control DAF-16/FoxO target gene expression. However, in contrast to AKT-1, EAK proteins inhibit nuclear DAF-16/FoxO activity without influencing its subcellular localization (Zhang et al., 2008; Alam et al., 2010). The precise mechanism by which EAK proteins inhibit nuclear DAF-16/FoxO remains elusive.

Gene	Predicted product	Human ortholog	Expression pattern
eak-1	?	?	?
eak-2	?	?	XXX cells
eak-3	N-myristoylated protein	?	XXX cells
eak-4	N-myristoylated protein	?	XXX cells
eak-5	*sdf-9*	?	XXX cells
eak-6	Protein tyrosine phosphatase	?	XXX cells[1]
eak-7	N-myristoylated TLDc protein	KIAA1609	XXX cells, neurons, intestine, other tissues

Table 1.1: Seven EAK proteins were identified from the *eak* screen.
[1]*eak-6* is also expressed in the M1 pharyngeal motor neuron.

The expression pattern of the *eak* genes provides some clues as to their function. Strikingly, of the cloned *eak* genes, all but *eak-7* are expressed exclusively in the two neuroendocrine XXX cells (Hu et al., 2006; Zhang et al., 2008; Alam et al., 2010). Interestingly, the XXX cells do not express DAF-16/FoxO (Hu et al., 2006), suggesting the *eak* genes encode molecules with endocrine activity. The XXX cells play a known role in dauer arrest; laser ablation of both XXX cells results in dauer arrest (Ohkura et al., 2003), and the cells are the site of synthesis of DAs, the steroid hormone ligands for the nuclear hormone receptor DAF-12 (Ohkura et al., 2003; Motola et al., 2006). In the

presence of DAs, DAF-12 promotes bypass of dauer arrest (Motola et al., 2006). Collectively, this indicates the XXX cells normally function to inhibit dauer, likely through the production of DAs. Based on their expression in the XXX cells and epistasis to DA biosynthesis enzyme *daf-9*, the XXX-specific EAKs are thought to potentiate DA synthesis or secretion (Hu et al., 2006; Zhang et al., 2008).

In contrast to other *eak* genes, *eak-7* is expressed in multiple tissues in the worm, including tissues which also express *daf-16*/FoxO (Alam et al., 2010). Additionally, unlike the other *eak* genes, *eak-7* loss-of-function mutation results in a longevity phenotype. *eak-7* mutants live approximately 25% longer than wild-type animals, and this life span extension requires DAF-16/FoxO as well as the DAF-16/FoxO cofactors HSF-1 and SMK-1 (Alam et al., 2010). *eak-7* mutation strongly enhances life span extension in animals lacking a germline (Alam et al., 2010), indicating that EAK-7 functions in parallel to signals from the reproductive system to regulate DAF-16/FoxO and longevity.

Based on its presence in the same cells as DAF-16/FoxO and the strength of its phenotypes, EAK-7 is likely the most downstream component of the known EAK pathway proteins. Nevertheless, how EAK-7 controls nuclear DAF-16/FoxO activity remains unclear. The structure of EAK-7 provides few clues as to its function; it contains a consensus N-myristoylation (N-myr) motif and a TLDc (*T*BC- and *L*ysM-*d*omain-*c*ontaining) domain, the function of which is poorly understood. The N-myr motif likely targets EAK-7 to the plasma membrane, as a functional EAK-7::GFP fusion protein localizes to the plasma membrane and does not appear to translocate in adult animals (Alam et al., 2010). Thus, EAK-7 likely regulates nuclear DAF-16/FoxO activity indirectly. Interestingly, *eak-7* mutation increases steady-state DAF-16/FoxO protein levels in *akt-1* mutants without altering *daf-16/FoxO* transcript levels (Alam et al., 2010), suggesting that EAK-7 may modulate DAF-16/FoxO synthesis or turnover.

Collectively, the EAK proteins define a novel, conserved endocrine pathway that acts in parallel to PI3kinase/Akt and the germline to regulate the activity of nuclear DAF-

16/FoxO. Continued investigation of the *C. elegans* EAK pathway promises to reveal new insights into mechanisms of FoxO regulation. In light of the potential role of FoxO transcription factors in mammalian aging and the pathogenesis of aging-associated diseases, EAK proteins could emerge as promising targets for the development of new drugs to treat Type 2 diabetes, cancer, and osteoporosis.

Outstanding questions

The following unresolved question provides the *raison d'être* of this dissertation: How does the EAK pathway inhibit the activity DAF-16/FoxO? Several independent lines of inquiry address this question and comprise the subsequent chapters of this dissertation. First, elucidation of the uncloned *eaks* may shed light on the function of the entire pathway; as such, in Chapter 2, this dissertation takes up the question, what is the nature of *eak-2*, and by what mechanism does it inhibit DAF-16 FoxO? Second, the evidence outlined above indicates the steroid hormone pathway defined by DA and DAF-12 influence DAF-16/FoxO phenotypes and might represent a mechanism of action of the EAKs. This dissertation pursues this hypothesis by investigating the role of the steroid hormone pathway in the control of DAF-16/FoxO-dependent longevity, as described in Chapter 3. Lastly, an approach to uncover new molecules required to confer EAK inhibitory signal to DAF-16/FoxO is described, along with preliminary findings, in Chapter 4 and Chapter 5. In sum, this work sheds light on novel regulators of FoxO transcription factors, and expands our understanding of FoxO regulation beyond its canonical control by PI3kinase/Akt signaling.

References

Alam, H., Williams, T.W., Dumas, K.J., Guo, C., Yoshina, S., Mitani, S., and Hu, P.J. (2010). EAK-7 Controls Development and Life Span by Regulating Nuclear DAF-16/FoxO Activity. Cell Metabolism *12*, 30–41.

Ambrogini, E., Almeida, M., Martin-Millan, M., Paik, J.-H., DePinho, R.A., Han, L., Goellner, J., Weinstein, R.S., Jilka, R.L., O'Brien, C.A., et al. (2010). FoxO-Mediated Defense against Oxidative Stress in Osteoblasts Is Indispensable for Skeletal Homeostasis in Mice. Cell Metabolism *11*, 136–146.

Andjelković, M., Alessi, D.R., Meier, R., Fernandez, A., Lamb, N.J., Frech, M., Cron, P., Cohen, P., Lucocq, J.M., and Hemmings, B.A. (1997). Role of translocation in the activation and function of protein kinase B. The Journal of Biological Chemistry *272*, 31515–31524.

Anselmi, C. V (2009). Association of the FOXO3A locus with extreme longevity in a southern Italian centenarian study. Rejuvenation Res. *12*, 95–104.

Berdichevsky, A., Viswanathan, M., Horvitz, H.R., and Guarente, L. (2006). C. elegans SIR-2.1 Interacts with 14-3-3 Proteins to Activate DAF-16 and Extend Life Span. Cell *125*, 1165–1177.

Berman, J.R., and Kenyon, C. (2006). Germ-Cell Loss Extends C. elegans Life Span through Regulation of DAF-16 by kri-1 and Lipophilic-Hormone Signaling. Cell *124*, 1055–1068.

Blüher, M., Kahn, B.B., and Kahn, C.R. (2003). Extended longevity in mice lacking the insulin receptor in adipose tissue. Science (New York, N.Y.) *299*, 572–574.

Brunet, A., Kanai, F., Stehn, J., Xu, J., Sarbassova, D., Frangioni, J. V, Dalal, S.N., DeCaprio, J.A., Greenberg, M.E., and Yaffe, M.B. (2002). 14-3-3 transits to the nucleus and participates in dynamic nucleocytoplasmic transport. The Journal of Cell Biology *156*, 817–828.

Calnan, D.R., and Brunet, a (2008). The FoxO code. Oncogene *27*, 2276–2288.

Dong, X.C., Copps, K.D., Guo, S., Li, Y., Kollipara, R., DePinho, R.A., White, M.F., and Dong XC Guo S, Li Y, Kollipara R, DePinho RA, White MF, C.K.D. (2008). Inactivation of hepatic Foxo1 by insulin signaling is required for adaptive nutrient homeostasis and endocrine growth regulation. Cell Metabolism *8*, 65–76.

Dumas, K.J., Guo, C., Wang, X., Burkhart, K.B., Adams, E.J., Alam, H., and Hu, P.J. (2010). Functional divergence of dafachronic acid pathways in the control of C. elegans development and lifespan. Developmental Biology *340*, 605–612.

Flachsbart, F., Caliebe, A., Kleindorp, R., BlanchÃ©, Hã©., Von Eller-Eberstein, H., Nikolaus, S., Schreiber, S., and Nebel, A. (2009). Association of FOXO3A variation with human longevity confirmed in German centenarians. Proceedings of the National Academy of Sciences *106*, 2700–2705.

Furuyama, T., Nakazawa, T., Nakano, I., and Mori, N. (2000). Identification of the differential distribution patterns of mRNAs and consensus binding sequences for mouse DAF-16 homologues. Biochem. J. *349*, 629–634.

Gerisch, B., Weitzel, C., Kober-Eisermann, C., Rottiers, V., and Antebi, A. (2001). A Hormonal Signaling Pathway Influencing C. elegans Metabolism, Reproductive Development, and Life Span. Developmental Cell *1*, 841–851.

Giannakou, M.E., Goss, M., Jünger, M.A., Hafen, E., Leevers, S.J., and Partridge, L. (2004). Long-lived Drosophila with overexpressed dFOXO in adult fat body. Science (New York, N.Y.) *305*, 361.

Gil, E.B., Malone Link, E., Liu, L.X., Johnson, C.D., and Lees, J.A. (1999). Regulation of the insulin-like developmental pathway of Caenorhabditis elegans by a homolog of the PTEN tumor suppressor gene. Proceedings of the National Academy of Sciences of the United States of America *96*, 2925–2930.

Gottlieb, S., and Ruvkun, G. (1994). daf-2, daf-16 and daf-23: Genetically Interacting Genes Controlling Dauer Formation in Caenorhabditis elegans. Genetics *137*, 107–120.

Greer, E.L., and Brunet, A. (2008). FOXO transcription factors in ageing and cancer. Acta Physiologica (Oxford, England) *192*, 19–28.

Greer, E.L., and Brunet, A. (2009). Different dietary restriction regimens extend lifespan by both independent and overlapping genetic pathways in C. elegans. Aging Cell *8*, 113–127.

Henderson, S.T., and Johnson, T.E. (2001). daf-16 integrates developmental and environmental inputs to mediate aging in the nematode Caenorhabditis elegans. Current Biology *11*, 1975–1980.

Hertweck, M., Göbel, C., and Baumeister, R. (2004). C. elegans SGK-1 Is the Critical Component in the Akt/PKB Kinase Complex to Control Stress Response and Life Span. Developmental Cell *6*, 577–588.

Holzenberger, M., Dupont, J., Ducos, B., Leneuve, P., Géloën, A., Even, P.C., Cervera, P., and Le Bouc, Y. (2003). IGF-1 receptor regulates lifespan and resistance to oxidative stress in mice. Nature *421*, 182–187.

Hsin, H., and Kenyon, C. (1999). Signals from the reproductive system regulate the lifespan of C. elegans. Nature *399*,.

Hu, P.J., Xu, J., and Ruvkun, G. (2006). Two Membrane-Associated Tyrosine Phosphatase Homologs Potentiate C. elegans AKT-1/PKB Signaling. PLoS Genet *2*, e99.

Huang, H., Regan, K.M., Wang, F., Wang, D., Smith, D.I., Van Deursen, J.M., and Tindall, D.J. (2005). Skp2 inhibits FOXO1 in tumor suppression through ubiquitin-mediated degradation. Proceedings of the National Academy of Sciences of the United States of America *102*, 1649–1654.

Hwangbo, D.S., Gershman, B., Tu, M.P., Palmer, M., and Tatar, M. (2004). Drosophila dFOXO controls lifespan and regulates insulin signalling in brain and fat body. Nature *429*, 562–566.

Jia, K., Albert, P.S., and Riddle, D.L. (2002). DAF-9, a cytochrome P450 regulating C. elegans larval development and adult longevity. Development *129*, 221–231.

Kaestner, K.H., Knochel, W., and Martinez, D.E. (2000). Unified nomenclature for the winged helix/forkhead transcription factors. Genes & Dev. *14*, 142–146.

Kenyon, C., Chang, J., Gensch, E., Rudner, A., and Tabtiang, R.A. (1993). C. elegans mutant that lives twice as long as wild type. Nature *366*, 461–464.

Kimura, K.D., Tissenbaum, H.A., Liu, Y., and Ruvkun, G. (1997). daf-2, an Insulin Receptor-Like Gene That Regulates Longevity and Diapause in Caenorhabditis elegans. Science *277*, 942–946.

Larsen, P.L., Albert, P.S., and Riddle, D.L. (1995). Genes that regulate both development and longevity in Caenorhabditis elegans. Genetics *139*, 1567–1583.

Lee, R.Y.N., Hench, J., and Ruvkun, G. (2001). Regulation of C. elegans DAF-16 and its human ortholog FKHRL1 by the daf-2 insulin-like signaling pathway. Current Biology *11*, 1950–1957.

Li, J., Tewari, M., Vidal, M., and Lee, S.S. (2007). The 14-3-3 protein FTT-2 regulates DAF-16 in Caenorhabditis elegans. Developmental Biology *301*, 82–91.

Li, Y. (2009). Genetic association of FOXO1A and FOXO3A with longevity trait in Han Chinese populations. Hum. Mol. Genet. *18*, 4897–4904.

Lin, K., Dorman, J.B., Rodan, A., and Kenyon, C. (1997). daf-16: An HNF-3/forkhead family member that can function to double the life-span of Caenorhabditis elegans. Science *278*, 1319–1322.

Lin, K., Hsin, H., Libina, N., and Kenyon, C. (2001). Regulation of the Caenorhabditis elegans longevity protein DAF-16 by insulin/IGF-1 and germline signaling. Nat Genet *28*, 139–145.

Lunetta, K.L. (2007). Genetic correlates of longevity and selected age-related phenotypes: a genome-wide association study in the Framingham Study. BMC Med. Genet. *8*, S13.

Matsumoto, M., Pocai, A., Rossetti, L., DePinho, R.A., and Accili, D. (2007). Impaired Regulation of Hepatic Glucose Production in Mice Lacking the Forkhead Transcription Factor Foxo1 in Liver. Cell Metabolism *6*, 208–216.

Mazet, F., Yu, J.-K., Liberles, D. a., Holland, L.Z., and Shimeld, S.M. (2003). Phylogenetic relationships of the Fox (Forkhead) gene family in the Bilateria. Gene *316*, 79–89.

Motola, D.L., Cummins, C.L., Rottiers, V., Sharma, K.K., Li, T., Li, Y., Suino-Powell, K., Xu, H.E., Auchus, R.J., Antebi, A., et al. (2006). Identification of ligands for DAF-12 that govern dauer formation and reproduction in C. elegans. Cell *124*, 1209–1223.

Nakae, J., Kitamura, T., Kitamura, Y., Biggs, W.H., Arden, K.C., and Accili, D. (2003). The Forkhead Transcription Factor Foxo1 Regulates Adipocyte Differentiation. Developmental Cell *4*, 119–129.

Obsilova, V., Vecer, J., Herman, P., Pabianova, A., Sulc, M., Teisinger, J., Boura, E., and Obsil, T. (2005). 14-3-3 Protein interacts with nuclear localization sequence of forkhead transcription factor FoxO4. Biochemistry *44*, 11608–11617.

Ogg, S., Paradis, S., Gottlieb, S., Patterson, G.I., Lee, L., Tissenbaum, H.A., and Ruvkun, G. (1997). The Fork head transcription factor DAF-16 transduces insulin-like metabolic and longevity signals in C. elegans. Nature *389*, 994–999.

Ohkura, K., Suzuki, N., Ishihara, T., and Katsura, I. (2003). SDF-9, a protein tyrosine phosphatase-like molecule, regulates the L3/dauer developmental decision through hormonal signaling in C. elegans. Development *130*, 3237–3248.

Paik, J.-H., Kollipara, R., Chu, G., Ji, H., Xiao, Y., Ding, Z., Miao, L., Tothova, Z., Horner, J.W., Carrasco, D.R., et al. (2007). FoxOs Are Lineage-Restricted Redundant Tumor Suppressors and Regulate Endothelial Cell Homeostasis. Cell *128*, 309–323.

Paradis, S., Ailion, M., Toker, A., Thomas, J.H., and Ruvkun, G. (1999). A PDK1 homolog is necessary and sufficient to transduce AGE-1 PI3 kinase signals that regulate diapause in Caenorhabditis elegans. Genes & Development *13*, 1438–1452.

Paradis, S., and Ruvkun, G. (1998). Caenorhabditis elegans Akt/PKB transduces insulin receptor-like signals from AGE-1 PI3 kinase to the DAF-16 transcription factor. Genes & Development *12*, 2488–2498.

Pawlikowska, L. (2009). Association of common genetic variation in the insulin/IGF1 signaling pathway with human longevity. Aging Cell *8*, 460–472.

Quevedo, C., Kaplan, D.R., and Derry, W.B. (2007). AKT-1 regulates DNA-damage-induced germline apoptosis in C. elegans. Current Biology : CB *17*, 286–292.

Rached, M.T., Kode, A., Silva, B.C., Jung, D.Y., Gray, S., Ong, H., Paik, J.H., DePinho, R.A., Kim, J.K., Karsenty, G., et al. (2010). FoxO1 expression in osteoblasts regulates glucose homeostasis through regulation of osteocalcin in mice. J Clin Invest *120*, 357–368.

Riddle, D.L., Swanson, M.M., and Albert, P.S. (1981). Interacting genes in nematode dauer larva formation. Nature *290*, 668–671.

Stambolic, V., Suzuki, a, De la Pompa, J.L., Brothers, G.M., Mirtsos, C., Sasaki, T., Ruland, J., Penninger, J.M., Siderovski, D.P., and Mak, T.W. (1998). Negative regulation of PKB/Akt-dependent cell survival by the tumor suppressor PTEN. Cell *95*, 29–39.

Taguchi, A., Wartschow, L.M., and White, M.F. (2007). Brain IRS2 signaling coordinates life span and nutrient homeostasis. Science (New York, N.Y.) *317*, 369–372.

Taniguchi, C.M., Emanuelli, B., and Kahn, C.R. (2006). Critical nodes in signalling pathways: insights into insulin action. Nature Reviews. Molecular Cell Biology *7*, 85–96.

Thomas, J.H., Birnby, D.A., and Vowels, J.J. (1993). Evidence for parallel processing of sensory information controlling dauer formation in Caenorhabditis elegans. Genetics *134*, 1105–1117.

Ullrich, A., Bell, J.R., Chen, E.Y., Herrera, R., Petruzzelli, L.M., Dull, T.J., Gray, A., Coussens, L., Liao, Y.-C., Tsubokawa, M., et al. (1985). Human insulin receptor and its relationship to the tyrosine kinase family of oncogenes. Nature *313*, 756–761.

Ullrich, A., Gray, A., Tam, A.W., Yang-Feng, T., Tsubokawa, M., Collins, C., Henzel, W., Le Bon, T., Kathuria, S., and Chen, E. (1986). Insulin-like growth factor I receptor primary structure: comparison with insulin receptor suggests structural determinants that define functional specificity. The EMBO Journal *5*, 2503–2512.

Vanhaesebroeck, B., and Alessi, D. (2000). The PI3K–PDK1 connection: more than just a road to PKB.

Vowels, J.J., and Thomas, J.H. (1992). Genetic Analysis of Chemosensory Control of Dauer Formation in Caenorhabditis elegans. Genetics *130*, 105–123.

Willcox, B.J., Donlon, T.A., He, Q., Chen, R., Grove, J.S., Yano, K., Masaki, K.H., Willcox, D.C., Rodriguez, B., and Curb, J.D. (2008). FOXO3A genotype is strongly associated with human longevity. Proceedings of the National Academy of Sciences *105*, 13987–13992.

Yamawaki, T.M., Berman, J.R., Suchanek-Kavipurapu, M., McCormick, M., Gaglia, M.M., Lee, S.-J.J., and Kenyon, C. (2010). The somatic reproductive tissues of C. elegans promote longevity through steroid hormone signaling. PLoS Biology *8*,.

Zhang, Y., Xu, J., Puscau, C., Kim, Y., Wang, X., Alam, H., and Hu, P.J. (2008). Caenorhabditis elegans EAK-3 inhibits dauer arrest via nonautonomous regulation of nuclear DAF-16/FoxO activity. Developmental Biology *315*, 290–302.

Chapter 2: Functional divergence of dafachronic acid pathways in the control of *Caenorhabditis elegans* development and life span[1]

Abstract

Steroid hormone and insulin/insulin-like growth factor signaling (ILS) pathways control development and life span in the nematode *Caenorhabditis elegans* by regulating the activity of the nuclear receptor DAF-12 and the FoxO transcription factor DAF-16, respectively. The DAF-12 ligands Δ^4- and Δ^7-dafachronic acid (DA) promote bypass of the dauer diapause and proper gonadal migration during larval development; in adults, DAs influence life span. Whether Δ^4- and Δ^7-DA have unique biological functions is not known. We identified the 3-β-hydroxysteroid dehydrogenase (3βHSD) family member HSD-1, which participates in Δ^4-DA biosynthesis, as an inhibitor of DAF-16/FoxO activity. Whereas ILS promotes the cytoplasmic sequestration of DAF-16/FoxO, HSD-1 inhibits nuclear DAF-16/FoxO activity without affecting DAF-16/FoxO subcellular localization. Thus, HSD-1 and ILS inhibit DAF-16/FoxO activity *via* distinct and complementary mechanisms. In adults, HSD-1 was required for full life span extension in ILS mutants, indicating that HSD-1 interactions with ILS are context-dependent. In contrast to the Δ^7-DA biosynthetic enzyme DAF-36, HSD-1 is dispensable for proper gonadal migration and life span extension induced by germline ablation. These findings provide insights into the molecular interface between DA and ILS pathways and suggest that Δ^4- and Δ^7-DA pathways have unique as well as overlapping biological functions in the control of development and life span.

[1] Originally published in *Developmental Biology* (2010; 340(2), 605-612) with authors listed as Dumas, K.J., Guo, C., Wang, X., Burkhart, K.B., Adams, E.J., Alam, H., and Hu, P.J.

Introduction

In replete environments, *Caenorhabditis elegans* larvae undergo four molts during reproductive development. When faced with unfavorable conditions, they enter diapause, arresting in an alternative third larval stage known as dauer. Dauers are adapted for survival and dispersal and resume development to adulthood once ambient conditions improve (Riddle, 1988).

The elucidation of signal transduction pathways that regulate dauer arrest has provided a glimpse into how organisms integrate environmental cues with developmental programs. Genetic analysis has defined an intricate signaling network that controls the transition to diapause (Hu, 2007; Fielenbach and Antebi, 2008). A pathway regulated by the DAF-11 guanylyl cyclase (Birnby et al., 2000) acts in sensory neurons to promote reproductive development by potentiating the expression of insulin-like (Pierce et al., 2001; Li et al., 2003) and transforming growth factor-beta (TGFβ)-like (Ren et al., 1996; Schackwitz et al., 1996; Murakami et al., 2001) ligands. These ligands regulate gene expression by activating conserved insulin-like and TGFβ-like signal transduction pathways in target tissues.

A hormone biosynthetic pathway also regulates dauer arrest by synthesizing dafachronic acids (DAs), which are steroid ligands for the nuclear receptor DAF-12 (Motola et al., 2006). The cytochrome P450 DAF-9 (Gerisch et al., 2001; Jia et al., 2002) acts on distinct precursors to generate two DAs, Δ^4- and Δ^7-DA (Motola et al., 2006). Precursors for Δ^4- and Δ^7-DA are thought to be synthesized by the 3-β-hydroxysteroid dehydrogenase (3βHSD) family member HSD-1 (Patel et al., 2008) and the Rieske oxygenase DAF-36 (Rottiers et al., 2006), respectively (Figure 2.1). DA binding to DAF-12 promotes reproductive development, whereas unliganded DAF-12 promotes dauer arrest (Motola et al., 2006). Although synthetic Δ^7-DA is more potent than synthetic Δ^4-DA in dauer rescue bioassays (Sharma et al., 2009), exogenous Δ^4-DA rescues *daf-36* mutant phenotypes (Rottiers et al., 2006; Gerisch et al., 2007), indicating that Δ^4-DA can

compensate for a reduction in Δ^7-DA *in vivo*. Whether Δ^4-DA and Δ^7-DA have distinct biological functions is not known.

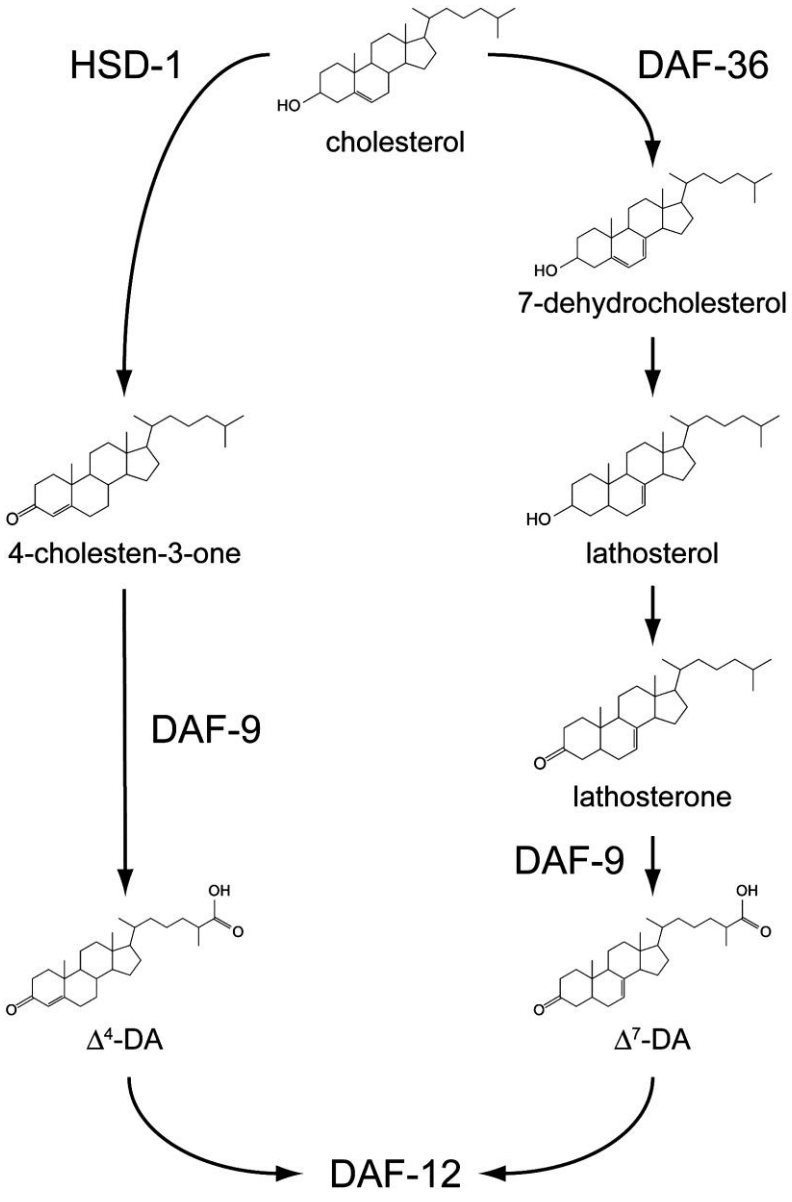

Figure 2.1. Hypothetical model of dafachronic acid (DA) biosynthetic pathways. Adapted from Rottiers *et al*.(Rottiers et al., 2006) and Patel *et al.* (Patel et al., 2008).

daf-12 mutations suppress dauer arrest in *daf-11* and *daf-7/TGFβ* pathway mutants (Thomas et al., 1993), indicating that DAF-12 is required for dauer arrest in these mutants and suggesting that DAF-12 acts downstream of DAF-11 and DAF-7/TGFβ pathways. In contrast, the relationship between the DA pathway and the insulin-like pathway appears to be complex. Whereas reduced insulin-like signaling results in constitutive dauer arrest, *daf-12* mutations cause a synthetic non-dauer larval arrest phenotype in the context of reduced insulin-like signaling (Vowels and Thomas, 1992; Larsen et al., 1995). Furthermore, exogenous Δ^4-DA fully rescues dauer arrest in *daf-9* and *daf-7/TGFβ* mutants but causes non-dauer larval arrest in some strains harboring mutations in the insulin receptor (InsR) ortholog DAF-2 (Motola et al., 2006). The molecular basis for these interactions between DA and insulin-like signaling remains poorly understood.

Upon engagement by insulin-like ligands, DAF-2/InsR promotes reproductive development by activating a conserved phosphoinositide 3-kinase (PI3K)/Akt pathway (Morris et al., 1996; Paradis and Ruvkun, 1998; Paradis et al., 1999). Dauer arrest caused by reductions in DAF-2/InsR signaling is fully suppressed by mutations in the FoxO transcription factor DAF-16 (Vowels and Thomas, 1992; Gottlieb and Ruvkun, 1994), indicating that DAF-16/FoxO is the major target of DAF-2/InsR pathway signaling and that DAF-2/InsR antagonizes DAF-16/FoxO. DAF-2/InsR activation of PI3K/Akt signaling results in DAF-16/FoxO phosphorylation by Akt and its subsequent cytoplasmic sequestration *via* binding to 14-3-3 proteins (Berdichevsky et al., 2006; Hertweck et al., 2004; Lee et al., 2001; Li et al., 2007; Lin et al., 2001).

Although the inhibition of FoxO transcription factors by Akt in both *C. elegans* and mammals is well established, multiple lines of evidence support the existence of a second pathway that acts in parallel to PI3K/Akt signaling to inhibit FoxO. DAF-16/FoxO that is constitutively nuclear by virtue of either mutation of its consensus Akt/PKB phosphorylation sites or inactivation of either AKT-1 or the 14-3-3 protein FTT-2 is not fully active (Lin et al., 2001; Hertweck et al., 2004; Berdichevsky et al., 2006; Zhang et al., 2008), suggesting that a pathway acting in parallel to AKT-1 inhibits the activity of

nuclear DAF-16/FoxO. To identify components of this pathway, we performed a genetic screen for enhancers of the dauer arrest phenotype seen in *akt-1* null mutants (*eak* mutants) (Hu et al., 2006; Zhang et al., 2008). Here we report the cloning and characterization of *eak-2*. Surprisingly, *eak-2* is allelic to *hsd-1* (Patel et al., 2008). This finding provided us with an opportunity to examine the interface between *C. elegans* insulin-like and DA pathways in dauer regulation and life span control.

Materials and Methods

Strains

The following alleles were used, in the N2 Bristol wild-type background, *hsd-1(mg345)*, *hsd-1(mg433)* (Patel et al., 2008), *daf-9(k182)* (Gerisch et al., 2001), *daf-36(k114)* (Rottiers et al., 2006), *glp-1(e2141)* (Priess et al., 1987), *daf-16(mgDf47)* (Ogg et al., 1997), *daf-12(rh61rh411)* (Antebi et al., 2000), *akt-1(mg306)* (Hu et al., 2006), *eak-3(mg344)* (Zhang et al., 2008), *daf-2(e1370)* (Kimura et al., 1997), *sqt-1(sc13) age-1(hx546)* (Morris et al., 1996), *pdk-1(sa709)* (Paradis et al., 1999), *eak-4(mg348)* (Hu et al., 2006), and *sdf-9(mg337)* (Hu et al., 2006). DAF-16::GFP localization was assayed using strain TJ356 (*zIs356)* IV, which contains an integrated C-terminal translational fusion of the DAF-16A isoform in-frame to GFP (Henderson and Johnson, 2001). Strains CF1330 and CF1371 harbor extrachromosomal arrays encoding wild-type GFP::DAF-16/FoxO and a constitutively nuclear GFP::DAF-16/FoxO mutant lacking all AKT phosphorylation sites, respectively (Lin et al., 2001).

eak-2 mutant isolation, mapping, and sequencing

Isolation, mapping, and sequencing of *eak-2* alleles were performed as described for *eak-3* (Zhang et al., 2008).

hsd-1 cDNA isolation

hsd-1 cDNA isolation was performed as described for *eak-3* (Zhang et al., 2008), except that total RNA was isolated from fluorescent XXX cells that had been FACS-purified

from cultured embryonic cells containing an integrated *sdf-9*p::RFP transgene (Hu et al., 2006).

*hsd-1*p::GFP construction and analysis

The *hsd-1* promoter (corresponding to nucleotides 24173-24413 of YAC Y6B3B, as annotated by the National Center for Biotechnology Information, was amplified from genomic DNA, a fragment containing GFP and the *unc-54* 3' UTR was amplified using pPD95.75 as a template, and the two PCR products were fused using overlap extension PCR to create *hsd-1*p::GFP. *hsd-1*p::GFP and the transformation marker plasmid pRF4 were coinjected at concentrations of 40 ng/μl and 60 ng/μl respectively into animals containing an integrated *sdf-9*p::RFP transgene. Transgenic animals were generated, animals were visualized using an Olympus BX61 upright microscope, and fluorescence was analyzed using SlideBook 4.1 digital microscopy software (Intelligent Imaging Innovations, Inc., Denver, CO, USA) as described (Hu et al., 2006).

Gonadal migration assays

Egg lays were performed on standard NGM plates at 20°C, and L4 larvae were scored for gonadal migration defects (Mig phenotype) using a Nikon SMZ800 stereomicroscope. Mig phenotypes were confirmed by visualization on an Olympus BX61 upright microscope at 200X magnification.

Life span assays

Life span assays were performed as described (Hu et al., 2006), except that the 5-fluorodeoxyuridine (FUDR) concentration used in life span assays was 0.025 mg/ml. For life span assays on *glp-1(e2141)* strains, animals were cultured at 25°C after egg lay, and L4 animals were picked to NGM plates containing nystatin but lacking FUDR and incubated at 20°C.

Dauer assays

Dauer assays were performed as described (Hu et al., 2006). To test rescue of dauer arrest by various sterols, 10μl of 100μM sterol stock solution was mixed with 90μl of concentrated *E. coli* OP50 suspension, and the mix was aliquotted onto 6-cm NGM plates and allowed to dry overnight at room temperature. These plates were then used for standard dauer assays on *hsd-1;akt-1* double mutant animals at 25°C. Final concentration of exogenous sterols was 111nM. For assays of strains harboring extrachromosomal DAF-16/FoxO transgenes, gravid transgenic animals were picked for egg lays based on the Rol phenotype. Progeny were incubated at 25°C and assayed for dauer arrest 48-60 hours after egg lay. Animals that bypassed dauer arrest were scored as Rol or non-Rol. Only Rol bypassors were included in calculations of dauer arrest penetrance.

Quantitative real-time reverse transcriptase PCR

After four-hour egg lay, animals were grown at 25°C for 24 hours prior to harvesting. Total RNA isolation, cDNA synthesis, and quantitative real-time reverse transcriptase PCR were performed using gene-specific primers as described (Zhang et al., 2008).

DAF-16::GFP localization

Animals harboring an integrated DAF-16::GFP transgene were grown at 25°C and analyzed as described (Zhang et al., 2008). To obtain a distribution of DAF-16::GFP localization patterns in a population of animals, single animals were categorized as exhibiting nuclear, nuclear and cytoplasmic, or cytoplasmic fluorescence, and percentages of animals exhibiting each pattern were calculated for each strain.

Results

Animals harboring the *akt-1(mg306)* null mutation arrest as dauers at 27°C but develop reproductively at 25°C (Hu et al., 2006). To identify mutations that enhance the *akt-1(mg306)* dauer arrest phenotype, we mutagenized *akt-1(mg306)* animals and screened for rare F_2 dauers at 25°C. After excluding mutants whose dauer arrest phenotype was either not suppressed by *daf-16/FoxO* RNAi or did not require the presence of the *akt-*

1(mg306) mutation, we identified 21 independent mutants that define seven *eak* genes. Four *eak* genes have been cloned: *eak-3*, *eak-4*, *sdf-9* (which is allelic to *eak-5*), and *eak-6*. They encode plasma membrane-associated proteins that function in a single pathway to promote reproductive development by acting in parallel to AKT-1 to inhibit DAF-16/FoxO activity nonautonomously (Hu et al., 2006; Zhang et al., 2008).

e*ak-2* is defined by two independent alleles, *mg334* and *mg345*. We cloned *eak-2* and found that it is allelic to the 3βHSD family member *hsd-1* (see Supporting Information for details), which was originally identified in a screen for enhancers of the *ncr-1* dauer arrest phenotype (Patel et al., 2008). HSD-1 is thought to participate in the biosynthesis of DAs. DAF-9, which is expressed in the XXX cells, the hypodermis, and the hermaphrodite spermatheca (Gerisch et al., 2001; Jia et al., 2002), catalyzes the final steps in the biosynthesis of two distinct DAs, Δ^4-DA and Δ^7-DA, from the precursors 4-cholesten-3-one and lathosterone (Motola et al., 2006) (Figure 2.1). The predicted biochemical activity of HSD-1 and the expression pattern of *hsd-1*p::GFP (Supplemental Figure 2.3; (Patel et al., 2008) suggest that HSD-1 and DAF-9 participate in Δ^4-DA biosynthesis in the XXX cells, whereas DAF-36 and hypodermal DAF-9 synthesize Δ^7-DA (Figure 2.1).

hsd-1 mutants undergo dauer arrest in a DAF-16/FoxO- and DAF-12-dependent manner

hsd-1 single mutants do not have a strong dauer arrest phenotype at 25°C (Figures 2.2B and 2.2C). However, they do undergo dauer arrest at 27°C when cultured on NGM plates lacking supplemental cholesterol (Figure 2.2A). Dauer arrest in these conditions required both DAF-16/FoxO and DAF-12, indicating that HSD-1 promotes reproductive development by antagonizing DAF-16/FoxO and DAF-12. *hsd-1* mutation also enhanced the dauer arrest phenotype of other DA biosynthetic mutants (Figure 2.2B). As previously shown (Patel et al., 2008), precursors of both Δ^4- and Δ^7-DA rescued the *hsd-1* dauer arrest phenotype (Supplemental Figure 2.4).

Since *hsd-1* mutations strongly enhance the dauer arrest phenotype of *akt-1* mutants (Figures 2.2B and 2.2C), we tested the interactions of *hsd-1* with other *daf-2/InsR* pathway mutants. *hsd-1* mutations also enhanced the dauer arrest phenotypes of *age-1/PI3K* and *pdk-1* mutants, consistent with HSD-1 acting in parallel to the PI3K/Akt pathway (Figure 2.2C). The strong dauer arrest phenotype of *hsd-1;akt-1* double mutants also required both DAF-16/FoxO and DAF-12 function (Figure 2.2C). *hsd-1* mutation also enhanced the dauer arrest phenotype of *daf-2(e1370)* mutants; whereas *daf-2(e1370)* animals develop reproductively at 15°C, a significant fraction of *hsd-1;daf-2* double mutant animals arrested as dauers at 15°C (Figure 2.2D). *daf-2* mutants harboring the *hsd-1(mg433)* molecular null mutation had a stronger dauer arrest phenotype than *daf-2* mutants harboring the *hsd-1(mg345)* missense mutation (Figure 2.2D), suggesting that *hsd-1(mg345)* is a non-null allele.

Since HSD-1 likely functions in DA biosynthesis, we tested other DA biosynthetic mutants for their ability to enhance the dauer arrest phenotype of *akt-1(mg306)*. The *daf-9(k182)* partial loss-of-function mutation (Gerisch et al., 2001) also enhanced the dauer arrest phenotype of *akt-1* mutants (Figure 2.2B). The *daf-36* gene is located on the same cosmid as *akt-1*, hindering the construction of a *daf-36 akt-1* double mutant. However, we previously showed that RNAi of *akt-1* enhances dauer arrest in a *daf-36* mutant background (Zhang et al., 2008). Thus, mutations predicted to reduce the synthesis of either Δ^4- or Δ^7-DA or both DAs enhance the dauer arrest phenotype of *akt-1* mutants. These findings indicate that DAs act in parallel to AKT-1 to inhibit dauer arrest. Taken together with the observation that precursors of both Δ^4- and Δ^7-DA rescue dauer arrest in *hsd-1;akt-1* double mutants (Supplemental Figure 2.4), they suggest that Δ^4- and Δ^7-DA act redundantly to promote reproductive development.

hsd-1 mutation did not enhance the dauer arrest phenotype of other *eak* mutants (Figures 2.2B and 2.2C), suggesting that HSD-1 and the other EAK proteins act in the same pathway and in parallel to the PI3K/Akt pathway in dauer regulation.

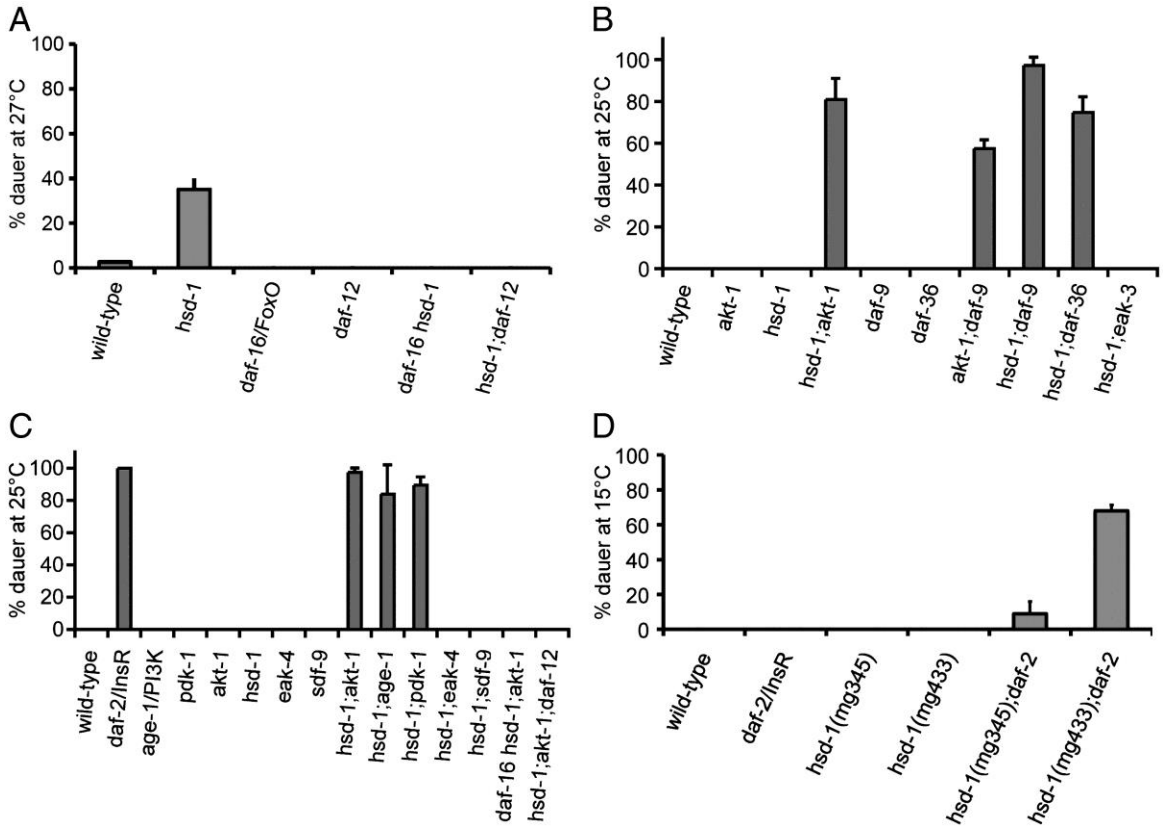

Figure 2.2: HSD-1 regulation of dauer arrest.
(A.) *hsd-1(mg433)* animals arrest as dauers at 27°C on NGM plates lacking supplemental cholesterol in a DAF-16/FoxO- and DAF-12-dependent manner. (B.) Synthetic dauer arrest phenotypes at 25°C in combinations of *hsd-1* and *akt-1* mutations with mutations in DA biosynthetic pathway components. (C.) The *hsd-1(mg433)* mutation enhances dauer arrest at 25°C in PI3K/Akt pathway mutants but not in other *eak* mutants. (D.) *hsd-1* mutations enhance dauer arrest at 15°C in *daf-2(e1370)* mutants. Error bars indicate standard deviation.

HSD-1 regulates DAF-16/FoxO target gene expression in a DAF-16/FoxO and DAF-12-dependent manner

The requirement of DAF-16/FoxO for dauer arrest in *hsd-1* mutants suggests that *hsd-1* mutation increases DAF-16/FoxO activity. To test this, we used quantitative real-time reverse transcriptase PCR (qPCR) to measure endogenous mRNA levels of three direct DAF-16/FoxO target genes: *sod-3* (Oh et al., 2006), *mtl-1* (Murphy et al., 2003), and *dod-3* (Murphy et al., 2003) (Figure 2.3). As previously observed (Zhang et al., 2008), *akt-1* mutation increases transcript levels of all three genes. This is consistent with the increased nuclear localization of DAF-16/FoxO caused by reduction of AKT-1 activity (Hertweck et al., 2004; Zhang et al., 2008). Intriguingly, *hsd-1* mutation had divergent effects on different transcripts. *hsd-1* mutation modestly increased *sod-3* transcript levels and synergized with *akt-1* mutation to further increase *sod-3* mRNA levels (Figure 2.3A). This increase in *sod-3* expression required both DAF-12 and DAF-16/FoxO activity, consistent with what we have previously observed with *eak-3* mutation (Zhang et al., 2008). Thus, HSD-1 inhibits *sod-3* expression in a DAF-12- and DAF-16/FoxO-dependent manner. Since DAF-16/FoxO activates *sod-3* transcription directly (Oh et al., 2006), this result suggests that in this context, DAF-12 acts either upstream of or in parallel to DAF-16/FoxO to promote *sod-3* expression.

In contrast, *hsd-1* mutation reduced the expression of *mtl-1* and *dod-3* in both wild-type and *akt-1* mutant backgrounds (Figures 2.3B and 2.3C). Thus, HSD-1 promotes the expression of *mtl-1* and *dod-3*. *akt-1* mutation increased *mtl-1* and *dod-3* expression in an *hsd-1* mutant background, and this increase required both DAF-12 and DAF-16/FoxO activity (Figures 2.3B and 2.3C). These results indicate that HSD-1 has distinct effects on the expression of subsets of DAF-16/FoxO target genes and that both DAF-12 and DAF-16/FoxO are required for maximal expression of *mtl-1* and *dod-3* in *hsd-1;akt-1* double mutants.

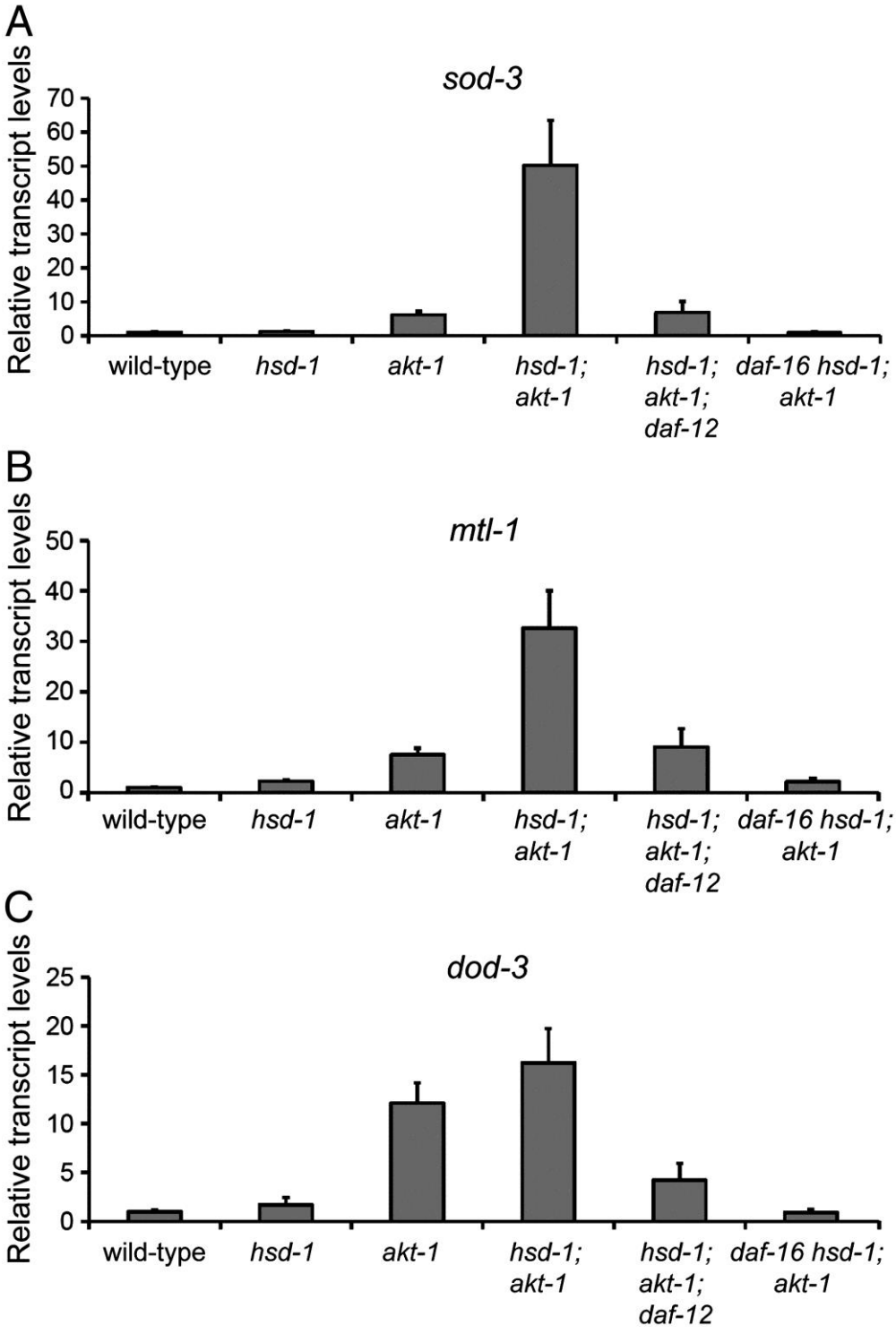

Figure 2.3. HSD-1 regulation of DAF-16/FoxO target gene expression.
Quantification of endogenous transcripts corresponding to the DAF-16/FoxO target genes (A.) *sod-3*, (B.) *mtl-1*, and (C.) *dod-3* in various mutant strains. Error bars indicate standard deviation.

HSD-1 inhibits nuclear DAF-16/FoxO activity without influencing DAF-16/ FoxO subcellular localization

To gain further insight into how HSD-1 regulates DAF-16/FoxO activity, we examined the localization of a functional DAF-16::GFP fusion protein (Henderson and Johnson, 2001) in wild-type, *akt-1* mutant, and *hsd-1* mutant animals (Figures 2.4A and 2.4B). As previously reported, most wild-type animals exhibited diffuse fluorescence corresponding to cytoplasmic localization (Henderson and Johnson, 2001; Zhang et al., 2008). *akt-1* mutation promoted nuclear localization of DAF-16::GFP, as shown by the increase in percentage of animals exhibiting nuclear or nuclear and cytoplasmic fluorescence compared to wild-type (two-sided t-test: $p = 0.017$; Figure 2.4B). In contrast, the distribution of DAF-16::GFP fluorescence patterns in *hsd-1* single mutants was indistinguishable from that of wild-type animals (two-sided t-test: $p = 0.562$; Figure 2.4B). Thus, in contrast to AKT-1, which inhibits DAF-16/FoxO by promoting its translocation from the nucleus to the cytoplasm, HSD-1 inhibits DAF-16/FoxO activity without influencing its subcellular localization. Multiple efforts to construct an *hsd-1;akt-1* double mutant strain harboring DAF-16::GFP were unsuccessful, preventing us from determining whether *hsd-1* mutation promotes the nuclear localization of DAF-16::GFP in an *akt-1* mutant background.

To directly test the hypothesis that HSD-1 inhibits nuclear DAF-16/FoxO activity, we assayed the ability of *hsd-1* mutation to activate a constitutively nuclear GFP::DAF-16 fusion protein that lacks all Akt phosphorylation sites (DAF-16^{AM}) (Lin et al., 2001). Transgenic animals expressing DAF-16^{AM} exhibit constitutive nuclear fluorescence but do not arrest as dauers or live long (Lin et al., 2001), suggesting that in wild-type animals, nuclear DAF-16/FoxO is inhibited by a pathway that does not promote its relocalization to the cytoplasm. As previously reported, DAF-16^{AM} animals did not arrest as dauers at 25°C in a wild-type background (Figure 2.4B). *hsd-1* mutation strongly enhanced the 25°C dauer arrest phenotype of animals harboring DAF-16^{AM} but did not promote dauer arrest in animals harboring a wild-type GFP::DAF-16 transgene (Figure 2.4B). Thus, the effect of *hsd-1* mutation on dauer arrest is greatly enhanced in contexts

in which DAF-16/FoxO is nuclear, strongly suggesting that HSD-1 inhibits nuclear DAF-16/FoxO activity.

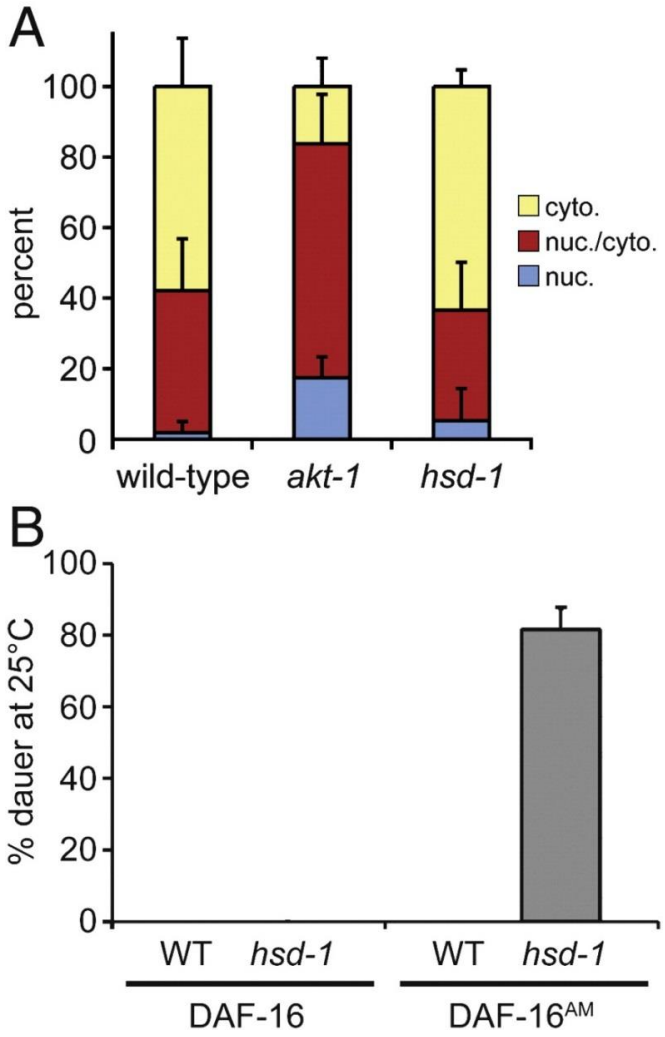

Figure 2.4 HSD-1 inhibits nuclear DAF-16/FoxO activity without promoting its translocation from the nucleus to the cytoplasm.
(A.) Percentage of animals exhibiting cytoplasmic, nuclear and cytoplasmic, or nuclear DAF-16::GFP localization. Error bars: s.d. N = 62 (wild-type), 77 (*akt-1(mg306)*), and 62 (*hsd-1(mg433)*). (B.) The *hsd-1(mg433)* mutation enhances dauer arrest at 25°C in animals harboring a constitutively nuclear GFP::DAF-16/FoxO mutant lacking all Akt phosphorylation sites (DAF-16^{AM}) but not in animals harboring wild-type GFP::DAF-16. Error bars indicate standard deviation.

HSD-1 is required for life span extension in DAF-2/InsR mutants

To determine whether HSD-1 plays a role in life span control, we assayed the life span of *hsd-1* mutants (Figure 2.5). The life spans of *hsd-1* single mutants were comparable to that of wild-type animals. We previously showed that *akt-1* mutants exhibit a slight increase in mean and median life span (Hu et al., 2006; Zhang et al., 2008); upon reduction of the FUDR concentration by 75%, we now observe significant life span extension in *akt-1* mutants compared to wild-type or *hsd-1* mutants (Figure 2.5A; $P < 0.0001$ by the log-rank test). Two independent *hsd-1* mutant alleles modestly suppressed the life span extension of *akt-1* mutants, and this was of borderline statistical significance ($P = 0.0128$ for *akt-1 vs. hsd-1(mg345);akt-1* and 0.0548 for *akt-1 vs. hsd-1(mg433);akt-1*). This result contrasts with the strong enhancement of dauer arrest in *akt-1* mutants by *hsd-1* mutation (Figures 2.2B and 2.2C).

In light of the trend toward suppression of life span extension of *akt-1* mutants by *hsd-1* mutation, we determined the effect of *hsd-1* mutation on the life span of *daf-2/InsR* mutants. Surprisingly, *hsd-1* mutation significantly reduced the life span of *daf-2(e1370)* mutants (Figure 2.5B; $P < 0.0001$). This effect is unlikely to be a consequence of general frailty due to *hsd-1* mutation, as *hsd-1* single mutants have life spans that are comparable to wild-type (Figure 2.5). Thus, although HSD-1 does not influence life span substantially in wild-type animals, it is required for maximal life span extension when insulin-like signaling is reduced. The suppression of *daf-2(e1370)* life span extension by *hsd-1* mutation contrasts with its enhancement of *daf-2(e1370)* dauer arrest (Figure 2.2D) and suggests that HSD-1 can either antagonize or potentiate DAF-16/FoxO activity, depending upon the biological context.

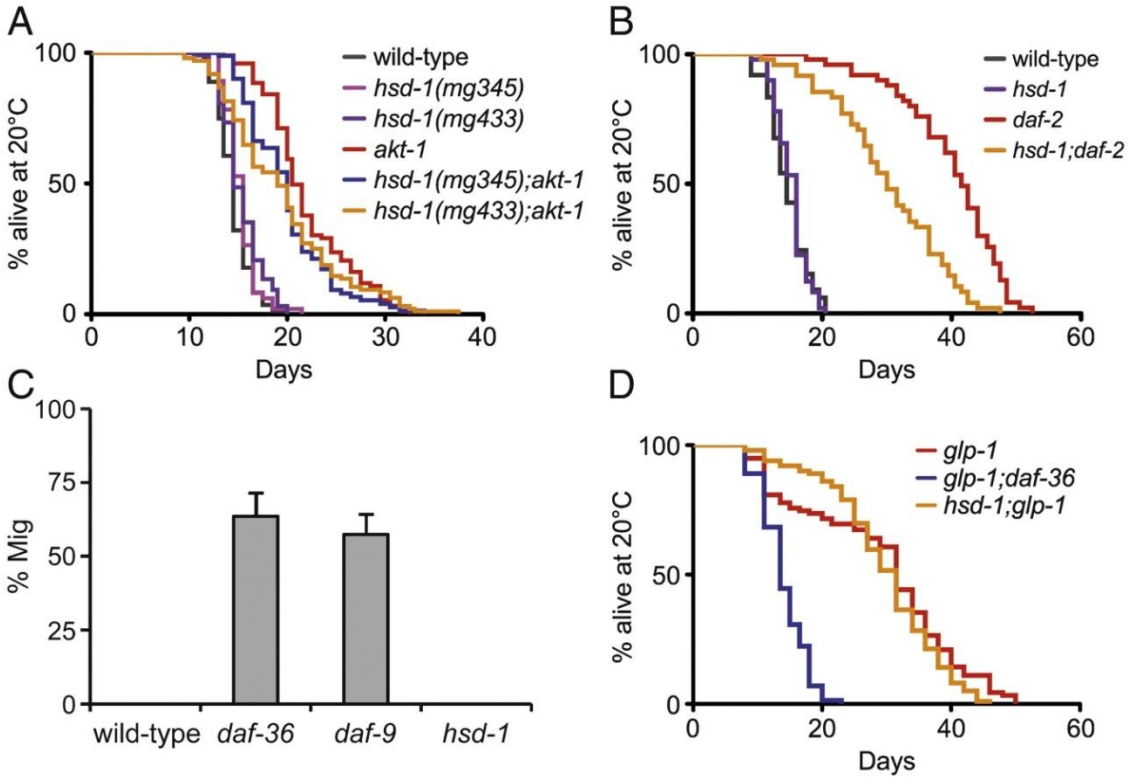

Figure 2.5. Impact of *hsd-1* mutation on life span and gonadal migration.
(A.) Effect of *hsd-1* mutations on life span at 20°C in various genetic backgrounds. (B.) Effect of the *hsd-1(mg433)* mutation on life span extension in *daf-2(e1370)* mutants at 20°C. (C.) Percentage of wild-type and mutant populations exhibiting the Mig phenotype at 20°C. Error bars indicate standard deviation. (D.) Life span extension in *glp-1(e2141)* mutant animals does not require *hsd-1*.

HSD-1 is not required for proper gonadal migration or life span extension in animals lacking a germline

In addition to their dauer-constitutive phenotypes, *daf-9* and *daf-36* loss-of-function mutants and *daf-12* ligand binding domain mutants exhibit developmental abnormalities in gonadal migration (Mig phenotype) (Antebi et al., 2000; Gerisch et al., 2001; Jia et al., 2002; Rottiers et al., 2006). In these mutants, the gonadal leader cells fail to turn dorsally and continue to migrate away from the primordial vulva (Figures 2.6A and 2.6B). Since exogenous Δ^4-DA rescues the Mig phenotype of *daf-9* mutants (Motola et al., 2006) and HSD-1 is thought to participate in Δ^4-DA biosynthesis (Patel et al., 2008), we examined *hsd-1* mutant animals for the Mig phenotype. Surprisingly, in contrast to *daf-9* and *daf-36*

mutants, which exhibited high penetrance Mig phenotypes (Figures 2.6A and 2.6C), *hsd-1* null mutants did not have discernible gonadal migration abnormalities (Figures 2.6B and 2.6C). Thus, unlike DAF-9 and DAF-36, HSD-1 is not required for proper gonadal migration during larval development.

DAF-9, DAF-36, and DAF-12 are also required for life span extension in animals lacking a germline (Berman and Kenyon, 2006; Rottiers et al., 2006). Since HSD-1 is required for full life span extension in *daf-2(e1370)* mutant animals (Figure 2.5B), we tested the role of HSD-1 in life span extension caused by germline ablation. As previously shown (Rottiers et al., 2006), DAF-36 was required for life span extension in *glp-1(e2141)* mutants lacking a germline (Figure 2.6D). In contrast, HSD-1 was completely dispensable for life span extension in *glp-1* mutants. Thus, whereas HSD-1 and DAF-36 play similar roles in dauer regulation (Figures 2.2B), they have distinct functions in the control of gonadal migration and life span.

Discussion

We have shown that the 3βHSD family member HSD-1 acts in parallel to AKT-1 to regulate dauer arrest via DAF-16/FoxO and DAF-12. This is supported by three major lines of evidence. First, *hsd-1* mutation strongly enhances the dauer arrest phenotype of an *akt-1* null mutant in a DAF-16/FoxO- and DAF-12-dependent manner (Figure 2.2C). *hsd-1* mutation also synergizes with *akt-1* mutation to enhance expression of the DAF-16/FoxO target gene *sod-3* in a DAF-16/FoxO- and DAF-12-dependent manner (Figure 2.3A). Finally, *hsd-1* mutation enhances dauer arrest in animals expressing a constitutively nuclear DAF-16/FoxO mutant that lacks all Akt phosphorylation sites (Figure 2.4C). The observations that *daf-9* mutation also enhances dauer arrest in an *akt-1* null mutant (Figure 2.2B) and that *akt-1* RNAi induces dauer arrest and DAF-16/FoxO target gene expression in a *daf-36* mutant (Zhang et al., 2008) are consistent with the postulated role of HSD-1 in synthesizing the Δ^4-DA precursor 4-cholesten-3-one (Patel et al., 2008) (Figure 2.1). Taken together, these data suggest that DAs act in parallel to AKT-1 to promote reproductive development *via* DAF-16/FoxO and DAF-12.

Based on their observation that DAF-16::GFP localizes to the nucleus in *hsd-1;ncr-1* double mutants, Patel *et al.* have proposed that steroid signaling promotes reproductive development by inhibiting DAF-16/FoxO nuclear localization (Patel et al., 2008). However, they did not address the question of how HSD-1 itself regulates DAF-16/FoxO activity. We find that, in contrast to *akt-1* mutation, which promotes the translocation of a functional DAF-16::GFP fusion protein from the cytoplasm to the nucleus, *hsd-1* mutation does not influence DAF-16::GFP localization (Figures 2.4A and 2.4B). Furthermore, *hsd-1* mutation strongly promotes dauer arrest in animals expressing a constitutively nuclear DAF-16/FoxO mutant that lacks all of its Akt phosphorylation sites while having no effect on animals expressing wild-type DAF-16/FoxO (Figure 2.4C). HSD-1 also acts in the same dauer regulatory pathway as other EAK proteins (Figures 2.2B and 2.2C), none of which influences DAF-16/FoxO localization (Zhang et al., 2008). Based on these data, we favor a model whereby HSD-1 inhibits the activity of nuclear-localized DAF-16/FoxO without promoting its translocation from the nucleus to the cytoplasm. It is possible that *hsd-1* mutation has indirect effects on other signaling pathways that may promote DAF-16/FoxO nuclear translocation in an *ncr-1* mutant background (Patel et al., 2008).

Surprisingly, whereas *hsd-1* mutation enhanced the dauer arrest phenotype of DAF-2/InsR pathway mutants, including *daf-2(e1370)* (Figures 2.2B-D), it suppressed the life span extension phenotype of *daf-2(e1370)* (Figure 2.5B). Thus, HSD-1 can either potentiate or antagonize DAF-2/InsR signaling depending upon the biological context (Figure 2.6). This could be due to context-dependent effects of the Δ^4-DA/DAF-12 interaction, the interaction of Δ^4-DA with nuclear receptors other than DAF-12 during adulthood, or a possible role for HSD-1 in the biosynthesis of distinct steroid hormones during larval development and adulthood.

Whereas mutations in *hsd-1* and *daf-36* have similar effects on dauer arrest (Figure 2.2B; (Rottiers et al., 2006), they differ in their impact on life span extension and gonadal migration (Figures 2.5C, D and Supplemental Figure 2.6, (Antebi et al., 2000; Gerisch et al., 2001; Rottiers et al., 2006)). In contrast to *daf-36* mutation, *hsd-1* mutation does not

cause defects in gonadal migration and does not suppress life span extension caused by germline ablation (Figure 2.5C and D). Thus, Δ^4- and Δ^7-DA pathways may have overlapping and distinct functions in the control of development and life span. Since HSD-1 is the only putative DA biosynthetic enzyme that is specifically expressed in the XXX cells (Supplemental Figure 2.3, (Gerisch et al., 2001; Rottiers et al., 2006; Patel et al., 2008)), this result suggests that Δ^4-DA synthesized in the XXX cells does not influence gonadal migration or life span in the context of germline ablation. This could be due to the presence of DAs synthesized in other tissues that suffice to promote normal gonadal migration in *hsd-1* mutants and life span extension in *hsd-1;glp-1* double mutants. Indeed, the ability of exogenous Δ^4-DA to rescue both the gonadal migration phenotype as well as the suppression of *glp-1(e2141)* life span extension caused by *daf-9* mutation (Motola et al., 2006; Gerisch et al., 2007) indicates that Δ^4-DA can regulate these processes. However, the partial suppression of life span extension in *daf-2(e1370)* mutants by *hsd-1* mutation suggests that other DAs that may compensate for loss of HSD-1 activity to promote normal gonadal migration and life span in germline-ablated animals are not sufficient to do so in the context of reduced insulin-like signaling.

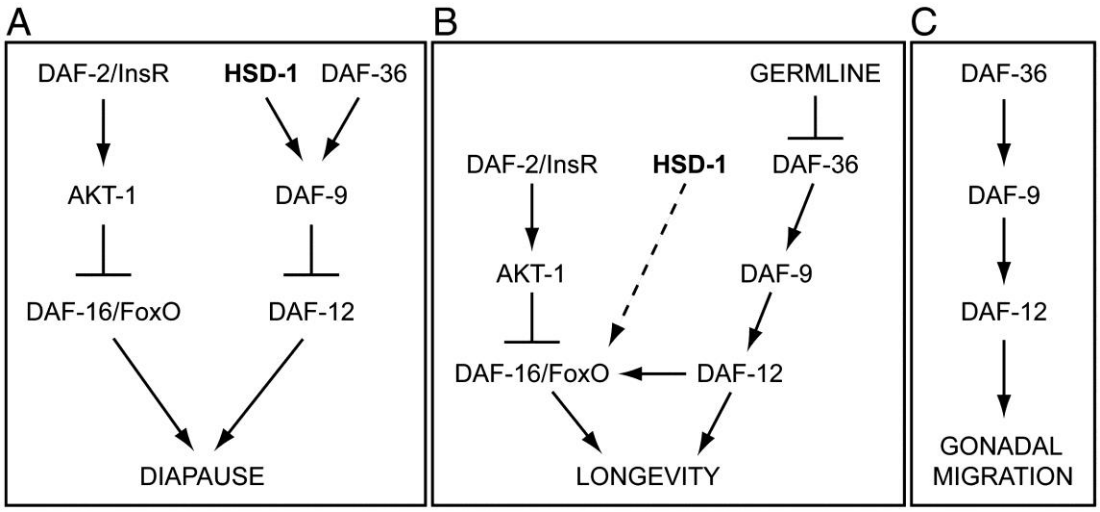

Figure 2.6. Hypothetical models of insulin-like and DA pathways in the control of diapause, longevity, and gonadal migration.
(A.) HSD-1 and DAF-36 act in canonical DA biosynthetic pathways to promote reproductive development. (B.) HSD-1 does not participate in life span control by the germline pathway but promotes life span extension in animals with reduced insulin-like signaling. (C.) Regulation of gonadal migration does not require HSD-1.

In aggregate, our data support distinct roles for DA pathways in dauer regulation, the control of life span, and gonadal migration (Figure 2.6). In dauer regulation, HSD-1 and DAF-36 act in parallel to AKT-1 to promote reproductive development *via* DAF-12 and DAF-16/FoxO (Figure 2.6A). During adulthood, DAF-36 is required for life span extension in animals lacking a germline. In contrast, HSD-1 is dispensable for life span extension caused by germline ablation but required for life span extension in animals with reduced insulin-like signaling (Figure 2.6B). HSD-1 has no apparent role in the regulation of gonadal migration by DAs (Figure 6C). Since neither the biochemical activities of HSD-1 and DAF-36 nor the steroid profiles of *hsd-1* and *daf-36* mutants have been characterized, the caveat must be considered that differences in levels of and/or the anatomical site of DA synthesis could contribute to differences in *hsd-1* and *daf-36* mutant phenotypes.

Our model of HSD-1 as a regulator of nuclear DAF-16/FoxO activity suggests that human SDR42E1, the putative HSD-1 ortholog, could play an important role in the regulation of FoxO transcription factor activity in physiological or pathophysiological states in which PI3K/Akt pathway activity is low. For example, FoxO1 localizes to hepatocyte nuclei in fasted wild-type as well as diabetic mice (Aoyama et al., 2006). In light of recent reports highlighting the role of hepatic FoxO1 in glucose homeostasis (Matsumoto et al., 2007; Dong et al., 2008), SDR42E1 could be a critical regulator of nuclear FoxO1 activity and glucose metabolism in the liver. FoxO1 also localizes to the nucleus in response to dietary restriction in tumors lacking activating PI3K/Akt pathway mutations, and FoxO1 overexpression sensitizes such tumors to dietary-restriction-induced apoptosis (Kalaany and Sabatini, 2009); in this context, SDR42E1 could modulate the apoptotic response of tumors to dietary restriction. Finally, the association of FoxO3 polymorphisms with extreme human longevity (Willcox et al., 2008; Flachsbart et al., 2009) suggests the possibility that HSD-1 control of life span may also be phylogenetically conserved.

Supplemental Material

Cloning of *eak-2*

We used single nucleotide polymorphism mapping to localize *eak-2* to the right arm of chromosome I. The *hsd-1* gene lies within this interval. The *hsd-1* null allele *mg433* (Patel et al., 2008) did not complement *eak-2(mg334)* or *eak-2(mg345)*, and sequencing of predicted exons and splice junctions in the *hsd-* open reading frame identified distinct point mutations in both *eak-2* alleles. Injection of a genomic fragment containing the putative *hsd-1* promoter, open reading frame, and 3'untranslated region rescued the dauer arrest phenotype of *hsd-1;akt-1* double mutants. Therefore, *eak-2* is allelic to *hsd-1*.

Comparative sequence analysis indicates that HSD-1 is most closely related to human SDR42E1, which is one of six human 3βHSD family members (Supplemental Figure 2.1). Both *hsd-1* alleles that emerged from the *eak* screen contain missense mutations that are predicted to alter amino acid residues that are conserved in mammalian SDR42E1; the *mg334* mutation is a G-to-A transition predicted to change alanine 387 to valine (A387V), and the *mg345* mutation is a C-to-T transition predicted to change glycine 200 in the 3βHSD catalytic domain to glutamate (G200E; Supplemental Figure 2.2). Although 3βHSDs are known to participate in sterol biosynthesis (Simard et al., 2005), the function of mammalian SDR42E1 is not known.

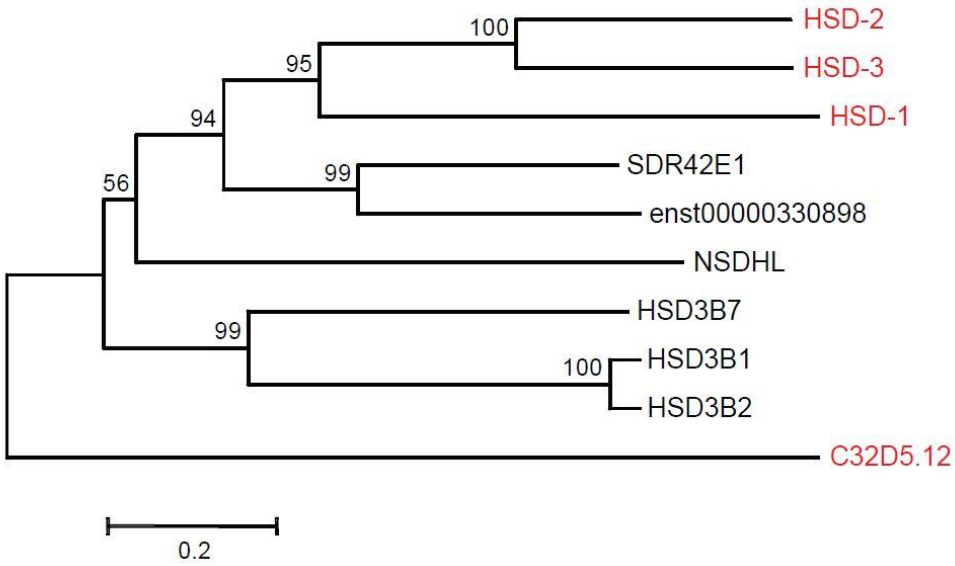

Supplemental Figure 2.1: Phylogenetic relationship among *C. elegans* and human 3βHSD family members.
A phylogeny tree was constructed based on amino acid sequences using the neighbor-joining method (Saitou and Nei, 1987). *C. elegans* and human sequences are denoted in red and black font, respectively. Numbers on the internal branches indicate bootstrap percentages greater than 50%. The scale bar indicates branch length.

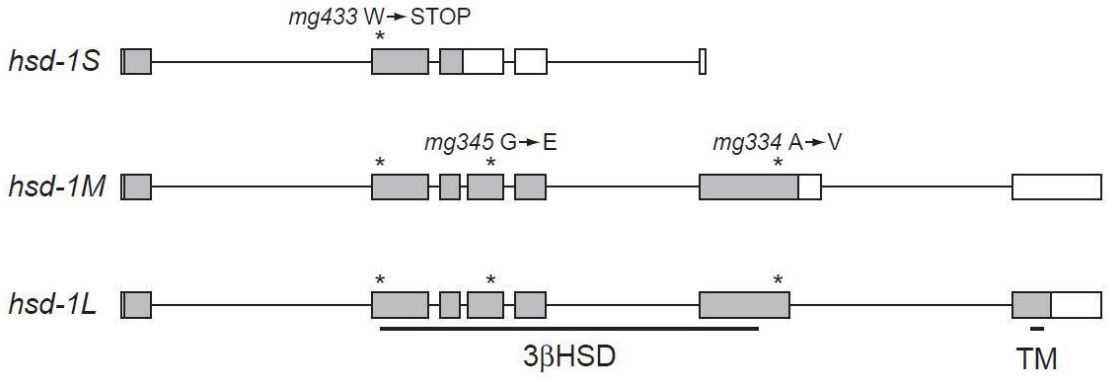

Supplemental Figure 2.2: *hsd-1* cDNA structures.
Structures of three *hsd-1* cDNAs are shown. Exons are depicted as rectangles and introns as lines. Open reading frame sequences are shaded. Asterisks indicate the location of mutations in mutant alleles *mg433* (Patel et al., 2008), *mg345*, and *mg334*. The region of homology to 3βHSDs (Simard et al., 2005) and a predicted transmembrane (TM) domain are denoted.

We identified three distinct cDNA isoforms using reverse transcriptase PCR, 5' RACE, and 3' RACE (Supplemental Figure 2.2). *hsd-1L* corresponds to the predicted *hsd-1*cDNA structure in WormBase and encodes a protein of 462 amino acids containing both the 3βHSD domain and a C-terminal transmembrane domain. *hsd-1M* is generated by lack of splicing of the sixth intron and encodes a 414-amino-acid protein that diverges from HSD-1L in its 12 C-terminal amino acids and lacks the C-terminal transmembrane domain.

In contrast to *hsd-1L* and *hsd-1M*, the structures of which were confirmed with multiple independent cDNA isolates, a single *hsd-1S* clone was isolated that is generated by lack of splicing of the third intron and encodes a 164-amino-acid protein diverging from the longer HSD-1 isoforms in its 5 C-terminal amino acids. The biological significance of *hsd-1S* is not clear, as *hsd-1S* is predicted to encode a protein that would be missing most of the 3βHSD domain (Supplemental Figure 2.2). Furthermore, the molecular lesions in *mg334* and *mg345* do not affect the predicted amino acid sequence of HSD-1S. If HSD-1S is a biologically relevant isoform, its activity is not sufficient to compensate for the loss of HSD-1M and HSD-1L. The previously identified nonsense mutation *mg433* is predicted to affect all three HSD-1 isoforms (Supplemental Figure 2.2), consistent with it being a candidate null allele (Patel et al., 2008).

hsd-1 promoter analysis

The predicted *hsd-1* initiation codon is only 217 nucleotides downstream of the predicted translation termination codon of the immediate upstream gene *lagr-1*, suggesting that *lagr-1* and *hsd-1* may be cotranscribed in an operon. However, whereas the genomic structure of the vast majority of *C. elegans* operons is conserved in *C. briggsae*, the *C. briggsae lagr-1* and *hsd-1* genes are not contiguous (Stein et al., 2003). Furthermore, the single clone we isolated that corresponded to the 5' end of the *hsd-1* cDNA contained an SL1 leader sequence, suggesting that *hsd-1* may be transcribed from a promoter that lies between *lagr-1* and *hsd-1* (Blumenthal, 2005). To determine whether the *hsd-1-lagr-1* intergenic fragment has promoter activity, we injected an *hsd-1* genomic fragment

containing the 217-bp sequence between *hsd-1* and *lagr-1*, the *hsd-1* open reading frame, and the *hsd-1* 3'untranslated region into *hsd-1;akt-1* double mutant animals. This transgene rescued *hsd-1;akt-1* dauer arrest in six of six independent transgenic lines, indicating that the 217-bp promoter contiguous with the *hsd-1* gene is sufficient to drive *hsd-1* expression in a physiologically relevant manner. Taken together with the pharyngeal expression of a *lagr-1*p::GFP fusion (Henricson et al., 2004), this result suggests that *hsd-1* and *lagr-1* are transcribed from distinct promoters and do not comprise an operon.

A GFP fusion containing the putative *lagr-1* promoter, the *lagr-1* open reading frame, and the *lagr-1-hsd-1* intergenic region drives expression specifically in the XXX cells (Patel et al., 2008) To determine where the *hsd-1* promoter is active, we constructed an *hsd-1*p::GFP promoter fusion in which GFP expression is controlled solely by the 217-bp *lagr-1-hsd-1* intergenic region and assayed transgenic animals for green fluorescence. The *hsd-1* promoter was active specifically in the endocrine XXX cells (Supplemental Figure 2.3), suggesting that this promoter is active both in isolation as well as in its genomic context.

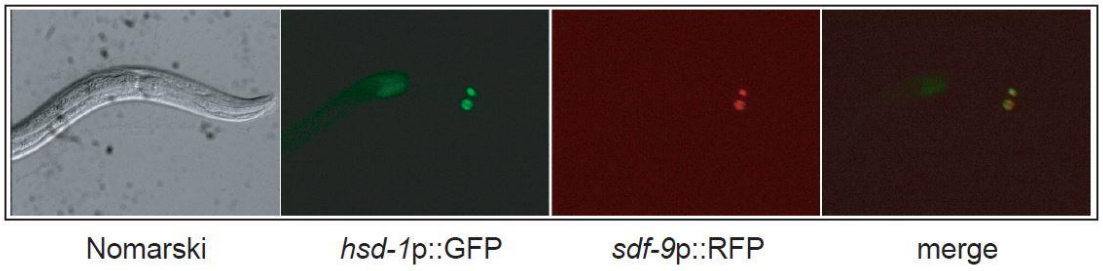

Supplemental Figure 2.3: The *hsd-1* promoter drives expression specifically in the XXX cells.
A representative late L1 larva harboring *hsd-1*p::GFP and *sdf-9*p::RFP (Hu et al., 2006) transgenes is shown.

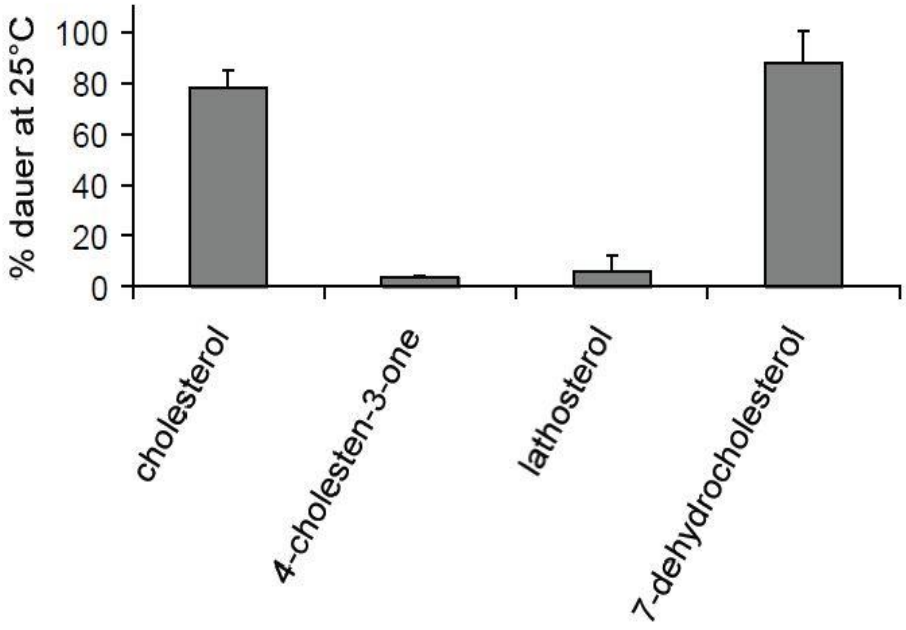

Supplemental Figure 2.4: Dafachronic acid precursors rescue the dauer arrest phenotype of *hsd-1;akt-1* double mutants.
Data are represented as mean + standard deviation. See Supplemental Figure 2.1 for molecular structures.

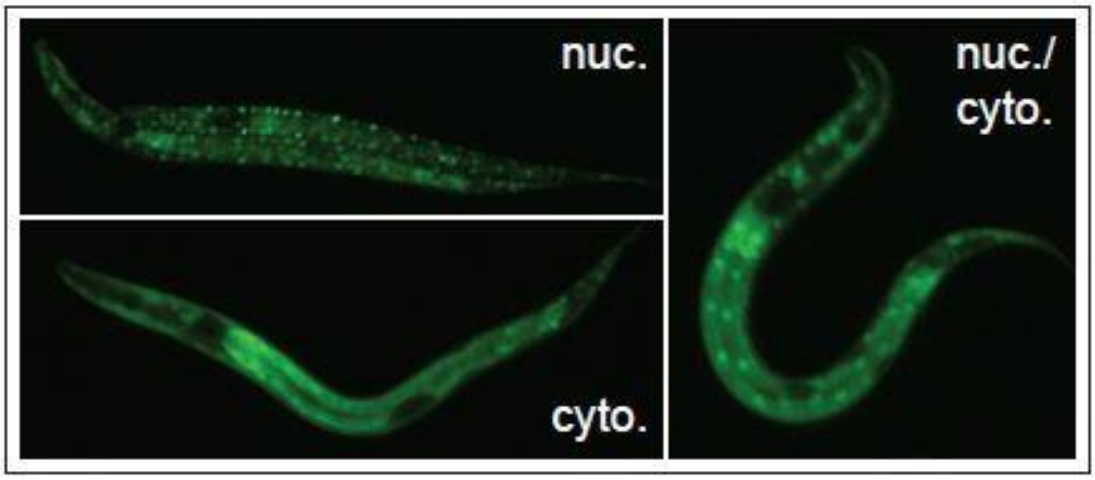

Supplemental Figure 2.5: Subcellular DAF-16::GFP localization.
Examples of animals exhibiting nuclear (nuc.; upper left panel), cytoplasmic (cyto.; lower left panel), and both nuclear and cytoplasmic (nuc./cyto.; right panel) DAF-16::GFP localization.

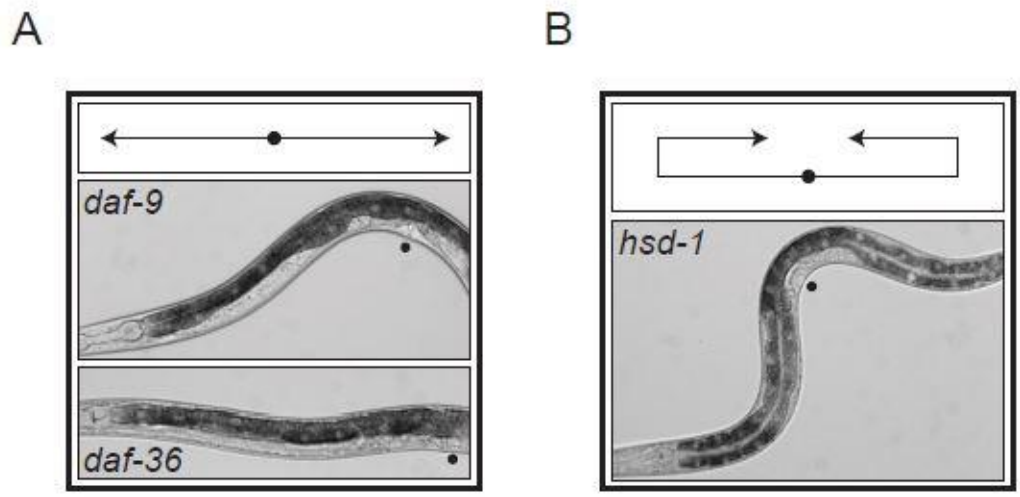

Supplemental Figure 2.6: *hsd-1* mutants do not exhibit the gonadal migration (Mig) phenotype characteristic of other DA biosynthetic mutants.
(A.) Gonadal migration (Mig) phenotype. A schematic of the Mig defect is shown in the upper panel. The vulva is denoted by a black dot. Examples of the Mig phenotype in representative *daf-9(k182)* (middle panel) and *daf-36(k114)* (lower panel) animals are shown. (B.) Normal gonadal migration. A schematic (upper panel) and normal gonadal migration in a representative *hsd-1(mg433)* animal (lower panel) are shown.

References

Antebi, A., Yeh, W.-H., Tait, D., Hedgecock, E.M., and Riddle, D.L. (2000). daf-12 encodes a nuclear receptor that regulates the dauer diapause and developmental age in C. elegans. Genes & Development *14*, 1512–1527.

Berdichevsky, A., Viswanathan, M., Horvitz, H.R., and Guarente, L. (2006). C. elegans SIR-2.1 Interacts with 14-3-3 Proteins to Activate DAF-16 and Extend Life Span. Cell *125*, 1165–1177.

Berman, J.R., and Kenyon, C. (2006). Germ-Cell Loss Extends C. elegans Life Span through Regulation of DAF-16 by kri-1 and Lipophilic-Hormone Signaling. Cell *124*, 1055–1068.

Birnby, D.A., Link, E.M., Vowels, J.J., Tian, H., Colacurcio, P.L., and Thomas, J.H. (2000). A transmembrane guanylyl cyclase (DAF-11) and Hsp90 (DAF-21) regulate a common set of chemosensory behaviors in caenorhabditis elegans. Genetics *155*, 85–104.

Blumenthal, T. (2005). Trans-splicing and operons. WormBook 1–9.

Dong, X.C., Copps, K.D., Guo, S., Li, Y., Kollipara, R., DePinho, R.A., White, M.F., and Dong XC Guo S, Li Y, Kollipara R, DePinho RA, White MF, C.K.D. (2008). Inactivation of hepatic Foxo1 by insulin signaling is required for adaptive nutrient homeostasis and endocrine growth regulation. Cell Metabolism *8*, 65–76.

Fielenbach, N., and Antebi, A. (2008). C. elegans dauer formation and the molecular basis of plasticity. Genes & Development *22*, 2149–2165.

Flachsbart, F., Caliebe, A., Kleindorp, R., BlanchÃ©, Hã©., Von Eller-Eberstein, H., Nikolaus, S., Schreiber, S., and Nebel, A. (2009). Association of FOXO3A variation with human longevity confirmed in German centenarians. Proceedings of the National Academy of Sciences *106*, 2700–2705.

Gerisch, B., Rottiers, V., Li, D., Motola, D.L., Cummins, C.L., Lehrach, H., Mangelsdorf, D.J., and Antebi, A. (2007). A bile acid-like steroid modulates Caenorhabditis elegans life span through nuclear receptor signaling. Proceedings of the National Academy of Sciences *104*, 5014–5019.

Gerisch, B., Weitzel, C., Kober-Eisermann, C., Rottiers, V., and Antebi, A. (2001). A Hormonal Signaling Pathway Influencing C. elegans Metabolism, Reproductive Development, and Life Span. Developmental Cell *1*, 841–851.

Gottlieb, S., and Ruvkun, G. (1994). daf-2, daf-16 and daf-23: Genetically Interacting Genes Controlling Dauer Formation in Caenorhabditis elegans. Genetics *137*, 107–120.

Henderson, S.T., and Johnson, T.E. (2001). daf-16 integrates developmental and environmental inputs to mediate aging in the nematode Caenorhabditis elegans. Current Biology *11*, 1975–1980.

Henricson, A., Sonnhammer, E.L., Baillie, D.L., and Gomes, A. V (2004). Functional characterization in Caenorhabditis elegans of transmembrane worm-human orthologs. BMC Genomics *5*, 85.

Hertweck, M., Göbel, C., and Baumeister, R. (2004). C. elegans SGK-1 Is the Critical Component in the Akt/PKB Kinase Complex to Control Stress Response and Life Span. Developmental Cell *6*, 577–588.

Hu, P.J. (2007). Dauer. WormBook 1–19.

Hu, P.J., Xu, J., and Ruvkun, G. (2006). Two Membrane-Associated Tyrosine Phosphatase Homologs Potentiate C. elegans AKT-1/PKB Signaling. PLoS Genet *2*, e99.

Jia, K., Albert, P.S., and Riddle, D.L. (2002). DAF-9, a cytochrome P450 regulating C. elegans larval development and adult longevity. Development *129*, 221–231.

Kalaany, N.Y., and Sabatini, D.M. (2009). Tumours with PI3K activation are resistant to dietary restriction. Nature *458*, 725–731.

Kimura, K.D., Tissenbaum, H.A., Liu, Y., and Ruvkun, G. (1997). daf-2, an Insulin Receptor-Like Gene That Regulates Longevity and Diapause in Caenorhabditis elegans. Science *277*, 942–946.

Larsen, P.L., Albert, P.S., and Riddle, D.L. (1995). Genes that regulate both development and longevity in Caenorhabditis elegans. Genetics *139*, 1567–1583.

Li, W., Kennedy, S.G., and Ruvkun, G. (2003). daf-28 encodes a C. elegans insulin superfamily member that is regulated by environmental cues and acts in the DAF-2 signaling pathway. Genes & Development *17*, 844–858.

Lin, K., Hsin, H., Libina, N., and Kenyon, C. (2001). Regulation of the Caenorhabditis elegans longevity protein DAF-16 by insulin/IGF-1 and germline signaling. Nat Genet *28*, 139–145.

Matsumoto, M., Pocai, A., Rossetti, L., DePinho, R.A., and Accili, D. (2007). Impaired Regulation of Hepatic Glucose Production in Mice Lacking the Forkhead Transcription Factor Foxo1 in Liver. Cell Metabolism *6*, 208–216.

Morris, J.Z., Tissenbaum, H.A., and Ruvkun, G. (1996). A phosphatidylinositol-3-OH kinase family member regulating longevity and diapause in Caenorhabditis elegans. Nature *382*, 536–539.

Motola, D.L., Cummins, C.L., Rottiers, V., Sharma, K.K., Li, T., Li, Y., Suino-Powell, K., Xu, H.E., Auchus, R.J., Antebi, A., et al. (2006). Identification of ligands for DAF-12 that govern dauer formation and reproduction in C. elegans. Cell *124*, 1209–1223.

Murakami, M., Koga, M., and Ohshima, Y. (2001). DAF-7/TGF-beta expression required for the normal larval development in C. elegans is controlled by a presumed guanylyl cyclase DAF-11. Mechanisms of Development *109*, 27–35.

Murphy, C.T., McCarroll, S.A., Bargmann, C.I., Fraser, A., Kamath, R.S., Ahringer, J., Li, H., and Kenyon, C. (2003). Genes that act downstream of DAF-16 to influence the life span of Caenorhabditis elegans. Nature *424*, 277–283.

Ogg, S., Paradis, S., Gottlieb, S., Patterson, G.I., Lee, L., Tissenbaum, H.A., and Ruvkun, G. (1997). The Fork head transcription factor DAF-16 transduces insulin-like metabolic and longevity signals in C. elegans. Nature *389*, 994–999.

Oh, S.W., Mukhopadhyay, A., Dixit, B.L., Raha, T., Green, M.R., Tissenbaum, H.A., and Wook Oh, S. (2006). Identification of direct DAF-16 targets controlling longevity, metabolism and diapause by chromatin immunoprecipitation. Nature Genetics *38*, 251–257.

Paradis, S., Ailion, M., Toker, A., Thomas, J.H., and Ruvkun, G. (1999). A PDK1 homolog is necessary and sufficient to transduce AGE-1 PI3 kinase signals that regulate diapause in Caenorhabditis elegans. Genes & Development *13*, 1438–1452.

Paradis, S., and Ruvkun, G. (1998). Caenorhabditis elegans Akt/PKB transduces insulin receptor-like signals from AGE-1 PI3 kinase to the DAF-16 transcription factor. Genes & Development *12*, 2488–2498.

Patel, D.S., Fang, L.L., Svy, D.K., Ruvkun, G., and Li, W. (2008). Genetic identification of HSD-1, a conserved steroidogenic enzyme that directs larval development in Caenorhabditis elegans. Development *135*, 2239–2249.

Pierce, S.B., Costa, M., Wisotzkey, R., Devadhar, S., Homburger, S.A., Buchman, A.R., Ferguson, K.C., Heller, J., Platt, D.M., Pasquinelli, A.A., et al. (2001). Regulation of DAF-2 receptor signaling by human insulin and ins-1, a member of the unusually large and diverse C. elegans insulin gene family. Genes & Development *15*, 672–686.

Priess, J.R., Schnabel, H., and Schnabel, R. (1987). The glp-1 locus and cellular interactions in early C. elegans embryos. Cell *51*, 601–611.

Ren, P., Lim, C.S., Johnsen, R., Albert, P.S., Pilgrim, D., and Riddle, D.L. (1996). Control of C. elegans larval development by neuronal expression of a TGF-beta homolog. Science *274*, 1389–1391.

Riddle, D.L. (1988). The Dauer Larva. In The Nematode Caenorhabditis Elegans, W.B. Wood editor, ed. (Plainview (New York): Cold Spring Harbor Laboratory Press), pp. 393–412.

Rottiers, Motola, Gerisch, Cummins, Nishiwaki, Mangelsdorf, and Antebi (2006). Hormonal Control of C. elegans Dauer Formation and Life Span by a Rieske-like Oxygenase. Developmental Cell *10*, 473–482.

Saitou, N., and Nei, M. (1987). The neighbor-joining method: a new method for reconstructing phylogenetic trees. Mol Biol Evol *4*, 406–425.

Schackwitz, W.S., Inoue, T., and Thomas, J.H. (1996). Chemosensory neurons function in parallel to mediate a pheromone response in C. elegans. Neuron *17*, 719–728.

Sharma, K.K., Wang, Z., Motola, D.L., Cummins, C.L., Mangelsdorf, D.J., and Auchus, R.J. (2009). Synthesis and activity of dafachronic acid ligands for the C. elegans DAF-12 nuclear hormone receptor. Molecular Endocrinology *23*, 640–648.

Simard, J., Ricketts, M.-L.L., Gingras, S., Soucy, P., Feltus, F.A., and Melner, M.H. (2005). Molecular biology of the 3beta-hydroxysteroid dehydrogenase/delta5-delta4 isomerase gene family. Endocr Rev *26*, 525–582.

Stein, L.D., Bao, Z., Blasiar, D., Blumenthal, T., Brent, M.R., Chen, N., Chinwalla, A., Clarke, L., Clee, C., Coghlan, A., et al. (2003). The genome sequence of Caenorhabditis briggsae: a platform for comparative genomics. PLoS Biology *1*, E45.

Thomas, J.H., Birnby, D.A., and Vowels, J.J. (1993). Evidence for parallel processing of sensory information controlling dauer formation in Caenorhabditis elegans. Genetics *134*, 1105–1117.

Vowels, J.J., and Thomas, J.H. (1992). Genetic Analysis of Chemosensory Control of Dauer Formation in Caenorhabditis elegans. Genetics *130*, 105–123.

Willcox, B.J., Donlon, T.A., He, Q., Chen, R., Grove, J.S., Yano, K., Masaki, K.H., Willcox, D.C., Rodriguez, B., and Curb, J.D. (2008). FOXO3A genotype is strongly associated with human longevity. Proceedings of the National Academy of Sciences *105*, 13987–13992.

Zhang, Y., Xu, J., Puscau, C., Kim, Y., Wang, X., Alam, H., and Hu, P.J. (2008). Caenorhabditis elegans EAK-3 inhibits dauer arrest via nonautonomous regulation of nuclear DAF-16/FoxO activity. Developmental Biology *315*, 290–302.

Chapter 3: The influence of steroid hormone signaling on life span control by *Caenorhabditis elegans* insulin-like signaling[2]

Abstract

Sterol-sensing nuclear receptors and insulin-like growth factor signaling play evolutionarily conserved roles in the control of aging. In the nematode Caenorhabditis elegans, bile-acid-like steroid hormones known as dafachronic acids (DAs) influence longevity by binding to and regulating the activity of the conserved nuclear receptor DAF-12, and the insulin receptor (InsR) ortholog DAF-2 controls life span by inhibiting the FoxO transcription factor DAF-16. How the DA/DAF-12 pathway interacts with DAF-2/InsR signaling to control life span is poorly understood. Here we specifically interrogate the roles of liganded and unliganded DAF-12 in life span control in the context of reduced DAF-2/InsR signaling. In animals with reduced DAF-2/InsR activity, mutations that either reduce DA biosynthesis or fully abrogate DAF-12 activity shorten life span, suggesting that liganded DAF-12 promotes longevity. In animals with reduced DAF-2/InsR activity induced by *daf-2*/InsR RNAi, both liganded and unliganded DAF-12 promote longevity. However, in *daf-2*/InsR mutants, liganded and unliganded DAF-12 act in opposition to control life span. Thus, multiple DAF-12 activities influence life span in distinct ways in contexts of reduced DAF-2/InsR signaling. Our findings establish new roles for a conserved steroid signaling pathway in life span control and elucidate interactions among DA biosynthetic pathways, DAF-12, and DAF-2/InsR signaling in aging.

[2] Originally published in *G3: Genes Genomes Genetics* (published online ahead of print March 18, 2013) with authors listed as Dumas, K.J., Guo, C., Shih, H., and Hu, P.J..

Introduction

Steroid hormones have critical functions in development and the maintenance of homeostasis throughout metazoan phylogeny. They exert their effects largely by binding to and regulating the activity of transcription factors of the nuclear receptor superfamily (Wollam and Antebi, 2011). In the nematode *C. elegans*, bile-acid-like steroid hormones known as dafachronic acids (DAs) are nuclear receptor ligands that control development and life span by binding to and regulating the activity of the nuclear receptor DAF-12 (Motola et al., 2006). Two structurally related DAs, Δ^4- and Δ^7-DA, differ in potency but appear to have similar functions in regulating larval development (Sharma et al., 2009).

Genetic analyses and rescue experiments with presumed DA biosynthetic intermediates are consistent with a model whereby Δ^4- and Δ^7-DA are synthesized from cholesterol via distinct pathways [Figure 3.1A; (Wollam et al., 2012)]. The Rieske oxygenase family member DAF-36 catalyzes the first step of Δ^7-DA biosynthesis by synthesizing 7-dehydrocholesterol [7-DHC; (Rottiers et al., 2006; Wollam et al., 2011; Yoshiyama-Yanagawa et al., 2011)]. 7-DHC is thought to be converted into lathosterol, the 3-OH group of which is subsequently oxidized by the 3-hydroxysteroid dehydrogenase DHS-16 to create lathosterone (Rottiers et al., 2006; Wollam et al., 2012). Lathosterone is a direct Δ^7-DA precursor which is a substrate for the cytochrome P450 family member DAF-9 (Motola et al., 2006). The enzyme that catalyzes the conversion of 7-DHC into lathosterol has not been identified.

DAF-9 catalyzes the final common step of DA biosynthesis, converting lathosterone into Δ^7-DA and 4-cholesten-3-one into Δ^4-DA (Motola et al., 2006). Whereas Δ^7-DA is detectable in lipid extracts from wild-type *C. elegans*, it is not detectable in extracts from *daf-36* or *daf-9* mutants, indicating that both DAF-36 and DAF-9 are required for Δ^7-DA synthesis *in vivo* (Motola et al., 2006; Wollam et al., 2011). Δ^4-DA has not been unequivocally identified in *C. elegans* extracts.

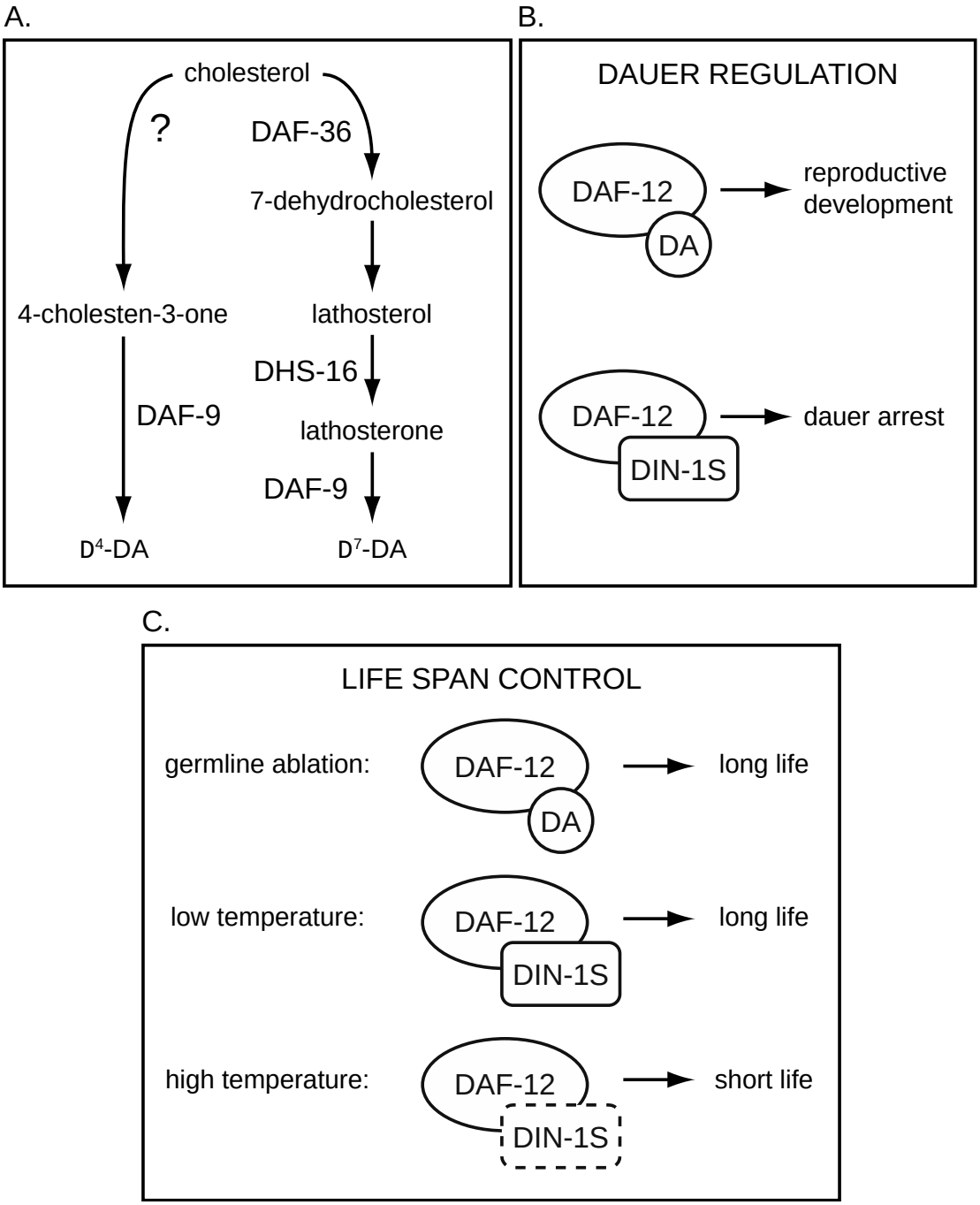

Figure 3.1: Models of dafachronic acid (DA) biosynthetic pathways and DAF-12 complexes in the control of dauer arrest and life span.
(A.) Hypothetical model of DA biosynthesis, adapted from WOLLAM *et al.* 2012. (B.) Liganded DAF-12 promotes reproductive development, whereas unliganded DAF-12 acts with DIN-1S to promote dauer arrest. (C.) Liganded DAF-12 promotes longevity in animals lacking a germline. Unliganded DAF-12 acts with DIN-1S to promote longevity at low temperatures (15°) but shortens life span at higher temperatures (20°-25°). The role of DIN-1S in life span control at higher temperatures is not known.

DAs and DAF-12 have multiple functions during larval development. In conditions of high population density, food scarcity, and high temperature, wild-type *C. elegans* larvae undergo developmental arrest in an alternative third larval stage known as dauer. Dauers are long-lived and resistant to environmental insults (Hu, 2007). *daf-9* mutants, which lack endogenous DAs (Motola et al., 2006), arrest as dauers constitutively, even when ambient conditions favor reproductive development (Gerisch et al., 2001; Jia et al., 2002). This dauer-constitutive phenotype is fully suppressed by exogenous DA (Motola et al., 2006; Giroux et al., 2008; Sharma et al., 2009) as well as by null mutations in *daf-12* (Gerisch et al., 2001). *daf-12* ligand binding domain mutants also have a dauer-constitutive phenotype (Antebi et al., 1998, 2000). Therefore, unliganded DAF-12 promotes dauer arrest. The dauer-constitutive phenotype of *daf-9* mutants and *daf-12* ligand binding domain mutants is also suppressed by mutations in *din-1S*, which encodes a transcriptional coregulator that binds to DAF-12 (Ludewig et al., 2004).

Taken together, these results support a model whereby unliganded DAF-12 acts together with DIN-1S to promote dauer arrest; DAs permit reproductive development by binding to DAF-12, thereby preventing its interaction with DIN-1S [Figure 3.1B; (Fielenbach and Antebi, 2008)]. DAs are also required during larval development for proper gonadal migration (Gerisch et al., 2001; Motola et al., 2006) and expression of *let-7*-family microRNAs that coordinate the timing of cell divisions (Bethke et al., 2009; Hammell et al., 2009). In adult males, DAs are required for normal mate searching behavior (Kleemann et al., 2008).

The roles of DAs and DAF-12 in the control of adult life span are complex. *daf-9* mutants are long-lived when cultured at 15° (Jia et al., 2002; Gerisch et al., 2007) but short-lived when cultured at temperatures between 20° and 25° (Gerisch et al., 2001, 2007; Jia et al., 2002; Lee and Kenyon, 2009). These temperature-dependent phenotypes are suppressed by *daf-12* loss-of-function mutations (Jia et al., 2002; Lee and Kenyon, 2009) and exogenous DA (Gerisch et al., 2007), suggesting that unliganded DAF-12 promotes longevity at low temperatures but shortens life span at higher temperatures (Figure 3.1C). *din-1S* mutation suppresses the life span extension conferred by *daf-9* mutation at low

temperatures (Ludewig et al., 2004), indicating that at 15°, unliganded DAF-12 and DIN-1S act together to extend life span (Figure 3.1C).

DAs and DAF-12 have a profound influence on life span in animals lacking a germline. Ablation of the germline extends adult life span at 20° by ~60%, and this life span extension requires DAF-9, DAF-36, DAF-12, and the FoxO transcription factor DAF-16 (Hsin and Kenyon, 1999; Gerisch et al., 2001, 2007). Exogenous DA restores life span extension in germline-ablated animals harboring *daf-9* or *daf-36* mutations (Gerisch et al., 2007), indicating that liganded DAF-12 promotes longevity in this context (Figure 3.1C).

Similar to germline ablation, loss-of-function mutations in *daf-2*, which encodes the sole *C. elegans* insulin/insulin-like growth factor receptor family member (InsR) (Kimura et al., 1997), extend *C. elegans* life span in a DAF-16/FoxO-dependent manner (Kenyon et al., 1993). Both DAF-2/InsR and the germline inhibit DAF-16/FoxO activity by promoting its translocation from the nucleus to the cytoplasm (Henderson and Johnson, 2001; Lee et al., 2001; Lin et al., 2001). In mutants that either lack a germline or have reduced DAF-2/InsR signaling, DAF-16/FoxO enters the nucleus, activating a gene regulatory program that promotes longevity (Murphy et al., 2003; McCormick et al., 2012).

How DAs and DAF-12 influence life span in the context of reduced DAF-2/InsR signaling is poorly understood. The *daf-9* missense allele *rh50* has distinct effects on life span in the context of specific *daf-2* mutant alleles. At 15°, *daf-9(rh50)* shortens the life span of both *daf-2(e1368)* (harboring a missense mutation in the DAF-2 ligand binding domain) and *daf-2(e1370)* (harboring a missense mutation in the tyrosine kinase domain) mutant animals. However, at 22.5°, *daf-9(rh50)* shortens *daf-2(e1368)* life span but lengthens *daf-2(e1370)* life span (Gerisch et al., 2001). Accordingly, exogenous Δ^4-DA prolongs the life span of *daf-2(e1368)* animals but does not significantly influence the life span of *daf-2(e1370)* animals (Gerisch et al., 2007). Furthermore, *daf-12* mutant alleles influence the life span of *daf-2/InsR* mutants in an allele-specific manner. For example,

the non-null allele *daf-12(m20)* [Supplemental Figure 3.1; (Antebi et al., 2000; Snow and Larsen, 2000)] suppresses the extended life span phenotype of *daf-2(e1365)* [harboring a mutation in the ligand binding domain; (Patel et al., 2008)] at all temperatures tested (Gems et al., 1998), whereas it enhances *daf-2(e1370)* life span extension at high temperatures (Larsen et al., 1995; Gems et al., 1998). In aggregate, these data underscore the need for further investigation into how steroid hormone signaling and DAF-2/InsR signaling interact in life span control. Specifically, the relative contributions of liganded and unliganded DAF-12 to life span control have not been defined. Prior studies on the interactions of *daf-12* and *daf-2/InsR* mutants in life span control were performed with non-null alleles of *daf-12* (Larsen et al., 1995; Gems et al., 1998), complicating the interpretation of these experiments.

Here we use null alleles of *daf-36* and *daf-12* to explore the relationship between DA pathways and DAF-2/InsR signaling in life span regulation. Our results are consistent with a model whereby both liganded and unliganded DAF-12 influence life span. Liganded DAF-12 promotes longevity in animals with reduced DAF-2/InsR signaling. Unliganded DAF-12 also extends life span in animals subjected to *daf-2/InsR* RNAi but shortens life span in *daf-2/InsR* mutants and in animals lacking a germline. These findings establish that distinct DAF-12 activities interact with DAF-2/InsR signaling to control life span.

Materials and Methods

C. elegans strains

The wild-type N2 Bristol strain was used. Mutant alleles used in this study are described in Supplemental Table 3.1. Compound mutants were constructed using standard techniques.

Dauer arrest assays

Dauer arrest assays were performed at the indicated temperatures in Percival I-36NL incubators (Percival Scientific, Inc., Perry, IA) as described (Hu et al., 2006). P-values

were calculated using Student's t-Test. Statistical analysis of all data is presented in Supplemental Table 3.2.

Life span assays

Life span assays were performed in Percival I-36NL incubators at the indicated temperatures. After alkaline hypochlorite treatment and two generations of growth, young adult animals were placed onto NGM plates containing 25 μg/ml (100 μM) 5-fluoro-2'-deoxyuridine (FUDR; Sigma) and 10 μg/ml nystatin (Sigma) that had been seeded with 20X concentrated *E. coli* OP50. Assays were conducted at 20˚ unless otherwise noted. Viability was assessed visually or with gentle prodding. For life span assays of strains carrying *glp-1(e2141)*, animals were raised at 25˚, and sterile young adult animals were placed onto NGM plates containing nystatin but lacking FUDR as described above. GraphPad Prism (GraphPad Software, La Jolla, CA) was used for data representation and statistical analysis. P-values were calculated using the Log-rank Test. Statistical analysis of all data is presented in Supplemental Table 3.2.

RNAi

Feeding RNAi was performed using variations of standard procedures (Boulton et al., 2002). For dauer assays, NGM plates containing 5 mM IPTG and 25 μg/ml carbenicillin were seeded with 500 μl of overnight culture of *E. coli* HT115 harboring either control L4440 vector or *daf-2* RNAi plasmid. Gravid animals cultured on control or *daf-2* RNAi plates were picked to assay plates for six-hour egg lays. Dauers were scored after progeny had been incubated at 25˚ for 48–60 hours. For life span assays, NGM plates containing 5 mM IPTG, 25 μg/ml carbenicillin, 25 μg/ml FUDR, and 10 μg/ml nystatin were seeded with 500 μl of 5X concentrated overnight culture of *E. coli* HT115 harboring either control L4440 vector or *daf-2* RNAi plasmid. Young adult animals cultured on standard NGM plates seeded with *E. coli* OP50 were picked to RNAi plates and scored for viability as described above.

Results

Modulation of DAF-2/InsR signaling by DAF-12

Two classes of *daf-2* mutants have distinct interactions with the non-null *daf-12(m20)* allele (Gems et al., 1998). The dauer-constitutive phenotype of Class 1 *daf-2* alleles (*e.g.*, the ligand binding domain mutant *e1368*), which are also long-lived and thermotolerant (Gems et al., 1998), is suppressed by *daf-12(m20)*. In contrast, Class 2 *daf-2* alleles (*e.g.*, the tyrosine kinase domain mutant *e1370*), which have pleiotropies in addition to the aforementioned Class 1 phenotypes, have a synthetic non-dauer larval arrest phenotype in combination with *daf-12(m20)* (Vowels and Thomas, 1992; Larsen et al., 1995; Gems et al., 1998).

Notably, *daf-12(m20)* is a nonsense mutation that specifically affects DAF-12A isoforms; it is predicted to truncate DAF-12A upstream of the C-terminal ligand binding domain, potentially resulting in a DAF-12A polypeptide that contains an intact zinc finger in the N-terminal DNA binding domain. The DAF-12B isoform, which contains the ligand binding domain but lacks the DNA binding domain, is not affected by *m20* [Supplemental Figure 3.1; (Antebi et al., 2000; Snow and Larsen, 2000)]. The influence of a *daf-12* null allele on the dauer-constitutive phenotype of *daf-2* mutants has not been explored.

To clarify the epistatic relationship between *daf-2* and *daf-12*, we constructed *daf-2;daf-12* double mutants using the *daf-12(rh61rh411)* null allele [Supplemental Figure 3.1 and Supplemental Table 3.1; heretofore referred to as "*daf-12* null"; (Antebi et al., 2000; Snow and Larsen, 2000)] and performed dauer arrest assays at 25°. As expected, both the Class 1 *daf-2(e1368)* ligand binding domain mutant as well as the Class 2 *daf-2(e1370)* tyrosine kinase domain mutant had strong dauer-constitutive phenotypes (Supplemental Figure 3.2). The dauer-constitutive phenotype of *daf-2(e1368)* was completely suppressed by *daf-12(null)*, consistent with the effect of *daf-12(m20)* on other Class 1 *daf-2* alleles (Gems et al., 1998). At 15°, *daf-2(e1370);daf-12(null)* double mutants developed reproductively into adults (data not shown). At 25°, they arrested as larvae that

were longer and wider than dauers and that lacked both dauer alae and pharyngeal remodeling (Supplemental Figure 3.2 and data not shown). This phenotype is comparable to that previously described for *daf-2(e1370);daf-12(m20)* double mutants (Vowels and Thomas, 1992; Larsen et al., 1995; Gems et al., 1998) and suggests that the DAF-12A isoforms that are affected by the *m20* mutation are the isoforms that prevent non-dauer larval arrest in *daf-2(e1370)* mutants at 25°.

daf-12(m20) also has disparate effects on the longevity of Class 1 and Class 2 *daf-2* mutants (Larsen et al., 1995; Gems et al., 1998). To gain insight into how DAF-12 influences life span in animals with reduced DAF-2/InsR signaling, we measured life spans of *daf-12(null)* animals in three contexts of reduced DAF-2/InsR activity. First, we performed *daf-2* RNAi in wild-type and *daf-12(null)* animals. *daf-2* RNAi does not induce dauer arrest in wild-type animals at 25° but enhances dauer arrest at 27° (Dillin et al., 2002a), suggesting that the extent to which RNAi reduces DAF-2 activity is less than that caused by Class 1 and Class 2 *daf-2* mutant alleles, which all have strong dauer-constitutive phenotypes at 25° (Gems et al., 1998). As previously observed (Dillin et al., 2002b), *daf-2* RNAi extended life span to an degree comparable to *daf-2* mutation (Figures 3.2A-C). Life span extension induced by *daf-2* RNAi was significantly attenuated in *daf-12(null)* animals (Figure 3.2A, 3.2D, and Supplemental Table 3.2: *daf-12(null)* animals subjected to *daf-2* RNAi exhibited a 34.5% decrease in median survival compared to wild-type animals on *daf-2* RNAi, $p < 0.0001$ by the Log-rank Test), suggesting that DAF-12 is required for life span extension in animals with reduced DAF-2/InsR activity. At 25°, *daf-12(null)* mutants live approximately as long as wild-type animals do (Figure 3.2A, $p = 0.0018$; Figure 3.2B, $p = 0.1787$; Figure 3.2C, $p = 0.0678$; Supplemental Table 3.2), indicating that the effect of *daf-12(null)* on the life span of animals subjected to *daf-2* RNAi is unlikely to be due to general frailty. Furthermore, RNAi of three unrelated genes in wild-type and *daf-12(null)* animals revealed that *daf-12(null)* animals do not have an Rde (RNAi-defective) phenotype (Supplemental Figure 3.3). This indicates that the relative reduction in life span extension caused by *daf-2* RNAi in *daf-12(null)* animals is unlikely to be due to reduced inactivation of *daf-2*.

We also assayed the life spans of *daf-2;daf-12(null)* double mutants. Interestingly, although *daf-2(e1368);daf-12(null)* animals had a shorter life span than Class 1 *daf-2(e1368)* single mutants, the effect of *daf-12(null)* on life span extension in the context of the Class 1 *daf-2(e1368)* mutation was significantly smaller than its effect in the context of *daf-2* RNAi (Figure 3.2B, 3.2D, and Supplemental Table 3.2: *daf-2(e1368);daf-12(null)* exhibited a 10.3% decrease in median survival compared to *daf-2(1368)* alone, $p < 0.0001$). Furthermore, *daf-2(e1370);daf-12(null)* animals lived as long as Class 2 *daf-2(e1370)* single mutants (Figure 3.2C, 3.2D, and Supplemental Table 3.2: 0% change in median survival of *daf-2(e1370);daf-12(null)* compared to *daf-2(e1370),* $p = 0.4275$). Taken together, these results suggest that DAF-12 is required for life span extension in the context of RNAi knock-down of *daf-2*, but is largely dispensable for longevity in the context of Class I *daf-2(e1368*) and Class II *daf-2(e1370*) mutants (see comparison of replicate experiments in Figure 3.2D).

A possible explanation for the differences in the influence of DAF-12 on life span between the contexts of *daf-2* RNAi and mutational reduction of DAF-2/InsR activity are the distinct food sources employed in each experimental condition. RNAi by feeding, as used to reduce *daf-2/InsR* activity, involves the use of an *E. coli* strain, HT115, which is distinct from standard lab food source, *E. coli* OP50. It has been shown that using HT115 in place of OP50 as a food source is sufficient to impact *C. elegans* longevity (Maier et al., 2010). To test whether *E. coli* strain differences influence the effect of *daf-12(null)* on life span in the context of reduced DAF-2/InsR activity, we performed life span assays on *daf-2(e1368)* and *daf-2(e1370)* mutant animals grown on *E. coli* HT115 (expressing empty vector control RNAi) as the food source. Under these conditions, *daf-2(e1368);daf-12* double mutants were not shorter lived than *daf-2(e1368)* single mutants (Figures 3.2D, 3.2E, and Supplemental Table 3.2: *daf-2(e1368);daf-12* animals exhibited a 0% change in median life span compared to *daf-2(e1368),* $p = 0.1989$). *daf-2(e1370);daf-12* double mutants grown on HT115 were shorter lived than *daf-2(e1370)* single mutants, but the difference in median life span was not statistically significant (Figures 3.2D, 3.2F, and Supplemental Table 3.2: 12.1% decrease in median life span compared to *daf-2(e1370),* $p = 0.1439$). These results suggest that the food source does

not account for the differential effects of *daf-12(null)* on longevity in the three contexts of reduced *daf-2/InsR* activity that we examined.

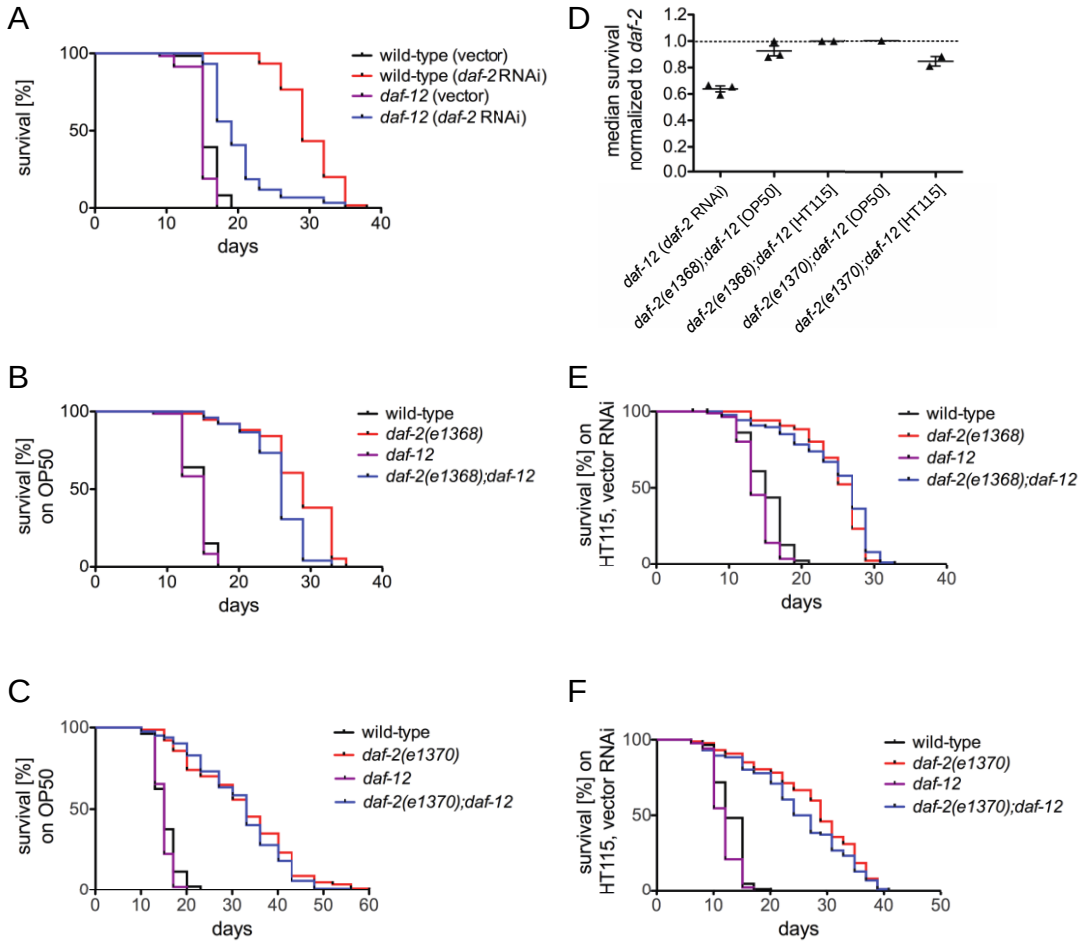

Figure 3.2: Modulation of life span by *daf-12(null)* mutation in animals with reduced DAF-2/InsR activity.
(A.) In the context of DAF-2/InsR activity reduction by *daf-2* RNAi, *daf-12(null)* mutation shortened median life span [*daf-12(null)* v. wild-type, $p < 0.0001$]. (B.) In the context of the Class 1 *daf-2(e1368)* allele, *daf-12(null)* shortened median life span [*daf-2(e1368);daf-12(null)* v. *daf-2(e1368)*, $p < 0.0001$]. (C.) *daf-12(null)* mutation did not shorten median life span of animals with DAF-2/InsR activity reduction via the Class 2 *daf-2(e1370)* allele [*daf-2(e1370);daf-12(null)* v. *daf-2(e1370)*, $p = 0.4275$]. (D.) Scatter plot of median survival of *daf-12(null)* animals normalized to *daf-12* wild-type animals in the three contexts of reduced DAF-2/InsR activity, separated by assay food source. Error bars indicate SEM. (E.-F.) Food source control experiments for (B.) and (C.), respectively. *E. coli* HT115 expressing vector control RNAi was used as the assay food source as opposed to *E. coli* OP50. For each experiment, greater than 60 animals were scored per genotype, and at least two experimental replicates were performed. See Supplemental Table 3.2 for all raw data and statistics.

Modulation of DAF-2/InsR signaling by DA biosynthetic components

Since DAF-12 is regulated by DA ligands (Motola et al., 2006), we explored the influence of mutations in DA biosynthetic pathway components on dauer arrest and life span in animals with reduced DAF-2 activity. Mutations in two genes encoding components of DA biosynthetic pathways, *daf-36* and *daf-9*, cause a dauer-constitutive phenotype (Gerisch et al., 2001; Jia et al., 2002; Rottiers et al., 2006). The null allele *daf-36(k114)*(Rottiers et al., 2006) (heretofore referred to as "*daf-36(null)*") and the partial loss-of-function allele *daf-9(k182)* enhanced the dauer-constitutive phenotype induced by *daf-2* RNAi at 25°C (Figure 3.3A). They also enhanced the dauer-constitutive phenotype of the Class 1 *daf-2(e1368)* ligand binding domain mutant at 20° (Figure 3.3B) and 15° (Supplemental Figure 3.4).

To elucidate interactions between DA biosynthetic pathways and DAF-2/InsR signaling in life span control, we performed life span assays in *daf-36(null)* and *daf-9(k182)* mutants in two contexts of reduced DAF-2/InsR activity: *daf-2* RNAi and *daf-2(e1368).* *daf-36(null)* and *daf-9(k182)* mutations both reduced life span extension induced by *daf-2* RNAi (Figure 3.3C: *daf-36(null)* exhibited a 25.8% decrease in life span compared to wild-type animals on *daf-2* RNAi, $p < 0.0001$; Figure 3.3D: *daf-9(k182)* exhibited a 28.1% decrease in median life span compared to wild-type, $p < 0.0001$; Supplemental Table 3.2). Since neither Δ^4- nor Δ^7-DA is detectable in *daf-36* null mutants (Wollam et al., 2011), these results suggest that DAs are required for maximal life span extension in animals subjected to *daf-2* RNAi. Similar to the case for DAF-12 (Figure 3.2), the requirement for DA biosynthesis in life span extension induced by reduced DAF-2/InsR activity is dependent on the context of InsR activity reduction, as the magnitude of life span reduction caused by *daf-36* and *daf-9* mutations was smaller in animals harboring the Class 1 *daf-2(e1368)* allele than in animals subjected to *daf-2* RNAi (Figure 3.3E: *daf-2(e1368);daf-36(null)* median life span was 10.3% less than that of *daf-2(e1368),* $p < 0.0001$; Figure 3.3F: *daf-2(e1368);daf-9(k182)* median life span was 10.3% less than that of *daf-2(e1368),* $p < 0.0001$; compare to Figures 3.3C-D; Supplemental Table 3.2; results summarized in Table 3.1).

The difference in response on *daf-2* RNAi compared to *daf-2/InsR* genetic mutation was not due to differences in the *E. coli* strain used as a food source, as *daf-2(e1368)* mutant animals had similar life spans when assayed on *E. coli* HT115 (with vector control RNAi) and *E. coli* OP50 (Figure 3.3G: on HT115, median life span of *daf-2(e1368);daf-36(null)* animals was 7.4% shorter than *daf-2(e1368)*, p = 0.4328; Figure 3.3H: on HT115, median life span of *daf-2(e1368);daf-9(k182)* animals was 7.4% shorter than *daf-2(e1368)*, p = 0.2991; Supplemental Table 3.2). Collectively, these data suggest that both DAs and DAF-12 contribute to life span extension in animals with reduced DAF-2/InsR activity.

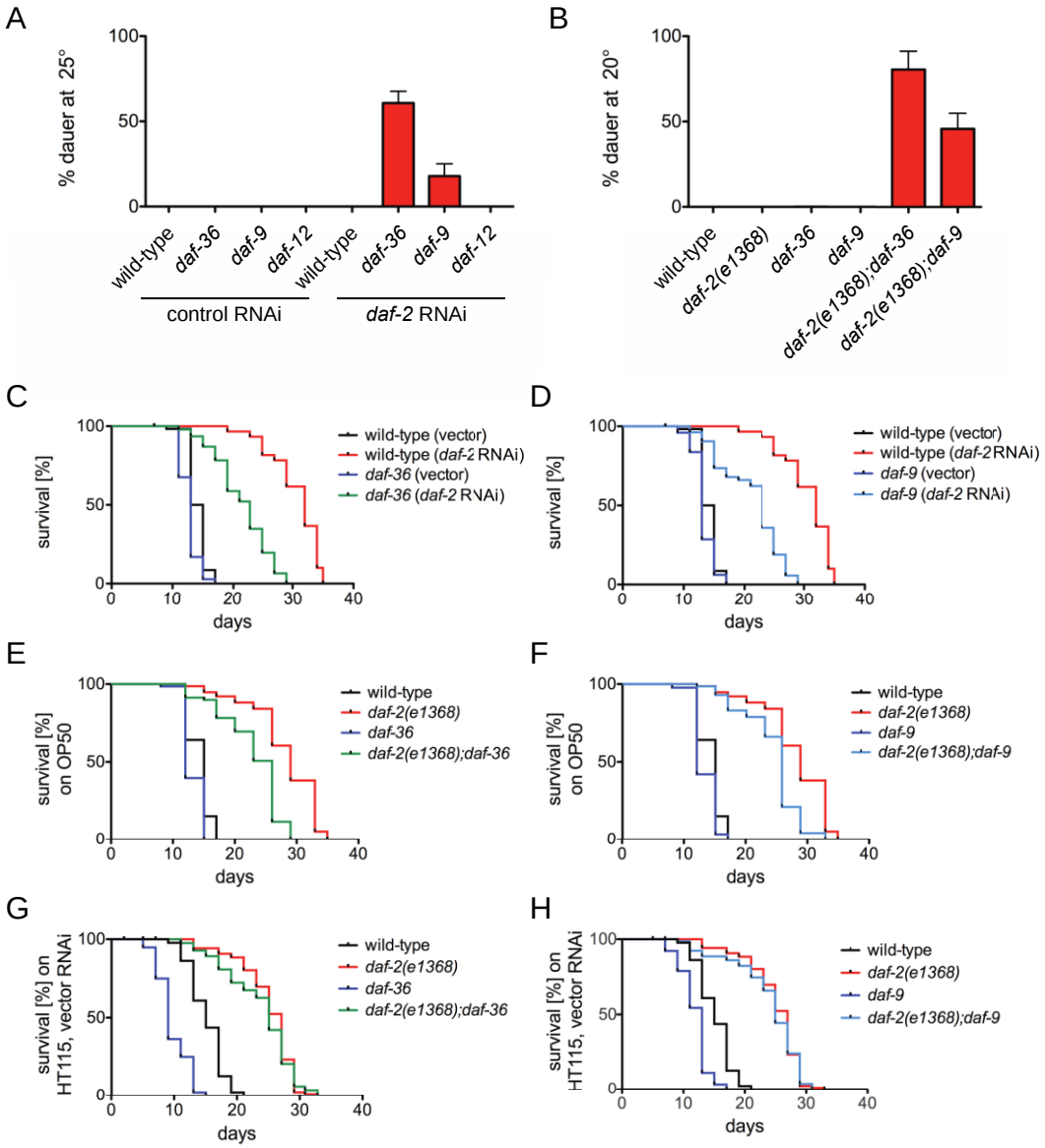

Figure 3.3: Mutations that reduce DA biosynthesis promote dauer arrest and shorten life span in animals with reduced DAF-2/InsR signaling.
(A.-B.) *daf-36(null)* and *daf-9(k182)* mutations enhance dauer arrest of animals subjected to *daf-2* RNAi, (A.), [wild-type on *daf-2* RNAi v. *daf-36(null)* on *daf-2* RNAi, p = 0.0009; wild-type on *daf-2* RNAi v. *daf-9(k182)* on *daf-2* RNAi, p = 0.0689], or harboring the Class I *daf-2(e1368)* allele, (B.), [*daf-2(e1368)* v. d*af-2(e1368);daf-36(null)*, p = 0.0017; *daf-2(e1368)* v. d*af-2(e1368);daf-9(k182)*, p = 0.0072]. Data represent the average of three replicate experiments, with a minimum of 400 animals scored per genotype. Error bars indicate SEM. (C.-D.) *daf-36(null)* or *daf-9(k182)* mutations reduce life span of animals subjected to d*af-2* RNAi [p < 0.0001] or (E.-F.) harboring the Class I *daf-2(e1368)* allele [p < 0.0001]. (G.-H.) Food source control experiments for (E.) and (F.), respectively. *E. coli* HT115 expressing vector control RNAi was used as the assay food source as opposed to *E. coli* OP50. For each life span experiment, greater than 60 animals were assayed per genotype. All raw data and statistics are presented in Supplemental Table 3.2.

Role of unliganded DAF-12 in life span control by DAF-2/InsR signaling

To elucidate the relative contributions of liganded and unliganded DAF-12 to life span control in animals with reduced DAF-2/InsR signaling, we determined the influence of *daf-12(null)* mutation on the life spans of *daf-36(null)* animals with reduced DAF-2/InsR activity. Since *daf-36(null)* animals do not make Δ^4- or Δ^7-DA (Wollam et al., 2011), DAF-12 activity in the context of *daf-36(null)* is largely attributable to unliganded DAF-12.

In animals subjected to *daf-2* RNAi, *daf-36(null)* mutation reduced life span (Figures 3.3C and 3.4A), as did the hypomorphic *daf-9(k182)* mutation (Figure 3.3D). *daf-36(null);daf-12(null)* animals subjected to *daf-2* RNAi had even shorter life spans than *daf-36(null)* single mutants subjected to *daf-2* RNAi (Figure 3.4A and Supplemental Table 3.2: *daf-36(null);daf-12(null)* had a 25.9% decrease in median life span compared to *daf-36(null)* on *daf-2* RNAi, $p < 0.0001$). From this finding, we infer that unliganded DAF-12 promotes longevity in the context of *daf-2* RNAi.

In the *daf-2(e1368)* background, *daf-36(null)* and *daf-9(k182)* mutations also reduced life span (Figures 3.3E, 3.3F, and 3.4B). However, in contrast to our findings with *daf-2* RNAi, *daf-12(null)* mutation did not further shorten the life spans of *daf-2(e1368);daf-36(null)* double mutant animals. Whereas *daf-12(null)* mutation shortened the life span of *daf-36(null)* animals subjected to *daf-2* RNAi (Figure 3.4A, 25.9% decrease in median life span, $p < 0.0001$), it extended the life span of *daf-2(e1368);daf-36(null)* animals fed *E. coli* OP50 (Figure 3.4B and Supplemental Table 3.2: 29.2% increase in median life span of *daf-2(e1368);daf-36(null);daf-12(null)* compared to *daf-2(e1368);daf-36(null),* $p < 0.0001$). The food source does not account for this difference; in contrast to the context of *daf-2* RNAi, *daf-12(null)* mutation did not shorten the life spans of *daf-2(e1368);daf-36(null)* mutant animals when animals were grown on *E. coli* HT115 (Figure 3.4C and Supplemental Table 3.2; 0% change in median life span comparing *daf-2(e1368);daf-36(null);daf-12(null)* to *daf-2(e1368);daf-36(null),* $p = 0.6097$). Because *daf-12* null mutation in the context of *daf-2(e1368)* mutation and the absence of DA is either beneficial or neutral to life span (Figures 3.4B-C), we conclude that unliganded DAF-12

shortens life span in *daf-2(e1368)* mutant animals. We were unsuccessful in our efforts to construct *daf-2(e1370);daf-36(null)* double mutants; this precluded an assessment of the influence of *daf-36(null)* mutation on life span in the *daf-2(e1370)* mutant background.

In aggregate, our results (summarized in Table 3.1) support roles for both liganded and unliganded DAF-12 in life span control in animals with reduced DAF-2/InsR signaling. Liganded DAF-12 promotes longevity in all contexts tested, whereas unliganded DAF-12 modulates life span in a context-dependent manner; in the context of reduced DAF-2/InsR signaling via *daf-2* RNAi, unliganded DAF-12 promotes longevity. In contrast, in the context of DAF-2/InsR signaling reduction via *daf-2(e1368)* mutation, unliganded DAF-12 is detrimental to life span.

Role of unliganded DAF-12 in life span control by the germline

Although both DAF-2/InsR and the germline control life span by regulating DAF-16/FoxO activity, they do so through distinct molecular pathways (Hsin and Kenyon, 1999; Berman and Kenyon, 2006; Ghazi et al., 2009). DA biosynthetic enzymes and DAF-12 are required for life span extension induced by germline ablation (Hsin and Kenyon, 1999; Gerisch et al., 2001, 2007; Yamawaki et al., 2010), suggesting that liganded DAF-12 is important in promoting longevity in animals lacking a germline. In light of our finding that unliganded DAF-12 can shorten life span in *daf-2* mutants (Figure 3.4B), we sought to determine whether unliganded DAF-12 also shortens life span in animals lacking a germline.

We confirmed previously established requirements for *daf-36* and *daf-12* in life span extension induced by germline ablation [Figure 3.4C; (Hsin and Kenyon, 1999; Gerisch et al., 2007; Yamawaki et al., 2010)]. Notably, in three of five replicate experiments, we found that *glp-1;daf-12(null)* animals lived longer than *glp-1;daf-36(null)* animals (Figure 3.4D and Supplemental Table 3.2). Since *daf-36(null)* animals do not make Δ^4- or Δ^7-DA (Wollam et al., 2011), this result suggested the possibility that unliganded DAF-12 shortens life span in animals lacking a germline. To determine whether this was the case, we examined the influence of *daf-12(null)* mutation on life span in germline-ablated

daf-36(null) animals. *glp-1;daf-36(null);daf-12(null)* triple mutant animals lived significantly longer than *glp-1;daf-36(null)* double mutant animals (Figure 3.4D and Supplemental Table 3.2: 27.3% increase in median life span of *glp-1;daf-36(null);daf-12(null)* compared to *glp-1;daf-36(null),* $p < 0.0001$), indicating that unliganded DAF-12 also shortens life span in germline-ablated animals. This result was recapitulated by control experiments performed on *E. coli* HT115 as the food source (Figure 3.4E and Supplemental Table 3.2: 18.2% increase in median life span of *glp-1;daf-36(null);daf-12(null)* compared to *glp-1;daf-36(null),* $p < 0.0001$). Thus, DAF-12 has at least two distinct activities that control life span in germline-ablated animals: liganded DAF-12 promotes longevity, whereas unliganded DAF-12 shortens life span. These findings are summarized in Table 3.1.

Role of the transcriptional coregulator DIN-1S in life span control by the germline

In animals lacking DAs, DIN-1S, the short isoform of the transcriptional coregulator DIN-1, acts in a complex with unliganded DAF-12 to promote dauer arrest [Figure 3.1B; (Ludewig et al., 2004)]. Since unliganded DAF-12 shortens life span in germline-ablated animals (Figure 3.4D), we examined the role of DIN-1S in life span control in animals lacking a germline by determining the impact of the *din-1S* null mutation *dh127* (Ludewig et al., 2004) (heretofore referred to as "*din-1S(null)*") on the life span of *glp-1;daf-36(null)* double mutant animals. *din-1S(null)* animals have life spans comparable to wild-type animals at 15° (Ludewig et al., 2004). Surprisingly, *din-1S(null)* completely suppressed the life span shortening effect of *daf-36(null)* on germline-ablated animals fed *E. coli* OP50 (Figure 3.4D and Supplemental Table 3.2: $p = 0.8829$ for the comparison of *din-1S(null);glp-1;daf-36(null)* to *glp-1* single mutant; *din-1S(null);glp-1;daf-36(null)* median life span was between 35.3% and 118.2% longer than that of *glp-1;daf-36(null)* in four replicate experiments, $p < 0.0001$ for each experiment). This result was replicated with *E. coli* HT115 as the food source (Figure 3.4E and Supplemental Table 3.2: $p = 0.0389$ for the comparison of *din-1S(null);glp-1;daf-36(null)* to *glp-1* single mutant; *din-1S(null);glp-1;daf-36(null)* median life span was 54.4% longer than that of *glp-1;daf-*

36(null), p <0.0001). Thus, in *daf-36(null)* animals lacking a germline, DIN-1S plays a major role in shortening life span.

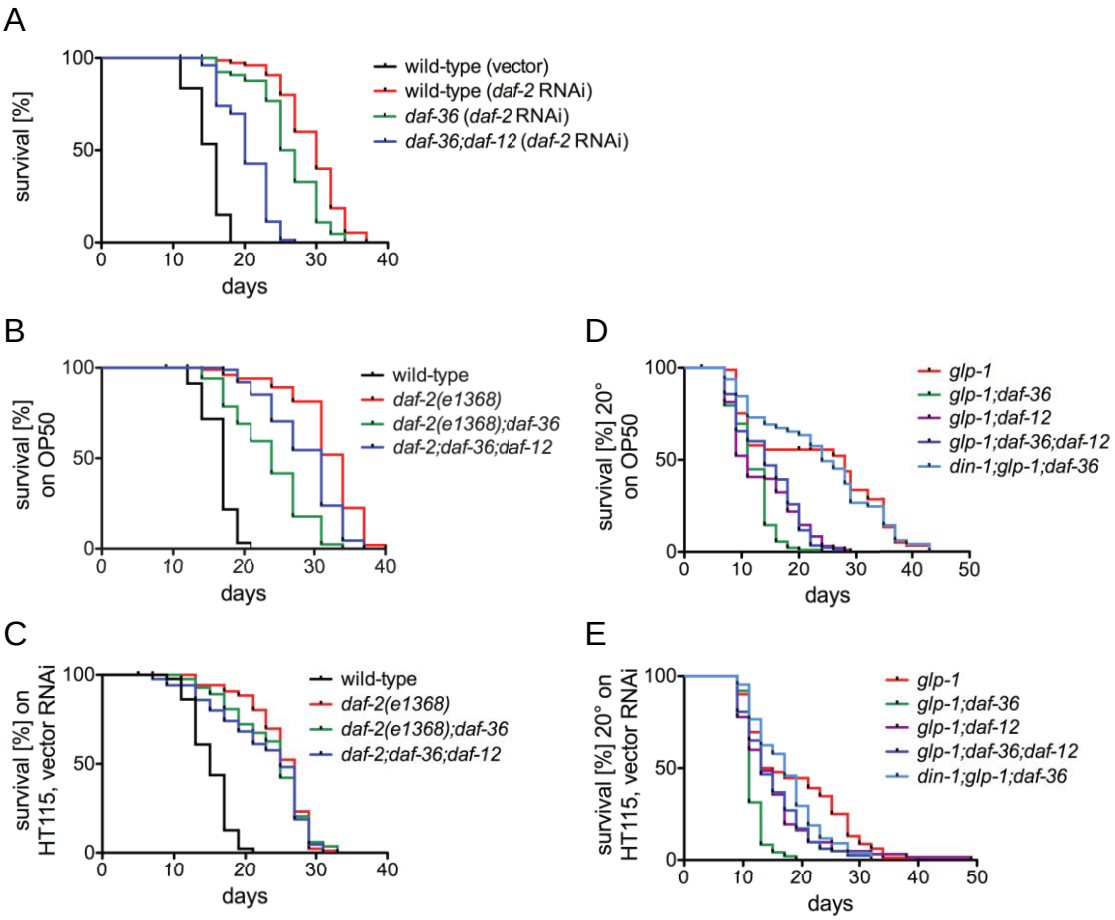

Figure 3.4: Unliganded DAF-12 influences life span in a context-dependent manner. *daf-12(null)* mutation further decreased median life span of *daf-36(null)* animals on *daf-2* RNAi [*daf-36(null);daf-12(null)* v. *daf-36(null)*, p < 0.0001]. (B., D.) In contrast, *daf-12(null)* mutation increased median life span of *daf-36(null)* in the context of *daf-2(e1368)*, (B.), and germline ablation (*glp-1* mutation), (D.) [*daf-2(e1368);daf-36(null);daf-12(null)* v. *daf-2(e1368);daf-36(null)*, p < 0.0001; *glp-1;daf-36(null);daf-12(null)* v. *glp-1;daf-36(null)*, p < 0.0001]. (D.) *din-1S(null)* abrogated life span shortening induced by *daf-36(null)* in the context of germline ablation [*din-1S(null);glp-1;daf-36(null)* v. *glp-1;daf-36(null)*, p < 0.0001]. (C., E.) Food source control experiments for (B.) and (D.), respectively. *E. coli* HT115 expressing vector control RNAi was used as the assay food source as opposed to *E. coli* OP50. For each experiment, greater than 60 animals were assayed per genotype, and at least two experimental replicates were performed. Raw data and statistics are presented in Supplemental Table 3.2.

Genetic context	Percent shortening of life span by *daf-12(null)*	Percent shortening of life span by *daf-36(null)*	Effect of *daf-12(null)* mutation on life span in *daf-36(null)*	Effect of liganded DAF-12 on life span	Effect of unliganded DAF-12 on life span
***daf-2* RNAi**	34.5 (< 0.0001) [Fig. 3.2A]	10.0 (< 0.0001) [Fig. 3.4A]	25.9 (< 0.0001) ↓ [Fig. 3.4A]	↑	↑
daf-2(e1368)	10.3 (< 0.0001) [Fig. 3.2B]	29.4 (< 0.0001) [Fig. 3.4B]	29.2 (< 0.0001) ↑ [Fig. 3.4B]	↑	↓
glp-1(e2141)	60.7 (< 0.0001) [Fig. 3.4D]	60.7 (< 0.0001) [Fig. 3.4D]	27.3 (< 0.0001) ↑ [Fig. 3.4D]	↑	↓

Table 3.1: Summary of effects of *daf-12* and *daf-36* null mutations on life span in three contexts of DAF-16 activation.
daf-2 RNAi, *daf-2(e1368)* mutation, and germline ablation (*glp-1(e2141)* animals raised at the restrictive temperature) were used to induce DAF-16-dependent life span extension. Percent change in median life span *vs.* the comparator (p value) are shown for each indicated experiment. Refer to Supplemental Table 3.2 for replicate experiments. Arrows indicate the direction of effect on life span (↓ decrease, ↑ increase). The two rightmost columns denote the qualitative effects of liganded and unliganded DAF-12 on life span.

Discussion

Although the interface between *C. elegans* hormonal signaling and the DAF-2/InsR pathway has been explored previously (Larsen et al., 1995; Gems et al., 1998), how these pathways interact to influence longevity remains obscure. Our work provides novel insights into the genetic interactions of liganded and unliganded DAF-12 with DAF-2/InsR signaling in life span control.

Liganded DAF-12 promotes longevity in animals with reduced DAF-2/InsR activity

Ambiguity about the role of DAF-12 in determining longevity is due at least in part to the use of the non-null *daf-12(m20)* allele in previous investigations (Larsen et al., 1995; Gems et al., 1998). We now show that the *daf-12(rh61rh411)* null allele and the non-null *daf-12(m20)* allele have distinct effects on the life spans of animals with reduced DAF-2/InsR signaling [Figure 3.2; (Larsen et al., 1995; Gems et al., 1998; McCulloch and Gems, 2007)]. Our results indicate that at high temperatures, DAF-12 promotes longevity in animals with reduced DAF-2/InsR signaling (Figure 3.2). The magnitude of this life-span-extending effect of DAF-12 is greater in animals subjected to *daf-2* RNAi than in animals harboring *daf-2* mutation, indicating that the specific context of reduced DAF-2/InsR activity influences the role of DAF-12 in life span control (Table 3.1). The disparity between our results and those obtained with the non-null *daf-12(m20)* allele (Larsen et al., 1995; Gems et al., 1998) suggests that the longevity-promoting effect of *daf-12(m20)* and other non-null *daf-12* mutations (that specifically affect DAF-12A isoforms) on the life span of *daf-2(e1370)* and other Class 2 *daf-2* mutants (Larsen et al., 1995; Gems et al., 1998; Antebi et al., 2000; McCulloch and Gems, 2007) may be attributable to a life-span-extending activity of either the DAF-12B isoform, which contains a ligand binding domain but no DNA binding domain, or truncated DAF-12A polypeptides containing most of the DNA binding domain but lacking the ligand binding domain (Antebi et al., 2000; Snow and Larsen, 2000). These DAF-12 polypeptides do not play a significant role in dauer regulation by DAF-2/InsR, as *daf-12(null)* and *daf-12(m20)* have similar effects on the dauer-constitutive phenotypes of *daf-2* mutants (Supplemental Figure 3.1).

The observation that mutations in either *daf-12* (Figure 3.2) or genes encoding DA biosynthetic components (Figure 3.2) reduce life span in animals with reduced DAF-2/InsR signaling is consistent with a model whereby liganded DAF-12 promotes longevity when DAF-2/InsR signaling is reduced (Figure 3.5A). Similar results indicate that liganded DAF-12 also promotes longevity in germline-ablated animals [Figure 3.4D; (Hsin and Kenyon, 1999; Gerisch et al., 2001, 2007; Yamawaki et al., 2010)]. The

magnitude of the effect of reducing the activity of DA biosynthetic components or DAF-12 on life span is greater in animals lacking a germline than in animals with reduced DAF-2/InsR activity [Figures 3.2-3.4 (Hsin and Kenyon, 1999; Gerisch et al., 2001, 2007; Yamawaki et al., 2010)]. The molecular basis for this observation is not known.

Unliganded DAF-12 has context-dependent influences on life span in animals with reduced DAF-2/InsR activity

Unliganded DAF-12 promotes longevity in animals cultured at low temperatures (Gerisch et al., 2001; Jia et al., 2002) but shortens life span in animals that are cultured at high temperatures (Lee and Kenyon, 2009). Here we show that in the context of reduced DAF-2/InsR signaling, unliganded DAF-12 can either extend or shorten life span. In *daf-36(null)* animals, which lack both Δ^4- and Δ^7-DA (Wollam and Antebi, 2011), DAF-12 extends life span in the context of *daf-2* RNAi (Figure 3.4A) but shortens life span in the contexts of the Class 1 *daf-2(e1368)* allele (Figure 3.4B) and germline ablation (Figure 3.4D). Since DAF-16/FoxO is a major target of both DAF-2/InsR signaling and germline signaling in life span control (Kenyon et al., 1993; Hsin and Kenyon, 1999), it is likely that the impact of unliganded DAF-12 on longevity is strongly influenced by relative levels of DAF-16/FoxO activity. This notion is supported by a recent report demonstrating that DAF-12 and DAF-16/FoxO mutually influence target gene expression in animals lacking a germline (McCormick et al., 2012).

The transcriptional coregulator DIN-1S shortens life span in animals lacking a germline

DIN-1S acts together with unliganded DAF-12 at 15° to promote longevity (Ludewig et al., 2004). Here we show for the first time that the DAF-12 coregulator DIN-1S plays a major role in life span control in germline-ablated animals. Both *daf-12(null)* and *din-1S(null)* suppressed the life-span-shortening effect of *daf-36(null)* on animals lacking a germline (Figure 3.4D-E). This is consistent with a model whereby unliganded DAF-12 and DIN-1S act together to shorten life span. The role of DIN-1S in life span control by unliganded DAF-12 in the context of reduced DAF-2/InsR signaling is not known.

Context-dependent life span control by DAF-12 complexes

Our results define new functions for DAF-12 complexes in life span control and underscore the context-dependence of these activities (Figure 3.5). As summarized in Table 3.1, liganded DAF-12 promotes longevity both in animals with reduced DAF-2/InsR activity (Figures 3.2A-C, E-F and 3.3C-H) as well as in animals lacking a germline (Figure 3.4D-E; (Gerisch et al., 2007; Yamawaki et al., 2010)). Unliganded DAF-12 also promotes longevity in animals subjected to *daf-2* RNAi (Figure 3.4A) but shortens life span in animals harboring *daf-2* mutations or lacking a germline (Figure 3.4B-E). The basis for the context-dependent influence of unliganded DAF-12 on life span may involve context-specific proteins and/or undiscovered DAF-12 ligands present in *daf-36(null)* animals that influence the transcriptional regulatory activity of DAF-12 complexes.

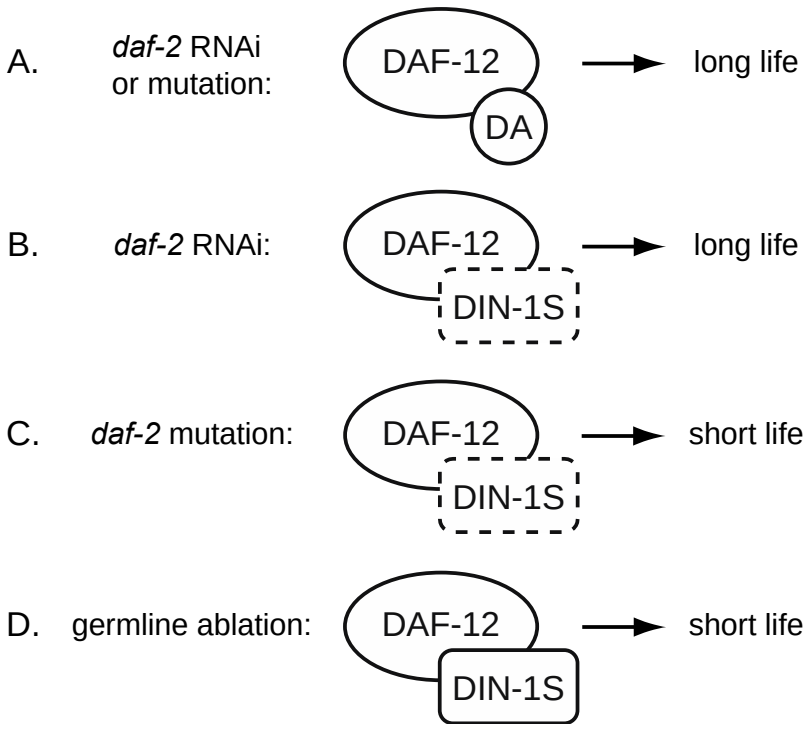

Figure 3.5: New functions of DAF-12 complexes in life span control.
(A.) Liganded DAF-12 promotes longevity in animals with reduced DAF-2 activity. (B.-C.) Unliganded DAF-12 promotes longevity in animals subjected to *daf-2* RNAi (B.) but shortens life span in *daf-2* mutant animals (C.). (D.) Unliganded DAF-12 acts together with DIN-1S to shorten life span in animals lacking a germline.

Supplemental Information

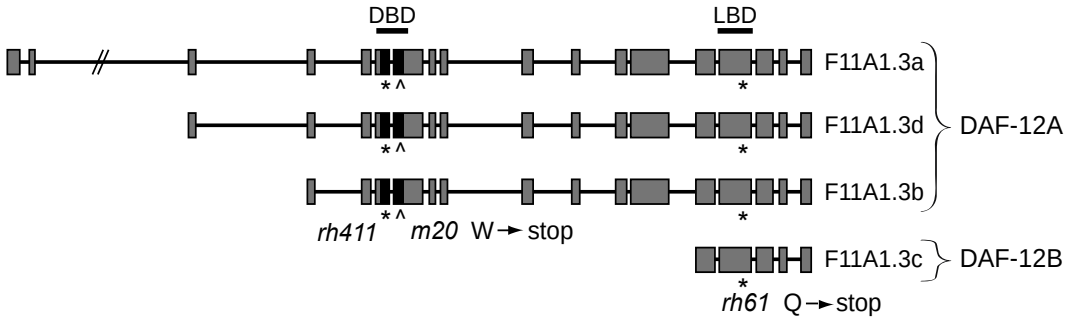

Supplemental Figure 3.1: *daf-12* gene structure, transcripts, and relevant mutations. The structure of *daf-12* transcripts is adapted from WormBase (WBGene00000908). Transcripts corresponding to DAF-12A and DAF-12B isoforms as first described in Antebi *et al.* 2000 and Snow and Larsen 2000 are shown. The location of molecular lesions is taken from Antebi *et al.* 2000 and Snow and Larsen 2000. The *m20* mutation is indicated by a caret, and the *rh411* mutation is indicated by an asterisk in the DNA binding domain. *rh411* is a small deletion/duplication after the first Zn finger in the DNA binding domain that results in an in-frame stop (Antebi et al., 2000). Abbreviations: DBD, DNA binding domain; LBD, ligand binding domain.

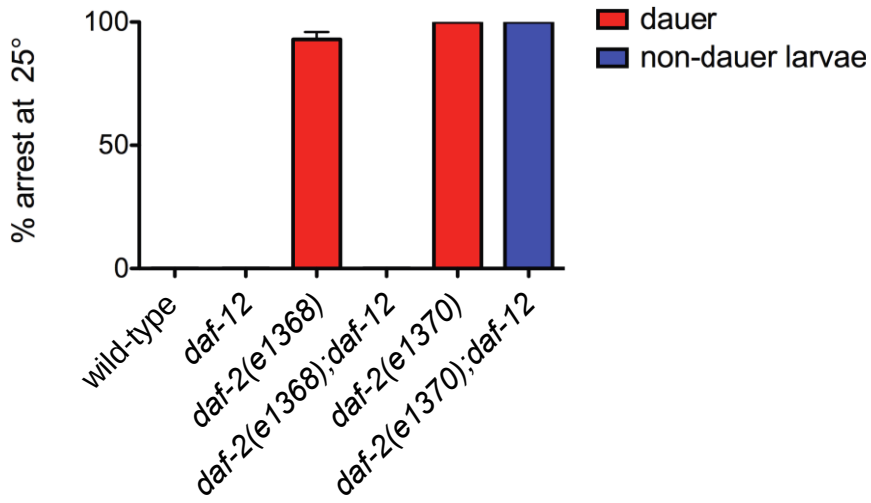

Supplemental Figure 3.2: Larval arrest phenotypes of *daf-2;daf-12(null)* mutants. *daf-12(null)* suppresses dauer arrest of *daf-2(e1368)* mutant animals [*daf-2(e1368)* v. d*af-2(e1368);daf-12(null),* $p < 0.0001$]. *daf-2(e1370);daf-12(null)* animals arrest as non-dauer larvae, see text for details. Data represent the average of at least two replicate experiments, with a minimum of 495 animals scored per genotype. Error bars represent SD. All raw data and statistics are presented in Supplemental Table 3.2.

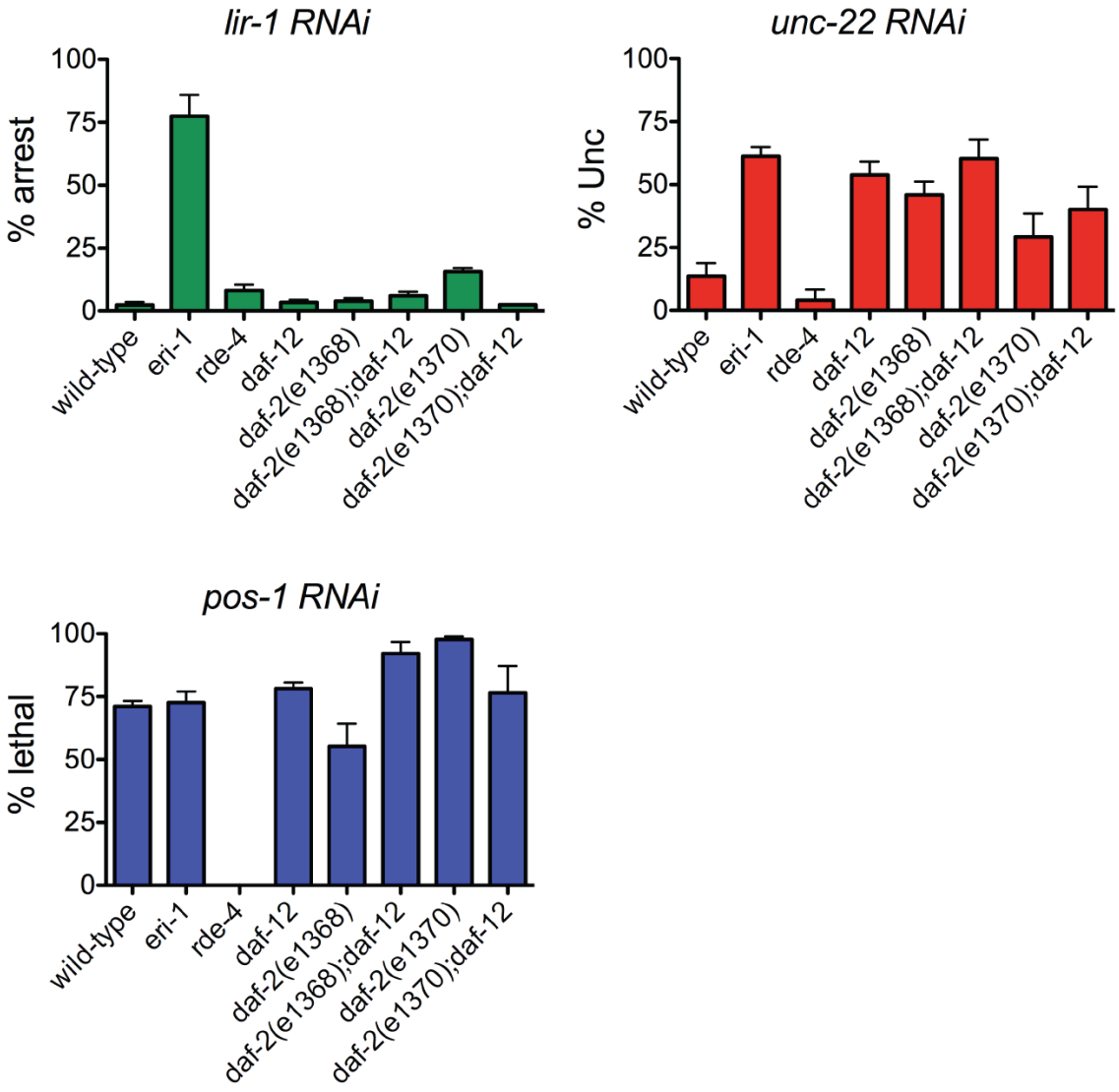

Supplemental Figure 3.3: *daf-12(null)* does not cause an RNAi-defective phenotype. Phenotypes of animals subjected to RNAi of *lir-1*, *unc-22*, and *pos-1* are shown. As controls, the *e*nhanced-*R*NA*i* strain *eri-1(mg366)* and the *R*NAi-*de*fective strain *rde-4 (ne301)* are shown. Error bars represent SEM.

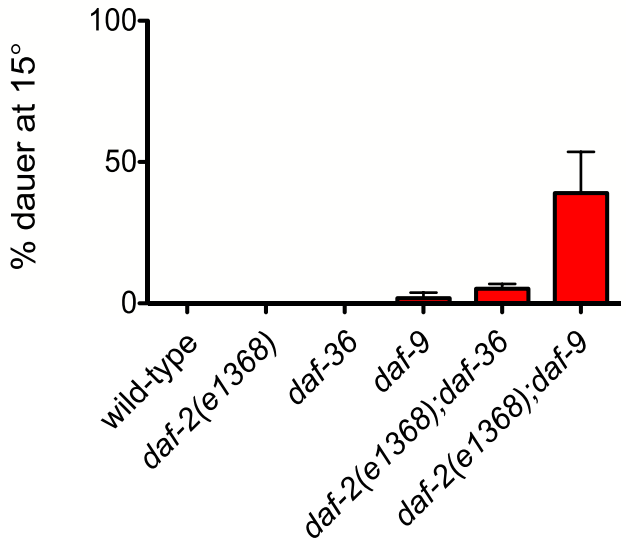

Supplemental Figure 3.4: Enhancement of the dauer-constitutive phenotype *daf-2(e1368)* by mutations in genes encoding DA biosynthetic pathway components. *daf-36(null)* and *daf-9(k182)* mutations enhance dauer arrest of animals harboring the Class I *daf-2(e1368)* allele [*daf-2(e1368)* v. d*af-2(e1368);daf-36(null),* p = 0.0388; *daf-2(e1368)* v. d*af-2(e1368);daf-9(k182),* p = 0.0561]. Data represent the average of three replicate experiments, with a minimum of 700 animals scored per genotype. Error bars represent SEM. All raw data and statistics are presented in Supplemental Table 3.2.

Supplemental Table 3.1: Mutant alleles used in this study.

Gene	Allele	Nature of mutation	Comments	Reference(s)
daf-2	*e1368*	missense, ligand binding domain	Class I	Gems *et al.* 1998; Kimura et al. 1997
daf-2	*e1370*	missense, tyrosine kinase domain	Class II	Gems *et al.* 1998; Kimura et al. 1997
daf-9	k182	missense	hypomorphic allele	Gerisch et al. 2001
daf-12	rh61rh411	nonsense (both mutations)	null; all isoforms affected	Antebi et al. 2000
daf-36	k114	nonsense	null; Δ^7-DA not detectable	Rottiers et al. 2006; Wollam et al. 2011
din-1S	dh127	nonsense	null	Ludewig et al. 2004
glp-1	e2141	missense	animals lack germline when raised at 25°	Priess et al. 1987

Supplemental Table 3.2: Life span and dauer statistics.

figure	assay temp	genotype	mean survival (in days)	+/- SD	# animals (censored)	median survival (in days)	P value (Log-rank) (comparison 1)	P value v. (comparison 1)	% change, median survival (v. compar. 1)	P value (Log-rank) (comparison 2)	P value v. (comparison 2)	% change, median survival (v. compar. 2)
Figure 2A	**25**	**wild-type (vector)**	**15.11**	**2.68**	**61(0)**	**15**	**n/a**	**wild-type (vector)**	**n/a n/a**	**n/a**	**n/a**	**n/a n/a**
		daf-12 (vector)	**15.00**	**1.59**	**58(0)**	**15**	**0.0018**	**wild-type (vector)**	**0.0 no change**	**n/a**	**n/a**	**n/a n/a**
		wild-type (daf-2 RNAi)	**30.05**	**3.61**	**60(0)**	**29**	**< 0.0001**	**wild-type (vector)**	**93.3 increase**	**n/a**	**n/a**	**n/a n/a**
		daf-12 (daf-2 RNAi)	**20.03**	**4.55**	**59(0)**	**19**	**< 0.0001**	**wild-type (daf-2 RNAi)**	**34.5 decrease**	**n/a**	**n/a**	**n/a n/a**
	25	wild-type (vector)	14.10	1.46	58(1)	14	n/a	wild-type (vector)	n/a n/a	n/a	n/a	n/a n/a
		daf-12 (vector)	12.74	1.52	53(6)	13	< 0.0001	wild-type (vector)	7.1 decrease	n/a	n/a	n/a n/a
		wild-type (daf-2 RNAi)	30.62	4.09	60(0)	32	< 0.0001	wild-type (vector)	128.6 increase	n/a	n/a	n/a n/a
		daf-12 (daf-2 RNAi)	19.65	3.95	57(1)	19	< 0.0001	wild-type (daf-2 RNAi)	40.6 decrease	n/a	n/a	n/a n/a
	25	wild-type (vector)	14.88	2.17	73(0)	16	n/a	wild-type (vector)	n/a n/a	n/a	n/a	n/a n/a
		daf-12 (vector)	14.15	1.72	72(0)	14	0.0038	wild-type (vector)	12.5 decrease	n/a	n/a	n/a n/a
		wild-type (daf-2 RNAi)	29.35	4.29	75(0)	30	< 0.0001	wild-type (vector)	87.5 increase	n/a	n/a	n/a n/a
		daf-12 (daf-2 RNAi)	20.14	4.11	65(2)	20	< 0.0001	wild-type (daf-2 RNAi)	33.3 decrease	n/a	n/a	n/a n/a
Figure 2B	**25**	**wild-type**	**14.23**	**1.81**	**106(0)**	**15**	**n/a**	**wild-type**	**n/a n/a**	**n/a**	**n/a**	**n/a n/a**
		daf-12	**13.86**	**1.84**	**72(0)**	**15**	**0.1787**	**wild-type**	**0.0 n/a**	**n/a**	**n/a**	**n/a n/a**
		daf-2(e1368)	**28.24**	**5.39**	**76(0)**	**29**	**< 0.0001**	**wild-type**	**93.3 increase**	**n/a**	**n/a**	**n/a n/a**
		daf-2(e1368);daf-12	**25.56**	**3.95**	**75(0)**	**26**	**< 0.0001**	**daf-2(e1368)**	**10.3 decrease**	**n/a**	**n/a**	**n/a n/a**
	25	wild-type	15.38	2.11	91(0)	17	n/a	wild-type	n/a n/a	n/a	n/a	n/a n/a
		daf-12	14.59	1.89	86(5)	14	0.0039	wild-type	17.6 decrease	n/a	n/a	n/a n/a
		daf-2(e1368)	24.67	5.17	81(0)	26	< 0.0001	wild-type	52.9 increase	n/a	n/a	n/a n/a
		daf-2(e1368);daf-12	23.53	5.54	78(4)	26	0.2228	daf-2(e1368)	0.0 no change	n/a	n/a	n/a n/a
	25	wild-type	14.29	1.10	102(0)	14	n/a	wild-type	n/a n/a	n/a	n/a	n/a n/a
		daf-2(e1368)	24.16	5.43	74(1)	25	< 0.0001	wild-type	78.6 increase	n/a	n/a	n/a n/a
		daf-2(e1368);daf-12	19.66	3.96	56(15)	22	< 0.0001	daf-2(e1368)	12.0 decrease	n/a	n/a	n/a n/a
Figure 2E *HT115 control for Figure 2B*	**25**	**wild-type**	**15.07**	**2.74**	**87(2)**	**15**	**n/a**	**wild-type**	**n/a n/a**	**n/a**	**n/a**	**n/a n/a**
		daf-12	**13.77**	**2.26**	**86(3)**	**13**	**0.0002**	**wild-type**	**13.3 decrease**	**n/a**	**n/a**	**n/a n/a**
		daf-2(e1368)	**24.93**	**4.37**	**86(4)**	**27**	**< 0.0001**	**wild-type**	**80.0 increase**	**n/a**	**n/a**	**n/a n/a**
		daf-2(e1368);daf-12	**24.61**	**5.81**	**88(1)**	**27**	**0.1989**	**daf-2(e1368)**	**0.0 no change**	**n/a**	**n/a**	**n/a n/a**
	25	wild-type	12.89	2.62	85(3)	12	n/a	wild-type	n/a n/a	n/a	n/a	n/a n/a
		daf-12	11.60	2.27	86(1)	12	0.0004	wild-type	0.0 no change	n/a	n/a	n/a n/a
		daf-2(e1368)	23.02	5.26	83(4)	24	< 0.0001	wild-type	100.0 increase	n/a	n/a	n/a n/a
		daf-2(e1368);daf-12	24.18	5.74	87(1)	24	0.0257	daf-2(e1368)	0.0 no change	n/a	n/a	n/a n/a
Figure 2C	**25**	**wild-type**	**15.31**	**2.70**	**77(2)**	**15**	**n/a**	**wild-type**	**n/a n/a**	**n/a**	**n/a**	**n/a n/a**
		daf-12	**14.76**	**1.81**	**84(0)**	**15**	**0.0678**	**wild-type**	**0.0 no change**	**n/a**	**n/a**	**n/a n/a**
		daf-2(e1370)	**32.34**	**11.39**	**77(0)**	**33**	**< 0.0001**	**wild-type**	**120.0 increase**	**n/a**	**n/a**	**n/a n/a**
		daf-2(e1370);daf-12	**31.77**	**9.86**	**82(0)**	**33**	**0.4275**	**daf-2(e1370)**	**0.0 no change**	**n/a**	**n/a**	**n/a n/a**
	20	wild-type	13.49	2.33	77(23)	13.5	n/a	wild-type	n/a n/a	n/a	n/a	n/a n/a
		daf-12	13.56	1.96	56(44)	13.5	0.08576	wild-type	0.0 no change	n/a	n/a	n/a n/a
		daf-2(e1370)	39.46	8.71	97(3)	41.5	< 0.0001	wild-type	207.4 increase	n/a	n/a	n/a n/a
		daf-2(e1370);daf-12	34.82	9.60	97(3)	36.5	< 0.0001	daf-2(e1370)	12.0 decrease	n/a	n/a	n/a n/a
	20	wild-type	15.49	1.76	85(15)	15.5	n/a	wild-type	n/a n/a	n/a	n/a	n/a n/a
		daf-12	15.20	1.70	74(26)	15.5	0.3576	wild-type	0.0 no change	n/a	n/a	n/a n/a
		daf-2(e1370)	41.03	12.54	97(3)	43.5	< 0.0001	wild-type	180.6 increase	n/a	n/a	n/a n/a
		daf-2(e1370);daf-12	38.34	11.23	100(0)	39.5	0.0161	daf-2(e1370)	9.2 decrease	n/a	n/a	n/a n/a
	20	daf-2(e1370)	39.37	9.88	101(0)	40	n/a	daf-2(e1370)	n/a n/a	n/a	n/a	n/a n/a
		daf-2(e1370);daf-12	39.90	9.22	99(1)	39	0.9095	daf-2(e1370)	2.5 decrease	n/a	n/a	n/a n/a
Figure 2F *HT115 control for Figure 2C*	**25**	**wild-type**	**12.89**	**2.62**	**85(3)**	**12**	**n/a**	**wild-type**	**n/a n/a**	**n/a**	**n/a**	**n/a n/a**
		daf-12	**11.60**	**2.27**	**86(1)**	**12**	**0.0004**	**wild-type**	**0.0 no change**	**n/a**	**n/a**	**n/a n/a**
		daf-2(e1370)	**27.60**	**8.85**	**87(1)**	**29**	**< 0.0001**	**wild-type**	**141.7 increase**	**n/a**	**n/a**	**n/a n/a**
		daf-2(e1370);daf-12	**25.23**	**9.17**	**86(0)**	**25.5**	**0.1439**	**daf-2(e1370)**	**12.1 decrease**	**n/a**	**n/a**	**n/a n/a**
	25	wild-type	15.07	2.74	87(2)	15	n/a	wild-type	n/a n/a	n/a	n/a	n/a n/a
		daf-12	13.77	2.26	86(3)	13	0.0002	wild-type	13.3 decrease	n/a	n/a	n/a n/a
		daf-2(e1370)	29.01	8.01	89(1)	31	< 0.0001	wild-type	106.7 increase	n/a	n/a	n/a n/a
		daf-2(e1370);daf-12	24.82	10.14	83(8)	25	0.1719	daf-2(e1370)	19.4 decrease	n/a	n/a	n/a n/a
Figure 3C	**25**	**wild-type (vector)**	**18.64**	**2.31**	**89(0)**	**18**	**n/a**	**wild-type (vector)**	**n/a n/a**	**n/a**	**n/a**	**n/a n/a**
		daf-36 (vector)	**17.55**	**3.34**	**73(1)**	**18**	**0.1054**	**wild-type (vector)**	**0.0 no change**	**n/a**	**n/a**	**n/a n/a**
		wild-type (daf-2 RNAi)	**29.62**	**3.79**	**82(5)**	**31**	**< 0.0001**	**wild-type (vector)**	**72.2 increase**	**n/a**	**n/a**	**n/a n/a**
		daf-36 (daf-2 RNAi)	**21.57**	**4.77**	**67(4)**	**23**	**< 0.0001**	**wild-type (daf-2 RNAi)**	**25.8 decrease**	**n/a**	**n/a**	**n/a n/a**
	25	wild-type (vector)	14.10	1.46	58(1)	14	n/a	wild-type (vector)	n/a n/a	n/a	n/a	n/a n/a
		daf-36 (vector)	12.72	1.52	36(24)	13	< 0.0001	wild-type (vector)	7.1 decrease	n/a	n/a	n/a n/a
		wild-type (daf-2 RNAi)	30.62	4.09	60(0)	32	< 0.0001	wild-type (vector)	128.6 increase	n/a	n/a	n/a n/a
		daf-36 (daf-2 RNAi)	21.57	4.65	46(13)	23	< 0.0001	wild-type (daf-2 RNAi)	28.1 decrease	n/a	n/a	n/a n/a
	25	wild-type (vector)	15.11	2.68	61(0)	15	n/a	wild-type (vector)	n/a n/a	n/a	n/a	n/a n/a
		daf-36 (vector)	14.52	2.05	54(2)	15	< 0.0001	wild-type (vector)	0.0 no change	n/a	n/a	n/a n/a
		wild-type (daf-2 RNAi)	30.05	3.61	60(0)	29	< 0.0001	wild-type (vector)	93.3 increase	n/a	n/a	n/a n/a
		daf-36 (daf-2 RNAi)	23.04	4.57	49(4)	23	< 0.0001	wild-type (daf-2 RNAi)	20.7 decrease	n/a	n/a	n/a n/a
Figure 3D	**25**	**wild-type (vector)**	**14.10**	**1.46**	**58(1)**	**14**	**n/a**	**wild-type (vector)**	**n/a n/a**	**n/a**	**n/a**	**n/a n/a**
		daf-9 (vector)	**13.29**	**1.73**	**49(10)**	**13**	**0.0153**	**wild-type (vector)**	**7.1 decrease**	**n/a**	**n/a**	**n/a n/a**
		wild-type (daf-2 RNAi)	**30.62**	**4.09**	**60(0)**	**32**	**< 0.0001**	**wild-type (vector)**	**128.6 increase**	**n/a**	**n/a**	**n/a n/a**
		daf-9 (daf-2 RNAi)	**21.34**	**5.20**	**53(6)**	**23**	**< 0.0001**	**wild-type (daf-2 RNAi)**	**28.1 decrease**	**n/a**	**n/a**	**n/a n/a**
Figure 3E	**25**	**wild-type**	**14.23**	**1.81**	**106(0)**	**15**	**n/a**	**wild-type**	**n/a n/a**	**n/a**	**n/a**	**n/a n/a**
		daf-36	**13.13**	**1.60**	**68(0)**	**12**	**< 0.0001**	**wild-type**	**20.0 decrease**	**n/a**	**n/a**	**n/a n/a**
		daf-2(e1368)	**28.24**	**5.39**	**76(0)**	**29**	**< 0.0001**	**wild-type**	**93.3 increase**	**n/a**	**n/a**	**n/a n/a**
		daf-2(e1368);daf-36	**22.84**	**4.94**	**69(0)**	**26**	**< 0.0001**	**daf-2(e1368)**	**10.3 decrease**	**n/a**	**n/a**	**n/a n/a**
	25	wild-type	17.38	2.01	58(14)	17	n/a	wild-type	n/a n/a	n/a	n/a	n/a n/a
		daf-36	13.24	1.64	29(42)	14	< 0.0001	wild-type	17.6 decrease	n/a	n/a	n/a n/a
		daf-2(e1368)	34.88	5.50	64(7)	37	< 0.0001	wild-type	117.6 increase	n/a	n/a	n/a n/a
		daf-2(e1368);daf-36	28.70	5.06	66(4)	31	< 0.0001	daf-2(e1368)	16.2 decrease	n/a	n/a	n/a n/a
	25	wild-type	16.48	2.23	92(1)	17	n/a	wild-type	n/a n/a	n/a	n/a	n/a n/a
		daf-2(e1368)	31.82	5.13	102(0)	34	< 0.0001	wild-type	100.0 increase	n/a	n/a	n/a n/a
		daf-2(e1368);daf-36	23.60	5.39	84(4)	24	< 0.0001	daf-2(e1368)	29.4 decrease	n/a	n/a	n/a n/a
	25	wild-type	15.38	2.11	91(0)	17	n/a	wild-type	n/a n/a	n/a	n/a	n/a n/a
		daf-36	13.39	2.97	67(15)	14	< 0.0001	wild-type	17.6 decrease	n/a	n/a	n/a n/a
		daf-2(e1368)	24.67	5.17	81(0)	26	< 0.0001	wild-type	52.9 increase	n/a	n/a	n/a n/a
		daf-2(e1368);daf-36	23.52	5.51	85(0)	26	0.1956	daf-2(e1368)	0.0 no change	n/a	n/a	n/a n/a
Figure 3G *HT115 control for Figure 3E*	**25**	**wild-type**	**15.07**	**2.74**	**87(2)**	**15**	**n/a**	**wild-type**	**n/a n/a**	**n/a**	**n/a**	**n/a n/a**
		daf-36	**9.58**	**2.54**	**45(45)**	**9**	**< 0.0001**	**wild-type**	**40.0 decrease**	**n/a**	**n/a**	**n/a n/a**
		daf-2(e1368)	**24.93**	**4.37**	**86(4)**	**27**	**< 0.0001**	**wild-type**	**80.0 increase**	**n/a**	**n/a**	**n/a n/a**
		daf-2(e1368);daf-36	**23.70**	**5.45**	**83(2)**	**25**	**0.4328**	**daf-2(e1368)**	**7.4 decrease**	**n/a**	**n/a**	**n/a n/a**
	25	wild-type	12.89	2.62	85(3)	12	n/a	wild-type	n/a n/a	n/a	n/a	n/a n/a
		daf-36	10.58	1.97	52(37)	10	< 0.0001	wild-type	16.7 decrease	n/a	n/a	n/a n/a
		daf-2(e1368)	23.02	5.26	83(4)	24	< 0.0001	wild-type	100.0 increase	n/a	n/a	n/a n/a
		daf-2(e1368);daf-36	14.26	5.19	78(6)	15	< 0.0001	daf-2(e1368)	37.5 decrease	n/a	n/a	n/a n/a

Supplemental Table 3.2, continued

figure	assay temp	genotype	mean survival *(in days)*	+/- SD	# animals (censored)	median survival *(in days)*	P value (Log-rank) *(comparison 1)*	P value v. *(comparison 1)*	% change, median survival *(v. compar. 1)*	P value (Log-rank) *(comparison 2)*	P value v. *(comparison 2)*	% change, median survival *(v. compar. 2)*
Figure 3F	**25**	**wild-type**	**14.23**	**1.81**	**106(0)**	**15**	**n/a**	**wild-type**	**n/a n/a**	**n/a**	**n/a**	**n/a n/a**
		daf-9	**13.24**	**1.79**	**88(0)**	**12**	**0.0002**	**wild-type**	**20.0 decrease**	**n/a**	**n/a**	**n/a n/a**
		daf-2(e1368)	**28.24**	**5.39**	**76(0)**	**29**	**< 0.0001**	**wild-type**	**93.3 increase**	**n/a**	**n/a**	**n/a n/a**
		daf-2(e1368);daf-9	**24.46**	**4.67**	**71(0)**	**26**	**< 0.0001**	**daf-2(e1368)**	**10.3 decrease**	**n/a**	**n/a**	**n/a n/a**
	25	wild-type	17.38	2.01	58(14)	17	n/a	wild-type	n/a n/a	n/a	n/a	n/a n/a
		daf-9	14.60	1.91	63(10)	14	< 0.0001	wild-type	17.6 decrease	n/a	n/a	n/a n/a
		daf-2(e1368)	34.88	5.50	64(7)	37	< 0.0001	wild-type	117.6 increase	n/a	n/a	n/a n/a
		daf-2(e1368);daf-9	30.33	6.57	69(2)	31	< 0.0001	daf-2(e1368)	16.2 decrease	n/a	n/a	n/a n/a
Figure 3H *HT115 control for Figure 3F*	**25**	**wild-type**	**15.07**	**2.74**	**87(2)**	**15**	**n/a**	**wild-type**	**n/a n/a**	**n/a**	**n/a**	**n/a n/a**
		daf-9	**11.80**	**2.32**	**90(0)**	**13**	**< 0.0001**	**wild-type**	**13.3 decrease**	**n/a**	**n/a**	**n/a n/a**
		daf-2(e1368)	**24.93**	**4.37**	**86(4)**	**27**	**< 0.0001**	**wild-type**	**80.0 increase**	**n/a**	**n/a**	**n/a n/a**
		daf-2(e1368);daf-9	**23.99**	**5.52**	**79(10)**	**25**	**0.2991**	**daf-2(e1368)**	**7.4 decrease**	**n/a**	**n/a**	**n/a n/a**
	25	wild-type	12.89	2.62	85(3)	12	n/a	wild-type	n/a n/a	n/a	n/a	n/a n/a
		daf-9	11.24	1.80	84(3)	11	< 0.0001	wild-type	8.3 decrease	n/a	n/a	n/a n/a
		daf-2(e1368)	23.02	5.26	83(4)	24	< 0.0001	wild-type	100.0 increase	n/a	n/a	n/a n/a
		daf-2(e1368);daf-9	21.37	4.62	83(3)	22	0.0005	daf-2(e1368)	8.3 decrease	n/a	n/a	n/a n/a
Figure 4A	**25**	**wild-type (vector)**	**14.88**	**2.17**	**73(0)**	**16**	**n/a**	**wild-type (vector)**	**n/a n/a**	**n/a**	**n/a**	**n/a n/a**
		daf-36 (vector)	**15.36**	**2.17**	**66(2)**	**16**	**0.1511**	**wild-type (vector)**	**0.0 no change**	**n/a**	**n/a**	**n/a n/a**
		daf-36;daf-12 (vector)	**13.95**	**1.61**	**74(0)**	**14**	**< 0.0001**	**wild-type (vector)**	**12.5 decrease**	**n/a**	**n/a**	**n/a n/a**
		wild-type (daf-2 RNAi)	**29.35**	**4.29**	**75(0)**	**30**	**< 0.0001**	**wild-type (vector)**	**87.5 increase**	**n/a**	**n/a**	**n/a n/a**
		daf-36 (daf-2 RNAi)	**26.11**	**4.52**	**64(5)**	**27**	**< 0.0001**	**wild-type (daf-2 RNAi)**	**10.0 decrease**	**n/a**	**n/a**	**n/a n/a**
		daf-36;daf-12 (daf-2 RNAi)	**20.28**	**3.36**	**71(6)**	**20**	**< 0.0001**	**wild-type (daf-2 RNAi)**	**33.3 decrease**	**< 0.0001**	**daf-36 (daf-2 RNAi)**	**25.9 decrease**
	25	wild-type (vector)	18.64	2.31	89(0)	18	n/a	wild-type (vector)	n/a n/a	n/a	n/a	n/a n/a
		daf-36 (vector)	17.55	3.34	73(1)	18	0.1054	wild-type (vector)	0.0 no change	n/a	n/a	n/a n/a
		daf-36;daf-12 (vector)	16.10	2.35	77(1)	16	< 0.0001	wild-type (vector)	11.1 decrease	n/a	n/a	n/a n/a
		wild-type (daf-2 RNAi)	29.62	3.79	82(5)	31	< 0.0001	wild-type (vector)	72.2 increase	n/a	n/a	n/a n/a
		daf-36 (daf-2 RNAi)	21.57	4.77	67(4)	23	< 0.0001	wild-type (daf-2 RNAi)	25.8 decrease	n/a	n/a	n/a n/a
		daf-36;daf-12 (daf-2 RNAi)	19.40	2.78	65(2)	18	< 0.0001	wild-type (daf-2 RNAi)	41.9 decrease	< 0.0001	daf-36 (daf-2 RNAi)	21.7 decrease
Figure 4B	25	**wild-type**	**16.48**	**2.23**	**92(1)**	**17**	**n/a**	**wild-type**	**n/a n/a**	**n/a**	**n/a**	**n/a n/a**
		daf-2(e1368)	**31.82**	**5.13**	**102(0)**	**34**	**< 0.0001**	**wild-type**	**100.0 increase**	**n/a**	**n/a**	**n/a n/a**
		daf-2(e1368);daf-36	**23.60**	**5.39**	**84(4)**	**24**	**< 0.0001**	**daf-2(e1368)**	**29.4 decrease**	**n/a**	**n/a**	**n/a n/a**
		daf-2(e1368);daf-36;daf-12	**28.52**	**5.12**	**88(0)**	**31**	**< 0.0001**	**daf-2(e1368)**	**8.8 decrease**	**< 0.0001**	**daf-2(e1368);daf-36**	**29.2 increase**
	25	wild-type	13.73	2.06	88(2)	14	n/a	wild-type	n/a n/a	n/a	n/a	n/a n/a
		daf-2(e1368)	27.43	7.28	109(0)	30	< 0.0001	wild-type	114.3 increase	n/a	n/a	n/a n/a
		daf-2(e1368);daf-36;daf-12	24.73	5.57	87(0)	26	< 0.0001	daf-2(e1368)	13.3 decrease	n/a	n/a	n/a n/a
	25	wild-type	16.43	2.61	88(2)	17	n/a	wild-type	n/a n/a	n/a	n/a	n/a n/a
		daf-2(e1368)	29.07	4.17	109(0)	29	< 0.0001	wild-type	70.6 increase	n/a	n/a	n/a n/a
		daf-2(e1368);daf-36	21.85	6.66	13(4)	20	< 0.0001	daf-2(e1368)	31.0 decrease	n/a	n/a	n/a n/a
		daf-2(e1368);daf-36;daf-12	26.62	4.42	87(0)	29	< 0.0001	daf-2(e1368)	0.0 no change	0.0234	daf-2(e1368);daf-36	45 increase
	25	wild-type	15.38	2.11	91(0)	17	n/a	wild-type	n/a n/a	n/a	n/a	n/a n/a
		daf-2(e1368)	24.67	5.17	81(0)	26	< 0.0001	wild-type	52.9 increase	n/a	n/a	n/a n/a
		daf-2(e1368);daf-36	23.52	5.51	85(0)	26	0.1956	daf-2(e1368)	0.0 no change	n/a	n/a	n/a n/a
		daf-2(e1368);daf-36;daf-12	23.18	5.48	82(7)	26	0.0712	daf-2(e1368)	0.0 no change	0.598	daf-2(e1368);daf-36	0.0 no change
	25	wild-type	16.66	3.02	98(1)	16	n/a	wild-type	n/a n/a	n/a	n/a	n/a n/a
		daf-2(e1368)	31.89	6.30	95(2)	34	< 0.0001	wild-type	112.5 increase	n/a	n/a	n/a n/a
		daf-2(e1368);daf-36	26.04	7.11	96(2)	29	< 0.0001	daf-2(e1368)	14.7 decrease	n/a	n/a	n/a n/a
		daf-2(e1368);daf-36;daf-12	28.10	6.31	97(3)	31	< 0.0001	daf-2(e1368)	8.8 decrease	0.0706	daf-2(e1368);daf-36	6.9 increase
Figure 4C *HT115 control for Figure 4B*	**25**	**wild-type**	**15.07**	**2.74**	**87(2)**	**15**	**n/a**	**wild-type**	**n/a n/a**	**n/a**	**n/a**	**n/a n/a**
		daf-2(e1368)	**24.93**	**4.37**	**86(4)**	**27**	**< 0.0001**	**wild-type**	**80.0 increase**	**n/a**	**n/a**	**n/a n/a**
		daf-2(e1368);daf-36	**23.70**	**5.45**	**83(2)**	**25**	**0.4328**	**daf-2(e1368)**	**7.4 decrease**	**n/a**	**n/a**	**n/a n/a**
		daf-2(e1368);daf-36;daf-12	**22.69**	**6.47**	**85(0)**	**25**	**0.238**	**daf-2(e1368)**	**7.4 decrease**	**0.6097**	**daf-2(e1368);daf-36**	**0.0 no change**
	25	wild-type	12.89	2.62	85(3)	12	n/a	wild-type	n/a n/a	n/a	n/a	n/a n/a
		daf-2(e1368)	23.02	5.26	83(4)	24	< 0.0001	wild-type	100.0 increase	n/a	n/a	n/a n/a
		daf-2(e1368);daf-36	14.26	5.19	78(6)	15	< 0.0001	daf-2(e1368)	37.5 increase	n/a	n/a	n/a n/a
		daf-2(e1368);daf-36;daf-12	23.12	5.86	86(0)	24	0.2774	daf-2(e1368)	0.0 no change	< 0.0001	daf-2(e1368);daf-36	60.0 increae
Figure 4D	**20**	**glp-1**	**20.50**	**11.97**	**72(25)**	**28**	**n/a**	**glp-1**	**n/a n/a**	**n/a**	**n/a**	**n/a n/a**
		glp-1;daf-36	**11.73**	**3.57**	**91(8)**	**11**	**< 0.0001**	**glp-1**	**60.7 decrease**	**n/a**	**n/a**	**n/a n/a**
		glp-1;daf-12	**13.33**	**6.09**	**96(4)**	**11**	**< 0.0001**	**glp-1**	**60.7 decrease**	**n/a**	**n/a**	**n/a n/a**
		glp-1;daf-36;daf-12	**14.20**	**5.52**	**91(7)**	**14**	**< 0.0001**	**glp-1**	**50.0 decrease**	**< 0.0001**	**glp-1;daf-36**	**27.3 increase**
		din-1;glp-1;daf-36	**22.38**	**11.22**	**53(44)**	**24**	**0.8829**	**glp-1**	**14.3 decrease**	**< 0.0001**	**glp-1;daf-36**	**118.2 increase**
	20	glp-1	23.34	9.83	90(0)	24	n/a	glp-1	n/a n/a	n/a	n/a	n/a n/a
		glp-1;daf-36	11.59	1.95	78(2)	11	< 0.0001	glp-1	54.2 decrease	n/a	n/a	n/a n/a
		glp-1;daf-12	15.33	5.39	84(0)	14	< 0.0001	glp-1	41.7 decrease	n/a	n/a	n/a n/a
		glp-1;daf-36;daf-12	13.79	6.53	80(3)	11	< 0.0001	glp-1	54.2 decrease	< 0.0001	glp-1;daf-36	0.0 n/a
		din-1;glp-1;daf-36	19.32	8.95	78(1)	16	0.008	glp-1	33.3 decrease	< 0.0001	glp-1;daf-36	45.5 increase
	20	glp-1	26.54	8.66	93(6)	29	n/a	glp-1	n/a n/a	n/a	n/a	n/a n/a
		glp-1;daf-36	13.53	2.67	89(13)	15	< 0.0001	glp-1	48.3 decrease	n/a	n/a	n/a n/a
		glp-1;daf-12	17.87	5.55	93(7)	17	< 0.0001	glp-1	41.4 decrease	n/a	n/a	n/a n/a
		glp-1;daf-36;daf-12	16.76	5.49	74(21)	17	< 0.0001	glp-1	41.4 decrease	< 0.0001	glp-1;daf-36	13.3 increase
	20	glp-1	27.46	9.23	67(16)	32	n/a	glp-1	n/a n/a	n/a	n/a	n/a n/a
		glp-1;daf-36	15.00	2.89	19(65)	17	< 0.0001	glp-1	46.9 decrease	n/a	n/a	n/a n/a
		glp-1;daf-12	17.28	4.84	76(9)	17	< 0.0001	glp-1	46.9 decrease	n/a	n/a	n/a n/a
		din-1;glp-1;daf-36	23.14	8.58	139(21)	23	< 0.0001	glp-1	28.1 decrease	< 0.0001	glp-1;daf-36	35.3 increase
	20	glp-1	25.61	9.17	69(15)	28	n/a	glp-1	n/a n/a	n/a	n/a	n/a n/a
		glp-1;daf-36	15.00	2.77	24(60)	17	< 0.0001	glp-1	39.3 decrease	n/a	n/a	n/a n/a
		glp-1;daf-12	18.84	6.48	77(6)	19	< 0.0001	glp-1	32.1 decrease	n/a	n/a	n/a n/a
		din-1;glp-1;daf-36	25.52	8.91	136(28)	26	0.7629	glp-1	7.1 decrease	< 0.0001	glp-1;daf-36	52.9 increase
Figure 4E *HT115 control for Figure 4D*	**20**	**glp-1**	**18.63**	**8.34**	**91(1)**	**14**	**n/a**	**glp-1**	**n/a n/a**	**n/a**	**n/a**	**n/a n/a**
		glp-1;daf-36	**11.57**	**1.90**	**53(35)**	**11**	**< 0.0001**	**glp-1**	**21.4 decrease**	**n/a**	**n/a**	**n/a n/a**
		glp-1;daf-12	**14.85**	**7.17**	**66(15)**	**13**	**0.0058**	**glp-1**	**7.1 decrease**	**n/a**	**n/a**	**n/a n/a**
		glp-1;daf-36;daf-12	**14.51**	**4.83**	**81(7)**	**13**	**0.0004**	**glp-1**	**7.1 decrease**	**< 0.0001**	**glp-1;daf-36**	**18.2 increase**
		din-1;glp-1;daf-36	**16.89**	**5.32**	**82(5)**	**17**	**0.0389**	**glp-1**	**21.4 increase**	**< 0.0001**	**glp-1;daf-36**	**54.5 increase**
	20	glp-1	18.03	8.68	97(2)	15	n/a	glp-1	n/a n/a	n/a	n/a	n/a n/a
		glp-1;daf-36	11.02	2.46	53(72)	11	< 0.0001	glp-1	26.7 decrease	n/a	n/a	n/a n/a
		glp-1;daf-12	14.80	6.22	96(2)	13	0.0004	glp-1	13.3 decrease	n/a	n/a	n/a n/a
		glp-1;daf-36;daf-12	16.08	6.16	95(5)	15	0.0163	glp-1	0.0 no change	< 0.0001	glp-1;daf-36	36.4 increase
		din-1;glp-1;daf-36	16.81	5.85	95(6)	18	0.0431	glp-1	20.0 increase	< 0.0001	glp-1;daf-36	63.6 increase

*__Bold typeface__ indicates replicate pictured in figure

Figure 3A Percent dauer at 25°

Column Statistics:

	wild-type (vector)	wild-type (*daf-2* RNAi)	*daf-36* (vector)	*daf-36* (*daf-2* RNAi)	*daf-9* (vector)	*daf-9* (*daf-2* RNAi)	*daf-12* (vector)	*daf-12* (*daf-2* RNAi)
Mean	0	0	0	60.7	0	17.9	0	0
Std. Deviation	0	0	0	12.0	0	12.5	0	0
Std. Error	0	0	0	6.9	0	7.2	0	0

Figure 3A, by replicate

condition:	wild-type (vector)			wild-type (*daf-2* RNAi)			*daf-36* (vector)			*daf-36* (*daf-2* RNAi)			*daf-9* (vector)			*daf-9* (*daf-2* RNAi)			*daf-12* (vector)			*daf-12* (*daf-2* RNAi)		
replicate number	mean	st. dev.	n	mean	st. dev.	n	mean	st. dev.	n	mean	st. dev.	n	mean	st. dev.	n	mean	st. dev.	n	mean	st. dev.	n	mean	st. dev.	n
1	0	0	411	0	0	136	0	0	236	60.9	0.0	70	0	0	245	13.0	14.1	208	0	0	493	0	0	407
2	0	0	655	0	0	321	0	0	113	48.7	13.0	321	0	0	205	32.2	15.0	436	0	0	502	0	0	533
3	0	0	336	0	0	367	0	0	56	72.6	8.6	522	0	0	51	8.6	10.3	75	0	0	441	0	0	259

Figre 3A, significance tests

comparison: **wild-type (*daf-2* RNAi) v. *daf-36* (*daf-2* RNAi)**

p = 9E-04
Student's t-Test (calculated using excel)
2-tailed, homoscedastic test

wild-type (*daf-2* RNAi) v. *daf-9* (*daf-2* RNAi)

p = 0.069
Student's t-Test (calculated using excel)
2-tailed, homoscedastic test

Figure 3B Percent dauer at 20°

Column Statistics:

	wild-type	*daf-36*	*daf-9*	*daf-2 (e1368)*	*daf-2 (e1368);daf-36*	*daf-2 (e1368) ;daf-9*
Mean	0	0.1	0	0	80.6	45.8
Std. Deviation	0	0.2	0	0	18.5	15.7
Std. Error	0	0.1	0	0	10.7	9.1

Figure 3B, by replicate

strain:	wild-type			*daf-36*			*daf-9*			*daf-2 (e1368)*			*daf-2 (e1368);daf-36*			*daf-2 (e1368) ;daf-9*		
replicate number	mean	st. dev.	n	mean	st. dev.	n	mean	st. dev.	n	mean	st. dev.	n	mean	st. dev.	n	mean	st. dev.	n
1	0	0	212	0.3	0.5	341	0	0	263	0	0	359	98.5	1.6	235	63.9	2.8	272
2	0	0	425	0.0	0.0	285	0	0	414	0	0	321	81.8	4.4	140	38.3	6.1	191
3	0	0	299	0.0	0.0	210	0	0	240	0	0	233	61.5	7.5	213	35.4	15.6	225

Figre 3B, significance tests

comparison: ***daf-2(e1368)* v. *daf-2(e1368); daf-36***

p = 0.002
Student's t-Test (calculated using excel)
2-tailed, homoscedastic test

daf-2(e1368)* v. *daf-2(e1368); daf-9

p = 0.007
Student's t-Test (calculated using excel)
2-tailed, homoscedastic test

Supplemental Table 3.2, continued

Figure S2 Percent arrest at 25°

Totals:	dauer			non-dauer larvae		
	mean	st. dev.	n	mean	st. dev.	n
wild-type	0	0	2474	0	0	2474
daf-12	0	0	1791	0	0	1791
daf-2 (e1368)	92.95	3.02	1503	0	0	1503
daf-2 (e1368);daf-12	0	0	495	0	0	495
daf-2 (e1370)	100	0	1216	0	0	1216
daf-2 (e1370);daf-12	0	0	1122	100	0	1122

Figure S2, by replicate

replicate #	strain	mean, dauer	st. dev.	mean, non-dauer larvae	st. dev.	N
1	wild-type	0	0	0	0	525
2	wild-type	0	0	0	0	549
3	wild-type	0	0	0	0	607
4	wild-type	0	0	0	0	793
1	*daf-2(e1368)*	94.53	1.55	0	0	693
2	*daf-2(e1368)*	91.37	3.59	0	0	810
1	*daf-2(e1370)*	100	0	0	0	437
2	*daf-2(e1370)*	100	0	0	0	362
3	*daf-2(e1370)*	100	0	0	0	417
1	*daf-12*	0	0	0	0	327
2	*daf-12*	0	0	0	0	471
3	*daf-12*	0	0	0	0	480
4	*daf-12*	0	0	0	0	513
1	*daf-2(e1368);daf-12*	0	0	0	0	318
2	*daf-2(e1368);daf-12*	0	0	0	0	177
1	*daf-2(e1370);daf-12*	0	0	100	0	299
2	*daf-2(e1370);daf-12*	0	0	100	0	421
3	*daf-2(e1370);daf-12*	0	0	100	0	402

Figre S2, significance tests

comparison: ***daf-2(e1368)* v. *daf-2(e1368);daf-12***
$p < 0.0001$
Student's t-Test (calculated using excel)
2-tailed, homoscedastic test

***daf-2(e1370)* v. *daf-2(e1370);daf-12*, dauer**
$p < 0.0001$
Student's t-Test (calculated using excel)
2-tailed, homoscedastic test

Supplemental Table 3.2, continued

Figure S4 Percent dauer at 15°

Column Statistics:

	wild-type	daf-36	daf-9	daf-2 (e1368)	daf-2 (e1368);daf-36	daf-2 (e1368);daf-9
Mean	0.0	0.0	1.9	0.0	5.2	39.0
Std. Deviation	0.0	0.0	3.3	0.0	3.0	25.4
Std. Error	0.0	0.0	1.9	0.0	1.7	14.6

Figure S4, by replicate

condition:	wild-type			*daf-36*			*daf-9*			*daf-2 (e1368)*			*daf-2 (e1368);daf-36*			*daf-2 (e1368);daf-9*		
replicate number	mean	st. dev.	n	mean	st. dev.	n	mean	st. dev.	n	mean	st. dev.	n	mean	st. dev.	n	mean	st. dev.	n
1	0.0	0.0	310.0	0.0	0.0	264.0	5.7	2.0	277.0	0.0	0.0	383.0	4.0	3.7	332.0	68.3	2.9	247.0
2	0.0	0.0	384.0	0.0	0.0	95.0	0.0	0.0	333.0	0.0	0.0	334.0	8.6	6.7	146.0	24.8	7.3	257.0
3	0.0	0.0	334.0	0.0	0.0	223.0	0.0	0.0	246.0	0.0	0.0	301.0	3.1	2.8	265.0	23.9	5.3	203.0

Figre S4, significance tests

comparison: ***daf-2(e1368) v. daf-2(e1368);daf-36***

p = 0.0

Student's t-Test (calculated using excel)

2-tailed, homoscedastic test

daf-2(e1368) v. daf-2(e1368);daf-9

p = 0.1

Student's t-Test (calculated using excel)

2-tailed, homoscedastic test

References

Antebi, a, Culotti, J.G., and Hedgecock, E.M. (1998). daf-12 regulates developmental age and the dauer alternative in Caenorhabditis elegans. Development (Cambridge, England) *125*, 1191–1205.

Antebi, A., Yeh, W.-H., Tait, D., Hedgecock, E.M., and Riddle, D.L. (2000). daf-12 encodes a nuclear receptor that regulates the dauer diapause and developmental age in C. elegans. Genes & Development *14*, 1512–1527.

Berman, J.R., and Kenyon, C. (2006). Germ-Cell Loss Extends C. elegans Life Span through Regulation of DAF-16 by kri-1 and Lipophilic-Hormone Signaling. Cell *124*, 1055–1068.

Bethke, A., Fielenbach, N., Wang, Z., Mangelsdorf, D.J., and Antebi, A. (2009). Nuclear Hormone Receptor Regulation of MicroRNAs Controls Developmental Progression. Science *324*, 95–98.

Boulton, S.J., Gartner, A., Reboul, J., Vaglio, P., Dyson, N., Hill, D.E., and Vidal, M. (2002). Combined functional genomic maps of the C. elegans DNA damage response. Science (New York, N.Y.) *295*, 127–131.

Dillin, A., Crawford, D.K., and Kenyon, C. (2002a). Timing requirements for insulin/IGF-1 signaling in C. elegans. Science *298*, 830–834.

Dillin, A., Hsu, A.L., Arantes-Oliveira, N., Lehrer-Graiwer, J., Hsin, H., Fraser, A.G., Kamath, R.S., Ahringer, J., and Kenyon, C. (2002b). Rates of behavior and aging specified by mitochondrial function during development. Science *298*, 2398–2401.

Fielenbach, N., and Antebi, A. (2008). C. elegans dauer formation and the molecular basis of plasticity. Genes & Development *22*, 2149–2165.

Gems, D., Sutton, A.J., Sundermeyer, M.L., Albert, P.S., King, K. V, Edgley, M.L., Larsen, P.L., Riddle, D.L., and Gems D Sundermeyer ML, Alber PS, King KV, Edgley ML, Larsen PL, Riddle DL, S.A.J. (1998). Two pleiotropic classes of daf-2 mutation affect larval arrest, adult behavior, reproduction and longevity in Caenorhabditis elegans. Genetics *150*, 129–155.

Gerisch, B., Rottiers, V., Li, D., Motola, D.L., Cummins, C.L., Lehrach, H., Mangelsdorf, D.J., and Antebi, A. (2007). A bile acid-like steroid modulates Caenorhabditis elegans lifespan through nuclear receptor signaling. Proceedings of the National Academy of Sciences *104*, 5014–5019.

Gerisch, B., Weitzel, C., Kober-Eisermann, C., Rottiers, V., and Antebi, A. (2001). A Hormonal Signaling Pathway Influencing C. elegans Metabolism, Reproductive Development, and Life Span. Developmental Cell *1*, 841–851.

Ghazi, A., Henis-Korenblit, S., and Kenyon, C. (2009). A transcription elongation factor that links signals from the reproductive system to lifespan extension in Caenorhabditis elegans. PLoS Genetics *5*, e1000639.

Giroux, S., Bethke, A., Fielenbach, N., Antebi, A., and Corey, E.J. (2008). Syntheses and biological evaluation of B-ring-modified analogues of dafachronic acid A. Organic Letters *10*, 3643–3645.

Hammell, C.M., Karp, X., and Ambros, V. (2009). A feedback circuit involving let-7-family miRNAs and DAF-12 integrates environmental signals and developmental timing in Caenorhabditis elegans. Proceedings of the National Academy of Sciences *106*, 18668–18673.

Henderson, S.T., and Johnson, T.E. (2001). daf-16 integrates developmental and environmental inputs to mediate aging in the nematode Caenorhabditis elegans. Current Biology *11*, 1975–1980.

Hsin, H., and Kenyon, C. (1999). Signals from the reproductive system regulate the lifespan of C. elegans. Nature *399*,.

Hu, P.J. (2007). Dauer. WormBook 1–19.

Hu, P.J., Xu, J., and Ruvkun, G. (2006). Two Membrane-Associated Tyrosine Phosphatase Homologs Potentiate C. elegans AKT-1/PKB Signaling. PLoS Genet *2*, e99.

Jia, K., Albert, P.S., and Riddle, D.L. (2002). DAF-9, a cytochrome P450 regulating C. elegans larval development and adult longevity. Development *129*, 221–231.

Kenyon, C., Chang, J., Gensch, E., Rudner, A., and Tabtiang, R.A. (1993). C. elegans mutant that lives twice as long as wild type. Nature *366*, 461–464.

Kimura, K.D., Tissenbaum, H.A., Liu, Y., and Ruvkun, G. (1997). daf-2, an Insulin Receptor-Like Gene That Regulates Longevity and Diapause in Caenorhabditis elegans. Science *277*, 942–946.

Kleemann, G., Jia, L., and Emmons, S.W. (2008). Regulation of Caenorhabditis elegans male mate searching behavior by the nuclear receptor DAF-12. Genetics *180*, 2111–2122.

Larsen, P.L., Albert, P.S., and Riddle, D.L. (1995). Genes that regulate both development and longevity in Caenorhabditis elegans. Genetics *139*, 1567–1583.

Lee, R.Y.N., Hench, J., and Ruvkun, G. (2001). Regulation of C. elegans DAF-16 and its human ortholog FKHRL1 by the daf-2 insulin-like signaling pathway. Current Biology *11*, 1950–1957.

Lee, S.J., and Kenyon, C. (2009). Regulation of the longevity response to temperature by thermosensory neurons in Caenorhabditis elegans. Curr. Biol. *19*, 715–722.

Lin, K., Hsin, H., Libina, N., and Kenyon, C. (2001). Regulation of the Caenorhabditis elegans longevity protein DAF-16 by insulin/IGF-1 and germline signaling. Nat Genet *28*, 139–145.

Ludewig, A.H., Kober-Eisermann, C., Weitzel, C., Bethke, A., Neubert, K., Gerisch, B., Hutter, H., and Antebi, A. (2004). A novel nuclear receptor/coregulator complex controls C. elegans lipid metabolism, larval development, and aging. Genes & Development *18*, 2120–2133.

Maier, W., Adilov, B., Regenass, M., and Alcedo, J. (2010). A neuromedin U receptor acts with the sensory system to modulate food type-dependent effects on C. elegans lifespan. PLoS Biology *8*, e1000376.

McCormick, M., Chen, K., Ramaswamy, P., and Kenyon, C. (2012). New genes that extend Caenorhabditis elegans' lifespan in response to reproductive signals. Aging Cell *11*, 192–202.

McCulloch, D., and Gems, D. (2007). Sex-specific effects of the DAF-12 steroid receptor on aging in Caenorhabditis elegans. Ann N Y Acad Sci *1119*, 253–259.

Motola, D.L., Cummins, C.L., Rottiers, V., Sharma, K.K., Li, T., Li, Y., Suino-Powell, K., Xu, H.E., Auchus, R.J., Antebi, A., et al. (2006). Identification of ligands for DAF-12 that govern dauer formation and reproduction in C. elegans. Cell *124*, 1209–1223.

Murphy, C.T., McCarroll, S.A., Bargmann, C.I., Fraser, A., Kamath, R.S., Ahringer, J., Li, H., and Kenyon, C. (2003). Genes that act downstream of DAF-16 to influence the lifespan of Caenorhabditis elegans. Nature *424*, 277–283.

Patel, D.S., Garza-Garcia, A., Nanji, M., McElwee, J.J., Ackerman, D., Driscoll, P.C., and Gems, D. (2008). Clustering of genetically defined allele classes in the Caenorhabditis elegans DAF-2 insulin/IGF-1 receptor. Genetics *178*, 931–946.

Rottiers, Motola, Gerisch, Cummins, Nishiwaki, Mangelsdorf, and Antebi (2006). Hormonal Control of C. elegans Dauer Formation and Life Span by a Rieske-like Oxygenase. Developmental Cell *10*, 473–482.

Sharma, K.K., Wang, Z., Motola, D.L., Cummins, C.L., Mangelsdorf, D.J., and Auchus, R.J. (2009). Synthesis and activity of dafachronic acid ligands for the C. elegans DAF-12 nuclear hormone receptor. Molecular Endocrinology *23*, 640–648.

Snow, M.I., and Larsen, P.L. (2000). Structure and expression of daf-12: a nuclear hormone receptor with three isoforms that are involved in development and aging in

Caenorhabditis elegans. Biochimica Et Biophysica Acta (BBA) - Gene Structure and Expression *1494*, 104–116.

Vowels, J.J., and Thomas, J.H. (1992). Genetic Analysis of Chemosensory Control of Dauer Formation in Caenorhabditis elegans. Genetics *130*, 105–123.

Wollam, J., and Antebi, A. (2011). Sterol regulation of metabolism, homeostasis, and development. Annual Review of Biochemistry *80*, 885–916.

Wollam, J., Magner, D.B., Magomedova, L., Rass, E., Shen, Y., Rottiers, V., Habermann, B., Cummins, C.L., and Antebi, A. (2012). A novel 3-hydroxysteroid dehydrogenase that regulates reproductive development and longevity. PLoS Biology *10*, e1001305.

Wollam, J., Magomedova, L., Magner, D.B., Shen, Y., Rottiers, V., Motola, D.L., Mangelsdorf, D.J., Cummins, C.L., and Antebi, A. (2011). The Rieske oxygenase DAF-36 functions as a cholesterol 7-desaturase in steroidogenic pathways governing longevity. Aging Cell.

Yamawaki, T.M., Berman, J.R., Suchanek-Kavipurapu, M., McCormick, M., Gaglia, M.M., Lee, S.-J.J., and Kenyon, C. (2010). The somatic reproductive tissues of C. elegans promote longevity through steroid hormone signaling. PLoS Biology *8*,.

Yoshiyama-Yanagawa, T., Enya, S., Shimada-Niwa, Y., Yaguchi, S., Haramoto, Y., Matsuya, T., Shiomi, K., Sasakura, Y., Takahashi, S., Asashima, M., et al. (2011). The conserved Rieske oxygenase DAF-36/Neverland is a novel cholesterol-metabolizing enzyme. The Journal of Biological Chemistry *286*, 25756–25762.

Chapter 4: The p120RasGAP family member GAP-3 is a novel regulator of dauer arrest and longevity in *Caenorhabditis elegans*[3]

Abstract

In *C. elegans*, reducing insulin/insulin-like growth factor signaling (ILS) promotes dauer arrest and extends life span by promoting the translocation of DAF-16/FoxO to the nucleus, where it can induce transcriptional programs that promote survival. The ILS pathway in *C. elegans* consists of conserved PI3K and Akt components that antagonize DAF-16/FoxO by promoting its cytoplasmic sequestration. We have discovered the EAK pathway, a novel, conserved pathway that inhibits DAF-16/FoxO in parallel to PI3K/Akt signaling. The EAK pathway inhibits nuclear DAF-16/FoxO activity without promoting its translocation to the cytoplasm. How the EAK pathway inhibits DAF-16/FoxO is not known. To illuminate the mechanism underlying EAK pathway inhibition of nuclear DAF-16/FoxO activity, we identified a suppressor of *eak-7;akt-1* dauer arrest (*seak* gene). In this study, we implicate *gap-3* as a *seak* gene. GAP-3 is homologous to human RASA1, which was first identified as a RasGAP that antagonizes Ras by promoting its GTPase activity, and is one of three putative RasGAPs encoded in the *C. elegans* genome. A spontaneous missense mutation in the RasGAP domain of *gap-3* suppresses the dauer arrest and life span phenotypes of *eak-7;akt-1* double mutant animals. Two independent loss-of-function alleles of *gap-3* also suppress *eak-7;akt-1* dauer arrest, confirming *gap-3* as a *seak* gene. In contrast, mutations in *gap-1* and *gap-2* did not influence *eak-7;akt-1* dauer arrest. Notably, the *let-60*/Ras gain-of-function allele *n1046* suppresses *eak-7;akt-1* dauer arrest to a lesser degree than *gap-3* loss-of-function alleles, suggesting that GAP-3 may have Ras-independent functions in the control of dauer arrest. These results implicate GAP-3 as a novel regulator of dauer arrest and longevity.

[3] In preparation for submission with authors listed as Dumas, K.J., Flibotte, S., Moerman, D., and Hu, P.J..

Introduction

In *Caenorhabditis elegans*, an insulin/insulin-like growth factor signaling (ILS) pathway, a TGF-β-like pathway, and a steroid hormone pathway function to control normal reproductive development in a manner that is appropriate for an organism's given environment. In unfavorable environments, signaling through these pathways is abrogated and normal reproductive development is aborted; animals instead undergo arrest in an alternative developmental stage known as dauer. Dauer arrest requires the activity of the FoxO transcription factor DAF-16; in the absence of DAF-16/FoxO, animals develop reproductively, bypassing the dauer stage even in the absence of ILS activity.

In mammals and in worms, ILS inhibits FoxO transcription factors via phosphorylation by Akt and subsequent nuclear export and cytoplasmic sequestration. Nuclear localization, while necessary for FoxO activity, is not sufficient for its full activation (Lin et al., 2001; Tsai et al., 2003). Once in the nucleus, *C. elegans* DAF-16/FoxO is regulated by the EAK pathway, a conserved pathway that functions in parallel to AKT-1 to inhibit the activity of DAF-16/FoxO (Williams et al., 2010).

EAK-7 and AKT-1 normally synergize to inhibit the activity of DAF-16/FoxO. AKT-1 inhibits DAF-16/FoxO by phosphorylating FoxO, triggering its nuclear export and cytoplasmic sequestration. In the absence of *akt-1*, DAF-16/FoxO accumulates in the nucleus. EAK-7, in contrast, regulates the activity of specifically the nuclear pool of DAF-16/FoxO. *eak-7* mutation has no effect on the subcellular localization of DAF-16/FoxO, but it is able to enhance phenotypes associated with FoxO activity, including dauer arrest and longevity, doing so particularly in contexts which promote nuclear accumulation of DAF-16/FoxO (Alam et al., 2010).

The exact mechanism by which the EAK pathway inhibits nuclear DAF-16/FoxO remains unknown. EAK-7 is likely the most downstream component of the pathway based on the strength of its mutant phenotypes as well as its expression pattern; *eak-7* is the only EAK that is expressed in the same cells as DAF-16/FoxO, and, in contrast to the

other EAKs, mutation of *eak-7* alone is sufficient to promote longevity in otherwise wild-type animals. EAK-7 is conserved, yet the function of the protein is unknown. EAK-7 likely regulates DAF-16/FoxO indirectly, as it is tethered to the plasma membrane via a functional N-myristoylation motif.

Because the mechanism of EAK inhibition of DAF-16/FoxO remains obscure, we are interested in uncovering molecules which might be required to relay EAK pathway signals to DAF-16/FoxO. Here, we report the fortuitous identification of a conserved Ras GTPase activating protein, GAP-3, as a novel regulator of *eak-7;akt-1* dauer arrest and longevity. These findings define a novel function for *gap-3* and inform the design of a broader approach to uncover new factors that mediate the EAK pathway signal.

Materials and Methods

Whole genome sequencing

Genomic DNA was isolated from the *seak* strain and the non-suppressed *eak-7;akt-1* double mutant strain by phenol-chloroform extraction and subjected to whole genome sequencing using the Illumina HiSeq2000 platform. Approximately 30-40X genome coverage was obtained using 100-nucleotide paired-end reads.

Sequence analysis

Sequence reads were mapped to the WormBase reference genome build WS220 using the short read aligner BWA (Li and Durbin, 2009). Single nucleotide variants (SNVs) were identified with the help of the SAMtools toolbox (Li et al., 2009). Each SNV was annotated with a custom-made Perl script and gene information available from WormBase version WS220. Sequences of the *seak* mutant strain was compared to that of the non-suppressed *eak-7;akt-1* parental strain. All non-synonymous changes and predicted splice junction mutations were considered for subsequent analysis.

Dauer arrest assays

Dauer arrest assays were performed at the indicated temperatures in Percival I-36NL incubators (Percival Scientific, Inc., Perry, IA) as described (Hu et al., 2006).

Life span assays

Life span assays were performed in Percival I-36NL incubators at 20°C. After alkaline hypochlorite treatment and two generations of growth, young adult animals were placed onto NGM plates containing 25 μg/ml (100 μM) 5-fluoro-2'-deoxyuridine (FUDR; Sigma) and 10 μg/ml nystatin (Sigma) that had been seeded with 20X concentrated *E. coli* OP50. Assays were conducted at 20˚. Viability was assessed visually or with gentle prodding. GraphPad Prism (GraphPad Software, La Jolla, CA) was used for data representation and statistical analysis.

RNAi

Feeding RNAi was performed using variations of standard procedures (Kamath et al., 2001). NGM plates containing 5 mM IPTG and 25 μg/ml carbenicillin were seeded with 500 μl of overnight culture of *E. coli* HT115 harboring either control L4440 vector or indicated RNAi plasmid. Gravid animals cultured on NGM plates seeded with *E. coli* OP50 were picked to assay plates for six-hour egg lays at 20°C. Dauers were scored after progeny had been incubated at the assay temperature for 48–60 hours.

DAF-16A:GFP localization

daf-16(mu86);zIs356;akt-1(mg306) animals (*akt-1* mutants harboring a DAF-16A::GFP transgene as the only source of DAF-16) and *gap-3(ga139);daf-16(mu86);zIs356;akt-1(mg306)* were cultured on OP50 *E. coli* at 20°C. L3 or L4 larvae were mounted on glass slides using a thin pad of 2% agarose and 10 mM sodium azide to paralyze the animals. Images were captured using an Olympus BX61 epifluorescence compound microscope equipped with a Hamamatsu ORCA ER camera and Slidebook 4.0.1 digital microscopy software (Intelligent Imaging Innovations) and processed using ImageJ software. Images were captured within twenty minutes of mounting animals on slides to prevent variations

in DAF-16A::GFP localization due to prolonged stress induced by mounting. Images were then blinded and animals sorted into categories 1 through 5 based on the extent of nuclear localization of DAF-16A::GFP. 1 indicates that all cells have only cytoplasmic GFP, and 5 indicates that all cells have exclusively nuclear GFP.

Results

Identification of a spontaneous dauer suppressor mutation

Animals harboring a loss-of-function mutation in *akt-1* have an increase in nuclear localization of DAF-16 (Hertweck et al., 2004), as AKT-1 is responsible for inhibitory phosphorylation of DAF-16 which leads to its cytoplasmic sequestration. EAK-7 functions to inhibit specifically the nuclear pool of DAF-16; in its absence, DAF-16 activity increases, promoting enhanced dauer arrest and increased longevity (Alam et al., 2010). Together, loss-of-function mutations of both *eak-7* and *akt-1* synergize to increase DAF-16 activity (Alam et al., 2010). Animals harboring both mutations arrest as dauers at elevated temperatures (*e.g.* 25°C) as a result of this DAF-16 activation. The strong dauer-constitutive phenotype of *eak-7;akt-1* double mutants is fully suppressed by *daf-16/FoxO* loss-of-function mutations (Alam et al., 2010). In the process of using *eak-7;akt-1* double mutant animals as a constitutive dauer control, we isolated a strain of animals that spontaneously lost its dauer arrest phenotype at 25°C, while maintaining the *eak-7* and *akt-1* loss-of-function mutations.

Dauer arrest delays the onset of the reproductive period in *C. elegans* (Hu, 2007). Because of this delay in reaching sexual maturity, there is selection pressure on the population that favors the accumulation of spontaneous mutations which promote bypass of the dauer stage. Thus, isolation of a strain that lost its arrest phenotype suggested to us that the strain acquired a *de novo* mutation that suppressed dauer, potentially in a gene whose activity was normally required to activate DAF-16.

Identification of *gap-3* as a *seak* gene

We therefore pursued identification of the spontaneous suppressor of *eak-7;akt-1* (*seak*) mutation via whole-genome DNA sequencing. We isolated and sequenced genomic DNA from the *eak-7;akt-1;seak* strain and an *eak-7;akt-1* strain that maintained fully penetrant dauer arrest. Sequences of the two strains were compared, revealing only two non-synonymous mutations that were present in the *eak-7;akt-1;seak* strain but absent in the *eak-7;akt-1* control (Table 4.1). Linkage analysis revealed the *seak* phenotype was not X-linked, instead showing linkage to LG I, implicating the missense allele *dp17* in the gene *gap-3* as the putative *seak* mutation. *dp17* is predicted to cause a leucine to phenylalanine change in the protein encoded by *gap-3.*

LG	location	orig. base	new base	gene	orig AA	new AA	annotation
I	1988832	G	A	Y20F4.3	L	F	*gap-3* (GTPase Activating Protein family)
X	11670202	G	A	T04F8.6	S	N	orthologous to *H. sapiens* ninein

Table 4.1: Candidate *seak* mutations.
SNVs identified by whole genome sequencing that are present in *eak-7;akt-1;seak* and absent in *eak-7;akt-1*.

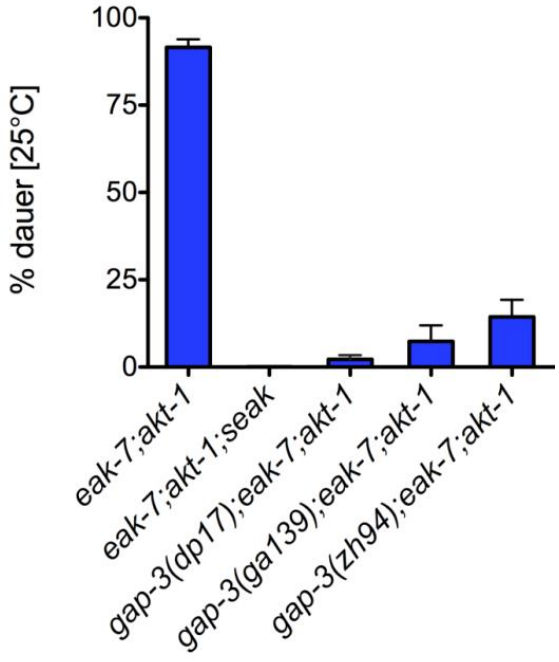

Figure 4.1: *gap-3* is a *seak* gene.
Isolated *gap-3(dp17)* in animals harboring *eak-7;akt-1* mutations recapitulates the dauer suppression phenotype of the seak strain, as do loss-of-function alleles of *gap-3*, *ga139* and *zh94*. Data are from one representative experiment. Error bars indicate SEM.

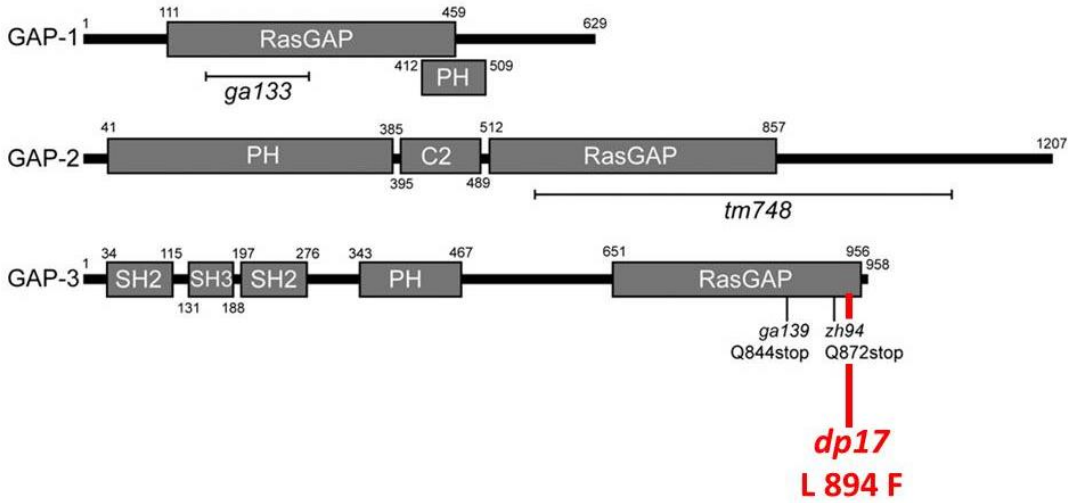

Figure 4.2: Genetic structure of *gap-1, gap-2,* and *gap-3,* the three putative RasGAPs encoded in the *C. elegans* genome.
Introns are represented by lines, exons by boxes. Three alleles of *gap-3* lie within the RasGAP domain.

gap-3 inactivation suppresses dauer arrest in *eak-7;akt-1* double mutants

We outcrossed *eak-7;akt-1;seak* to separate the two spontaneous mutations in the strain (Table 4.1), then tested the dauer arrest phenotype of *gap-3(dp17);eak-7;akt-1*. We found that *gap-3(dp17)* recapitulates the suppression of *eak-7;akt-1;seak* (Figure 4.1), confirming that the mutation in *gap-3* is responsible for the seak phenotype. We tested the ability of known loss-of-function alleles of *gap-3*, *ga139* and *zh94* (Stetak et al., 2008), to suppress *eak-7;akt-1* dauer arrest. We found that both alleles recapitulate the seak phenotype, indicating that the new *dp17* allele is likely a loss-of-function mutation, and suggesting that activity of GAP-3 is required for dauer arrest in *eak-7;akt-1* mutants.

Suppression of dauer arrest is specific to *gap-3*

gap-3 encodes the putative *C. elegans* p120 RasGAP, the ortholog of human RASA1 (Stetak et al., 2008), which functions to turn off the activity of Ras. Ras proteins play key roles in signal transduction from receptor tyrosine kinases; as a small G protein, Ras alternates between its active and inactive state by hydrolyzing bound GTP to GDP. GTP-bound Ras is active and stimulates the activation of downstream mitogen activated protein kinase (MAPK) signaling pathways, canonically the Raf/Mek/Erk MAPK pathway. In contrast, GDP-bound Ras is inactive. Ras possesses weak intrinsic GTP-hydrolysis activity, but this activity is promoted by the action of GTPase-activating proteins (GAPs). GAPs therefore promote the inactivation of the Ras small GTPase by accelerating the hydrolysis of GTP to GDP.

Most eukaryotes have multiple RasGAPs whose domain structures define four subfamilies; the p120 subfamily, the Neurofibromin 1 (NF1) subfamily, the Gap1 subfamily, and the synGAP subfamily. The *C. elegans* genome encodes three putative RasGAPs, Gap1 subfamily member *gap-1,* synGAP member *gap-2,* and *gap-3,* the sole p120 RasGAP subfamily member. No clear NF1 ortholog exists in *C. elegans*.

The domain structure of *gap-3,* illustrated in Figure 4.2, is typical of all p120 RasGAPs. *gap-3* contains a Src homology 3 (SH3) domain flanked by two SH2 domains, a

pleckstrin homology (PH) domain, and a C-terminal catalytic domain that is common to all RasGAP subfamilies (Stetak et al., 2008). Notably, the *dp17* allele we isolated resides within the C-terminal RasGAP domain of the protein, as do both *ga139* and *zh94*.

The *C. elegans* genome encodes one Ras protein, LET-60 (Beitel et al., 1990; Han et al., 1990). Analogous to mammals, a MAPkinase pathway defined by *lin-45*/Raf, *mek-2*/Mek, and *mpk-1*/MAPK functions downstream of LET-60/Ras (Han et al., 1993; Lackner et al., 1994; Wu and Han, 1994; Kornfeld et al., 1995; Wu et al., 1995). LET-60 was first discovered based on its role in regulating normal vulval development in the worm. GAP-1 is the predominant inhibitor of LET-60/Ras in vulval development, whereas GAP-3 is the main LET-60/Ras inhibitor in meiotic progression of the germ cells (Stetak et al., 2008). In some tissues, all three RasGAPs cooperate to regulate LET-60/Ras.

We asked whether *seak* activity was specific to *gap-3* or a trait of all three RasGAPs. We built loss-of-function mutations of *gap-1* and *gap-2* into the *eak-7;akt-1* mutant background and tested their impact on dauer arrest. We found that neither *gap-1(ga133)* nor *gap-2(tm748)* mutation recapitulates the dauer suppression conferred by *gap-3* mutation (Figure 4.3), suggesting *seak* activity is specific to *gap-3*.

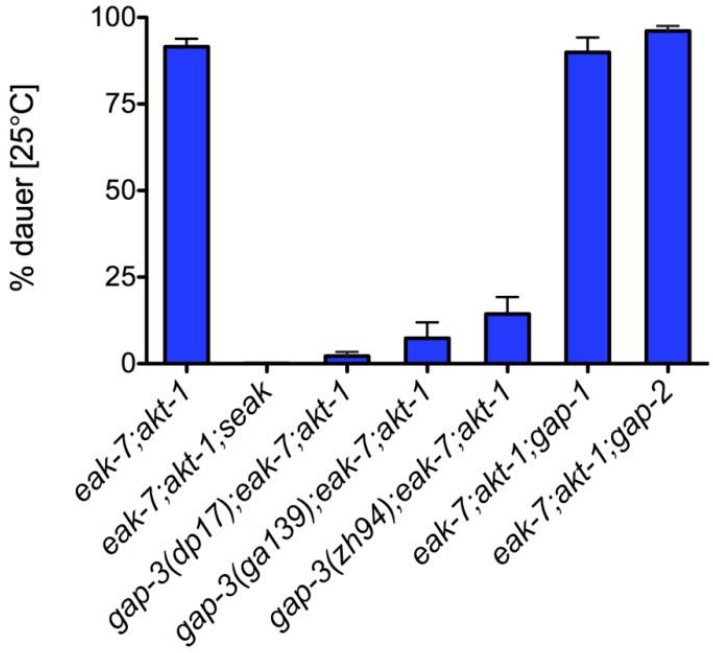

Figure 4.3: *seak* activity is specific to *gap-3*.
Mutation of neither *gap-1* nor *gap-2* does not suppress *eak-7;akt-1* dauer arrest. Data are from one representative experiment. Error bars indicate SEM.

gap-3 inactivation suppresses life span in *eak-7;akt-1* double mutants

Because genes required for dauer arrest frequently also impinge on longevity regulation in *C. elegans*, we tested the impact of *gap-3* mutation on the life span extension phenotype of *eak-7;akt-1* mutants. Consistent with its function as a suppressor of dauer arrest, *gap-3* mutation partially suppressed life span extension *eak-7;akt-1* (Figure 4.4). Importantly, *gap-3* single mutant life span is not different from wild-type, suggesting *gap-3* is not suppressing life span simply due to increased frailty (data not shown).

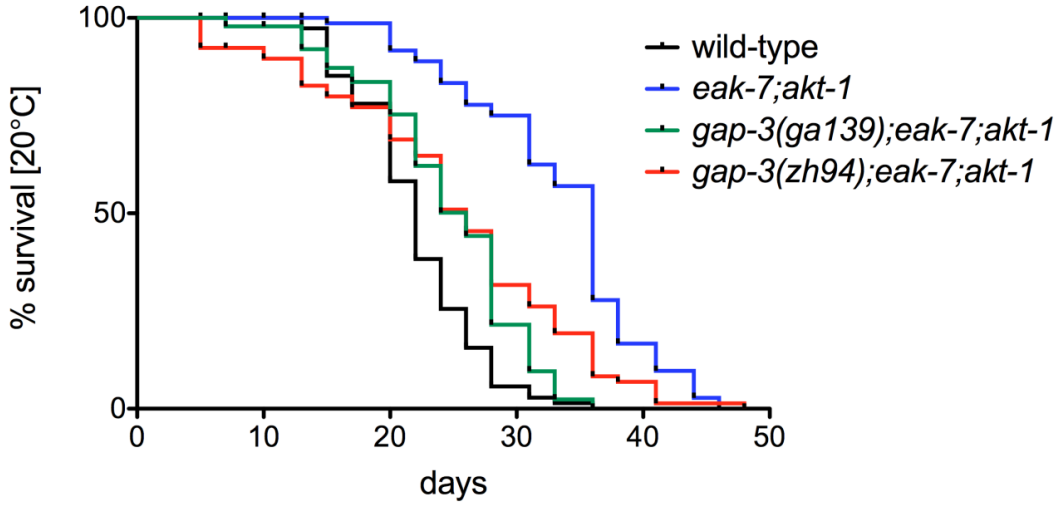

Figure 4.4: *gap-3* inactivation partially suppresses life span extension of *eak-7;akt-1* mutant animals.
Data are from one representative experiment with approximately 100 animals assayed per genotype.

gap-3 inactivation does not suppress dauer arrest of other dauer-constitutive mutants.

To unravel how *gap-3* functions to promote dauer arrest, we set out to determine if *gap-3* mutation confers general suppression of dauer arrest, or if it is specific to dauer arrest in the context of *eak-7* and/or *akt-1* mutation. We found that *gap-3(ga139)* mutation suppresses arrest of *eak-7* single mutants, but has no impact on *akt-1* single mutants (Figure 4.5). In contrast, *gap-3(zh94)* suppresses both *eak-7* and *akt-1* arrest with high penetrance, suggesting allelic differences between the two loss-of-function mutations (see Figure 4.2 for the nature of the alleles). Interestingly *gap-3* inactivation does not completely suppress either *eak-7* or *akt-1* single mutant, but suppresses the double mutant completely, suggesting that GAP-3 might play a role in regulating DAF-16 in the specific context of activation downstream of both *eak-7* and *akt-1* mutation. We pursued this question further by testing the ability of *gap-3* mutation to suppress arrest of other dauer constitutive mutants.

In addition to the EAK pathway and the ILS pathway, a TGFβ-like pathway regulates dauer arrest in a DAF-16-dependent manner. In the TGFβ-like pathway, a TGFβ-like ligand, DAF-7 (Ren et al., 1996), and its receptors promote reproductive development by regulating the activity of three SMAD transcription factor-like molecules DAF-3, DAF-8, and DAF-14, and a Sno transcription factor homolog DAF-5 (Georgi et al., 1990; Estevez et al., 1993; Patterson et al., 1997; Inoue and Thomas, 2000; da Graca et al., 2004; Tewari et al., 2004; Park et al., 2010). Animals with loss-of-function mutations in the SMAD-like transcription factors *daf-8* and *daf-14* have dauer-constitutive phenotypes at elevated temperatures. We tested the ability of *gap-3(ga139)* mutation to suppress *daf-8* and *daf-14* dauer arrest and found that *gap-3(ga139)* modestly suppresses arrest of both *daf-8* and *daf-14* mutants; however, the effect was not statistically significant in either case (Figure 4.5, p = 0.1523 for comparison of *gap-3(ga139);daf-8 to daf-8*; p = 0.0544 for comparison of *gap-3(ga139);daf-14* to *daf-14*). Collectively, these data suggest that GAP-3 regulates dauer arrest predominately in the context of both *eak-7* and *akt*-1 loss.

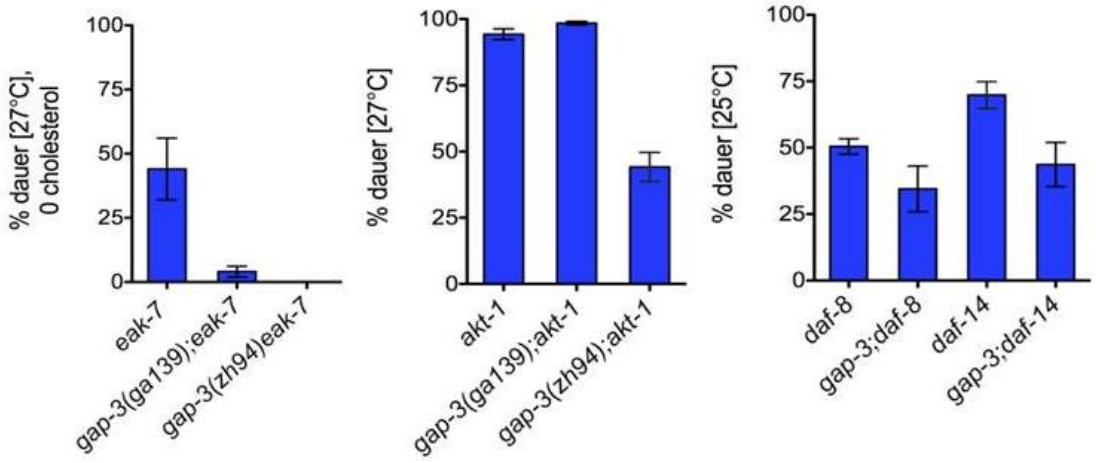

Figure 4.5*: gap-3(ga139)* mutation suppresses dauer arrest of *eak-7* single mutants but not of *akt-1(null)* nor TGFβ-like pathway mutants, *daf-8* and *daf-14*.
Data are from one representative experiment. Error bars indicate SEM.

gap-3 inactivation does not change nuclear localization of DAF-16::GFP

Insulin and TGFβ-like regulates dauer arrest by affecting the subcellular localization of DAF-16. Signaling through ILS and TGFβ-like signaling results in nuclear exclusion of DAF-16, inhibiting its activity as a transcription factor. A possible explanation for the suppression of dauer arrest when *gap-3* activity is reduced is that GAP-3 might normally function to promote nuclear accumulation of DAF-16. To test this hypothesis, we assayed the localization of a DAF-16a::GFP fusion protein in the context of *gap-3(ga139)* and *akt-1(null)* mutations. As expected, animals harboring the DAF-16a::GFP fusion construct and an *akt-1(null)* mutation have predominately nuclear DAF-16a::GFP. *gap-3* mutation does not change the nucleocytoplasmic distribution of DAF-16a::GFP (Figure 4.6), suggesting that the mechanism of suppression of dauer arrest by *gap-3* mutation is not mediated by exclusion of DAF-16 from the nucleus.

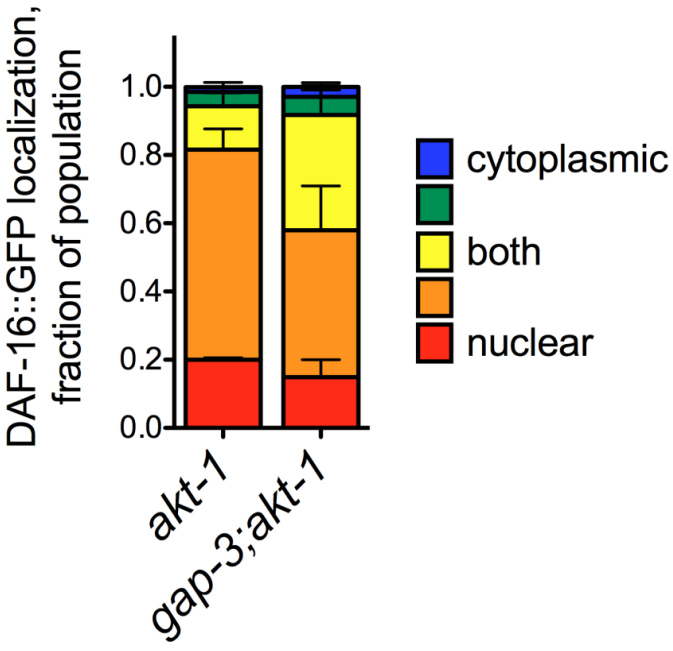

Figure 4.6: GAP-3 inactivation does not change DAF-16::GFP nuclear localization. Data are pooled from three experiments with approximately 30 animals scored per genotype, per experiment. Error bars indicate SEM.

Suppression of dauer arrest by *gap-3* inactivation is independent of LET-60/Ras

We asked whether GAP-3 activation of DAF-16 is mediated by LET-60/Ras, the canonical target of *gap-3* GAP activity. We reasoned that if dauer suppression due to *gap-3* loss-of-function was mediated by activation of Ras, then an activating mutation in Ras should phenocopy *gap-3* loss-of-function. A gain-of-function allele of *let-60/Ras* exists which renders Ras insensitive to inactivation by GAP. We built *let-60(n1046)* into the *eak-7;akt-1* background and tested its dauer arrest phenotype. We found that Ras activation does not fully recapitulate dauer suppression in the *eak-7;akt-1* background, suggesting that, at least in part, GAP-3 function is LET-60/Ras-independent (Figure 4.7).

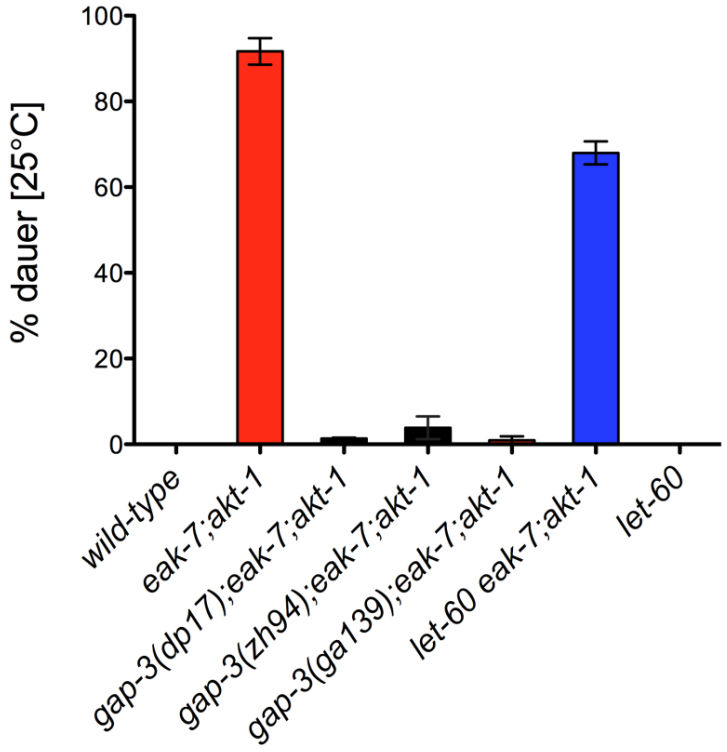

Figure 4.7: An activating mutation in *let-60/Ras* that renders Ras insensitive to inactivation by GAP activity does not recapitulate *gap-3* loss-of-function mutations. Data are from one representative experiment. Error bars indicate SEM.

This Ras-independence spurred us to pursue identification of the causative small GTPase, as we hypothesized that *gap-3* most likely impacts dauer arrest through its function as a GAP. The *C. elegans* genome encodes fifty-two small GTPases, eleven of which are in the Ras/Rap/Ral superfamily. We performed an RNAi screen of all small GTPases present in the genome-wide RNAi feeding libraries (36 out of 52 total small GTPases, including *let-60*, were screened) to identify potential causative small GTPases. We reasoned that reducing the activity of the causative small GTPase by RNAi in the *gap-3;eak-7;akt-1* mutant should restore dauer arrest. We tested all clones corresponding to small GTPases that were present in the library and found that none of the clones tested, including *let-60*, rescued dauer arrest after one or two generations of feeding RNAi. In addition to the lack of complete coverage of all small GTPases, this experiment is subject to the caveat that not all tissues are responsive to RNAi. Therefore, if GAP-3 exerts its function in a tissue refractory to RNAi, such as the nervous system or pharynx, this assay will likely be unable to detect a causative GTPase. It is noteworthy that *gap-3* RNAi has no effect on *eak-7;akt-1* dauer arrest (Supplemental Figure 4.1), suggesting that indeed *gap-3* might function in a RNAi refractory tissue.

We took a second approach to identify the GTPase that might interact with GAP-3, pursuing a yeast-two hybrid screen of small GTPases. Using full length *gap-3* as well as RasGAP domain constructs of both mutant and wild-type *gap-3*, we screened the small GTPases present in the wORFeome (worm Open Reading Frame collection; 42 of 52 small GTPases, including *let-60*, were screened). *gap-3* constructs were tested as both bait and prey. This analysis failed to identify any interacting GTPases. In addition to having incomplete coverage of all small GTPases, this approach is typified by a high false-negative rate. Despite the failure of these two approaches, we do not exclude the possibility that GAP-3 activity in the context of dauer arrest is mediated by its interaction with a small GTPase.

Discussion

The signaling pathways controlling the dauer decision in *C. elegans* are well described; they include the ILS pathway, TGFβ-like pathway, and the dafachronic acid/DAF-12

pathways. Genetic screens to identify new components of these dauer regulatory pathways appear to be saturated, suggesting all known components of the pathways have been identified. Despite this, here we describe the fortuitous identification of a novel regulator of dauer arrest, *gap-3*, whose mutation occurred spontaneously in a genetic background that promotes the activation of the DAF-16/FoxO transcription factor.

We implicate the RASA1 ortholog *gap-3* as a suppressor of the constitutive dauer arrest phenotype of *eak-7;akt-1* double mutant animals (suppressor of *eak-7;akt-1*, *seak* mutant). *eak-7;akt-1* animals harbor activated DAF-16/FoxO; a spontaneous, loss-of-function point mutation in the RasGAP domain of *gap-3* abrogates dauer arrest in this context, suggestion that GAP-3 normally functions to promote dauer arrest, possibly by promoting the activation of DAF-16/FoxO. Furthermore, we find that *seak* activity is specific to *gap-3* (Figure 4.3) and likely does not require LET-60/Ras (Figure 4.7).

Surprisingly, the *gap-3* loss-of-function allele *ga139* does not significantly impact dauer arrest of *akt-1* single mutants (Figure 4.5), despite inhibiting *eak-7;akt-1* double mutant arrest completely (Figure 4.2 and 4.3). This, together with the observation that *gap-3* mutation does not change the subcellular localization of DAF-16/FoxO (Figure 4.6), suggests that *gap-3* might mediate specifically the EAK pathway signal to DAF-16/FoxO. This hypothesis is consistent with the effect of *gap-3* mutation on life span, as mutation shortens life span of *eak-7;akt-1* mutant animals, but does not reduce life span back to wild-type levels (Figure 4.4), suggesting residual DAF-16 activity persists in the absence of GAP-3. It is not yet known how *gap-3* mutation affects the ability of DAF-16 to activate gene expression. Expression profiling experiments of DAF-16 target genes will be revealing in this regard.

We hypothesize that *gap-3* mutation suppresses dauer arrest independently of LET-60/Ras activation based on our finding that the activating allele *let-60(n1046)* does not phenocopy dauer suppression of *gap-3* loss-of-function mutations (Figure 4.7). This prompted an attempt to identify the causative GTPase by two approaches, a yeast-two-hybrid screen and a targeted RNAi screen. Both approaches yielded no candidates.

Notably, LET-60/Ras was tested in each screen; *let-60* knock-down by RNAi did not restore dauer arrest *in gap-3;eak-7;akt-1* mutants, nor did a *let-60* construct physically interact with any of the *gap-3* constructs tested in the two-hybrid approach. We do not rule out the possibility that *gap-3* interacts with a small GTPase given these results. Instead, we continue to pursue this line of inquiry by other methodologies.

A GAP-3 function that is independent of Ras/MAPK activity has not yet been described. Given the conservation of *gap-3*, this novel mechanism might have relevance to disease in humans. Interestingly, patients with loss of function mutations in the RASA1, the human ortholog of *gap-3*, have clinical phenotypes distinct from patients with Ras activating mutations, supporting the hypothesis that p120 GAPs might function independently of Ras.

In summary, this work identifies GAP-3 as a novel regulator of *C. elegans* dauer arrest and longevity, possibly via its interaction with the EAK pathway. We hypothesize that activity of *gap-3* in the EAK pathway might be the reason that, despite saturation of genetic screens in the context of canonical dauer regulatory pathways, *gap-3* has never before emerged from a dauer suppressor screen. In light of this discovery, we believe the *eak-7;akt-1* mutant background in which *gap-3* was discovered provides a uniquely sensitized background from which to uncover novel DAF-16 modulators. Moving forward, we will pursue a forward genetic screen to identify more *seak* genes. *seak* gene identity promises to shed light on the mechanism by which the EAK pathway regulates the activity of DAF-16/FoxO.

Supplemental Information

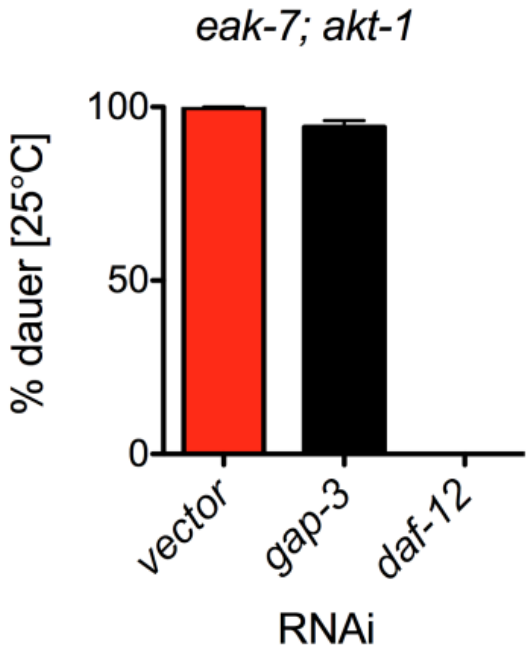

Supplemental Figure 4.1: *gap-3* RNAi does not suppress *eak-7;akt-1* dauer arrest. An RNAi construct corresponding to the RasGAP domain of *gap-3* was constructed and used for feeding RNAi to animals harboring eak-7 and akt-1 mutations. *gap-3* RNAi did not suppress arrest of *eak-7;akt-1* animals, in contrast to *daf-12* RNAi control, which suppressed arrest completely ($p < 0.0001$).

References

Alam, H., Williams, T.W., Dumas, K.J., Guo, C., Yoshina, S., Mitani, S., and Hu, P.J. (2010). EAK-7 Controls Development and Life Span by Regulating Nuclear DAF-16/FoxO Activity. Cell Metabolism *12*, 30–41.

Beitel, G.J., Clark, S.G., and Horvitz, H.R. (1990). Caenorhabditis elegans ras gene let-60 acts as a switch in the pathway of vulval induction. Nature *348*, 503–509.

Estevez, M., Attisano, L., Wrana, J.L., Albert, P.S., Massague, J., and Riddle, D.L. (1993). The daf-4 gene encodes a bone morphogenetic protein receptor controlling C. elegans dauer larva development. Nature *365*, 644–649.

Georgi, L.L., Albert, P.S., and Riddle, D.L. (1990). daf-1, a C. elegans gene controlling dauer larva development, encodes a novel receptor protein kinase. Cell *61*, 635–645.

Da Graca, L.S., Zimmerman, K.K., Mitchell, M.C., Kozhan-Gorodetska, M., Sekiewicz, K., Morales, Y., and Patterson, G.I. (2004). DAF-5 is a Ski oncoprotein homolog that functions in a neuronal TGF beta pathway to regulate C. elegans dauer development. Development *131*, 435–446.

Han, M., Aroian, R. V, and Sternberg, P.W. (1990). The let-60 locus controls the switch between vulval and nonvulval cell fates in Caenorhabditis elegans. Genetics *126*, 899–913.

Han, M., Golden, A., Han, Y., and Sternberg, P.W. (1993). C. elegans lin-45 raf gene participates in let-60 ras-stimulated vulval differentiation. Nature *363*, 133–140.

Hertweck, M., Göbel, C., and Baumeister, R. (2004). C. elegans SGK-1 Is the Critical Component in the Akt/PKB Kinase Complex to Control Stress Response and Life Span. Developmental Cell *6*, 577–588.

Hu, P.J. (2007). Dauer. WormBook 1–19.

Hu, P.J., Xu, J., and Ruvkun, G. (2006). Two membrane-associated tyrosine phosphatase homologs potentiate C. elegans AKT-1/PKB signaling. PLoS Genetics *2*, e99.

Inoue, T., and Thomas, J.H. (2000). Suppressors of transforming growth factor-beta pathway mutants in the Caenorhabditis elegans dauer formation pathway. Genetics *156*, 1035–1046.

Kamath, R.S., Martinez-Campos, M., Zipperlen, P., Fraser, A.G., and Ahringer, J. (2001). Effectiveness of specific RNA-mediated interference through ingested double-stranded RNA in Caenorhabditis elegans. Genome Biology *2*, RESEARCH0002.

Kornfeld, K., Guan, K.L., and Horvitz, H.R. (1995). The Caenorhabditis elegans gene mek-2 is required for vulval induction and encodes a protein similar to the protein kinase MEK. Genes & Development *9*, 756–768.

Lackner, M.R., Kornfeld, K., Miller, L.M., Horvitz, H.R., and Kim, S.K. (1994). A MAP kinase homolog, mpk-1, is involved in ras-mediated induction of vulval cell fates in Caenorhabditis elegans. Genes & Development *8*, 160–173.

Li, H., and Durbin, R. (2009). Fast and accurate short read alignment with Burrows-Wheeler transform. Bioinformatics *25*, 1754–1760.

Li, H., Handsaker, B., Wysoker, A., Fennell, T., Ruan, J., Homer, N., Marth, G., Abecasis, G., and Durbin, R. (2009). The Sequence Alignment/Map format and SAMtools. Bioinformatics *25*, 2078–2079.

Lin, K., Hsin, H., Libina, N., and Kenyon, C. (2001). Regulation of the Caenorhabditis elegans longevity protein DAF-16 by insulin/IGF-1 and germline signaling. Nat Genet *28*, 139–145.

Park, D., Estevez, A., and Riddle, D.L. (2010). Antagonistic Smad transcription factors control the dauer/non-dauer switch in C. elegans. Development *137*, 477–485.

Patterson, G.I., Koweek, A., Wong, A., Liu, Y., and Ruvkun, G. (1997). The DAF-3 Smad protein antagonizes TGF-beta-related receptor signaling in the Caenorhabditis elegans dauer pathway. Genes & Development *11*, 2679–2690.

Ren, P., Lim, C.S., Johnsen, R., Albert, P.S., Pilgrim, D., and Riddle, D.L. (1996). Control of C. elegans larval development by neuronal expression of a TGF-beta homolog. Science *274*, 1389–1391.

Stetak, A., Gutierrez, P., and Hajnal, A. (2008). Tissue-specific functions of the Caenorhabditis elegans p120 Ras GTPase activating protein GAP-3. Developmental Biology *323*, 166–176.

Tewari, M., Hu, P.J., Ahn, J.S., Ayivi-Guedehoussou, N., Vidalain, P.O., Li, S., Milstein, S., Armstrong, C.M., Boxem, M., Butler, M.D., et al. (2004). Systematic interactome mapping and genetic perturbation analysis of a C. elegans TGF-beta signaling network. Molecular Cell *13*, 469–482.

Tsai, W.C., Bhattacharyya, N., Han, L.Y., Hanover, J.A., and Rechler, M.M. (2003). Insulin inhibition of transcription stimulated by the forkhead protein Foxo1 is not solely due to nuclear exclusion. Endocrinology *144*, 5615–5622.

Williams, T.W., Dumas, K.J., and Hu, P.J. (2010). EAK proteins: novel conserved regulators of C. elegans lifespan. Aging *2*, 742–747.

Wu, Y., and Han, M. (1994). Suppression of activated Let-60 ras protein defines a role of Caenorhabditis elegans Sur-1 MAP kinase in vulval differentiation. Genes & Development *8*, 147–159.

Wu, Y., Han, M., and Guan, K.L. (1995). MEK-2, a Caenorhabditis elegans MAP kinase kinase, functions in Ras-mediated vulval induction and other developmental events. Genes & Development *9*, 742–755.

Chapter 5: Post-embryonic control of *Caenorhabditis elegans* DAF-2 insulin-like signaling by the conserved dosage compensation protein DPY-21[4]

Abstract

During embryogenesis, an essential process known as dosage compensation is initiated to equalize gene expression from sex chromosomes. Although much is known about how dosage compensation is established, the consequences of modulating the stability of dosage compensation post-embryonically are not known. Here we define a role for the *Caenorhabditis elegans* dosage compensation complex (DCC) in the regulation of DAF-2 insulin-like signaling. In a screen for dauer regulatory genes that control the activity of the FoxO transcription factor DAF-16, we isolated three mutant alleles of *dpy-21*, which encodes a conserved DCC component. Knockdown of multiple DCC components in hermaphrodite and male animals indicates that the dauer suppression phenotype of *dpy-21* mutants is due to a defect in dosage compensation *per se*. In *dpy-21* mutants, expression of several X-linked genes that promote dauer bypass is elevated, including four genes encoding components of the DAF-2 insulin-like pathway that antagonize DAF-16/FoxO activity. Accordingly, *dpy-21* mutation reduced the expression of DAF-16/FoxO target genes by promoting the exclusion of DAF-16/FoxO from nuclei. Thus, dosage compensation enhances dauer arrest by repressing X-linked genes that promote reproductive development through the inhibition of DAF-16/FoxO nuclear translocation. This work is the first to establish a specific post-embryonic function for dosage compensation in any organism. The influence of dosage compensation on dauer arrest, a larval developmental fate governed by the integration of multiple environmental inputs and signaling outputs, suggests that the dosage compensation machinery may respond to

[4] In revision for publication in *Genetics* with authors listed as Dumas, K.J., Delaney, C.E., Flibotte, S., Moerman, D., Csankovszki, G., and Hu, P.J..

external cues by modulating signaling pathways through chromosome-wide regulation of gene expression.

Introduction

In the nematode *Caenorhabditis elegans*, the DAF-2 insulin-like growth factor receptor (IGFR) ortholog promotes reproductive development and aging by inhibiting the FoxO transcription factor DAF-16 through the AGE-1 phosphoinositide 3-kinase (PI3K) and the conserved kinases PDK-1, AKT-1, and AKT-2 (Fielenbach and Antebi, 2008; Kenyon, 2010). *daf-2* mutants were first isolated in genetic screens for dauer-constitutive mutants (Riddle et al., 1981). In replete environments, hatched embryos develop reproductively by traversing four larval stages (L1-L4) prior to adulthood. In conditions of increased population density, reduced food availability, or elevated temperature, L1 larvae enter a distinct developmental pathway that culminates in arrest as an alternative, long-lived, morphologically distinct third larval stage known as dauer (Riddle, 1988). *daf-2/IGFR*, *age-1/PI3K*, *pdk-1*, and *akt-1* loss-of-function mutants all have dauer-constitutive phenotypes; *i.e.*, they undergo dauer arrest in conditions in which wild-type animals develop reproductively(Riddle et al., 1981; Vowels and Thomas, 1992; Gottlieb and Ruvkun, 1994; Morris et al., 1996; Kimura et al., 1997; Paradis et al., 1999; Ailion and Thomas, 2003). The dauer-constitutive phenotype of these mutants requires DAF-16/FoxO, as loss of *daf-16/FoxO* function fully suppresses dauer arrest in *daf-2/IGFR*, *age-1/PI3K*, *pdk-1*, and *akt-1* mutants (Vowels and Thomas, 1992; Gottlieb and Ruvkun, 1994; Larsen et al., 1995; Paradis et al., 1999; Ailion and Thomas, 2003). Taken together, these data indicate that the DAF-2/AGE-1/PDK-1/AKT-1 pathway promotes reproductive development by inhibiting DAF-16/FoxO.

Two other conserved signaling pathways play important roles in dauer regulation. The transforming growth factor-β (TGFβ)-like ligand DAF-7 inhibits dauer arrest in parallel to the DAF-2/IGFR pathway by signaling through the Type I TGFβ receptor homolog DAF-1 and the Type II receptor homolog DAF-4 to regulate the SnoN homolog DAF-5 and the SMAD homologs DAF-3, DAF-8, and DAF-14 (Fielenbach and Antebi, 2008).

Downstream of the DAF-2/IGFR and DAF-7/TGFβ pathways, a hormone biosynthetic pathway consisting of DAF-36 (Rottiers et al., 2006), DHS-16 (Wollam et al., 2012), and DAF-9 (Gerisch et al., 2001; Jia et al., 2002) makes Δ^7-dafachronic acid (Δ^7-DA), a steroid ligand that prevents dauer arrest by binding to the DAF-12 nuclear receptor (Motola et al., 2006).

Although insulin- and insulin-like ligand-induced inhibition of FoxO transcription factors through nuclear export and cytoplasmic sequestration is a well-established mechanism of FoxO regulation, nuclear translocation is not sufficient to fully activate FoxO (Lin et al., 2001; Tsai et al., 2003). In *C. elegans*, the EAK proteins comprise a conserved pathway that acts in parallel to AKT-1 to control the activity of nuclear DAF-16/FoxO (Williams et al., 2010). *eak* mutations, while causing a weak dauer-constitutive phenotype in isolation, strongly enhance the dauer-constitutive phenotype caused by *akt-1* mutations (Hu et al., 2006; Zhang et al., 2008; Alam et al., 2010; Dumas et al., 2010). EAK-7, which is likely the most downstream component of the known EAK pathway, is a conserved protein of unknown function that is expressed in the same tissues as DAF-16/FoxO. Although EAK-7 likely regulates the nuclear pool of DAF-16/FoxO, it is situated at the plasma membrane (Alam et al., 2010), suggesting that it controls DAF-16/FoxO activity via unknown intermediary molecules.

We conducted a genetic screen to identify new FoxO regulators that may mediate EAK-7 action. Herein we describe our initial findings, which reveal an unexpected role for dosage compensation in controlling dauer arrest, insulin-like signaling, and FoxO transcription factor activity.

Materials and Methods

C. elegans strains and maintenance

The following strains were used in this study: N2 Bristol, CB4856 (Wicks et al., 2001), and TJ356 [DAF-16::GFP(*zIs356*)] (Henderson and Johnson, 2001). The following mutant alleles were used: *akt-1(mg306)* (Hu et al., 2006), *akt-1(ok525)* (Hertweck et al.,

2004), *akt-2(ok393)* (Hertweck et al., 2004), *daf-1(m40)* (Georgi et al., 1990), *daf-2(e1368)* (Kimura et al., 1997), *daf-8(e1393)* (Park et al., 2010), *daf-9(dh6)* and *daf-9(k182)* (Gerisch et al., 2001), *daf-12(rh61rh411)* (Antebi et al., 2000), *daf-14(m77)* (Inoue and Thomas, 2000), *daf-16(mu86)* (Lin et al., 1997), *daf-36(k114)* (Rottiers et al., 2006), *dpy-21(e428)* (Yonker and Meyer, 2003), *dpy-28(y1)* (Meyer and Casson, 1986), *eak-7(tm3188)* (Alam et al., 2010), and *sdc-2(y46)* (Nusbaum and Meyer, 1989). Double, triple, and quadruple mutant animals were constructed by conventional methods. Animals were maintained on nematode growth media (NGM) plates seeded with *E. coli* OP50.

Suppressor of *eak-7;akt-1 (seak)* screen

eak-7(tm3188);akt-1(ok525) double mutant animals were mutagenized using N-ethyl-N-nitrosourea (ENU) at a concentration of 0.5 mM in M9 buffer for four hours at room temperature, with gentle agitation (De Stasio and Dorman, 2001). *eak-7(tm3188)* and *akt-1(ok525)* both harbor deletion mutations that are likely to be null alleles (Hertweck et al., 2004; Alam et al., 2010); these alleles were chosen to minimize the chances of isolating informational suppressors such as tRNA anticodon mutants or mutants defective in nonsense-mediated mRNA decay. After mutagenesis egg lays were performed with F_1 animals at 25°, and rare F_2 dauer bypassors were isolated for further analysis. The dauer suppressor phenotype was verified for sixteen independent mutants, indicating that these are bonafide *seak* mutants. Approximately 1200 haploid genomes were screened.

Whole genome sequencing

Genomic DNA was isolated from each of the sixteen *seak* strains and the non-mutagenized *eak-7;akt-1* double mutant strain by phenol-chloroform extraction and subjected to whole genome sequencing using the Illumina HiSeq2000 platform. Approximately 30-40X genome coverage was obtained using 100-nucleotide paired-end reads.

Sequence analysis

Sequence reads were mapped to the WormBase reference genome build WS220 using the short read aligner BWA (Li and Durbin, 2009). Single nucleotide variants (SNVs) were identified with the help of the SAMtools toolbox (LI *et al.* 2009). Each SNV was annotated with a custom-made Perl script and gene information available from WormBase version WS220. Sequences of the *seak* mutant strains were compared to that of the non-mutagenized *eak-7;akt-1* parental strain. All non-synonymous changes and predicted splice junction mutations were considered for subsequent analysis. A total of 664 such SNVs were identified among the sixteen *seak* strains.

Mapping

Single nucleotide polymorphism mapping was performed using the polymorphic Hawaiian CB4856 strain and a set of 48 primer pairs distributed throughout the genome (eight per chromosome) that flank DraI restriction site polymorphisms (Davis et al., 2005). Since the mutagenesis was performed on *eak-7;akt-1* double mutant animals, we constructed a "Hawaiianized" *eak-7(tm3188);akt-1(ok525)* double mutant strain for mapping. This was generated by outcrossing the original *eak-7;akt-1* double mutant ten times with CB4856 and identifying *eak-7;akt-1* double mutant recombinants harboring CB4856 polymorphisms at sites flanking *eak-7* and *akt-1*. Hawaiianized *eak-7(tm3188);akt-1(ok525)* double mutants arrested as dauers to the same extent as *eak-7(tm3188);akt-1(ok525)* double mutants in the Bristol background, indicating that the CB4856 background does not strongly influence dauer arrest in *eak-7;akt-1* double mutant animals.

Mapping was performed by crossing *seak* mutant hermaphrodites (*eak-7;akt-1;seak*) with Hawaiianized *eak-7;akt-1* males and isolating F_2 dauers and bypassors. After confirming the dauer-constitutive and suppressor phenotypes in the following generation, F_2 dauers and bypassors were pooled and assayed for all 48 DraI SNPs (Davis et al., 2005).

Dauer arrest assays

Dauer arrest assays were performed at the indicated temperatures in Percival I-36NL incubators (Percival Scientific, Inc., Perry, IA) as described (Hu et al., 2006). In assays involving *daf-9(k182)* and *daf-36(k114)* mutants, supplemental cholesterol was not added to the NGM assay plates (Gerisch et al., 2001; Rottiers et al., 2006). In assays involving *daf-9(dh6)* mutants, animals were propagated on NGM plates supplemented with 10 nM Δ^7-DA to rescue the constitutive dauer phenotype of *daf-9(dh6)* (Sharma et al., 2009). Gravid animals raised on Δ^7-DA were transferred to NGM plates without Δ^7-DA and allowed to lay eggs for the dauer assay. Raw data and statistical analysis of all dauer assays are presented in Table S1.

RNAi

Feeding RNAi was performed using variations of standard procedures (Kamath et al., 2001). For dauer assays, NGM plates containing 5 mM IPTG and 25 μg/ml carbenicillin were seeded with 500 μl of overnight culture of *E. coli* HT115 harboring either control L4440 vector or indicated RNAi plasmid. Gravid animals cultured on NGM plates seeded with *E. coli* OP50 were picked to assay plates for six-hour egg lays at 20°. Dauers were scored after progeny had been incubated at the assay temperature for 48–60 hours.

Male dauer assay

eak-7;akt-1 males were crossed with *eak-7;akt-1* hermaphrodites. Mated hermaphrodites were picked for egg lays on RNAi plates. The dauer arrest phenotype of male and hermaphrodite cross progeny was scored. The sex of dauers was determined by allowing the animals to recover to adulthood.

RNA preparation and real-time quantitative PCR

100-200 adult animals were allowed to lay eggs for 6 hours at 20° on NGM plates seeded with *E. coli* OP50. After egg lay, adults were removed and eggs were shifted to 25°. L2 larvae were harvested 24 hours later, washed twice in M9 buffer, then frozen in TRIzol reagent (Invitrogen, catalog #15596-026). RNA was extracted using TRIzol, cleaned

using the RNeasy Mini Kit (Qiagen, catalog #74104), and treated with DNAse (Qiagen, RNase-Free DNase Set, catalog #79254). mRNA was reverse transcribed using the SuperScript First-Strand Synthesis System for RT-PCR and oligo-dT primers (Invitrogen, catalog #11904-018). 10 ng of cDNA was used as template for real-time quantitative PCR amplification using the Absolute Blue QPCR SYBR Green Mix (Thermo Scientific, catalog #AB-4166/B) in a 15 µl reaction volume. Reactions were run on an Eppendorf realplex Mastercycler®. Primer sequences are presented in Table S2. Relative expression levels of each gene were determined using the $\Delta\Delta 2C_t$ method (Nolan et al., 2006). Gene expression levels were normalized relative to actin (*act-1*) in the same sample, and then relative to the levels of the same gene in the control sample (wild-type/N2 Bristol or *eak-7;akt-1* siblings, as indicated). Measurements were performed in triplicate, with three or four biological replicates for each condition.

DAF-16A:GFP localization

daf-16(mu86);zIs356;akt-1(mg306) animals (*akt-1* mutants harboring a DAF-16A::GFP transgene as the only source of DAF-16) were cultured for two generations on *dpy-21* RNAi or vector control at 20°. L2 or L3 larvae were mounted on glass slides using a thin pad of 2% agarose and 10 mM sodium azide to paralyze the animals. Images were captured using an Olympus BX61 epifluorescence compound microscope equipped with a Hamamatsu ORCA ER camera and Slidebook 4.0.1 digital microscopy software (Intelligent Imaging Innovations) and processed using ImageJ software. Images were captured within twenty minutes of mounting animals on slides to prevent variations in DAF-16A::GFP localization due to prolonged stress induced by mounting. Images were then blinded and animals sorted into categories 1 through 5 (Supplemental Figure 5.2) based on the extent of nuclear localization of DAF-16A::GFP. 1 indicates that all cells have only cytoplasmic GFP, and 5 indicates that all cells have exclusively nuclear GFP.

Results

A genetic screen for novel DAF-16/FoxO regulators

We pursued a genetic approach to identify molecules that mediate EAK-7 regulation of DAF-16/FoxO. The strong dauer-constitutive phenotype of *eak-7;akt-1* double mutants is fully suppressed by *daf-16/FoxO* loss-of-function mutations (Alam et al., 2010). We reasoned that screening for loss-of-function mutations that suppress the dauer-constitutive phenotype of *eak-7;akt-1* double mutants might identify genes encoding novel DAF-16/FoxO activators. Therefore, we mutagenized *eak-7(null);akt-1(null)* double mutant animals with *N*-ethyl-*N*-nitrosourea (ENU) and screened for rare F_2 suppressors of the *eak-7;akt-1* dauer-constitutive phenotype (*seak* mutants). Sixteen independent mutant strains were validated as bonafide *seak* mutants based on consistent high penetrance of the *seak* phenotype in subsequent generations.

To identify molecular lesions in these mutant strains, we isolated and sequenced genomic DNA isolated from non-outcrossed *seak* mutants and the original non-mutagenized *eak-7;akt-1* double mutant. Subsequently, each *seak* mutant was subjected to low-resolution single nucleotide polymorphism (SNP) mapping with the polymorphic CB4856 strain (Wicks et al., 2001; Davis et al., 2005).

dpy-21 inactivation suppresses dauer arrest in *eak-7;akt-1* double mutants

Three independent *seak* strains harbored distinct non-synonymous mutations in the conserved gene *dpy-21* (alleles *dp253, dp579* and *dp381*; Figure 5.1A). Each allele is predicted to be a missense mutation affecting a conserved residue in the conserved C-terminal region of DPY-21 (Figure 5.1A; (Yonker and Meyer, 2003)). Low-resolution SNP mapping indicated that the genomic region containing *dpy-21* is linked to the dauer suppression phenotype in each of these three strains. *dpy-21* RNAi also suppressed the dauer-constitutive phenotype of *eak-7;akt-1* double mutants (Figure 5.1B). Moreover, the *dpy-21(e428)* null allele [hereafter referred to as "*dpy-21(null)*"] (Yonker and Meyer, 2003), as well as *dpy-21(dp253),* isolated from other mutagenesis-induced SNVs present in the original *seak* strain, also strongly suppressed the dauer-constitutive phenotype of

eak-7;akt-1 double mutants (Figure 5.1C). Taken together, these data indicate that *dpy-21* inactivation suppresses the dauer-constitutive phenotype of *eak-7;akt-1* double mutants. Therefore, the three mutant alleles that emerged from our screen (Figure 5.1A) are likely *dpy-21* loss-of-function mutations.

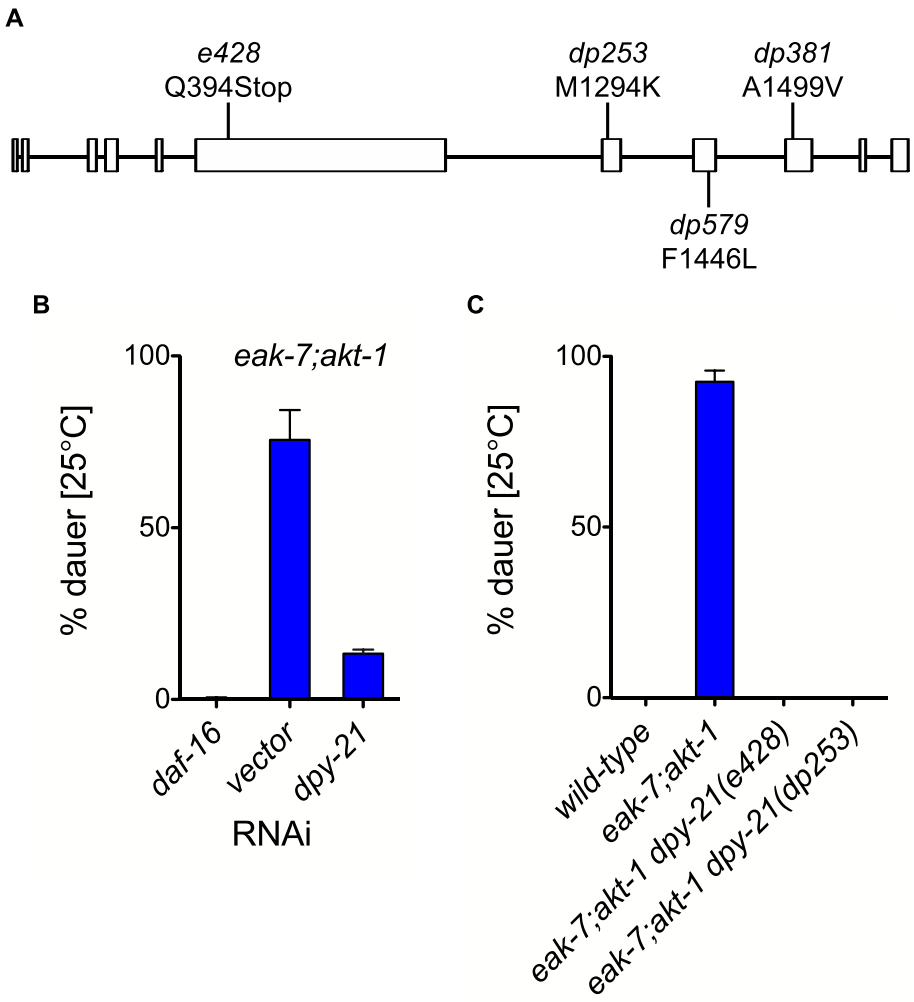

Figure 5.1: *dpy-21* inactivation suppresses the dauer phenotype of *eak-7;akt-1* mutants.
(A) Genomic structure of the *dpy-21* locus and locations of the *e428* null allele and three alleles isolated in this study. Exons are denoted by boxes and introns by lines. (B-C) Effect of reduction of *dpy-21*activity on the dauer-constitutive phenotype of *eak-7;akt-1* double mutants at 25°C. (B) *dpy-21* RNAi suppresses dauer arrest of *eak-7;akt-1* mutants (13.4% mean dauer arrest in animals exposed to *dpy-21* RNAi compared to 75.6% in animals exposed to control vector, $p = 0.0004$ by two-sided t-test). Data are from one representative experiment with greater than 250 animals assayed per condition. (C) *dpy-21(null)* and *dpy-21(dp253)* suppress dauer arrest of *eak-7;akt-1* mutants (0% mean dauer arrest in *eak-7;akt-1 dpy-21(e428)* triple mutants compared to 94.2% in *eak-7;akt-1* double mutants, $p < 0.0001$; 0% mean dauer arrest in *eak-7;akt-1 dpy-21(dp253)* triple mutants, $p < 0.0001$). Data are pooled from three replicate experiments with at least 1000 animals assayed per genotype. (B-C) Error bars indicate SEM. Raw data and statistics are presented in Supplemental Table 5.1.

DPY-21 is a general regulator of dauer arrest

To determine whether DPY-21 influences dauer arrest generally as opposed to specifically in the context of *eak-7* and *akt-1* mutation, we determined the effect of reducing DPY-21 activity on dauer arrest in the background of other dauer-constitutive mutations using both *dpy-21* RNAi and *dpy-21(null)* genetic mutation. Dauer arrest is controlled by three major signal transduction pathways; in addition to the DAF-2/IGFR pathway, the DAF-7 TGFβ-like pathway and the DAF-9 DA pathway also promote reproductive development by inhibiting dauer arrest (Fielenbach and Antebi, 2008). We tested the effect of *dpy-21* inactivation on dauer arrest in animals harboring mutations in each of these three pathways that confer a dauer-constitutive phenotype.

Reducing the activity of *dpy-21* suppressed dauer arrest in animals with reduced DAF-2/IGFR signaling. *dpy-21* RNAi modestly but significantly suppressed the 25° dauer-constitutive phenotype of animals harboring *daf-2(e1368),* which contains a missense mutation in the ligand-binding domain of DAF-2/IGFR (Kimura et al., 1997) (Figure 5.2A), and *dpy-21(null)* strongly suppressed *daf-2(e1368)* dauer arrest (Figure 5.2B). Additionally, *dpy-21(null)* suppressed the 27° dauer arrest phenotype of *akt-1(ok525),* a likely null allele harboring a 1251-base-pair deletion eliminating the kinase domain (Hertweck et al., 2004) (Supplemental Figure 5.1A). These data indicate that DPY-21 promotes dauer arrest in the context of reduced DAF-2/IGFR signaling.

In the TGFβ-like pathway, a ligand (DAF-7 (Ren et al., 1996)) and its receptors (the Type I- and Type II- TGFβ receptor-like molecules DAF-1 (Georgi et al., 1990) and DAF-4 (Estevez et al., 1993), respectively) promote reproductive development by regulating the activity of three SMAD-like molecules (DAF-3 (Patterson et al., 1997), DAF-8 (Park et al., 2010), and DAF-14 (Inoue and Thomas, 2000)) and a Sno transcription factor homolog (DAF-5 (Da Graca et al., 2004; Tewari et al., 2004)). *dpy-21* inactivation also suppresses the dauer-constitutive phenotypes of mutants in the DAF-7/TGFβ-like pathway. Reducing *dpy-21* activity either by RNAi or via *dpy-21(null)* mutation modestly suppresses dauer arrest caused by the *daf-1(m40)* and *daf-14(m77)*

nonsense mutations (Georgi et al., 1990; Inoue and Thomas, 2000) (Figures 5.2C-D), indicating that DPY-21 also promotes dauer arrest in the context of reduced DAF-7 TGFβ-like signaling. The effect of *dpy-21* knockdown on the dauer-constitutive phenotype caused by the *daf-8(e1393)* missense allele is unclear; *dpy-21* RNAi suppresses *daf-8(e1393)* dauer arrest, but *dpy-21(null)* slightly enhances *daf-8(e1393)* dauer arrest (Supplemental Figure 5.1B).

In the dafachronic acid (DA) pathway, multiple biosynthetic enzymes [DAF-36 (Rottiers et al., 2006), DHS-16 (Wollam et al., 2012), and DAF-9 (Gerisch et al., 2001; Jia et al., 2002)] participate in the biosynthesis of Δ^7-dafachronic acid (Δ^7-DA), a steroid ligand that promotes reproductive development by binding to and inactivating the DAF-12 nuclear receptor (Motola et al., 2006). DAF-9 and DAF-12 act downstream of the DAF-2/IGFR and DAF-7/ TGFβ-like pathways to control dauer arrest (Gerisch et al., 2001, 2007; Jia et al., 2002; Mak and Ruvkun, 2004). We tested the effect of *dpy-21* inactivation on the dauer-constitutive phenotype of *daf-9(dh6)* animals, which harbor a null mutation *in daf-9* that completely abrogates DA biosynthesis (Gerisch et al., 2001; Motola et al., 2006) (hereafter referred to as "*daf-9(null)").* Neither *dpy-21* RNAi (Figure 5.2E) nor *dpy-21(null)* (Figure 5.2F) influenced the dauer-constitutive phenotype of *daf-9(null)* mutants at 25°. In contrast, *dpy-21(null)* modestly suppressed the 27° dauer-constitutive phenotypes caused by the hypomorphic *daf-9(k182)* mutation (Gerisch et al., 2001) and the *daf-36(k114)* null mutation (Rottiers et al., 2006), which reduces the biosynthesis of dafachronic acids (Wollam et al., 2011) (Supplemental Figure 5.1C).

Overall, these data indicate that DPY-21 is required for dauer arrest in the context of reduced DAF-2/IGFR signaling and plays a modest role in controlling DAF-7/TGFβ-like and DA hormonal signaling.

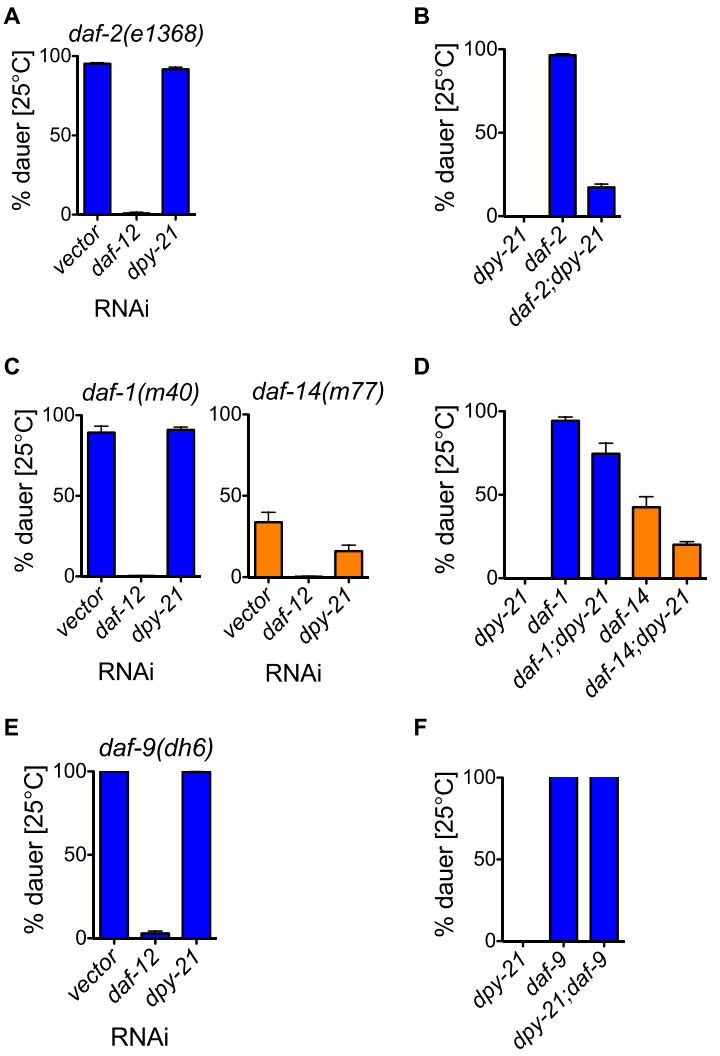

Figure 5.2: DPY-21 is a general regulator of dauer arrest.
Effect of reduction of *dpy-21*activity on the dauer-constitutive phenotypes of DAF-2/IGFR pathway, DAF-7/TGFβ-like pathway, and dafachronic acid pathway mutants. (A) *dpy-21* RNAi suppresses dauer arrest of *daf-2(e1368)* mutants (91.7% mean dauer arrest in animals exposed to *dpy-21* RNAi compared to 95.2% in animals exposed to control vector, p = 0.0275 by two-sided t-test). Data are pooled from three replicate experiments with at least 1000 animals assayed per genotype. (B) *dpy-21(null)* suppresses dauer arrest of *daf-2(e1368)* (17.2% mean dauer arrest in *daf-2;dpy-21* compared to 96.5% in *daf-2*, p < 0.0001). Data are pooled from three replicate experiments with at least 1300 animals assayed per genotype. (C) *dpy-21* RNAi does not influence or suppresses modestly dauer arrest of mutants with reduced DAF-7/TGFβ-like pathway signaling (91.0% mean dauer arrest in *daf-1* mutant animals exposed to *dpy-21* RNAi compared to 89.3% in animals exposed to control vector, p = 0.7064; 16.0% mean dauer arrest in *daf-14* mutant animals exposed to *dpy-21* RNAi compared to 33.8% in animals exposed to control vector, p = 0.0321). Data are pooled from two replicate experiments with at least 550 animals assayed per condition. (D) *dpy-21(null)* suppresses dauer arrest of *daf-1* and *daf-14* mutants (74.5% mean dauer arrest in *daf-1;dpy-21* compared to 94.3% in *daf-1*, p = 0.01; 20.0% mean dauer arrest in *daf-14;dpy-21* compared to 42.5% in *daf-14*, p = 0.0037). Data are pooled from three replicate experiments with at least 750 animals assayed per genotype. (E and F) Neither *dpy-21* RNAi nor *dpy-21(null)* influence dauer arrest in *daf-9(null)* mutant animals (E) p = 0.2153 for *dpy-21* RNAi v. vector control. Data are pooled from three replicate experiments with at least 800 animals per condition (F) p = 0.9503 for *dpy-21(null);daf-9(null)* v. *daf-9(null)*. Data are from one representative experiment with at least 250 animals per genotype. (A-F) Error bars indicate SEM. Raw data and statistics are presented in Supplemental Table 5.1.

Dosage compensation influences dauer arrest

DPY-21 was originally identified as one of ten components of the *C. elegans* dosage compensation complex (DCC) (Yonker and Meyer, 2003). This multi-protein complex mediates dosage compensation by assembling on both hermaphrodite X chromosomes to reduce X-linked gene expression by approximately 50%, thereby equating X-linked gene expression between XX hermaphrodites and XO males (Meyer, 2010). Based on its established role in dosage compensation, we sought to determine whether the suppression of dauer arrest by DPY-21 inactivation was a consequence of reduced dosage compensation *per se* as opposed to impairment of a DPY-21 activity that is independent of dosage compensation. To test this, we determined the effect of RNAi inactivation of each of the nine other DCC components on the dauer-constitutive phenotype of *eak-7;akt-1* double mutants. Strikingly, we found that reducing the activity of most DCC components by RNAi suppresses the dauer-constitutive phenotype of *eak-7;akt-1* double mutants (Figure 5.3A). It is noteworthy that, whereas loss-of-function mutations in most DCC components results in lethality (Riddle DL, 1997), RNAi-based inactivation of individual DCC components RNAi for multiple generations is not lethal (data not shown), suggesting that RNAi directed against these genes does not completely abrogate their function. Thus, the differential penetrance of dauer suppression observed after RNAi-based knockdown of DCC components could be a consequence of variable efficacy of RNAi against each targeted gene.

To further evaluate the role of other DCC components in dauer regulation, we reduced the activity of two DCC components via genetic mutation. *y1* is a temperature-sensitive missense allele of *dpy-28* (Plenefisch et al., 1989), which encodes a core DCC subunit (Tsai et al., 2008), and *y46* is a weak allele of *sdc-2* (Nusbaum and Meyer, 1989), which encodes a hermaphrodite-specific protein that targets the DCC to X chromosomes (Dawes et al., 1999). In accordance with our RNAi-based findings, both *dpy-28(y1)* and *sdc-2(y46)* completely suppress the dauer-constitutive phenotype of *eak-7;akt-1* double mutant animals (Figures 5.3B and 5.3C, respectively). Together, these results implicate the DCC itself in the control of dauer arrest.

Reducing DCC activity could suppress dauer arrest due to a reduction in dosage compensation. Alternatively, the dauer suppression phenotype could be a consequence of perturbing a novel, dosage-compensation-independent function of the DCC. To distinguish between these two possibilities, we took advantage of the observation that mutations that disrupt dosage compensation, while causing severe phenotypes in XX hermaphrodite animals, are phenotypically silent in XO male animals owing to the fact that the DCC does not repress X-linked gene expression in males (Meyer, 2010). Therefore, we compared the effect of DCC component RNAi on the dauer-constitutive phenotype of *eak-7;akt-1* hermaphrodites and males. In contrast to what was observed in *eak-7;akt-1* hermaphrodites, DCC component RNAi had no effect on the dauer-constitutive phenotype of *eak-7;akt-1* male siblings. In comparison, *daf-16/FoxO* and *daf-12* RNAi fully suppressed dauer arrest in *eak-7;akt-1* hermaphrodites and males (Figure 5.3A). Because DCC-mediated repression does not occur in males, these data suggest that the DCC controls dauer arrest through dosage compensation *per se*.

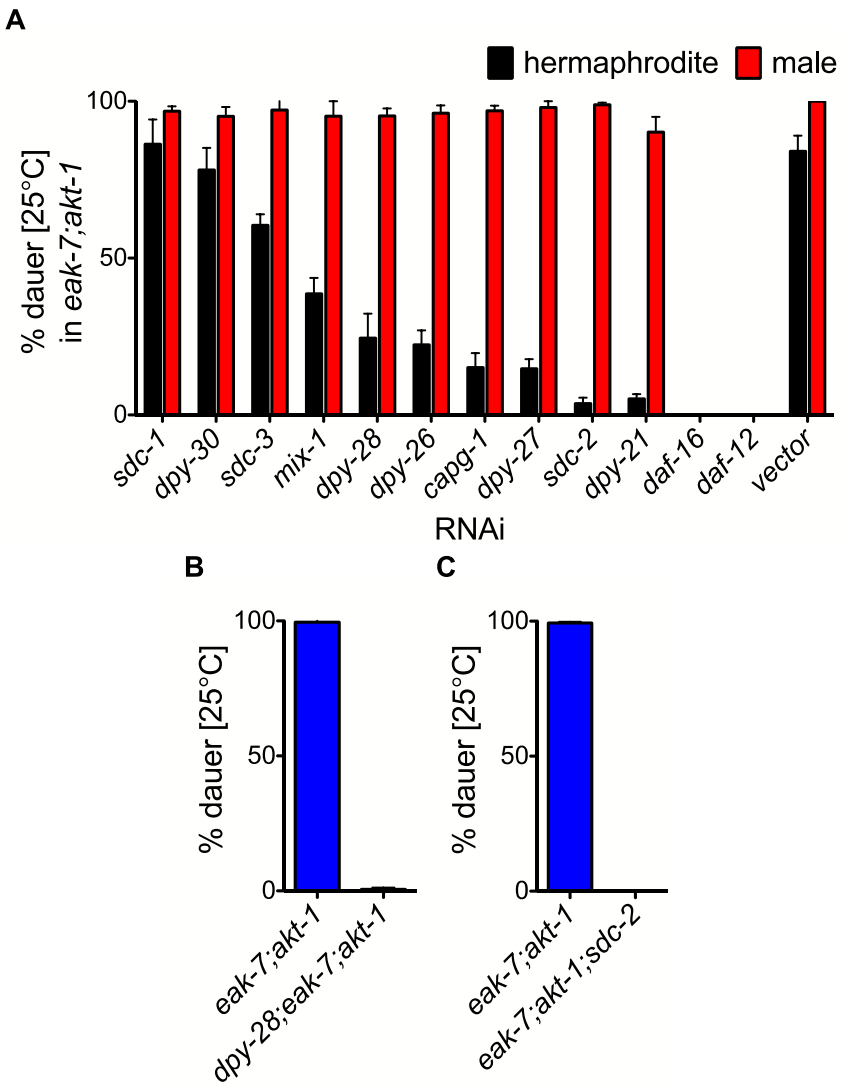

Figure 5.3: Dosage compensation influences dauer arrest.
Effect of RNAi of individual dosage compensation complex components on the dauer-constitutive phenotype of *eak-7;akt-1* hermaphrodites (black bars) and males (red bars). Reducing expression of most dosage compensation complex components by RNAi mediated knock-down suppresses arrest of *eak-akt-1* hermaphrodites ($p < 0.05$ for all DCC components except for *sdc-1* and *dpy-30*, which were not significantly different from vector, as calculated by a one-way ANOVA). Dauer arrest in male animals subjected to DCC component RNAi clone was not statistically different from vector control for any RNAi clone tested. In contrast, *daf-16* and *daf-12* RNAi caused significant suppression of dauer arrest in both hermaphrodite and male animals ($p < 0.001$ for comparison between *daf-16* or *daf-12* RNAi and vector control). Data are from a single experiment, representative of three replicates, with 100-800 animals scored per RNAi condition, per sex. Error bars indicate SEM. Raw data and statistics are presented in Supplemental Table 5.1.

Dauer inhibitory genes are upregulated in *dpy-21* mutants

Dosage compensation could potentially influence dauer arrest by controlling the expression of X-linked genes that normally function to inhibit dauer arrest. *C. elegans* has nine known X-linked dauer regulatory genes, most of which encode proteins that inhibit dauer arrest: *mrp-1* (Yabe et al., 2005), *daf-3* (Patterson et al., 1997), *pdk-1* (Paradis et al., 1999), *ncr-1* (Li et al., 2004), *daf-9* (Gerisch et al., 2001; Jia et al., 2002), *ist-1*(Wolkow et al., 2002), *daf-12* (Antebi et al., 2000), *ftt-2* (Li et al., 2007), and *akt-2* (Paradis and Ruvkun, 1998). Six of these genes have previously been shown to be upregulated approximately 2-fold in embryos defective in dosage compensation (Jans et al., 2009) (Supplemental Table 5.2). Notably, four of these genes, *ist-1*, *pdk-1*, *akt-2*, and *ftt-2*, encode components of the DAF-2/IGFR pathway, and the products of all four genes inhibit DAF-16/FoxO activity (Paradis and Ruvkun, 1998; Paradis et al., 1999; Wolkow et al., 2002; Li et al., 2007).

We quantified expression of these nine dauer regulatory genes in *eak-7;akt-1 dpy-21* triple mutant animals and their *eak-7;akt-1* double mutant siblings in animals raised at 25° for 24 hours after hatching (this time point corresponds to the L2 transition, following which animals commit developmentally to either dauer arrest or reproductive development). Expression of most of the X-linked dauer regulatory genes was increased approximately 2-fold in *eak-7;akt-1 dpy-21* triple mutants compared to *eak-7;akt-1* double mutant siblings, consistent with their modulation by dosage compensation [Figure 5.4A, left panel, and Supplemental Figure 5.3; (Jans et al., 2009)]. All four genes encoding DAF-2/IGFR pathway components that inhibit DAF-16/FoxO were upregulated in the context of *dpy-21* mutation (*ist-1*: 2.87-fold increase in *eak-7;akt-1 dpy-21* compared to *eak-7;akt-1*; *pdk-1*: increased 1.77-fold; *akt-2*: increased 3.46-fold; *ftt-2*: increased 1.57-fold). An increase in expression of these proteins would be predicted to inhibit DAF-16/FoxO activity by promoting its phosphorylation, nuclear export, and/or retention in the cytoplasm.

Strikingly, the expression of *daf-9*, the cytochrome P450 family member that catalyzes the final step in DA biosynthesis (Motola et al., 2006), was increased in the context of *dpy-21* mutation to a much greater extent than would be expected based on a reduction in dosage compensation. In four independent biological replicates, *daf-9* expression increased approximately 8- to 30-fold in *eak-7;akt-1 dpy-21* triple mutants compared to *eak-7;akt-1* siblings. This may be a consequence of suppression of the *eak-7;akt-1* dauer-constitutive phenotype by *dpy-21(null)*, as hypodermal *daf-9* expression is induced in reproductively growing *daf-2* mutant larvae but repressed in *daf-2* mutant dauers (Gerisch and Antebi, 2004). Notably, although many X-linked genes are upregulated approximately two-fold in mutants defective in dosage compensation, the influence of the DCC on the expression of individual X-linked genes is highly variable (Jans et al., 2009).

To determine whether changes in the expression of autosomal dauer inhibitory genes contribute to suppression of *eak-7;akt-1* dauer arrest by *dpy-21* inactivation, we quantified the expression of eleven autosomal dauer inhibitory genes in *eak-7;akt-1 dpy-21* triple mutants and their *eak-7;akt-1* double mutant siblings (Figure 5.4A, right panel, and Supplemental Figure 5.3). In contrast to X-linked dauer regulatory genes, expression of autosomal dauer inhibitory genes either did not change or increased only modestly in *eak-7;akt-1 dpy-21* triple mutants compared to eak-7;akt-1 sibling controls (Figure 5.4A, compare left and right panels). This finding is consistent with a model whereby *dpy-21* mutation suppresses dauer arrest via the perturbation of dosage compensation.

DPY-21 promotes DAF-16/FoxO nuclear localization

Our genetic analysis suggests that DPY-21 controls dauer arrest primarily by influencing DAF-2/IGFR signaling (Figure 5.2). The upregulation of four X-linked genes encoding DAF-2/IGFR pathway components that inhibit DAF-16/FoxO activity in the context of *dpy-21* mutation (Figure 5.4A) is predicted to result in DAF-16/FoxO inhibition due to increased nuclear export and cytoplasmic sequestration of DAF-16/FoxO. If this is the major mechanism through which DPY-21 controls dauer arrest, then *dpy-21* inactivation should promote the nuclear export of DAF-16/FoxO. To test this model, we determined the effect of *dpy-21* RNAi on the subcellular localization of a functional DAF-16A::GFP

fusion protein (Henderson and Johnson, 2001) in *daf-16(null);akt-1(null)* double mutant animals (Figures 5.4B and Supplemental Figure 5.2). As previously shown (Zhang et al., 2008; Alam et al., 2010; Dumas et al., 2010), DAF-16A::GFP was nuclear in many *akt-1(null)* animals cultured on *E. coli* containing a control RNAi construct. Exposure of animals of the same genotype to *dpy-21* RNAi promoted the nuclear export and cytoplasmic retention of DAF-16A::GFP. Therefore, DPY-21 promotes the nuclear localization of DAF-16A::GFP.

DPY-21 activates DAF-16/FoxO

To determine the impact of *dpy-21* inactivation on DAF-16/FoxO activity in dauer regulation, we quantified the expression of the DAF-16/FoxO target genes *sod-3, mtl-1*, and *dod-3* (Murphy et al., 2003; Oh et al., 2006) in *eak-7;akt-1 dpy-21* triple mutants and their *eak-7;akt-1* double mutant siblings grown at 25° for 24 hours after hatching. As previously shown (Alam et al., 2010), the expression of all three genes is increased in a *daf-16/FoxO*-dependent manner in *eak-7;akt-1* double mutants (Figure 5.4C). *dpy-21* null mutation strongly reduced the expression of at least two of the three genes in the *eak-7;akt-1* double mutant background, though not to the same extent as a *daf-16* null mutation. These results are consistent with a model whereby DPY-21 activates DAF-16/FoxO, as *dpy-21* mutation results in significant but incomplete inhibition of DAF-16/FoxO activity.

If suppression of the dauer-constitutive phenotype of *eak-7;akt-1* double mutants by *dpy-21* mutation (Figure 5.1C) is due to DAF-16/FoxO inhibition secondary to increases in the expression of *ist-1, ftt-2, pdk-1,* and *akt-2* (Figure 5.4), then reducing the expression of *ist-1, ftt-2, pdk-1,* and *akt-2* expression by approximately two-fold in *eak-7;akt-1 dpy-21* triple mutants should restore the dauer-constitutive phenotype. As a first step toward testing this hypothesis, we determined the dauer-constitutive phenotype of *eak-7;akt-1 dpy-21* triple mutants that were heterozygous for the *akt-2(ok393)* null mutation. To test this model, we sought to reduce the expression of one of the X-linked DAF-2/IGFR pathway genes, *akt-2*, to see if abrogating the *dpy-21(null)*-induced expression increase was sufficient to rescue dauer arrest in *eak-7;akt-1 dpy-21(null)* animals. We used *akt-*

2(ok393) null heterozygousity to reduce expression of *akt-2* by approximately half, and then asked whether dauer arrest was restored in the progeny of *eak-7;akt-1 dpy-21;akt-2/+* parents compared to controls with wild-type *akt-2*. *akt-2(ok393) null* mutation is known to synergize with *akt-1* mutation to promote dauer arrest, such that *akt-1;akt-2* double homozygous mutant animals arrest constitutively as dauers and do not recover (Alam et al., 2010). We found that *eak-7;akt-1 dpy-21(null)* mutants heterozygous for *akt-2(ok393)* threw less than 25% dauer progeny, indicating that there was not rescue of dauer arrest beyond that expected from normal Mendelian segregation of the mutant *akt-2(ok393)* allele in the progeny (Figure 5.4D). Supporting this inference, all dauer progeny from *eak-7;akt-1 dpy-21;akt-2/+* parents never recovered from dauer after several days at permissive temperature (data not shown), suggesting their genotype was indeed *eak-7;akt-1 dpy-21;akt-2* and not *eak-7;akt-1 dpy-21;akt-2/+*.

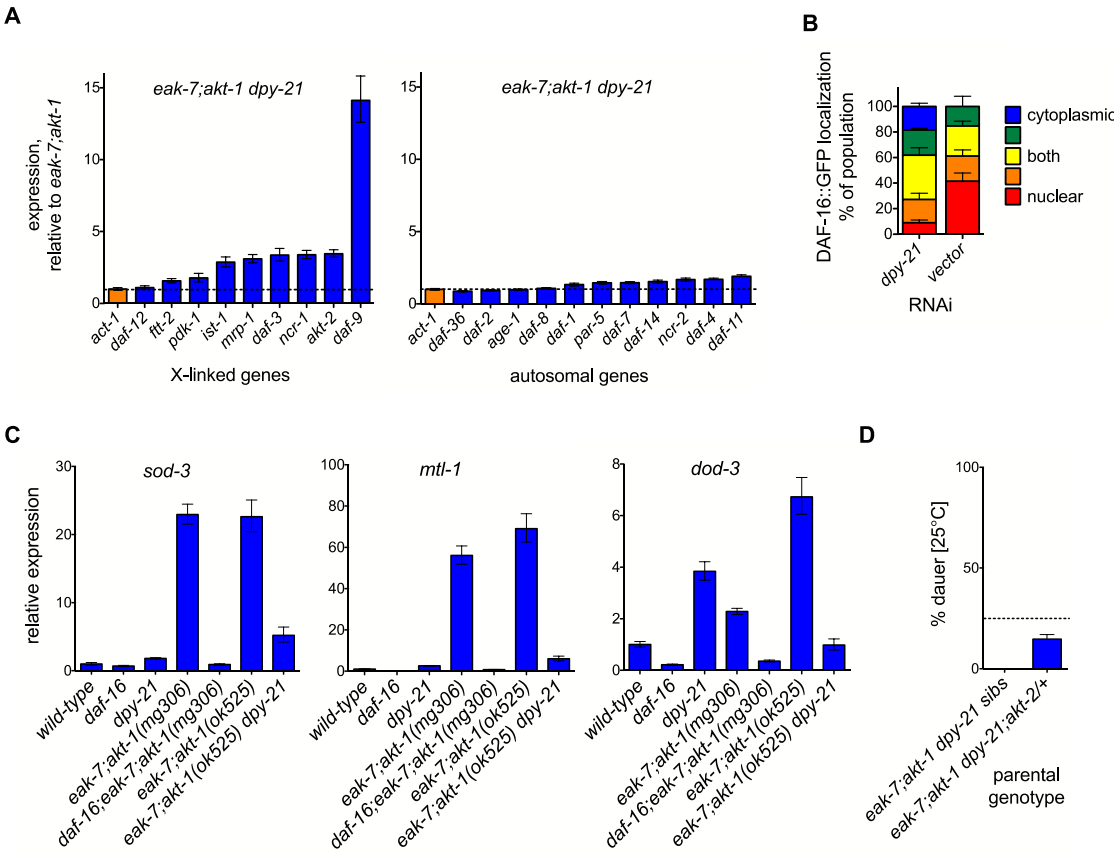

Figure 5.4: DPY-21 activates DAF-16/FoxO.
(A) Effect of *dpy-21(null)* on the expression of X-linked and autosomal dauer inhibitory genes (blue bars) at the L2 stage in dauer-inducing conditions. Data are normalized to expression levels of actin (*act-1*, orange bars), which is not X-linked. Expression in *eak-7;akt-1 dpy-21* relative to expression in *eak-7;akt-1* is shown. The dashed line indicates relative expression of one. Data are from a single representative experiment. Error bars indicate 95% confidence interval. Replicate data are presented in Supplemental Figure 5.3. (B) DPY-21 promotes DAF-16/FoxO nuclear localization in an *akt-1(null)* background. Localization of DAF-16A::GFP was assessed in L2 or L3 *daf-16(null);akt-1(null)* double mutant animals after growth on *E. coli* harboring either control plasmid or *dpy-21* RNAi plasmid for two generations. DAF-16A::GFP localization was scored on 1 to 5 cytoplasmic/nuclear scale. 1 (blue) = all cells in the animal have completely cytoplasmic localization; 2 (green) = most cells in the animal have completely cytoplasmic localization; 3 (yellow) = cells have both nuclear and cytoplasmic localization; 4 (orange) = most cells in the animal have completely nuclear localization; 5 (red) = all cells in the animal have completely nuclear localization. See Supplemental Figure 5.2 for representative images. Data represent three replicate experiments of approximately 30 animals per condition. Error bars indicate SEM. (C) DPY-21 promotes DAF-16/FoxO target gene expression. *sod-3*, *mtl-1*, and *dod-3* expression were quantified in L2 larvae under dauer inducing-conditions. Data are normalized to expression levels of actin (*act-1*) and expressed relative to wild-type N2 Bristol expression. *eak-7;akt-*

1(ok525) animals are siblings of *eak-7;akt-1 dpy-21* animals. Data are from a single experiment. Error bars indicate 95% confidence interval. Replicate data are presented in Supplemental Figure 5.4. (D) Reducing *akt-2* expression does not rescue dauer arrest of *eak-7;akt-1 dpy-21(null)* triple mutants. Dauer arrest was assayed in the progeny of *eak-7;akt-1 dpy-21(null);akt-2/+* parents compared to *eak-7;akt-1 dpy-21(null)* sibling controls. *akt-2* heterozygousity did not rescue dauer arrest beyond the 25% predicted from segregation of the *akt-2* mutant allele in the assayed generation (14.72% dauer arrest in progeny of *eak-7;akt-1 dpy-21(null);akt-2/+* parents, $p = 0.0002$ for comparison v. theoretical mean value of 25% arrest, by one-sample t-test). Data are pooled from two replicate experiments with at least 500 animals assayed per parental genotype. Error bars indicate SEM. Raw data and statistics are presented in Supplemental Table 5.1.

Discussion

Although much is known about the molecular components of the dosage compensation machinery and its influence on X-linked gene expression in *C. elegans* and other organisms, the physiologic consequences of dosage compensation are poorly understood. We have discovered a new function for dosage compensation in the control of DAF-2/IGFR signaling and dauer arrest. To our knowledge, this represents the first report of a specific post-embryonic function for dosage compensation in any organism.

We have shown that *dpy-21* mutation suppresses dauer arrest due to a defect in dosage compensation (Figures 5.1, 5.2, and 5.3). Impaired compensation of X-linked gene expression results in the increased expression of dauer inhibitory genes, including four genes encoding DAF-2/IGFR signaling components that inhibit DAF-16/FoxO activity by promoting its nuclear export and cytoplasmic retention (Figure 5.4A). Accordingly, *dpy-21* inactivation induces the relocalization of DAF-16/FoxO from nuclei to cytoplasm (Figure 5.4B) and inhibits the expression of DAF-16/FoxO target genes (Figure 5.4C). Our results support a model in which DPY-21 (and presumably the DCC) controls dauer arrest and DAF-16/FoxO activity by modulating the expression of DAF-2/IGFR pathway components that influence the nucleocytoplasmic trafficking of DAF-16/FoxO (Figure 5.5).

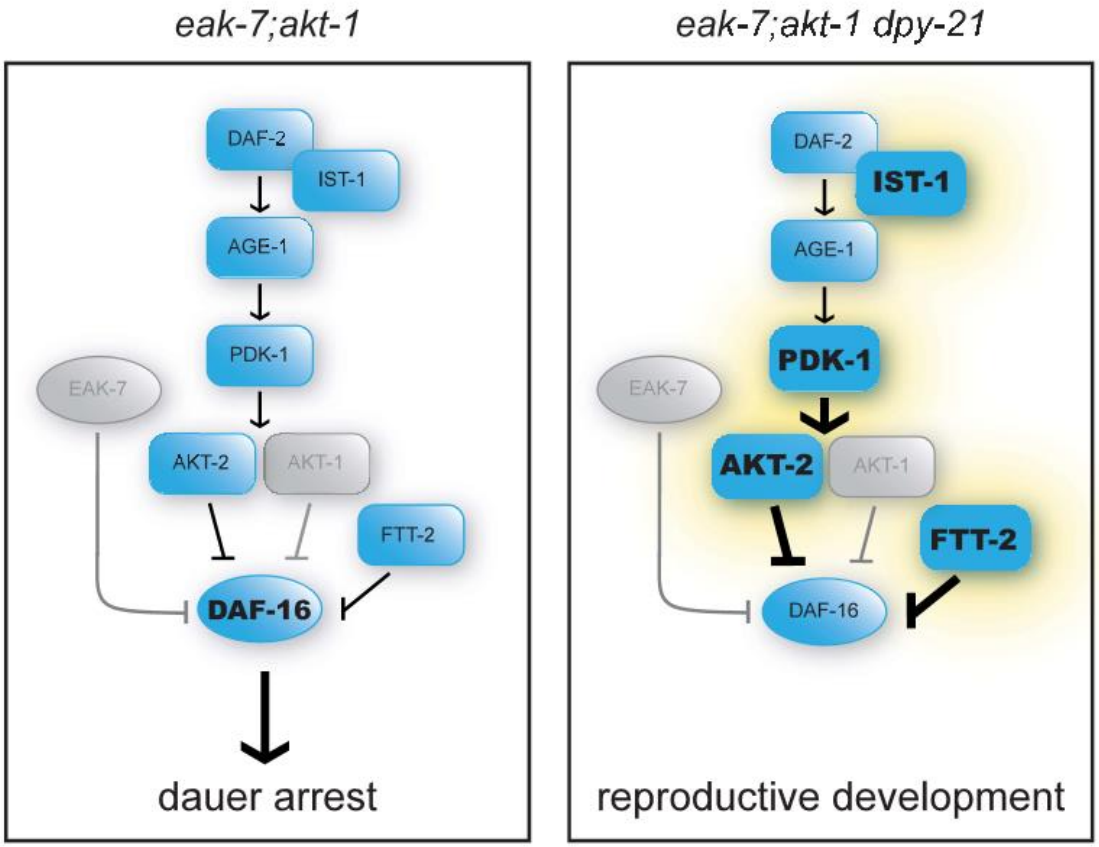

Figure 5.5: Model of DAF-2/IGFR pathway regulation by DPY-21.
In *eak-7;akt-1* double mutant animals, activated DAF-16/FoxO promotes dauer arrest (left panel). In *eak-7;akt-1 dpy-21* triple mutant animals, increased expression of *ist-1*, *pdk-1*, *akt-2*, and *ftt-2* contributes to suppression of dauer arrest by promoting the inhibition of DAF-16/FoxO (right panel).

While our data support a model whereby *dpy-21* mutation results in dauer suppression via DAF-16/FoxO inhibition as a result of DAF-2/IGFR pathway activation, we cannot rule out the contribution of the expression level increases of the multiple X-linked and autosomally encoded dauer inhibitory genes, as well as the potential contribution of other genes that we did not test that may change in response to *dpy-21* mutation. It is noteworthy that all genes tested have dauer constitutive phenotype when mutated, indicating that the normal function of the molecules encoded by these genes is to

suppress dauer. All targets assayed either increased or did not change; given the impact of these targets on dauer arrest, any increases would be predicted to contribute to suppression of dauer. Because of this, the dauer suppression phenotype we observe in *dpy-21* mutant animals might be a consequence of expression changes of many genes simultaneously. Consistent with this, reducing *akt-2* expression via heterozygous deletion of *akt-2* (via *akt-2(ok393) null* allele), did not rescue dauer arrest in the *eak-7;akt-1 dpy-21(null)* mutant population (Figure 5.4D), suggesting that expression level changes in just one gene are insufficient to cause the observed *seak* phenotype. Thus, dauer suppression in *dpy-21(null)* mutant animals may be a result of the concurrent increase in expression of *akt-2, ist-1, pdk-1* and *ftt-2*, but we cannot exclude the contribution of molecules in other dauer regulatory pathways acting either upstream or downstream of DAF-16/FoxO to control dauer arrest.

The observation that *dpy-21(null)* suppresses the dauer-constitutive phenotypes of DAF-2/IGFR pathway mutants to a greater extent that it suppresses DAF-7/TGFβ-like pathway mutants (Figure 5.2) supports the model that the major impact of DPY-21 on dauer regulation occurs through the modulation of DAF-16/FoxO subcellular localization. In addition to regulation of localization by the DAF-2/IGFR pathway, the DAF-7/TGFβ-like pathway can also influence DAF-16/FoxO nuclear localization, as *daf-7* mutation promotes nuclear accumulation of DAF-16/FoxO (Lee et al., 2001; Shaw et al., 2007); whether the TGFβ-like pathway regulates nuclear localization of DAF-16/FoxO independently or via regulation of the DAF-2/IGFR pathway is unclear. The key role of the DAF-2/IGFR pathway in the regulation of DAF-16/FoxO nuclear localization thus correlates with the strength of dauer suppression we observe in the context of *dpy-21* mutation; dauer arrest of DAF-2/IGFR pathway mutants was strongly suppressed, in contrast to modest suppression of arrest in TGFβ-like pathway mutants and dafachronic acid/DAF-12 pathway mutants (Figure 5.2, Supplemental Figure 5.1).

The establishment of a role for dosage compensation in the control of dauer arrest and insulin-like signaling may serve as a platform for investigations into other post-embryonic processes that might be influenced by dosage compensation, whether dosage

compensation is physiologically regulated, and whether it is dysregulated in human disease. Indeed, a recent study in mice suggests that sex chromosome dosage *per se* can influence metabolic phenotypes independently of gonadal sex (Chen et al., 2012). Furthermore, skewing of X chromosome inactivation increases with age in human females and is attenuated in cohorts of female centenarians (Gentilini et al., 2012), suggesting a correlation between dysregulation of dosage compensation and the aging process. To date, studies on dosage compensation have largely focused on the establishment of dosage compensation during embryogenesis; mechanisms governing the post-embryonic stability of dosage compensation remain poorly understood. Further inquiry into the function and regulation of dosage compensation in post-embryonic contexts has the potential to illuminate new functions for dosage compensation and provide insights into the pathogenesis of human disease.

Supplemental Information

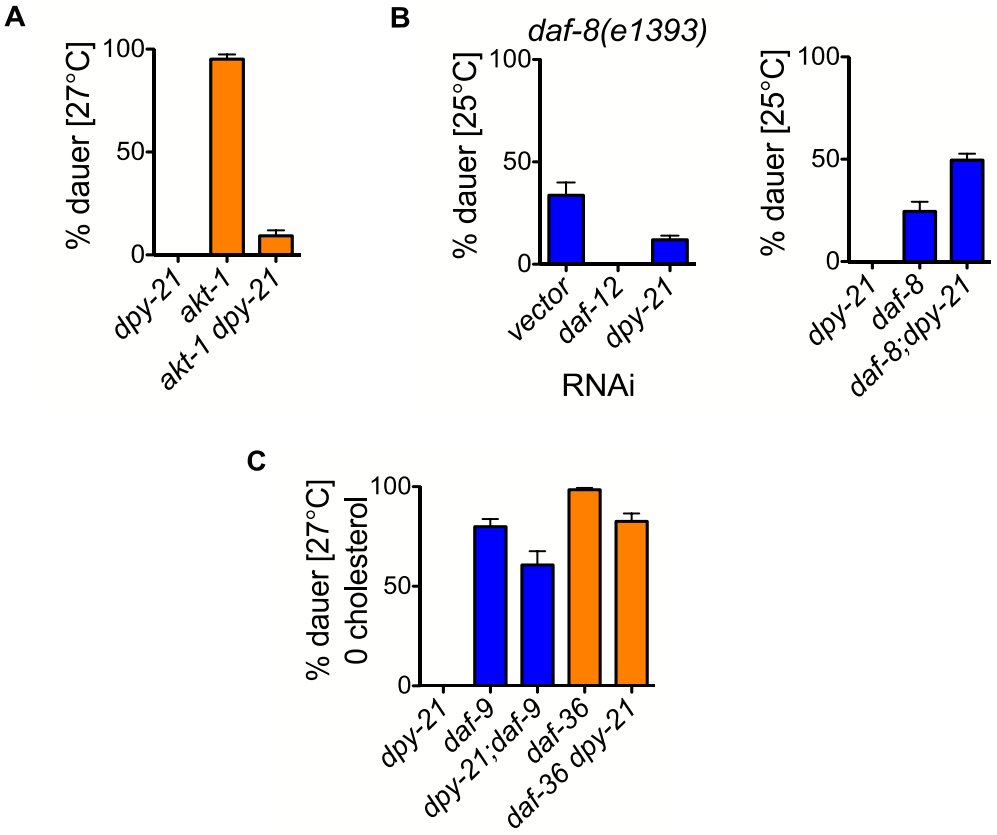

Supplemental Figure 5.1: DPY-21 regulates dauer arrest.
(A) *dpy-21(null)* suppresses 27°C dauer arrest of *akt-1* mutant animals (6.3% dauer arrest in *akt-1 dpy-21* mutants compared to 92.5% arrest in *akt-1*, P <0.0001). Data are pooled from four replicate experiments with at least 700 animals scored per genotype. (B) *dpy-21* RNAi suppresses the dauer-constitutive phenotype of the TGFβ-like pathway mutant *daf-8(e1393)* (11.9% dauer arrest in *daf-8* mutants exposed to *dpy-21* RNAi compared to 33.7% arrest in animals exposed to control vector, p = 0.0289). Data are from a single representative experiment with at least 450 animals scored per condition. In contrast, *dpy-21(null)* enhances dauer arrest of *daf-8* mutant animals (49.6% dauer arrest in *daf-8; dpy-21* mutants compared to 24.5% arrest in *daf-8*, p = 0.0004). Data are pooled from three replicate experiments with at least 950 animals scored per genotype. (C) *dpy-21(null)* suppresses 27°C, dauer arrest of *daf-9(k182)* and *daf-36(k114)* mutants raised on plates without supplemental cholesterol (60.7% dauer arrest in *dpy-21;daf-9* mutants compared to 79.9% arrest in *daf-9*, p = 0.0269; 82.6% dauer arrest in *daf-36 dpy-21* mutants compared to 98.4% arrest in *daf-36*, p = 0.0004). Data are pooled from four replicate experiments with at least 450 animals scored per genotype. (A-C) Error bars indicate SEM. Raw data and statistics are presented in Supplemental Table 5.1.

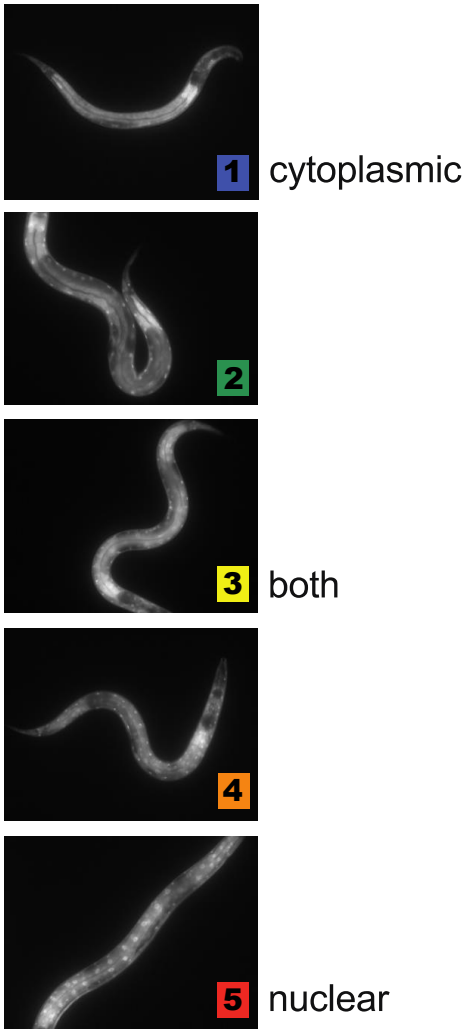

Supplemental Figure 5.2: Representative images of animals exhibiting cytoplasmic and nuclear DAF-16A::GFP localization.
The scale ranges from "1" (all cells have completely cytoplasmic localization) to "5" (all cells have completely nuclear localization).

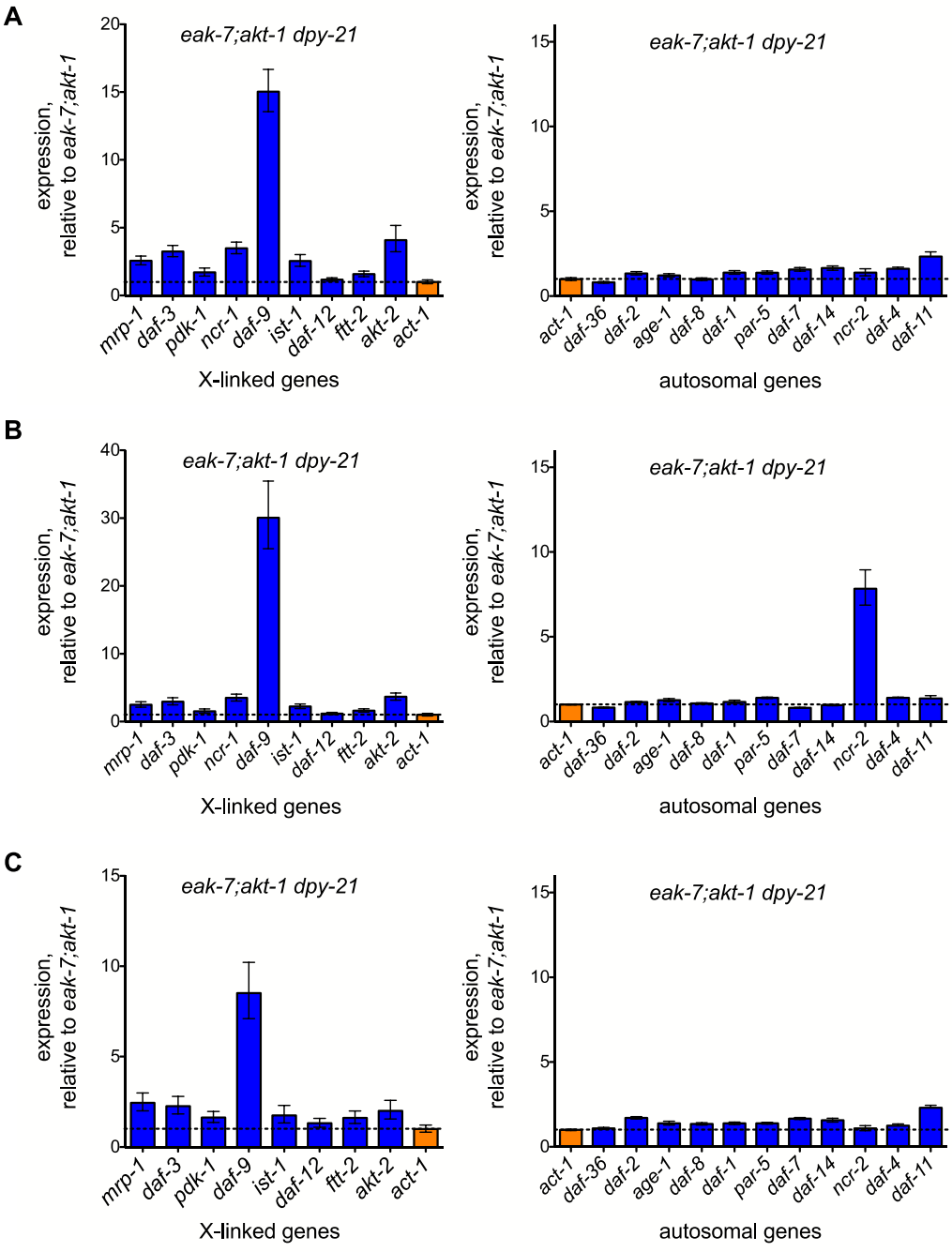

Supplemental Figure 5.3: X-linked and autosomal gene expression replicate data. Data are normalized to actin (*act-1*, orange bar) and expressed relative to *eak-7;akt-1 dpy-21(wt)* expression. Dashed line indicates relative expression of one. Each row corresponds to one biological replicate, with X-linked and autosomally encoded dauer inhibitory gene expression profiled from the same sample. Error bars indicate 95% confidence interval.

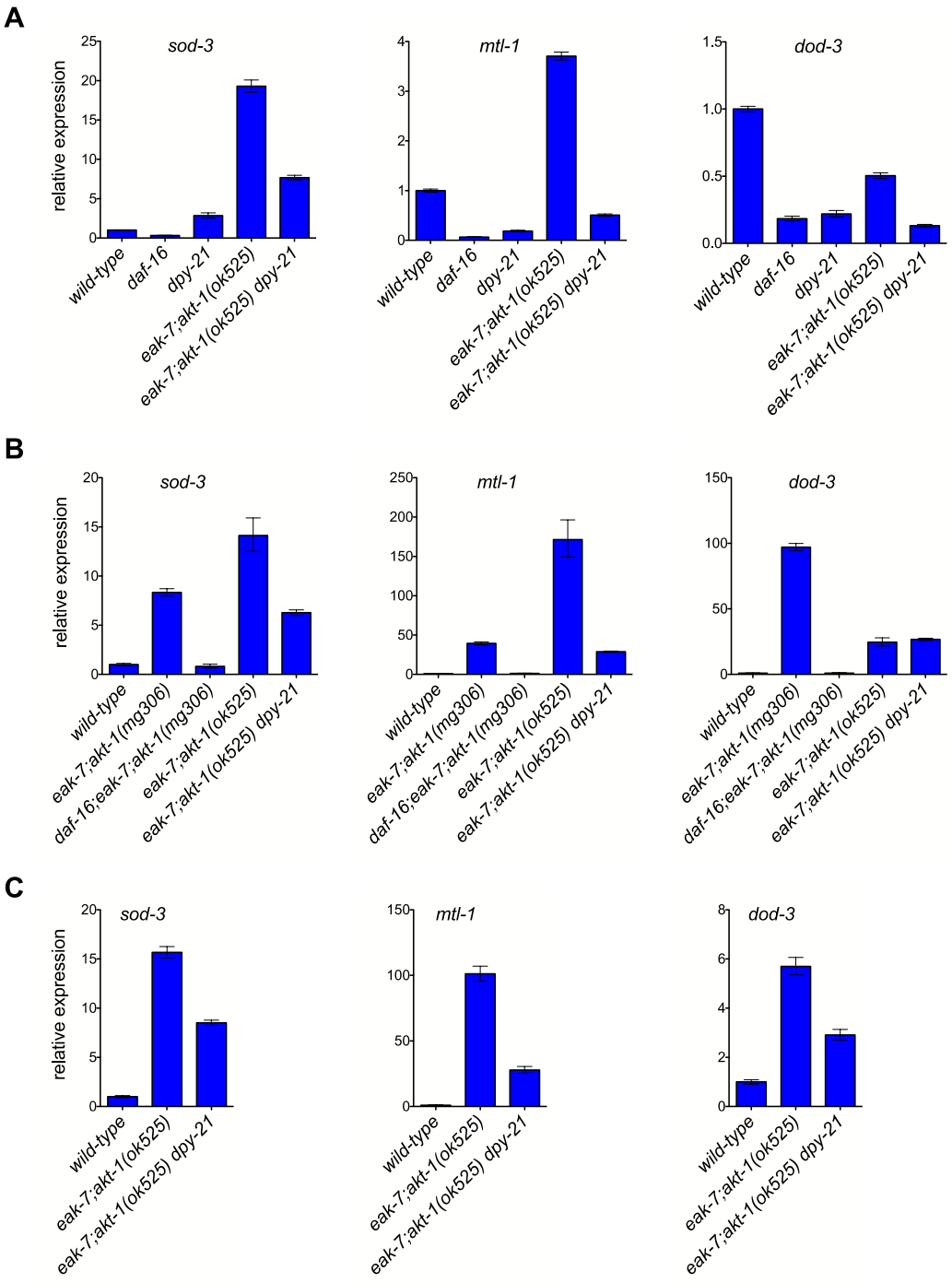

Supplemental Figure 5.4: DAF-16/FoxO target gene expression replicate data. Data are normalized to actin (*act-1*) and expressed relative to wild-type N2 Bristol expression. *eak-7;akt-1(ok525)* animals are siblings of *eak-7;akt-1 dpy-21* animals. Data in each row are from a single biological replicate. Error bars indicate 95% confidence interval.

Supplemental Table 5.1: Raw data and statistics for dauer assays.

FIGURE 1

Figure 1B

eak-7;akt-1	RNAi		
	dpy-21	*daf-16*	*vector*
Mean	13.35	0.33	75.58
Std. Deviation	2.31	0.65	17.40
Std. Error	1.16	0.33	8.70
n	287	268	302
# experiments	1		
comparison	v. vector RNAi	v. vector RNAi	
p value	0.0004	< 0.0001	
sig level	***	****	

Figure 1C
genotype:

	wild-type	*eak-7;akt-1*	*eak-7;akt-1 dpy-21(e428)*	*eak-7;akt-1 dpy-21(dp253)*
Mean	0.00	94.19	0.07	0.05
Std. Deviation	0.00	11.40	0.21	0.17
Std. Error	0.00	2.69	0.07	0.05
n	1094	3123	1098	1534
# experiments	3			
comparison	*v. wild-type*	*v. eak-7;akt-1*	*v. eak-7;akt-1*	*v. eak-7;akt-1*
p value	< 0.0001	< 0.0001	< 0.0001	< 0.0001
sig level	****	****	****	****

FIGURE 2

Figure 2B, D, F
genotype:

	dpy-21	*daf-1*	*daf-1;dpy-21*	*daf-14*	*daf-14;dpy-21*	*daf-2*	*daf-2;dpy-21*	*daf-9(dh6)*	*dpy-21;daf-9(dh6)*
Mean	0.00	94.31	74.50	42.51	20.04	96.46	17.18	100.00	100.00
Std. Deviation	0.00	6.81	19.16	19.10	5.50	2.43	5.95	0.00	0.00
Std. Error	0.00	2.27	6.39	6.37	1.83	0.81	1.98	0.00	0.00
n	430	1101	783	833	1308	1453	1360	452	286
# experiments	1	3		3		3		1	
comparison	*daf-1;dpy-21 v. daf-1*			*daf-14;dpy-21 v. daf-14*		*daf-2;dpy-21 v. daf-2*		*dpy-21;daf-9(dh6) v. daf-9(dh6)*	
p value	0.01			0.0037		< 0.0001		0.9503	
sig level	**			**		****		ns	

Figure 2A
daf-2(e1368)

	RNAi		
	vector	*daf-12*	*dpy-21*
Mean	95.23	0.81	91.73
Std. Deviation	1.91	1.93	3.87
Std. Error	0.64	0.64	1.29
n	1000	1461	1316
# experiments	3		
comparison	v. vector RNAi	v. vector RNAi	
p value	< 0.0001	0.0275	
sig level	****	*	

Figure 2C
daf-1(m40)

	RNAi		
	vector	*daf-12*	*dpy-21*
Mean	89.26	0.27	90.95
Std. Deviation	9.79	0.41	4.15
Std. Error	4.00	0.17	1.69
n	588	909	1020
# experiments	2		
comparison	v. vector RNAi	v. vector RNAi	
p value	< 0.0001	0.7064	
sig level	****	ns	

Figure 2E
daf-9(dh6)

	RNAi		
	vector	*daf-12*	*dpy-21*
Mean	100.00	2.90	99.69
Std. Deviation	0.00	3.75	0.68
Std. Error	0.00	1.32	0.23
n	841	1065	1289
# experiments	3		
comparison	v. vector RNAi	v. vector RNAi	
p value	< 0.0001	0.2153	
sig level	****	ns	

daf-14(m77)

	RNAi		
	vector	*daf-12*	*dpy-21*
Mean	33.78	0.33	16.02
Std. Deviation	15.02	0.60	8.97
Std. Error	6.13	0.24	3.66
n	1043	1044	1192
# experiments	2		
comparison	v. vector RNAi	v. vector RNAi	
p value	< 0.0001	0.0321	
sig level	****	*	

Supplemental Table 5.1, continued

FIGURE 3A

RNAi construct	hermaphrodite			male		
	Mean	Std. Deviation	n	Mean	Std. Deviation	n
capg-1	15.09	8.03	485	96.98	2.77	192
dpy-21	5.13	2.58	667	90.17	9.75	118
dpy-26	22.35	7.98	649	96.21	4.99	224
dpy-27	14.74	5.32	710	97.87	2.01	127
dpy-28	24.51	13.47	647	95.29	4.89	220
dpy-30	78.06	12.21	485	95.21	5.91	184
mix-1	38.59	8.82	137	95.24	8.25	22
sdc-1	86.29	13.71	547	96.79	2.76	174
sdc-2	3.61	3.29	420	98.91	1.06	182
sdc-3	60.44	6.15	435	97.17	4.00	99
vector	84.05	8.62	800	100.00	0.00	161
daf-16	0.00	0.00	300	0.00	0.00	221
daf-12	0.00	0.00	303	0.00	0.00	242

Hermaphrodites

One-way analysis of variance

P value	< 0.0001
P value summary	****
Number of groups	13
F	47.59
R square	0.9565

Dunnett's Multiple Comparison Test

	Mean Diff.	q	P < 0.05?	Summary	95% CI of diff
vector vs capg-1	68.96	10.25	Yes	***	48.91 to 89.01
vector vs dpy-21	78.92	11.73	Yes	***	58.87 to 98.97
vector vs dpy-26	61.7	9.173	Yes	***	41.65 to 81.74
vector vs dpy-27	69.31	10.3	Yes	***	49.26 to 89.35
vector vs dpy-28	59.54	8.852	Yes	***	39.49 to 79.58
vector vs dpy-30	5.986	0.89	No	ns	-14.06 to 26.03
vector vs mix-1	45.46	6.759	Yes	***	25.41 to 65.51
vector vs sdc-1	-2.246	0.334	No	ns	-22.29 to 17.80
vector vs sdc-2	80.44	11.96	Yes	***	60.39 to 100.5
vector vs sdc-3	23.6	3.509	Yes	*	3.557 to 43.65
vector vs daf-16	84.05	12.5	Yes	***	64.00 to 104.1
vector vs daf-12	84.05	12.5	Yes	***	64.00 to 104.1

Males

One-way analysis of variance

P value	< 0.0001
P value summary	****
Number of groups	13
F	158.4
R square	0.985

Dunnett's Multiple Comparison Test

	Mean Diff.	q	P < 0.05?	Summary	95% CI of diff
vector vs capg-1	3.019	0.7884	No	ns	-8.304 to 14.34
vector vs dpy-21	9.832	2.773	No	ns	-0.6514 to 20.31
vector vs dpy-26	3.793	1.07	No	ns	-6.690 to 14.28
vector vs dpy-27	2	0.4606	No	ns	-10.84 to 14.84
vector vs dpy-28	4.712	1.329	No	ns	-5.772 to 15.19
vector vs dpy-30	4.794	1.352	No	ns	-5.689 to 15.28
vector vs mix-1	4.762	1.243	No	ns	-6.561 to 16.09
vector vs sdc-1	3.207	0.8374	No	ns	-8.116 to 14.53
vector vs sdc-2	1.088	0.2841	No	ns	-10.24 to 12.41
vector vs sdc-3	2.83	0.6517	No	ns	-10.01 to 15.67
vector vs daf-16	100	26.11	Yes	***	88.68 to 111.3
vector vs daf-12	100	26.11	Yes	***	88.68 to 111.3

FIGURE 3B

FIGURE 3C

Supplemental Table 5.1, continued

FIGURE 4D

parental genotype:	*eak-7;akt-1 dpy-21 sibs*	*eak-7;akt-1 dpy-21;akt-2/+*
Mean	0.04	14.72
Std. Deviation	0.22	10.75
Std. Error	0.04	2.29
n	1390	537
# experiments	2	
comparison	*eak-7;akt-1 dpy-21;akt-2/+ v.* 25%	
p value	0.0002	

FIGURE S1

Figure S1A

genotype:	*dpy-21*	*akt-1*	*akt-1 dpy-21*
Mean	0.00	92.46	6.28
Std. Deviation	0.00	7.08	5.59
Std. Error	0.00	2.04	1.61
n	430	827	744
# experiments	1	4	
comparison		*akt-1 dpy-21 v. akt-1*	
p value		< 0.0001	
sig level		****	

Figure S1B

genotype:	*dpy-21*	*daf-8*	*daf-8;dpy-21*
Mean	0.00	24.53	49.66
Std. Deviation	0.00	13.98	9.18
Std. Error	0.00	4.66	3.06
n	430	1665	970
# experiments	1	3	
comparison		*daf-8;dpy-21 v. daf-8*	
p value		0.0004	
sig level		***	

Figure S1B

daf-8(e1393)	RNAi *vector*	RNAi *daf-12*	RNAi *dpy-21*
Mean	33.73	0.00	11.94
Std. Deviation	10.77	0.00	3.46
Std. Error	6.22	0.00	2.00
n	483	503	491
# experiments	1		
comparison		v. vector RNAi	v. vector RNAi
p value		< 0.0001	0.0289
sig level		****	*

Figure S1C

genotype:	*dpy-21*	*daf-9(k182)*	*dpy-21;daf-9*	*daf-36*	*daf-36 dpy-21*
Mean	0.00	79.93	60.70	98.39	82.62
Std. Deviation	0.00	11.53	20.68	2.77	9.56
Std. Error	0.00	3.84	6.89	0.92	3.90
n	430	2598	930	1075	470
# experiments	1	4		4	
comparison		*dpy-21;daf-9 v. daf-9*		*daf-36 dpy-21 v. daf-36*	
p value		0.0269		0.0004	
sig level		*		***	

Supplemental Table 5.2: Primers used for real-time quantitative PCR.

Target	Forward Primer (5' to 3')	Reverse Primer (5' to 3')
sod-3	TATTAAGCGCGACTTCGGTTCCCT	CGTGCTCCCAAACGTCAATTCCAA
mtl-1	ATGGCTTGCAAGTGTGACTG	CACATTTGTCTCCGCACTTG
dod-3	AAAAAGCCATGTTCCCGAAT	GCTGCGAAAAGCAAGAAAAT
akt-2	TCGTGATATGAAACTCGAAAATTTGC	ATTCTGGTGTTCCGCAAAAGGTG
daf-12	AATGTTTAGAGTTCTTCGGTTTCTTC	T TCGTTCATCGGAGGATCAGAG
daf-3	AGCTGCGAAGGGAAGCAACA	CTCAATCCAAACTGGACAATCATG
daf-9	ATTCCCCACAAAACAATCGAAGAAT	GAGATTCAAACACGTTTGGATCG
ftt-2	ACAGAAACTCGGTTGTCGAGAAG	ATAGAAGAAGACAGAGAAGTTGAGAG
ist-1	ATTGAAGATAACAAAGTGACCAGAAG	TGCATGCTGAAGATCTTCTATTCG
mrp-1	CGACTGAATACGGTTATGGATAGT	CACAACATTTGCATCTTTTGCCATTG
ncr-1	GCGTGCGTTTTGTCGCCAAC	C AATCCCACCTTCCGCTTTAAG
pdk-1	TTTATACATACGCCCAACCGCGT	T TTCGATAGTCACCGAGTACCG
age-1	GGATCATTTGAAGAAAACCCTCTTC	TTTGGTAGACCATGATCCATTGAAG
daf-1	GTACTGTTAGATACCTTGCACC	CGGCAGAACATCTCCATCTTC
daf-11	TTGTTTCGGAGAAGCTGTTATATTAG	ACGACCAATTCCTTCAATAGTACG
daf-14	TTCAAATATCTCAAGCCAATCTTCTT	AGCTCGTAGTAAAATATGGTACAC
daf-2	CCGGTGCGAAGAACGGTG	CCCACGTAATATGAATAGCGTCC
daf-36	GGATGGAAAATGGGAAGTGAAATC	ACCATGCTGCTCTGCAACAAG
daf-4	AATCTCTAGACAAGTTCCCATTCT	CTCCTCCTTCTTATTCTGCTGA
daf-7	GCACACCACTTCAACTTGGC	GATCAGCTTGATGTAGTCGTAC
daf-8	ACATATCAAGACGTCTACTGTCTC	CATCGGATTATTCAAATGAGCCTG
ncr-2	CAATATGGCAATGTCTCTTGGAATC	TAGATCCATTACTGACAAGTGCAG
par-5	GGCTTACCAGGAGGCTCTTG	CAAGCGTGCTCTGGAGTGTTC
scd-2	ATAGAATCCAACTGCACGAACTG	CATATTGGACTCTTGCGAGATCT

Supplemental Table 5.3: Dosage compensation of X-linked dauer regulatory genes. Adapted from Jans *et al.* 2009, Supplemental Table 4, Dosage-Compensated Genes and Supplemental Table 5, Non-Compensated Genes. "Not listed" indicates a gene that was not defined as dosage-compensated or non-compensated in the study.

Gene	**Compensated?**	**Increase (fold) in *sdc-2* mutant**	**Increase (fold) in *dpy-27* mutant**
mrp-1	Yes	1.5	1.8
daf-3	Yes	1.8	1.7
ncr-1	Yes	2.0	1.7
ist-1	Yes	2.1	1.8
daf-12	Yes	2.6	2.1
akt-2	Yes	2.8	3.1
pdk-1	Not listed		
daf-9	Not listed		
ftt-2	Not listed		

References

Ailion, M., and Thomas, J.H. (2003). Isolation and Characterization of High-Temperature-Induced Dauer Formation Mutants in Caenorhabditis elegans. Genetics *165*, 127–144.

Alam, H., Williams, T.W., Dumas, K.J., Guo, C., Yoshina, S., Mitani, S., and Hu, P.J. (2010). EAK-7 Controls Development and Life Span by Regulating Nuclear DAF-16/FoxO Activity. Cell Metabolism *12*, 30–41.

Antebi, A., Yeh, W.-H., Tait, D., Hedgecock, E.M., and Riddle, D.L. (2000). daf-12 encodes a nuclear receptor that regulates the dauer diapause and developmental age in C. elegans. Genes & Development *14*, 1512–1527.

Chen, X., McClusky, R., Chen, J., Beaven, S.W., Tontonoz, P., Arnold, A.P., and Reue, K. (2012). The number of x chromosomes causes sex differences in adiposity in mice. PLoS Genetics *8*, e1002709.

Davis, M.W., Hammarlund, M., Harrach, T., Hullett, P., Olsen, S., and Jorgensen, E.M. (2005). Rapid single nucleotide polymorphism mapping in C. elegans. BMC Genomics *6*, 118.

Dawes, H.E., Berlin, D.S., Lapidus, D.M., Nusbaum, C., Davis, T.L., and Meyer, B.J. (1999). Dosage compensation proteins targeted to X chromosomes by a determinant of hermaphrodite fate. Science *284*, 1800–1804.

Dumas, K.J., Guo, C., Wang, X., Burkhart, K.B., Adams, E.J., Alam, H., and Hu, P.J. (2010). Functional divergence of dafachronic acid pathways in the control of C. elegans development and lifespan. Developmental Biology *340*, 605–612.

Estevez, M., Attisano, L., Wrana, J.L., Albert, P.S., Massague, J., and Riddle, D.L. (1993). The daf-4 gene encodes a bone morphogenetic protein receptor controlling C. elegans dauer larva development. Nature *365*, 644–649.

Fielenbach, N., and Antebi, A. (2008). C. elegans dauer formation and the molecular basis of plasticity. Genes & Development *22*, 2149–2165.

Gentilini, D., Castaldi, D., Mari, D., Monti, D., Franceschi, C., Di Blasio, A.M., and Vitale, G. (2012). Age-dependent skewing of X chromosome inactivation appears delayed in centenarians' offspring. Is there a role for allelic imbalance in healthy aging and longevity? Aging Cell *11*, 277–283.

Georgi, L.L., Albert, P.S., and Riddle, D.L. (1990). daf-1, a C. elegans gene controlling dauer larva development, encodes a novel receptor protein kinase. Cell *61*, 635–645.

Gerisch, B., and Antebi, A. (2004). Hormonal signals produced by DAF-9/cytochrome P450 regulate C. elegans dauer diapause in response to environmental cues. Development *131*, 1765–1776.

Gerisch, B., Rottiers, V., Li, D., Motola, D.L., Cummins, C.L., Lehrach, H., Mangelsdorf, D.J., and Antebi, A. (2007). A bile acid-like steroid modulates Caenorhabditis elegans lifespan through nuclear receptor signaling. Proceedings of the National Academy of Sciences *104*, 5014–5019.

Gerisch, B., Weitzel, C., Kober-Eisermann, C., Rottiers, V., and Antebi, A. (2001). A Hormonal Signaling Pathway Influencing C. elegans Metabolism, Reproductive Development, and Life Span. Developmental Cell *1*, 841–851.

Gottlieb, S., and Ruvkun, G. (1994). daf-2, daf-16 and daf-23: Genetically Interacting Genes Controlling Dauer Formation in Caenorhabditis elegans. Genetics *137*, 107–120.

Da Graca, L.S., Zimmerman, K.K., Mitchell, M.C., Kozhan-Gorodetska, M., Sekiewicz, K., Morales, Y., and Patterson, G.I. (2004). DAF-5 is a Ski oncoprotein homolog that functions in a neuronal TGF beta pathway to regulate C. elegans dauer development. Development *131*, 435–446.

Henderson, S.T., and Johnson, T.E. (2001). daf-16 integrates developmental and environmental inputs to mediate aging in the nematode Caenorhabditis elegans. Current Biology *11*, 1975–1980.

Hertweck, M., Göbel, C., and Baumeister, R. (2004). C. elegans SGK-1 Is the Critical Component in the Akt/PKB Kinase Complex to Control Stress Response and Life Span. Developmental Cell *6*, 577–588.

Hu, P.J., Xu, J., and Ruvkun, G. (2006). Two Membrane-Associated Tyrosine Phosphatase Homologs Potentiate C. elegans AKT-1/PKB Signaling. PLoS Genet *2*, e99.

Inoue, T., and Thomas, J.H. (2000). Suppressors of transforming growth factor-beta pathway mutants in the Caenorhabditis elegans dauer formation pathway. Genetics *156*, 1035–1046.

Jans, J., Gladden, J.M., Ralston, E.J., Pickle, C.S., Michel, A.H., Pferdehirt, R.R., Eisen, M.B., and Meyer, B.J. (2009). A condensin-like dosage compensation complex acts at a distance to control expression throughout the genome. Genes & Development *23*, 602–618.

Jia, K., Albert, P.S., and Riddle, D.L. (2002). DAF-9, a cytochrome P450 regulating C. elegans larval development and adult longevity. Development *129*, 221–231.

Kamath, R.S., Martinez-Campos, M., Zipperlen, P., Fraser, A.G., and Ahringer, J. (2001). Effectiveness of specific RNA-mediated interference through ingested double-stranded RNA in Caenorhabditis elegans. Genome Biology *2*, RESEARCH0002.

Kenyon, C.J. (2010). The genetics of ageing. Nature *464*, 504–512.

Kimura, K.D., Tissenbaum, H.A., Liu, Y., and Ruvkun, G. (1997). daf-2, an Insulin Receptor-Like Gene That Regulates Longevity and Diapause in Caenorhabditis elegans. Science *277*, 942–946.

Larsen, P.L., Albert, P.S., and Riddle, D.L. (1995). Genes that regulate both development and longevity in Caenorhabditis elegans. Genetics *139*, 1567–1583.

Lee, R.Y.N., Hench, J., and Ruvkun, G. (2001). Regulation of C. elegans DAF-16 and its human ortholog FKHRL1 by the daf-2 insulin-like signaling pathway. Current Biology *11*, 1950–1957.

Li, H., and Durbin, R. (2009). Fast and accurate short read alignment with Burrows-Wheeler transform. Bioinformatics *25*, 1754–1760.

Li, J., Brown, G., Ailion, M., Lee, S., and Thomas, J.H. (2004). NCR-1 and NCR-2, the C. elegans homologs of the human Niemann-Pick type C1 disease protein, function upstream of DAF-9 in the dauer formation pathways. Development *131*, 5741–5752.

Li, J., Tewari, M., Vidal, M., and Lee, S.S. (2007). The 14-3-3 protein FTT-2 regulates DAF-16 in Caenorhabditis elegans. Developmental Biology *301*, 82–91.

Lin, K., Dorman, J.B., Rodan, A., and Kenyon, C. (1997). daf-16: An HNF-3/forkhead family member that can function to double the life-span of Caenorhabditis elegans. Science *278*, 1319–1322.

Lin, K., Hsin, H., Libina, N., and Kenyon, C. (2001). Regulation of the Caenorhabditis elegans longevity protein DAF-16 by insulin/IGF-1 and germline signaling. Nat Genet *28*, 139–145.

Mak, H.Y., and Ruvkun, G. (2004). Intercellular signaling of reproductive development by the C. elegans DAF-9 cytochrome P450. Development *131*, 1777–1786.

Meyer, B.J. (2010). Targeting X chromosomes for repression. Current Opinion in Genetics & Development *20*, 179–189.

Meyer, B.J., and Casson, L.P. (1986). Caenorhabditis elegans compensates for the difference in X chromosome dosage between the sexes by regulating transcript levels. Cell *47*, 871–881.

Morris, J.Z., Tissenbaum, H.A., and Ruvkun, G. (1996). A phosphatidylinositol-3-OH kinase family member regulating longevity and diapause in Caenorhabditis elegans. Nature *382*, 536–539.

Motola, D.L., Cummins, C.L., Rottiers, V., Sharma, K.K., Li, T., Li, Y., Suino-Powell, K., Xu, H.E., Auchus, R.J., Antebi, A., et al. (2006). Identification of ligands for DAF-12 that govern dauer formation and reproduction in C. elegans. Cell *124*, 1209–1223.

Murphy, C.T., McCarroll, S.A., Bargmann, C.I., Fraser, A., Kamath, R.S., Ahringer, J., Li, H., and Kenyon, C. (2003). Genes that act downstream of DAF-16 to influence the lifespan of Caenorhabditis elegans. Nature *424*, 277–283.

Nolan, T., Hands, R.E., and Bustin, S.A. (2006). Quantification of mRNA using real-time RT-PCR. Nature Protocols *1*, 1559–1582.

Nusbaum, C., and Meyer, B.J. (1989). The Caenorhabditis elegans gene sdc-2 controls sex determination and dosage compensation in XX animals. Genetics *122*, 579–593.

Oh, S.W., Mukhopadhyay, A., Dixit, B.L., Raha, T., Green, M.R., Tissenbaum, H.A., and Wook Oh, S. (2006). Identification of direct DAF-16 targets controlling longevity, metabolism and diapause by chromatin immunoprecipitation. Nature Genetics *38*, 251–257.

Paradis, S., Ailion, M., Toker, A., Thomas, J.H., and Ruvkun, G. (1999). A PDK1 homolog is necessary and sufficient to transduce AGE-1 PI3 kinase signals that regulate diapause in Caenorhabditis elegans. Genes & Development *13*, 1438–1452.

Paradis, S., and Ruvkun, G. (1998). Caenorhabditis elegans Akt/PKB transduces insulin receptor-like signals from AGE-1 PI3 kinase to the DAF-16 transcription factor. Genes & Development *12*, 2488–2498.

Park, D., Estevez, A., and Riddle, D.L. (2010). Antagonistic Smad transcription factors control the dauer/non-dauer switch in C. elegans. Development *137*, 477–485.

Patterson, G.I., Koweek, A., Wong, A., Liu, Y., and Ruvkun, G. (1997). The DAF-3 Smad protein antagonizes TGF-beta-related receptor signaling in the Caenorhabditis elegans dauer pathway. Genes & Development *11*, 2679–2690.

Plenefisch, J.D., DeLong, L., and Meyer, B.J. (1989). Genes that implement the hermaphrodite mode of dosage compensation in Caenorhabditis elegans. Genetics *121*, 57–76.

Ren, P., Lim, C.S., Johnsen, R., Albert, P.S., Pilgrim, D., and Riddle, D.L. (1996). Control of C. elegans larval development by neuronal expression of a TGF-beta homolog. Science *274*, 1389–1391.

Riddle, D.L. (1988). The Dauer Larva. In The Nematode Caenorhabditis Elegans, W.B. Wood editor, ed. (Plainview (New York): Cold Spring Harbor Laboratory Press), pp. 393–412.

Riddle, D.L., Swanson, M.M., and Albert, P.S. (1981). Interacting genes in nematode dauer larva formation. Nature *290*, 668–671.

Riddle DL, B.T.M.B. et al. . editors. (1997). X Chromosome Dosage Compensation.

Rottiers, Motola, Gerisch, Cummins, Nishiwaki, Mangelsdorf, and Antebi (2006). Hormonal Control of C. elegans Dauer Formation and Life Span by a Rieske-like Oxygenase. Developmental Cell *10*, 473–482.

Sharma, K.K., Wang, Z., Motola, D.L., Cummins, C.L., Mangelsdorf, D.J., and Auchus, R.J. (2009). Synthesis and activity of dafachronic acid ligands for the C. elegans DAF-12 nuclear hormone receptor. Molecular Endocrinology *23*, 640–648.

Shaw, W.M., Luo, S., Landis, J., Ashraf, J., and Murphy, C.T. (2007). The C. elegans TGF-[beta] Dauer Pathway Regulates Longevity via Insulin Signaling. Current Biology *17*, 1635–1645.

De Stasio, E.A., and Dorman, S. (2001). Optimization of ENU mutagenesis of Caenorhabditis elegans. Mutation Research/Genetic Toxicology and Environmental Mutagenesis *495*, 81–88.

Tewari, M., Hu, P.J., Ahn, J.S., Ayivi-Guedehoussou, N., Vidalain, P.O., Li, S., Milstein, S., Armstrong, C.M., Boxem, M., Butler, M.D., et al. (2004). Systematic interactome mapping and genetic perturbation analysis of a C. elegans TGF-beta signaling network. Molecular Cell *13*, 469–482.

Tsai, C.J., Mets, D.G., Albrecht, M.R., Nix, P., Chan, A., and Meyer, B.J. (2008). Meiotic crossover number and distribution are regulated by a dosage compensation protein that resembles a condensin subunit. Genes & Development *22*, 194–211.

Tsai, W.C., Bhattacharyya, N., Han, L.Y., Hanover, J.A., and Rechler, M.M. (2003). Insulin inhibition of transcription stimulated by the forkhead protein Foxo1 is not solely due to nuclear exclusion. Endocrinology *144*, 5615–5622.

Vowels, J.J., and Thomas, J.H. (1992). Genetic Analysis of Chemosensory Control of Dauer Formation in Caenorhabditis elegans. Genetics *130*, 105–123.

Wicks, S.R., Yeh, R.T., Gish, W.R., Waterston, R.H., and Plasterk, R.H. (2001). Rapid gene mapping in Caenorhabditis elegans using a high density polymorphism map. Nat Genet *28*, 160–164.

Williams, T.W., Dumas, K.J., and Hu, P.J. (2010). EAK proteins: novel conserved regulators of C. elegans lifespan. Aging *2*, 742–747.

Wolkow, C.A., Munoz, M.J., Riddle, D.L., and Ruvkun, G. (2002). Insulin receptor substrate and p55 orthologous adaptor proteins function in the Caenorhabditis elegans daf-2/insulin-like signaling pathway. The Journal of Biological Chemistry *277*, 49591–49597.

Wollam, J., Magner, D.B., Magomedova, L., Rass, E., Shen, Y., Rottiers, V., Habermann, B., Cummins, C.L., and Antebi, A. (2012). A novel 3-hydroxysteroid dehydrogenase that regulates reproductive development and longevity. PLoS Biology *10*, e1001305.

Wollam, J., Magomedova, L., Magner, D.B., Shen, Y., Rottiers, V., Motola, D.L., Mangelsdorf, D.J., Cummins, C.L., and Antebi, A. (2011). The Rieske oxygenase DAF-36 functions as a cholesterol 7-desaturase in steroidogenic pathways governing longevity. Aging Cell.

Yabe, T., Suzuki, N., Furukawa, T., Ishihara, T., and Katsura, I. (2005). Multidrug resistance-associated protein MRP-1 regulates dauer diapause by its export activity in Caenorhabditis elegans. Development *132*, 3197–3207.

Yonker, S.A., and Meyer, B.J. (2003). Recruitment of C. elegans dosage compensation proteins for gene-specific versus chromosome-wide repression. Development *130*, 6519–6532.

Zhang, Y., Xu, J., Puscau, C., Kim, Y., Wang, X., Alam, H., and Hu, P.J. (2008). Caenorhabditis elegans EAK-3 inhibits dauer arrest via nonautonomous regulation of nuclear DAF-16/FoxO activity. Developmental Biology *315*, 290–302.

Chapter 6: Conclusions

This dissertation was motivated by the desire to understand novel paradigms of FoxO transcription factor regulation, based on the discovery that the EAK pathway inhibits the function of DAF-16/FoxO in parallel to PI3kinase/Akt signaling (Hu et al., 2006; Zhang et al., 2008; Alam et al., 2010). In each chapter, the function of a different protein involved in the regulation of DAF-16/FoxO was interrogated; collectively, these investigations expand the repertoire of known FoxO regulators and provide potential avenues to pursue to modulate the activity of this important transcription factor.

HSD-1 and dafachronic acids

In characterizing *eak-2/hsd-1*, we found that the 3βHSD family member acts in the EAK pathway, in parallel to AKT-1, to regulate dauer arrest via DAF-16/FoxO and DAF-12. Deletion of both *hsd-1* and *akt-1* synergize to increase expression of DAF-16 target genes; we discovered that this expression increase requires DAF-12, suggesting cooperativity between DAF-16 and DAF-12 at the level of transcriptional control.

Phenotypic observations of *hsd-1* mutants were consistent with the proposed role of HSD-1 in one arm of the bifurcated dafachronic acid biosynthesis pathway; synthesizing the Δ^4-dafachronic acid precursor, 4-cholesten-3-one (Patel et al., 2008). Collectively, this work suggested that DAs made by HSD-1 act in parallel to AKT-1 to promote reproductive development *via* inhibition of the activity of DAF-16/FoxO and the dauer-promoting function of unliganded DAF-12. Moreover, it suggested that the HSD-1 derived DAs promote life span in the context of *daf-2/InsR* mutation, but do not influence life span in the context of germline removal. This finding differentiated HSD-1-derived DA activity with that of DAs made by DAF-36, which are required for life span extension in the absence of the germline (Rottiers et al., 2006).

At the time of this study, the biochemical activities of HSD-1 and DAF-36 had not been characterized. Additionally, the steroid hormone profiles of *hsd-1* and *daf-36* mutants were unknown. Since this work, investigation of the *hsd-1* and other proposed DA biosynthetic enzyme mutants revealed that HSD-1 is not in fact required for 4-cholesten-3-one production as previously thought (Wollam et al., 2012), suggesting HSD-1 may act in an alternative parallel pathway to synthesize DA. This led to the revision of the model of DA biosynthesis (Figure 6.1), in which HSD-1 is no longer implicated in the synthesis of Δ^4-dafachronic acid.

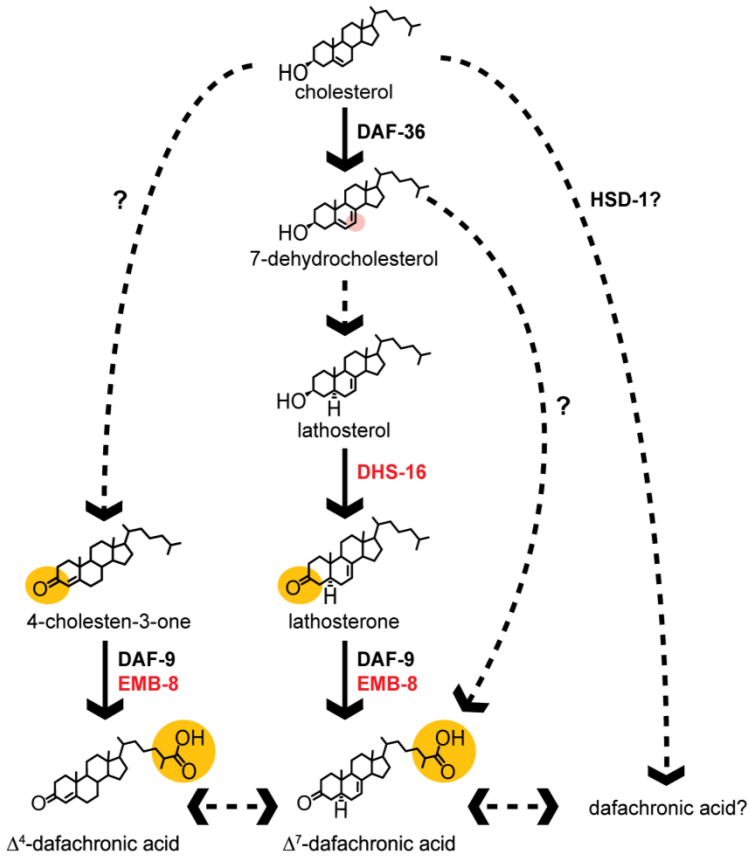

Figure 6.1: Revised model of dafachronic acid biosynthesis.
Adapted from Wollam et al., 2012.

In an additional line of inquiry, we collaborated with the Schroeder group to profile the metabolome of *hsd-1* mutants and controls (Mahanti et al. *in revision.*). Interestingly, this study failed to detect Δ^4-dafachronic acid in any animals tested, suggesting the

possibility that Δ^4-DA is not physiologically relevant. However, given that *hsd-1* is only expressed in the two XXX cells, failure to find Δ^4-DA could simply be indicative of a lack of sensitivity to detect the likely low-abundance DA. Surprisingly, metabolome profiling revealed two novel DAs that were differentially present in *hsd-1* mutants and controls. The first novel DA, dafa A, is not present in wild-type animals but is found in animals lacking functional HSD-1. The second, dafa-B, is detectable in wild-type animals, but is present at elevated levels in *hsd-1* mutants. This suggests that HSD-1 might normally act on dafa-A and dafa-B, potentially converting them into other DAs. We tested dafa-B and found that exogenous administration of it was able to rescue phenotypes associated with DA absence, including full rescue of enhanced life span in the context of germline ablation. This finding suggests that the presence of dafa-B, abundance of which is elevated in *hsd-1* mutants, might be responsible for the failure of *hsd-1* mutation to reduce germline longevity (Chapter 2; Dumas et al., 2010).

Our findings with *hsd-1* revealed a complex relationship between DAs, DAF-12 and DAF-16/FoxO-dependent life span regulation and supported the hypothesis that EAKs might exert their function via regulation of dafachronic acid synthesis or secretion. To investigate this further, we analyzed the role of DAs and DAF-12 in the control of DAF-16/FoxO-dependent life span, as described in Chapter 3. For these studies, we principally used *daf-36(null)* animals to infer the impact of DAs and DAF-12 in the regulation of life span, as these animals have been shown biochemically to lack Δ^4- and Δ^7-DA (Wollam et al., 2011). Although not included in the publication due to the unclear biochemistry of HSD-1, we found that *hsd-1(null)* animals behaved similarly to *daf-36* mutants in the context of *daf-2/InsR* mutant longevity. Collectively, this study revealed that unliganded DAF-12 is detrimental to life span in the context of strong reduction of DAF-2/InsR activity; however DAF-12 itself is dispensable for longevity in this context. In other words, as long as DAF-12 does not interact with its co-regulator DIN-1, as is the case when DA is present, DAF-12 activity is not required for longevity when DAF-2/InsR signaling is reduced. This suggests that unliganded DAF-12 works to oppose the activity of DAF-16/FoxO in the control of life span when ILS is strongly reduced; in contrast, in the presence of DA, DAF-12 does not play a significant role. If the EAK pathway

functions to promote DA biosynthesis or otherwise promote DA activity, but is not absolutely required for DA synthesis, this finding might explain why the majority of the EAKs (namely, *eak-3, eak-4, eak-5/sdf-9 and eak-6*) appear to play no role in life span regulation while strongly regulating dauer arrest (Hu et al., 2006; Zhang et al., 2008).

seak gene identification

Shifting focus away from the complexities of DAs and DAF-12 in DAF-16 regulation, we pursued a strategy to uncover suppressors of EAK activity (*seak* genes) in hopes that they would shed light on the mechanism of DAF-16/FoxO inhibition by the EAK pathway. We did this by identifying molecules which suppress dauer arrest of *eak-7;akt-1* animals when mutated. We postulated that SEAK proteins will normally function to promote DAF-16/FoxO activity, doing so by acting downstream of *eak-7*, downstream of PI3kinase/Akt, in parallel to both pathways, or, by potentially regulating a key downstream target of DAF-16/FoxO (Figure 6.2).

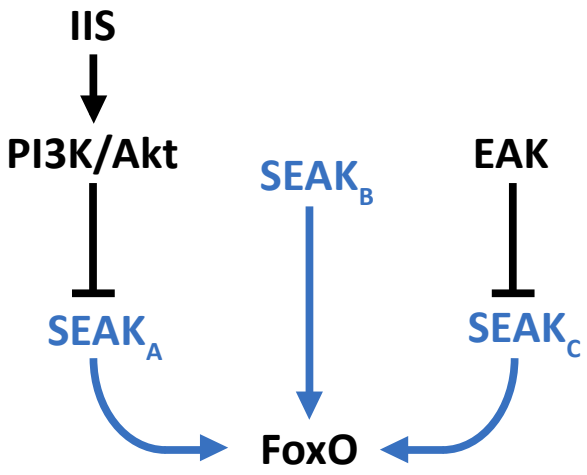

Figure 6.2: Hypothetical role of SEAK protein, suppressors of *eak-7;akt-1*.
SEAKs are predicted to activate FoxO by acting in position A, B, or C. It is also possible that *seak* genes will encode a key downstream target of DAF-16/FoxO.

GAP-3

To date, two *seak* genes have been characterized, *gap-3* (Chapter 4, identified as a spontaneous mutation in *eak-7;akt-1*) and *dpy-21* (Chapter 5, identified in our genetic screen). GAP-3 is potentially representative of the very molecules we sought to find; those that are required to relay the EAK-7 inhibitory signal to DAF-16/FoxO. We found that *gap-3* mutation abrogates dauer arrest of *eak-7;akt-1* mutants and *eak-7* single mutants, but does not substantially impact *akt-1* single mutant phenotypes. This suggests that GAP-3 might normally promote DAF-16/FoxO activity downstream of the EAK pathway. Furthermore, consistent with the mechanism of EAK pathway action, *gap-3* mutation does not alter DAF-16 nuclear-cytoplasmic shuttling. Future studies will address the effect of *gap-3* mutation on DAF-16 target gene expression and will further test the hypothesis that GAP-3 inhibits dauer arrest independently of LET-60/Ras.

DPY-21

In contrast to GAP-3, investigation of DPY-21 did not shed any new light onto the mechanism of EAK pathway action, but instead revealed a novel mechanism of DAF-16/FoxO activation by dosage compensation. DPY-21 appears to regulate DAF-16 via its function in the dosage compensation complex (DCC). The DCC binds to both X chromosomes in hermaphrodite animals and turns down gene expression from each by one half, thereby equilibrating expression levels to that of males with only one X chromosome. We discovered that deleting *dpy-21* was sufficient to increase expression of X-linked ILS pathway components, resulting in the inhibition of DAF-16/FoxO nuclear translocation and bypass of dauer arrest in dauer inducing conditions.

To our knowledge, this represents the first post-embryonic function for dosage compensation in any organism. Because dosage compensation can regulate dauer arrest, a transition that requires the complex integration of environmental sensing and signal transduction, we hypothesize that the activity of DCC may itself be controlled by external cues. Analogous to our observations with the ILS pathway, adjusting DCC activity could modulate other signaling pathways through chromosome-wide regulation of gene

expression, and therefore could impact diverse physiological processes. Future work will pick up this line of inquiry and will address whether DCC formation or activity is responsive to various environmental stimuli, and if so, what impact this has on physiology.

SEAK screen methodology and findings

Our forward genetic screen resulted in the isolation of sixteen independent seak mutant strains, three of which harbor mutant alleles of *dpy-21*. Thus, thirteen strains await identification of the causative *seak* mutation. We currently have hints as to the identity of *seak* candidate genes within several of the remaining strains. Namely, *egl-8,* orthologous to mammalian phospholipase C-β, has been confirmed as a *bona fide seak* gene. Investigation of *egl-8* as a DAF-16/FoxO regulator is underway. We isolated three independent alleles of *egl-8* in the seak screen, as was the case for *dpy-21*. We hypothesized that isolating three alleles of any given gene within a screen of our size (664 total SNVs) was highly significant; the confirmation of both *dpy-21* and *egl-8* (our only two triply-mutated genes) as *seak* genes supports this hypothesis.

Interestingly, one of our seak strains actually harbors a mutation in both *dpy-21* and *egl-8*. Finding one genome that simultaneously harbored mutations in two independent genes, both of which cause the same phenotype in isolation, was quite surprising to us. That said, we have not yet tested the ability of each mutation, in isolation, to suppress dauer arrest; it is possible that one of the two is non-functional and simply a coincidence. Moreover, our surprise might simply be illustrative of the novelty of the 'genome-sequence first, map later' approach that we took in this screen. It is likely that one of these two mutations would have been lost had we undertaken the traditional approach to mapping the causative mutation in this strain. It is therefore possible that this type of double-hit is common during mutagenesis and selection, but the traditional approach to identifying causative mutations has prevented us from detecting it until now. Looking forward, we foresee that the methodology we employed in the *seak* screen (*i.e.* pursuing genetic screens in conjunction with whole genome sequencing, prior to mapping) will

greatly accelerate genetic discovery, as its power is limited only by the cost of sequencing.

Moving forward, *seak* gene identification and characterization promises to be a fruitful strategy to inform our understanding of the biology of DAF-16/FoxO regulation. With luck, EAK proteins, together with SEAK proteins, might inform new avenues for therapeutic intervention for the many age-related diseases in which FoxO transcription factors play a role.

References

Alam, H., Williams, T.W., Dumas, K.J., Guo, C., Yoshina, S., Mitani, S., and Hu, P.J. (2010). EAK-7 Controls Development and Life Span by Regulating Nuclear DAF-16/FoxO Activity. Cell Metabolism *12*, 30–41.

Dumas, K.J., Guo, C., Wang, X., Burkhart, K.B., Adams, E.J., Alam, H., and Hu, P.J. (2010). Functional divergence of dafachronic acid pathways in the control of C. elegans development and lifespan. Developmental Biology *340*, 605–612.

Hu, P.J., Xu, J., and Ruvkun, G. (2006). Two Membrane-Associated Tyrosine Phosphatase Homologs Potentiate C. elegans AKT-1/PKB Signaling. PLoS Genet *2*, e99.

Mahanti P, Bose N, Bethke A, Judkins JJ, Wollam J, Dumas KJ, Malik RU, Hu PJ, Antebi A, S.F. Comparative metabolomics reveals endogenous ligands of a nuclear hormone receptor regulating C. elegans development and lifespan. *In Revision.*

Patel, D.S., Fang, L.L., Svy, D.K., Ruvkun, G., and Li, W. (2008). Genetic identification of HSD-1, a conserved steroidogenic enzyme that directs larval development in Caenorhabditis elegans. Development *135*, 2239–2249.

Rottiers, Motola, Gerisch, Cummins, Nishiwaki, Mangelsdorf, and Antebi (2006). Hormonal Control of C. elegans Dauer Formation and Life Span by a Rieske-like Oxygenase. Developmental Cell *10*, 473–482.

Wollam, J., Magner, D.B., Magomedova, L., Rass, E., Shen, Y., Rottiers, V., Habermann, B., Cummins, C.L., and Antebi, A. (2012). A novel 3-hydroxysteroid dehydrogenase that regulates reproductive development and longevity. PLoS Biology *10*, e1001305.

Wollam, J., Magomedova, L., Magner, D.B., Shen, Y., Rottiers, V., Motola, D.L., Mangelsdorf, D.J., Cummins, C.L., and Antebi, A. (2011). The Rieske oxygenase DAF-36 functions as a cholesterol 7-desaturase in steroidogenic pathways governing longevity. Aging Cell.

Zhang, Y., Xu, J., Puscau, C., Kim, Y., Wang, X., Alam, H., and Hu, P.J. (2008). Caenorhabditis elegans EAK-3 inhibits dauer arrest via nonautonomous regulation of nuclear DAF-16/FoxO activity. Developmental Biology *315*, 290–302.